IDENTIFICATION AND ANALYSIS OF PHOSPHODIESTERASE ISOENZYMES

A thesis submitted to the University of Glasgow for the degree of Doctor of Philosophy in the Faculty of Science

NEIL GRAHAM RENA B.Sc.(Hons)

Division of Biochemistry and Molecular Biology
Institute of Biomedical and Life Sciences (IBLS)
University of Glasgow

February, 1998

ProQuest LLC.
789 East Eisenhower Parkway
P.O. Box 1346
Ann Arbor, MI 48106 – 1346

Dedicated to my parents

ABSTRACT

The second messenger cAMP is involved in the mediation of a wide range of signals in response to a wide range of external stimuli, including processes as varied as neurotransmission, metabolism and embryonic development. Each of the components of the cAMP signalling system are encoded by families of genes. In the case of cAMP phosphodiesterases, the enzymes that hydrolyse cAMP, this variety produces proteins with different targeting, expression and kinetic characteristics. A full understanding of the differing functions of these isoenzymes may in the longer term allow drugs to be designed which allow specific interventions in human pathologies. To realise such an approach, it is important that each isoenzyme be identified and characterised. This thesis concentrates on the characterisation of four of these isoenzymes, namely PDE1B, PDE3B, PDE4A1 and PDE4A10.

In chapter three of this thesis, I use immunoblotting of cell fractions to examine the particulate association of transiently expressed full-length PDE3B. I show solubilisation of full-length PDE3B for the first time. In addition to this I determine the solubility of two deletion mutants which delete a putative membrane association domain. I demonstrate that a mutant with a deleted putative membrane association domain is still particulate, which strongly suggests that PDE3B possesses additional membrane association determinants. I also present data which suggests that PDE3B can be stimulated by protein kinase B.

In chapter four I examine a PKC-mediated induction of PDE1 in chinese hamster ovary cells. There was no sequence information for chinese hamster PDEs. This compelled me to design molecular probes to phylogenetically stable pieces of PDE1. Sequencing of amplification products of these probes reveal that PDE1B is the induced PDE1 form in chinese hamster ovary cells. Selective isoforms of PKC appear to mediate this stimulation.

Chapters five and six of this thesis are devoted to furthering knowledge of the number and primary structure of PDEs. In chapter five I identify mammalian homologues for the rat PDE RD1. Thus, RD1 becomes only the second PDE4A which

has been identified in human and rat. The putative membrane association sequences of RD1 are perfectly conserved across a range of mammalian species, supporting the notion that the sequences may have a conserved functional role. Serendipitously, this work exposes a rodent-lineage specific deletion of apparently ancient PDE4A sequence. This finding, which may be associated with functional alterations, may be a first step in the production of single state PDE inhibitors, since it suggests a possible target for such inhibitors. The deletion may also be of considerable interest to molecular taxonomists as a phylogenetic marker with the potential to solve previously intractable controversies over rodent phylogeny.

In chapter six of this thesis I identify, clone and express a novel human PDE4A splice variant, PDE4A10. I then make a survey of endogenous expression of this PDE in native brain and cell lines by RT-PCR. Furthermore, I identify almost the full open reading frame of the rat homologue of this splice variant. This PDE is therefore the third PDE4A which has been identified in both rat and human.

The work in chapter six also makes a wider contribution, by describing a novel method for producing precise overlaps in clones of DNA made by a modification of shotgun cloning. Shotgun cloning was already the easiest way to fragment a large piece of DNA into smaller ones. The innovation to shotgun cloning that I describe makes it easier and extends its utility. The overlaps of DNA fragments that result will allow the shotgun fragments to be ordered as they appeared in the original DNA sequence and if the ordered fragments are sized, this will produce a restriction map for the contig. This approach is considerably faster than existing methods for producing DNA contigs and restriction maps. If it is taken up, the ease and speed of this new technique should significantly hasten sequencing projects such as the Human Genome Project.

Acknowledgements

I would like to express my thanks to Professor Miles Houslay, for his generous support, understanding and friendly supervision during the last three years.

I would also like to thank the other members of the Gardiner Laboratory, whose friendship I enjoyed and whose technical experience I often called upon.

I am indebted to my family and friends who have tolerated my long absences from them. I am totally indebted to Michelle, whose tolerance and empathy seems infinite.

CONTENTS

FIGURE INDEX

Abbreviations

AKAP A-kinase anchoring protein

ATP adenosine trisphosphate

BSA bovine serum albumin

Ca^{2+}/CaM calcium/calmodulin

cAMP cyclic 3'5' adenosine mono phosphate

CAT chloramphenicol acetyl transferase

cGMP cyclic 3'5' guanosine mono phosphate

cDNA complementary DNA

CHO Chinese Hamster Ovary

CIAP calf intestinal alkaline phosphatase

Cilostimide[4,5-dihydro-6[4-(1H-imadazol-1-yl)phenyl[-5-methyl 392H)-pyrazone]

CRE cAMP response element

DAG diacylglycerol

DEAE diethylaminoethyl

DEPC diethylpyrocarbonate

DMEM Dulbecco's modification of Eagle's Medium

DMSO dimethylsulfoxide

DNA deoxyribonucleic acid

dNTP deoxynucleotide trisphosphate

DOTAP N-[1-(2,3-dioleoyloxy)propyl]-N,N,N-trimethylammoniummethylsulphate

DTT dithiothreitol

ECL Enhanced chemiluminescence

EDTA ethylenediaminetetra-acetic acid

EGTA ethylene glycolbis(ß-aminoethylether)-N,N,N',N'-tetra-acetic acid

EHNA erythro-9-(2-hydroxyl-3-nonyl)-adenine

FCS foetal Calf Serum

GDP guanosine diphosphate

GSK-3 glycogen synthase kinase-3

GSP gene specific primer

GTP guanosine trisphosphate

HeLa Henrietta Lacks

HEPES N-2-hydroxyethylpiperazine-N'-2-ethane-sulphonic acid

IBMX 1-isobutylmethyl-3-xanthine

IPTG isopropyl-ß-D-thiogalactopyranoside

KHEM potassium (K), HEPES, EGTA, Magnesium

LB Luria-Bertoni

LR linker region

MAP kinase mitogen activated protein kinase

mRNA messenger RNA

ORF open reading frame

ori origin of replication

PAGE polyacrylamide gel electrophoresis

PBS phosphate buffered saline

PCR polymerase chain reaction

PDE phosphodiesterase

PI 3-kinase Phosphatidyl inositol 3-kinase

PKA protein kinase A

PKB protein kinase B

PKC protein kinase C

PMA phorbol-12-myristate, 13-acetate

RACE rapid amplification of cDNA ends

RLM RNA ligase mediated

RNA ribonucleic acid

RT reverse transcription

SDS sodium dodecyl sulphate

TBE tris/borate/EDTA

TBS tris buffered saline

TE tris/EDTA

TEA triethanolamine

TEMED N,N,N',N'-tetramethylethylene diamine

TdT terminal deoxynucleotidyl transferase

Tris Tris(hydroxymethyl)methylamine

TSH thyroid stimulating hormone

UCR upstream conserved region

UTR untranslated region

UV ultraviolet

VSV vesicular stomatitis virus

INTRODUCTION

1.1 Intracellular signalling with cyclic nucleotides: cyclic nucleotide generation

The cyclic nucleotides cyclic 3'5' guanosine mono phosphate (cGMP) and cyclic 3'5' adenosine mono phosphate (cAMP) are second messengers which are found ubiquitously in mammalian cells. These cyclic nucleotides are involved in the transduction of signals by a wide variety of hormones and neurotransmitters and other agents. cAMP mediates a diverse range of effects. It can bring about acute, reversible changes in dynamically regulated processes such as neurotransmission, muscle contraction and it regulates metabolic processes such as glycogenolysis and lipolysis. Yet, in other contexts, cAMP can have long term effects on, for example, embryonic development, cell growth and differentiation. Most of the cellular effects of modulation of cAMP concentrations are due to the stimulatory effect of cAMP on protein kinase A (PKA) activity. PKA then phosphorylates key target proteins leading, ultimately, to alterations in cell functioning (1).

1.1.1 Agonist stimulation of G-protein coupled receptors (G-PCR)

cAMP signalling is initiated at the cell surface by regulation of G-protein coupled receptors (G-PCR). These numerous 'serpentine' receptors contain seven transmembrane domains each of about 22-28 amino acids. The N-terminal of the receptor is extracellular, of variable length and glycosylated, whilst the C-terminal tail is intracellular and, in certain receptors, this region contains phosphorylation sites for PKA and G-protein coupled receptor kinases (GRK) (2). Ligand occupancy of the receptor brings about interaction with the heterotrimeric guanine nucleotide regulatory protein (G-protein) family (3). These proteins consist of $\alpha\beta\gamma$ heterotrimers. There are multiple isoforms of each subunit and these isoforms have subtly different specificities for interactions with other signalling molecules including the other G-protein subunits themselves, such that the isoforms usually form heterotrimers with only a few of the other possible subunits (4). The alpha subunits are GTPases which bind to $\beta\gamma$-G via the α-G N-terminus, in a region which partly overlaps with the effector-binding region. The C-terminus of α-G is involved in specificity of the individual receptor/G-protein interactions (4). Receptor interaction with the adenylyl cyclase stimulatory G-protein G_s causes a conformational change which allows the α-G_s subunit of the G-protein to bind GTP and dissociate from the $\beta\gamma$-G heterodimer (3). Following this, binding of the α-G_s/GTP subunit stimulates the transmembrane enzyme adenylyl cyclase (see below). The conformational changes caused by GTP binding, which cause α-G_s dissociation have been elaborated in crystal structures of α-G of the light-activated heterotrimeric G-protein transducin bound to GTP and GDP (4). The activated conformation persists until GTP is hydrolysed to GDP by the intrinsic GTPase activity of the α subunit of the G-protein (4). This form is 'recycled' by reassociation with the $\beta\gamma$-G heterodimer (3). In addition to G_s linked G-PCR there is a family of receptors which are able to inhibit adenylate cyclase activity by interacting with the inhibitory guanine nucleotide regulatory protein, G_i (5) and certain receptors show a promiscuity in the G-proteins that they will couple with (2). The $\beta\gamma$-G heterodimer never disassociates and so acts as a functional monomer (4). This monomer is an active signalling molecule with many targets, amongst which are

examples of both positive and negative regulation (4). Regulatory targets include type-I adenylyl cyclase, which it inhibits, and type-II adenylyl cyclase, which it stimulates (6).

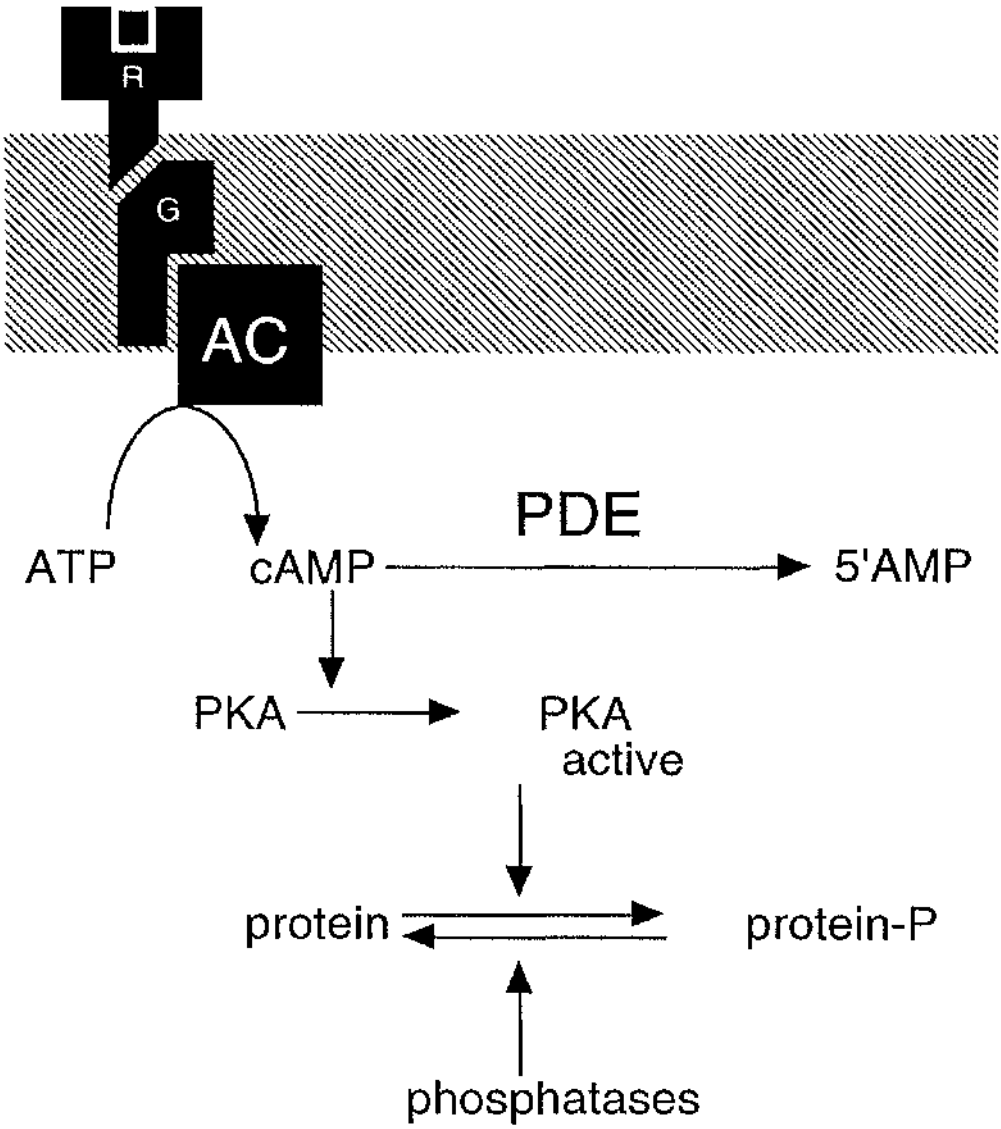

Figure 1.1.1. Schematic of G-protein coupled receptor mediated activation of Protein Kinase A

Ligand occupancy of G-protein coupled receptors (R, cell membrane is shown hatched) brings about activation of adenylyl cyclase (AC) through a G-protein mediated process (G). Adenylyl cyclase catalyses the synthesis of cAMP from ATP. cAMP, through association with the regulatory subunit of PKA, brings about catalytic subunit activation. PKA signalling then occurs by phosphorylation of substrate proteins. Phosphodiesterases allow the system to be reset by catalysing the breakdown of cAMP to 5'AMP.

1.1.2 Adenylyl Cyclases

G-proteins activated by cell-surface receptors alter cAMP signalling in a way that depends on which of the family of adenylyl cyclases (AC) the G-protein is co-localised with. To date, nine different classes of AC have been reported. AC enzymes are typically more than 1000 amino acids long with molecular weights of approximately 120kD but the distribution of AC forms varies (6). Members of the mammalian AC family all have a similar structure which is reminiscent of certain channels though no such activity has been reported for these enzymes (6). The structure consists of two sets of six transmembrane helices (M1 and M2) with very short connecting loops. M1 and M2 are separated by a much larger intracellular loop (C1a and C1b). There is a C-terminal tail at the end of the protein (C2a and C2b). C1a and C2a are very highly conserved and are thought to encode the catalytic domain of AC (6). Different AC forms often have contrasting regulatory properties (7). For example the activity of the AC I and III isoforms can be stimulated by calcium/calmodulin whereas the AC V, VI and IX isoforms are inhibited by calcium (6,8). The sequences that encode these regulatory domains are found within the intracellular loop and the long C-terminal tail. Furthermore, different AC have different catalytic properties and it has been suggested (7) that this can determine cAMP flux controls in the cell. Thus, in cells with 'high' cycling conditions brought about by AC with a high basal activity, such as AC-II, PKA is kept inactive by PDE with a high activity. In such a situation, elevation of cAMP levels can be brought about by stimulation of AC or inhibition of PDE. In contrast, in 'low' cycling conditions, where the AC basal activity is extremely low, as in the case of AC-VI, activation of AC is the only acute method by which the cAMP threshold can be breached since inhibition of PDE will cause a chronic build-up in cAMP concentration due to the low activity of AC. Thus cell-specific responses to ligands could in part be due to the cAMP 'poise' of the cell, as determined by the isoforms of AC expressed in the cell (7).

1.2 Hydrolysis of cAMP and cGMP by members of the 3'5' cyclic nucleotide phosphodiesterase (PDE) gene superfamily

cAMP phosphodiesterases antagonise effectors of adenylyl cyclases by hydrolysing 3',5' cyclic AMP to 5'-AMP. This is the only enzymatic route by which this can occur. In some cells (but not for example in hepatocytes (9)) cAMP can also be extruded through an energy driven process (10).

Mammalian phosphodiesterase activity is supplied by a large gene superfamily (see table 1.2), the members of which are all distantly related to the yeast PDE2 gene (see figure 1.2.) There is a second yeast PDE gene, PDE1, which has no mammalian homologues. Mammalian PDEs exhibit a common structural pattern with a conserved catalytic domain of ~300 amino acids and more divergent sequences in the N-terminal and C-terminal ends (11-18). PDE activity is classified into seven types (PDE1-7). These divisions were originally made on the basis of inhibitor/activator selectivity of phosphodiesterase activities eluted from purification columns. Since the identification of PDE genes, the genetic conservation which underlies these biochemical differences has become apparent such that it is now clear that the seven PDE types are groupings of highly homologous PDE genes. PDEs are highly conserved in evolution, such that species' homologues of a specific gene or cDNA are much more homologous than different PDE genes in the same species.

Type	Effectors	Substrate	Selective Inhibitor	Number of Genes	Splice Variants
1	Calcium/ CaM	cAMP/ cGMP	nicardipine vinpocetine	3	8+
2	cGMP stimulated	cAMP/ cGMP	EHNA	1	1
3	various	cAMP/ cGMP	cilostimide milrinone	2	2+
4	various	cAMP	rolipram RP73401	4	15+
5		cGMP	zaprinast	1	1
6		cGMP	none known	3	3
7		cAMP	none known	1	1

Table 1.2 General characteristics of the seven types of mammalian phosphodiesterase (19)

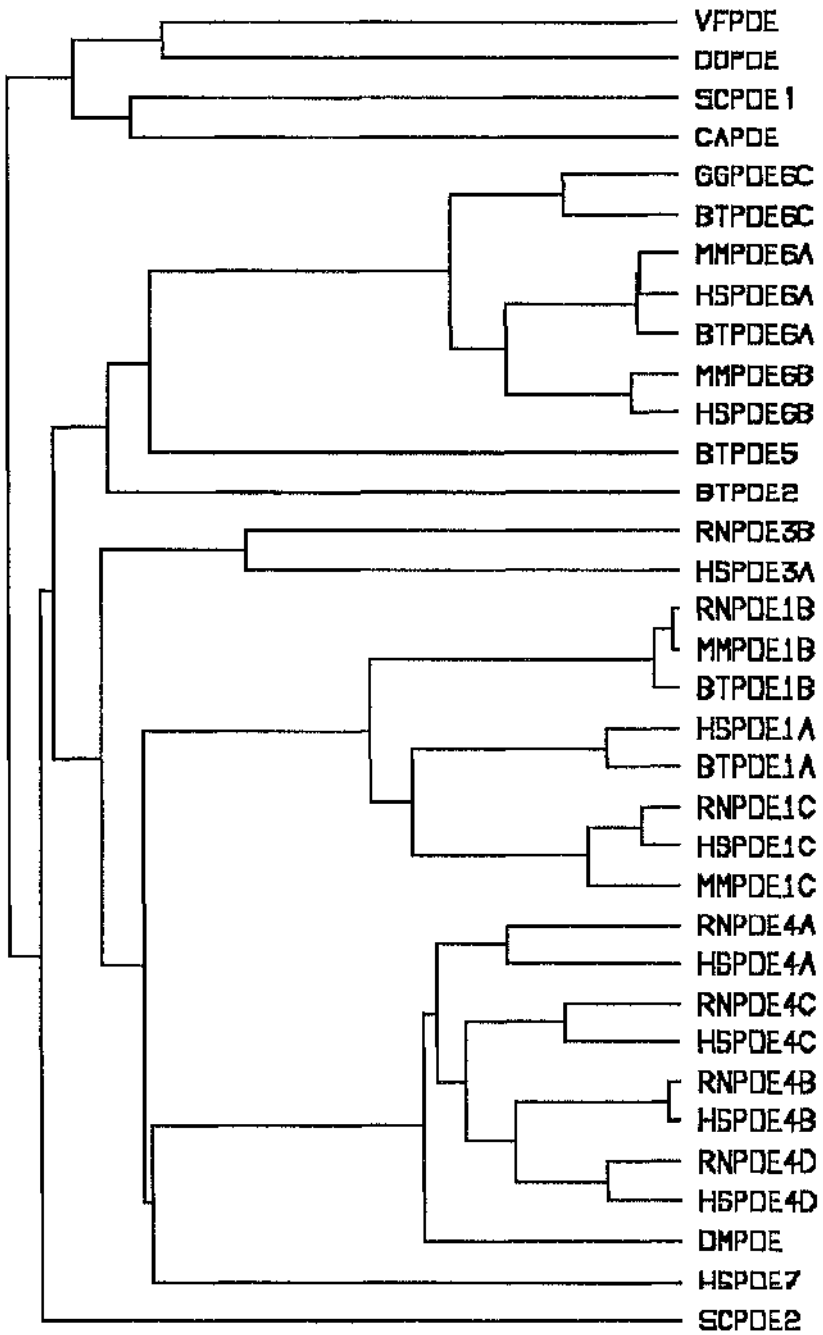

Figure 1.2 Conservation tree of phosphodiesterase genes

The conserved catalytic sequences of PDE genes in GenBank, were aligned according to instructions in the GCG suite of software. The most conserved sequences are chosen because substitutions here are more likely to represent neutral drift rather than adaptation. Thus, this figure represents the best estimation of the evolutionary ancestry of PDE genes. Genes are numbered according to the most recent nomenclature (see section 1.2.1.). Species are: BT *bos taurus*; CA *candida albicans*; DD *dictyostelium discoideum;* DM *drosophila melanogaster*; GG *gallus gallus;* HS *homo sapiens;* MM *mus musculus*; RN *rattus norvegicus*; SC *saccharomyces cerevisiae*; VF *vibrio fischeri*

1.2.1. Phosphodiesterase nomenclature

To describe the various PDE species and to provide a rational framework to allow accommodation of new forms, a Nomenclature Committee was set up in the early 1990s (11). This led to a change in PDE naming from a roman numeral-based system (type-I etc.) to one based on arabic numerals (PDE1 etc.). The new systematic PDE splice variant nomenclature is based upon (i) the first two letters indicating the source species (e.g., HS - homo sapiens; RN - rattus norvegicus), (ii) the name 'PDE' for cyclic nucleotide phosphodiesterase, (iii) an arabic numeral for the gene family, (iv) a single letter for the gene (e.g. A/B/C for each of the three PDE1 gene families), (v) an arabic numeral for the splice variant and (vi) a single letter for the report. Usually the same last numeral (v) is used to describe the same isoform in different species, for example the human splice variant most closely related to RNPDE4A1 is HSPDE4A1 (An important exception is HSPDE4A4, whose rat homologue is RNPDE4A5).

1.3 cAMP DEPENDENT PROTEIN KINASE A (PKA) MEDIATION OF cAMP SIGNALLING: MODELS FOR THE SPATIO-TEMPORAL PARTITIONING OF THE cAMP SIGNAL.

The generation of an intracellular response to elevated levels of cAMP is due to the action of protein kinase A (PKA) (20). Inactive PKA is a heterodimer consisting of both regulatory (R) and catalytic (C) units. cAMP activates PKA by binding to the regulatory subunits. This allows dissociation of free, active catalytic units which then mediate all of the various downstream physiological effects of cAMP signalling.

Spatio-temporal partitioning of the cAMP signal, so-called compartmentalisation, has been suggested as a mechanism for how in a single cell, two receptors coupled to adenylate cyclase can cause different effects on cell function via cyclic AMP signalling to PKA (21,22). The machinery for cAMP production can be localised to discrete regions of the plasma membrane in polar cells, as has been reported for various G-protein linked receptors and adenylate cyclase (3). The intracellular receptor system for cAMP, protein kinase A (PKA) may also be localised, in that the PKA-RI form is cytosolic but the PKA-RII form is almost exclusively particulate-associated by interaction with members of a family of A-kinase anchoring proteins (AKAPs)(21). These are a heterologous collection of proteins that have a common property of being able to bind PKA. AKAPs target pools of PKA-RII because different AKAPs have altered cellular distributions and associations with subcellular structures (21-23). Thus a system has been described which provides for distinct locations defining the sites of cAMP production and detection. Non-uniform intracellular distribution of cAMP has now been measured (24). A clear inference is that localised PKA-RII will be exposed to different cAMP concentrations leading to distinct responses dependent on whether the local cAMP concentration can breach the activation threshold of each PKA pool. If PDEs are targeted similarly to the other cAMP signalling components then selective PDE regulation immediately becomes an alternative way to manipulate the form of the cAMP response by defining spatially and temporally which PKA pools can respond to the cAMP signal, by selectively protecting specific PKA pools by lowering the local cAMP concentration (see figure

1.3).

The existence of the numerous evolutionarily conserved PDE forms is in itself consistent with the notion that such selective regulation of PDEs will take place because if these splice variants did not have differing roles they would not all be retained in evolution. Now evidence is accumulating regarding the distinct regulation, localisation and biochemistry that could form the molecular basis of spatio-temporal partitioning of the cAMP signal due to phosphodiesterase heterogeneity. Some of these examples are discussed below.

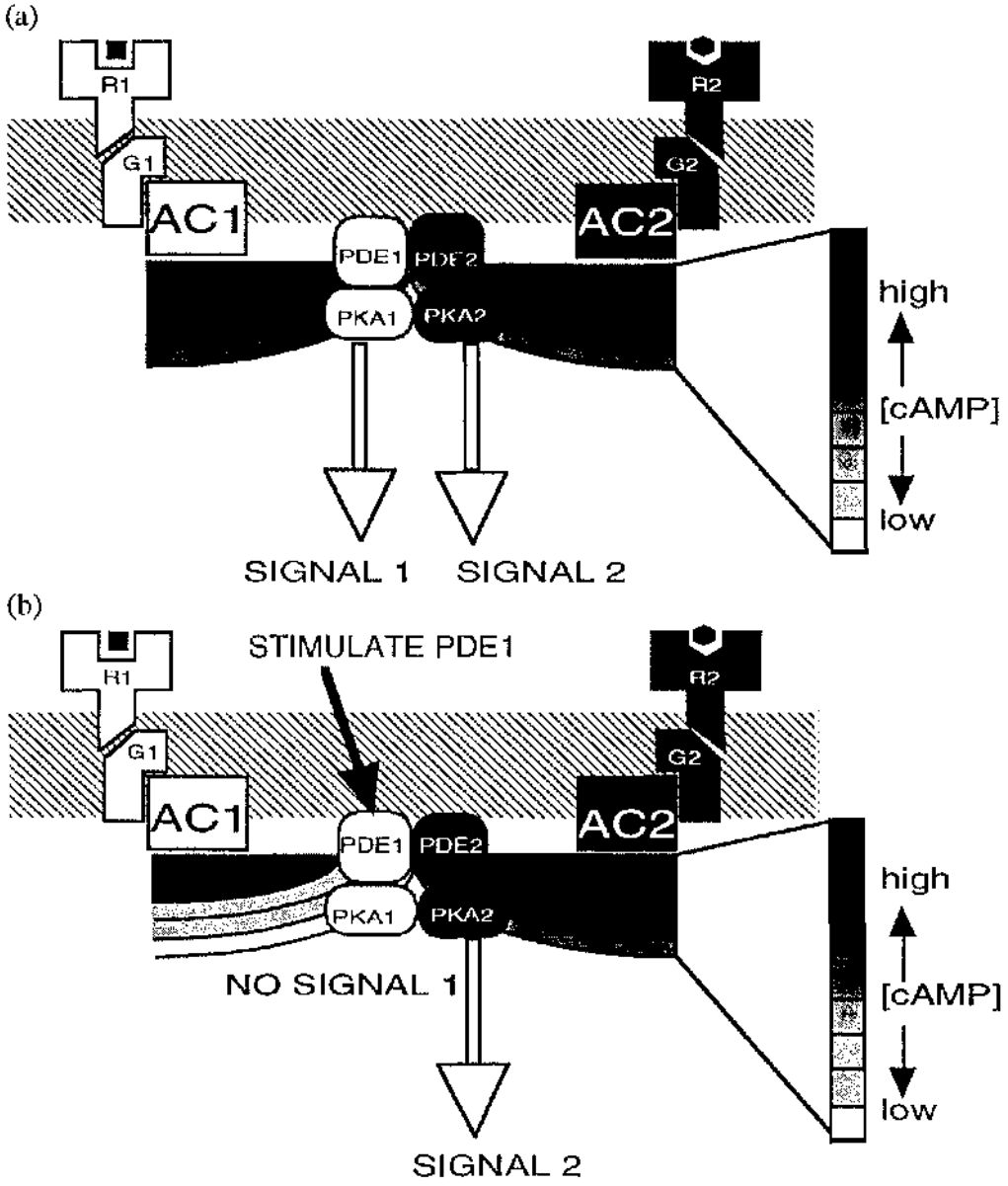

Figure 1.3. Model for compartmentalisation of the cAMP signalling system: potential for specific regulation of these channels by PDE.
(a) Components of cAMP signalling machinery, including receptors (R) G-proteins (G), PDE and PKA are targeted to subcellular locations (see text). These could form discrete groupings of signalling machinery (depicted as group 1 (white) and group 2 (black), in the diagram.) each populated by different isozymes of the various signalling enzymes (black and white in the diagram). At the cell membrane (hatched box) ligand occupancy is transduced by a G-protein mediated process to activate adenylyl cyclase producing enough cAMP to breach the activation threshold of both PDEs resulting in two downstream signals. (b) Selective stimulation of PDE is then able to selectively block a channelled cAMP signal, in the 'high' cycling cellular context (see section 1.1.2)

1.3.1. Experimental observations of compartmentalization due to PDEs

Specific PDE inhibitors have been used to implicate PDEs in many signalling mechanisms. Recently two reports have explicitly approached subcellular compartmentalization due to PDEs by use of PDE inhibitors. Jurevicius et al (25) showed that during β-adrenergic stimulation PDE activity stopped local cAMP pools diffusing into the cytosol. They found that in the absence of PDE inhibition, β-adrenergic-elevated cAMP levels in particulate fractions rise more than in cytosolic fractions. In contrast when PDE inhibitors were added simultaneously with isoproterenol treatment, a more equal division of cAMP accumulation was detected (25). These differences were shown to have a functional correlate in that treatment of the cells with isoproterenol alone had a much more spatially discrete effect on calcium channel gating than when isoproterenol was added in conjunction with PDE inhibitors. Thus PDEs are indeed able to insulate compartments of the cell from each other.

More recently (26), comparative analysis of the effect of inhibitors on the same cell line has led to the first evidence that different PDEs occupy different compartments and have different roles in the same cell. Chini et al (26) used PDE inhibitors specific for different PDE families to study cAMP signalling compartmentalization due to different PDE isoforms in rat kidney mesangial cells. In these cells, response to immunoinflammatory stimuli brings about accelerated proliferation and generation of reaction oxygen metabolites (ROM), both due to elevation of cAMP. It was found that PDE3 inhibitors raised PKA activity and specifically inhibited proliferation. In contrast, PDE4 inhibitors specifically blocked ROM whilst also raising PKA activity. All the effects of these inhibitors had potencies similar to their effect on PDEs.

1.4 PDE1 calcium/calmodulin stimulated PDE gene family: survey of complexity and distribution

PDE1 enzymes can hydrolyse both cAMP and cGMP, with their activities being stimulated by Ca^{2+}/CaM at physiological concentrations (12). Three genes (A,B,C) encode these enzymes, with additional complexity generated by alternative

mRNA splicing in PDE1A and PDE1C such that there are currently eight reported PDE1 isozymes. The PDE1 genes are most closely related to PDE4 and PDE7 in the PDE gene superfamily. PDE1A1, PDE1B (27,28) and PDE1C1-5 (29-31) are all expressed in discrete sections of the brain whereas PDE1A2 is identified in lung and heart (32).

PDE1A forms are about 59-61 kD in size, PDE1B is 63kD and PDE1C forms range in size from 71kD for PDE1C1 to 86kD for PDE1C2 (12).

PDE1A and PDE1B each have a K_m for cAMP which is approximately ten times higher than their K_m for cGMP which is in the low micromolar range (12). In contrast, PDE1C has a K_m for cAMP which is roughly equal to that for cGMP (31).

PDE1 forms possess the conserved PDE catalytic domain along with PDE1 specific sequences in the N-terminal. The PDE1A and PDE1C genes appear to be alternatively spliced (see table 1.4). PDE1C deviates from the normal pattern in that its splice-variants have gene-specific conserved sequences further towards its C-terminal than the catalytic domain. PDE1C also deviates from most other spliced PDEs in that it undergoes C-terminal as well as N-terminal alternative splicing. PDE1 conserved sequences have been shown to mediate regulation by PKA, Ca^{2+}/CaM or to be involved in autoregulation (see below).

Letter in figure	Transcript name	Clone Name	Accession Number	Size (amino acids)	Reference
PDE1A					
	BTPDE1A1	59kD CaM-PDE	L34069	514	(33)
	BTPDE1A2	61kD CaM-PDE	M90358	530	(32)
	HSPDE1A3	Hcam1	U40370	535	(29)
PDE1B					
	BTPDE1B1	63kD CaM-PDE	M94867	534	(34)
	HSPDE1B1		U56976	536	(35)
	MMPDE1B1		L01695	535	(28)
	RNPDE1B1		M94537	535	(36)
PDE1C					
	HSPDE1C1	Hcam3b	U40371	634	(29)
	MMPDE1C1		L76944	631	
	RNPDE1C2		L41045	768	(31)
	HSPDE1C3	Hcam3a	U40372	560*	(29)
	MMPDE1C4		L76947	655*	(30)
	MMPDE1C5		L76946	604	(30)

Table 1.4. PDE1 isoforms

A complete list of PDE1 isoforms is shown.

KEY:

* The reading frame is open at the 5' end

1.4.1. Regulation of the catalytic activity of PDE1

Ca^{2+}/calmodulin is able to stimulate all PDE 1 enzymes at least 10-fold. This effect is almost exclusively on the V_{max} (12). The mechanism of action of calmodulin binding is apparently to relieve inhibition by binding adjacent to an inhibitory domain found in the N-terminal of PDE1s. PDE1A2 apparently has a higher affinity for calmodulin than other PDE1s, owing to a second calmodulin binding domain in its unique, due to alternatively splicing, N-terminal sequence (33). Since the levels of calmodulin in cells do not vary it is likely that calmodulin binding is regulated directly by the level of Ca^{2+} in the cell (12). Such regulation is expected to allow interactions between Ca^{2+} and cAMP signalling. Such interplay is seen in the signal transduction of olfaction, where many signals trigger an increase in cAMP and an accompanying increase in Ca^{2+} by influx through cAMP gated channels. This calcium amplifies the cAMP signal by stimulation of adenylyl cyclase III but it has been suggested that it then also serves to reset the system by stimulation of PDE1C (12,30).

PDE1A1, PDE1A2 and PDE1B are all phosphorylated by PKA (37,38) and PDE1B can also be phosphorylated by CaM kinase II (37). Phosphorylation at serine 120 of PDE1A reduces the affinity of the protein for calmodulin. Thus, PKA can induce more cAMP production by inhibiting PDE1. An increase in Ca^{2+} concentration enables 'escape' from this feed-forward loop. It is not clear what the physiological role of this is. It has been suggested that in post synaptic endings feed-forward will allow rapid amplification of signals which cause a small increase in cAMP concentration. Ca^{2+} could then reset the system (12)

1.5. PDE2 cGMP STIMULATED PDE GENE FAMILY

Similarly to PDE1, PDE2 enzymes hydrolyse both cAMP and cGMP. PDE2, however, is more closely related to the cGMP specific PDE gene families, PDE5 & PDE6, than it is to other cAMP specific PDEs. To date, one cDNA for a PDE2 gene has been identified (39). This gene is expressed in a number of sections of the brain, in heart, trachea, lung, spleen and T-cells (39). In certain cell lines this sequence is only ever partly protected in RNAase protection analysis, implying the existence of

alternative splice variants. This is consistent with the finding that PDE2 can exist in both cytosolic and membrane-bound forms (40). A unique feature of PDE2 amongst PDE genes is that catalytic activity can be stimulated through the binding of cGMP to a flexible domain in the N-terminal region of PDE2 (41). This organisation of the gene was originally suggested when protease treatment of PDE2 was able to dissociate PDE catalytic activity from the cGMP binding site (41,42).

cGMP binding is thought to occur through a tandem repeat conserved in PDE5 (42) forming a domain which is able to bind cGMP. Consistent with this, site directed mutagenesis of key amino acids in this putative domain reduces the affinity of PDE2 for cGMP (43). It has been suggested that binding of cGMP brings about a conformational change in the cGMP binding domain and that the flexibility of this domain allows transduction of that conformational change to the catalytic domain (41).

1.6. PDE3 cGMP INHIBITED cAMP SPECIFIC PDE GENE FAMILY

There are two genes in the mammalian cAMP specific PDE3 gene family, these are named PDE3A and PDE3B. In the PDE gene superfamily these are most closely related to the other cAMP specific genes PDE1, PDE4 and PDE7. PDE3 gene products exhibit high affinities with a K_m for both cAMP and cGMP in the low micromolar range. This means that, in contrast to other PDEs (see section 1.6.2.1), cGMP can competitively inhibit cAMP hydrolysis at very low concentrations. Indeed PDE3 enzymes were originally termed 'cGMP-inhibited' PDEs after this characteristic. This name survives in many of the clone names of PDE3 (for example, the longest transcript of rat PDE3B which is called rcGIP-1 for rat cyclic GMP inhibited PDE).

PDE3 enzymes can be specifically inhibited by several drugs including cilostamide and OPC3911 and this has enabled understanding of the cellular functions that PDE3 is involved in. Such functions include (44): (1) myocardial contractility, which led to animal and clinical trials (45) for the PDE3 inhibitor milrinone in treatment of chronic heart failure; (2) inhibition of platelet aggregation (46); (3) relaxation of airway and vascular smooth muscle (47,48); (4) insulin mediated

adipocyte anti-lipolysis (49) and (5) insulin secretion (50). The last two of these are discussed in greater depth below.

Transcript name	Accession Number	Clone Name	Size (amino acids)	Reference
PDE3A				
HSPDE3A1	M91667	HcGIP-2	1141*	**(51)**
HSPDE3A2?			658	**(52)**
RNPDE3A	U38179	RcGIP-2	1141*	
PDE3B				
HSPDE3B	U38178	HcGIP-1	1112	**(53)**
RNPDE3B	Z22867	RcGIP-1	1108	**(54)**

Table 1.6. PDE3 isoforms

Information is shown on PDE3 cDNAs submitted to GenBank. cDNAs which are open at the 5' end are marked with an asterisk. In the case of RNPDE3B, the completeness of this reading frame is inferred by comparison with HSPDE3B.

1.6.1. PDE3 isoenzyme structure and distribution

The first cDNA that described a PDE3 form was isolated from a heart cDNA library and designated PDE3A (51). A cDNA (rcGIP-1) from a second gene, which was designated PDE3B was then identified in rat adipocyte libraries using a PDE3A probe (54). Though this reading frame is open at the 5' end, isolation of the human homologue of this PDE (HSPDE3B) indicates that the first ATG in rcGIP-1 is the initiator methionine. The first genomic sequence information on PDE3B has shown that human PDE3B is composed of 16 exons dispersed in more than 110Kb of the human genome (53). The two PDE3 genes have a gene primary structure which, beyond the common catalytic domain, shares elements not identified in other PDEs. Thus, they both possess a ~150 amino acid hydrophobic region in the N-terminus, as well as conserving the sequence which connects this domain to the catalytic domain (see figure 1.6.1). The role of these N-terminal domains in membrane association of PDE3B is discussed in chapter 3. PDE3 forms also possess a unique 44 amino acid insertion within the conserved catalytic region. The function of this region is not known but it is essential for PDE3 catalytic activity because even though its removal yields a catalytic domain more homologous to other PDE catalytic domains, this construct is inactive (55). Both PDE3 cDNAs encode proteins with predicted molecular weights of ~125kD. However, recombinant and native proteins of both genes migrate more slowly on SDS-PAGE gels than expected (56). This has been attributed to a cluster of positively charged residues conserved in the C-termini of both genes (54). In contrast to PDE1 and PDE4 there is no evidence for alternative splicing of PDE3 which could yield proteins with unique pieces of sequence. However, for PDE3A at least, truncated splice variants of the gene appear to exist both in RNA and as expressed protein (52).

PDE3A is expressed in heart and vascular smooth muscle while PDE3B is expressed in adipocytes, hepatocytes, renal collecting duct epithelium and developing spermatocytes (54,57) . Both PDE3 forms are expressed in the brain (57).

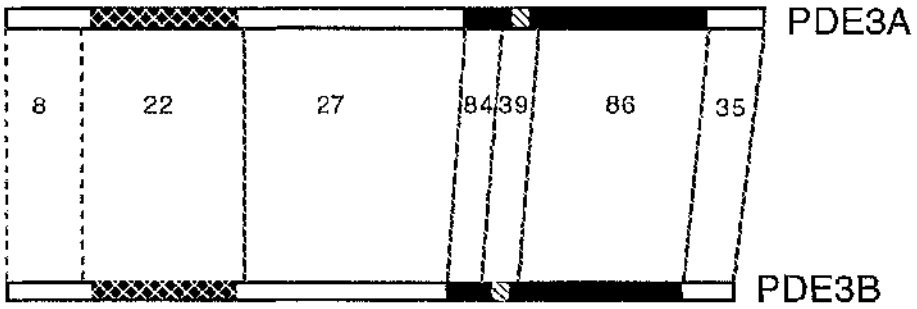

Figure 1.6.1. Schematic of domain structure of PDE3

The figure presented above shows the domain structure of PDE3A compared with PDE3B(based on a figure by Degerman et al (58)). The numbers represent the percentage of amino acid identities in between equivalent domains. The cross-hatched box is the hydrophobic putative membrane association domain of PDE3 (54) (see section 3.1). The black domain is the putative catalytic domain. The PDE3-specific catalytic insertion is the hatched box within the catalytic domain

1.6.2. Regulation of PDE3 catalytic activity

1.6.2.1. Regulation of PDE3 by cGMP

Several studies report that inhibition of PDE3 by cGMP signalling is of physiological importance. Nitrovasodilators, which up-regulate cGMP levels through stimulation of guanylyl cyclases, potentiate signals that are mediated by cAMP signalling and it has been proposed that this is due to cGMP inhibition of PDE3 leading to elevated cAMP levels (16). Examples of signals elevated in this way include anti-aggregatory effects of prostacyclin in rabbit platelets (46) and DNA synthesis in thymocytes (59). Thus regulation of cAMP levels can be positively or negatively coupled to changes in cGMP levels, dependent on whether PDE2 or PDE3 isozymes are present. This 'cross-talk' is likely to be particularly important in cellular contexts where cGMP levels are regulated, as is the case, for example, in the regulation of vasodilation (48).

1.6.2.2. The anti-lipolytic effect of insulin is mediated by stimulation of PDE3B

One of the physiological effects of insulin is antagonism of catecholamine induced release of free fatty acids (lipolysis). Early investigations by Beebe et al (60) studied lipolysis stimulated with thirteen cAMP analogues. Lipolysis stimulated by cAMP analogues which could be hydrolysed by adipocyte PDE could be antagonized by insulin. In contrast, lipolysis stimulated by analogues that PDE3B cannot hydrolyse was insensitive to insulin treatment. These results suggest that PDE3B mediates the anti-lipolytic signal of insulin and militate strongly against the other possibility that insulin might directly influence components of the signalling pathway downstream of cAMP/PKA. Subsequent experiments with specific PDE3 inhibitors such as cilostamide or OPC-3911 showed that they block insulin mediated anti-lipolysis, whilst PDE4 inhibitors are unable to mimic the inhibition (61,62). Thus it appears that PDE3 mediates the anti-lipolytic effect of insulin. The inactivation of PKA that ensues results in dephosphorylation and reduced activity of hormone sensitive lipase and lowered rates of lipolysis (63,64). An added level of complexity is that PKA itself is capable of stimulating PDE3B. A sustained PKA mediated PDE

stimulation was observed within ~2 minutes. Insulin mediated stimulation of PDE3 was also detected for a sustained time period but was maximal only after 15 minutes. Furthermore, stimulation with insulin and PKA synergistically activated PDE3, before rapidly tailing off, presumably due to hydrolysis of cAMP. It has been proposed that PKA stimulation of PDE3B acts as a short-term feedback loop for catecholamine stimulated lipolysis, whereas insulin can have more sustained effects on the levels of lipolysis in adipocytes (58,64).

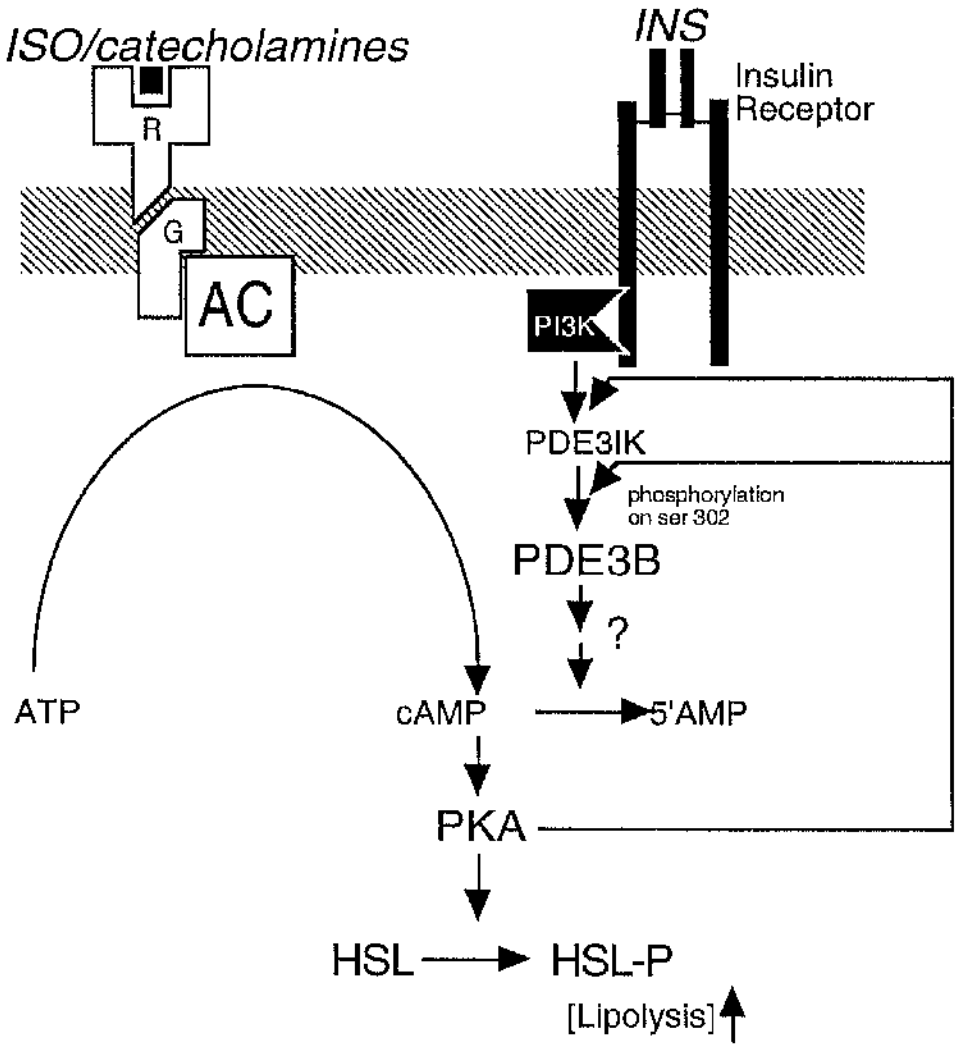

Figure 1.6.2.2. Mechanisms for the anti-lipolytic effect of insulin
Insulin antagonises catecholamine induced lipolysis by stimulating PDE3B, apparently by a PI 3-Kinase mediated signal (see section 1.6.2.2). The effect on PDE3B is phosphorylation of serine 302. Intriguingly, upregulation of PKA stimulates PDE3B on the same site, as part of a putative negative feedback loop. The effects of insulin and catecholamine regulation of lipolysis are ultimately mediated through PKA regulation of the level of phosphorylation of hormone sensitive lipase.

KEY:
PDE3IK= PDE3 insulin stimulated kinase
HSL= hormone sensitive lipase

1.6.2.3. The attenuation of insulin secretion by insulin-like growth factor 1 (IGF-1) is mediated by stimulation of PDE3B.

It has been shown that in both isolated pancreatic islets and an insulin-secreting cell-line, insulin secretion stimulated by glucose is reversed by IGF-1, apparently through a mechanism that reduces the concentration of cAMP (50). Experiments with selectively hydrolyzable cAMP analogues have implicated PDE3B in this attenuation of insulin secretion (50), much like the initial experiments on mediation of anti-lipolysis (60). Thus, insulin secretion induced by treatment with cAMP analogues can only be attenuated by IGF-1 if the analogues can be hydrolysed by PDE3B. These results suggest a direct role for PDE3B in the IGF-1 pathway rather than the possibility that IGF-1 might directly influence signalling components downstream of cAMP. Again similar to the experiments on anti-lipolysis, use of specific PDE3 inhibitors to block the IGF-1 signal confirmed the role of PDE3 in this pathway. The PDE3 involved was identified by confocal imaging which showed specific expression of PDE3B in the β cells of pancreatic islets of Langerhans. Furthermore, it was found that PDE3B activity was higher in immunoprecipitates following treatment with IGF-1. Thus, it seems that two aspects of insulin physiology, the regulation of insulin secretion and the regulation of lipolysis, are both controlled by modulation of cAMP concentrations by PDE3B. It remains to be seen how much of the rest of the two signalling pathways is conserved.

1.7 PDE4/*dunce* cAMP SPECIFIC PDE GENE FAMILY

The mammalian PDE4 gene family is highly homologous to the drosophila *dunce* locus which is involved in learning and short term memory processes as described below. Indeed, the first isolation of mammalian PDE4 cDNA was due to its homology with a drosophila dunce probe (65). Interestingly, PDE4 enzymes are potently inhibited by rolipram, a compound which exerts anti-depressant effects in man. The pharmacology of this compound and other PDE4 specific inhibitors indicates that PDE4 selective inhibitors may be of therapeutic use in a number of human disease states (reviewed in (19)). Moreover certain of these compounds are

able to distinguish between different conformations of PDE4 and it is emerging that these conformations, which can be selectively inhibited, are associated with different signals (see section 1.8).

Studies on rat (65-67), human (68) and mouse (69) models indicate that cAMP-specific PDEs, which are homologous to the *dunce* PDE are encoded by 4 genes in mammals, namely PDE4A-D. Individual PDE4 genes are evolutionarily conserved so that a human PDE4 gene is more closely related to its rat homologue than to the other human PDE4 genes (68).

The human PDE4 genes are found on three human chromosomes (one gene on each of chromosome 1 and 5 and two on chromosome 19). The murine PDE4s are located in the corresponding chromosomal regions of the mouse genome (69-72).

cDNA clones from each of the PDE4 genes have been isolated from both human and rat (65-68,70,71,73-91). Results for these studies indicate that each of the four PDE genes encode a multiplicity of transcripts. The most complete example of each transcript is listed in table 1.7. Figures 1.7.a and 1.7.b show these transcripts as alternatively spliced variants of the PDE4A-D gene loci. As can be seen, such transcripts have a structure consistent with their being generated by alternative mRNA splicing and, possibly, the use of alternative transcriptional start sites, with two splice junctions conserved from the dunce gene (92,93). Each of these splice variant transcripts are, presumably, under the regulation of a separate promoter. The almost universal use of the splice junctions conserved with the dunce PDE gene allows an informal distinction to be drawn between 'long' forms, which diverge at the first splice junction (splice site consensus: (F/L)(D/E)(L/A/V)(D/E)NG; junction 1 in figures 1.7a and 1.7b) and 'short' forms, which diverge at the second, more 3' splice junction (splice site consensus: E(D/E)(T/S/A)(G/C/Y)(L/Q)(K/Q)LA; junction 2 in figures 1.7a and 1.7b) (81). Nonetheless, there is little conservation between dunce and mammalian splice variant sequence. In contrast many of the individual splice variants are conserved between humans and rats (Table 2). For example, each of the three rat PDE4D transcripts are also present in human (87). For both humans and rats, there are some mRNAs for which no known counterpart has, to date, been identified

in the other species. Given the conservation of splice variants between mammals it is probable that these mRNAs exist but have yet to be isolated.

Analysis of PDE4 splice variants, and the proteins that they encode, demonstrates that different transcripts from a single human or rat gene encode proteins with different expression patterns, biochemical properties, regulation, and intracellular localisation (see below). This complexity may yet allow highly selective therapeutic inhibitors to be designed to individual variants.

	HUMAN ISOFORMS						RAT ISOFORMS				
Letter in figure	Transcript name	Accession Number	Clone name	Size (amino acids)	Ref.	No. in figure	Transcript name	Accession Number	Clone name	Size (amino acids)	Ref.
PDE4A											
A	HSPDE4A1A	U97584	hRD1	646[1]	(82)	A	RNPDE4A1A	M26715	RD1	610	(65)
	There is no human homologue of RD2				(82)	B	RNPDE4A2A	M26717 J04554	RD2	493	(65)
	There is no human homologue of RD3				(82)	C	RNPDE4A3A	M26716, J04554	RD3	585	(65)
D	HSPDE4A4B	L20965	PDE46	886	(68)	D	RNPDE4A5A	L27057	RPDE6	844	(68)
E	HSPDE4A5A	L20967	TM3	800**	(68)						
						F	RNPDE4A8A	L36437	RPDE39	763	(77)
						G	RNPDE4A9?[2]				(19)
H	HSPDE4A10A			810	This thesis	H	RNPDE4A10A			771*¥	This thesis
	HSPDE4A8A	U18088	2EL	323*	(71)						

PDE4B											
J	HSPDE4B1A	L20966	TM72	736	(68)		RNPDE4B1A§	J04563	DPD	562*	(66)
K	HSPDE4B2A	M97515		564	(83)	K	RNPDE4B2A	M25350 M28413	rat PDE4	564	(67)
L	HSPDE4B3A	U85048		721	(90)	L	RNPDE4B3A		PRPDE74	721	(90)
M	HSPDE4B4?	L12685	HPB102	516	(79)						
PDE4C											
N	HSPDE4C1B	Z46632		711	(85)	N	RNPDE4C1B§	L27061	RPDE36	536*	(76)
O	HSPDE4C2A	U88712		605	(78)						
P	HSPDE4C3A	U88713		699*	(78)						
Q	HSPDE4C4A	U66346		791*	(91)						
	HSPDE4C5A	U66347		426	(91)						
	HSPDE4C6A	U66348		518*$_2$	(91)						
	HSPDE4C7A	U66349		463*	(91)						
PDE4D											
R	HSPDE4D1B	U79571	DUN11	586	(87)	R	RNPDE4D1A	U09455	ratPDE3.1	584	(67)
S	HSPDE4D2B	U50158	PDE82	508	(87)	S	RNPDE4D2A	U09456	ratPDE3.2	505	(73)
T	HSPDE4D3A	L20970	PDE43	673	(68)	T	RNPDE4D3B	U09457	ratPDE3.3	672	(88)
U	HSPDE4D4	L20969	PDE39	809	(68)						
V	HSPDE4D5	S:1059276	PDE79	784*	(87)						

Table 1.7 PDE4 isoforms

A complete list of PDE4 cDNAs was compiled by Houslay et al (19) and there have been no published additions since then. The table above summarises this information, with all the splice variants of PDE4A-D shown. The most complete cDNA described for each isoform is listed and in the case where two such cDNAs have been reported, only the earliest report is listed.

* The reading frame is open at the 5' end. In some cases where both species' homologues exist, the completeness of a reading frame has been inferred in one species by comparison with the other. These open reading frames are not asterisked

**TM3 contains a number of intronic sequences which are removed from other PDE4As. It will only code for a 'long' form PDE4A of ~800 amino acids if these are removed (19).

$_1$This number is inferred only as full-length hRD1 has not yet been identified

$_2$RPDE66, Graeme Bolger unpublished

§ These cDNAs are truncated further towards the 3' end of the alternative splice junctions and so could be due to truncation of more than one splice variant

¥ By comparison to HSPDE4A10 it is anticipated that RNPDE4A10 will be 773 amino acids long.

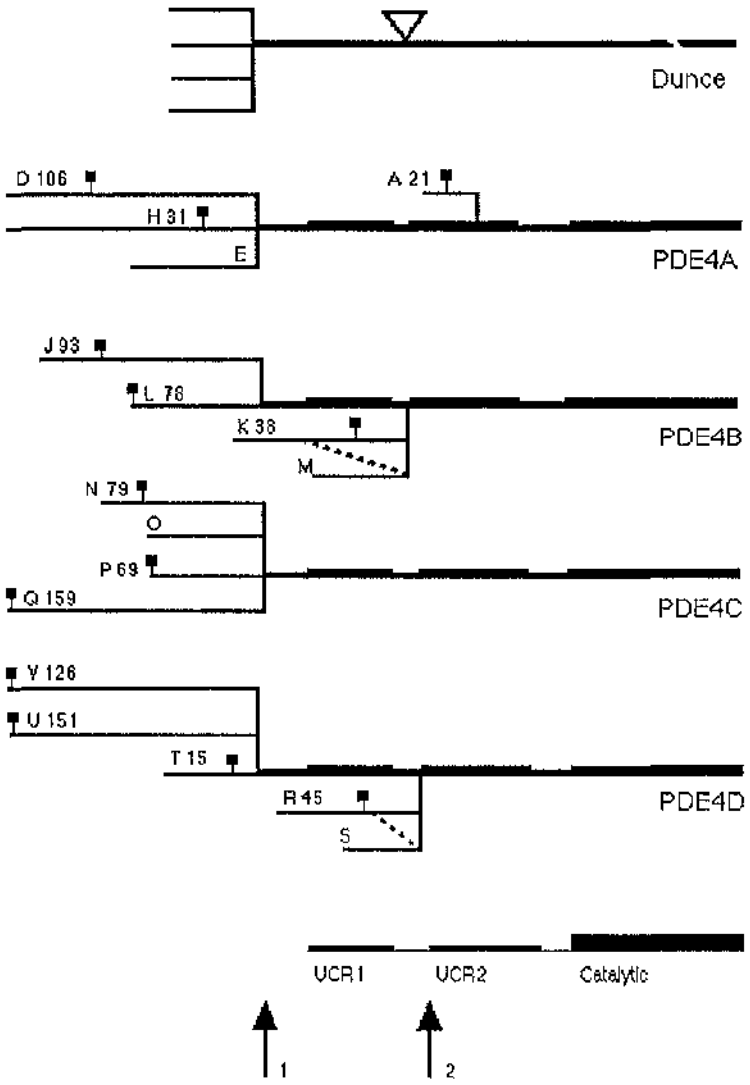

Figure 1.7.a Alternative splicing of human gene loci PDE4A-D

Transcripts of each human PDE4 gene are presented as splice variants of their gene locus, compared with dunce. Positions of UCR1, UCR2 and the catalytic domain are shown, with arrows showing the positions of the 'long' (1) and 'short' (2) splice junctions conserved from drosophila. The longest example of each transcript is presented in each case. Each letter refers to the transcript's entry in table 1.7. The numbers above each splice variant represent the number of unique 5' sequence in the transcript in amino acids. Note that some transcripts do not encode any unique amino acid sequence.

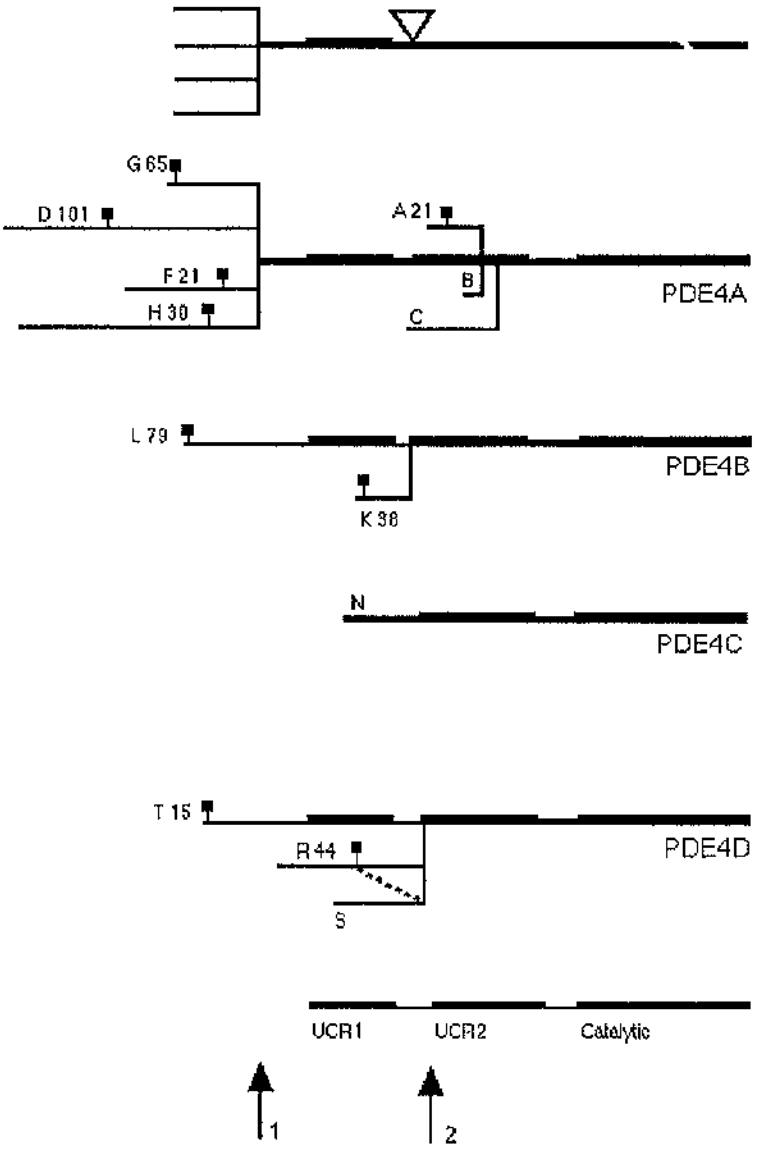

Figure 1.7.b Alternative splicing of rat gene loci PDE4A-D

Transcripts of each rat PDE4 gene are presented as splice variants of their gene locus, compared with dunce. Positions of UCR1, UCR2 and the catalytic domain are shown, with arrows showing the positions of the 'long' (1) and 'short' (2) splice junctions conserved from drosophila. The longest example of each transcript is presented in each case. Each letter refers to the transcript's entry in table 1.7. The numbers above each splice variant represent the number of unique 5' sequence in the transcript in amino acids. Note that some transcripts do not encode any unique amino acid sequence.

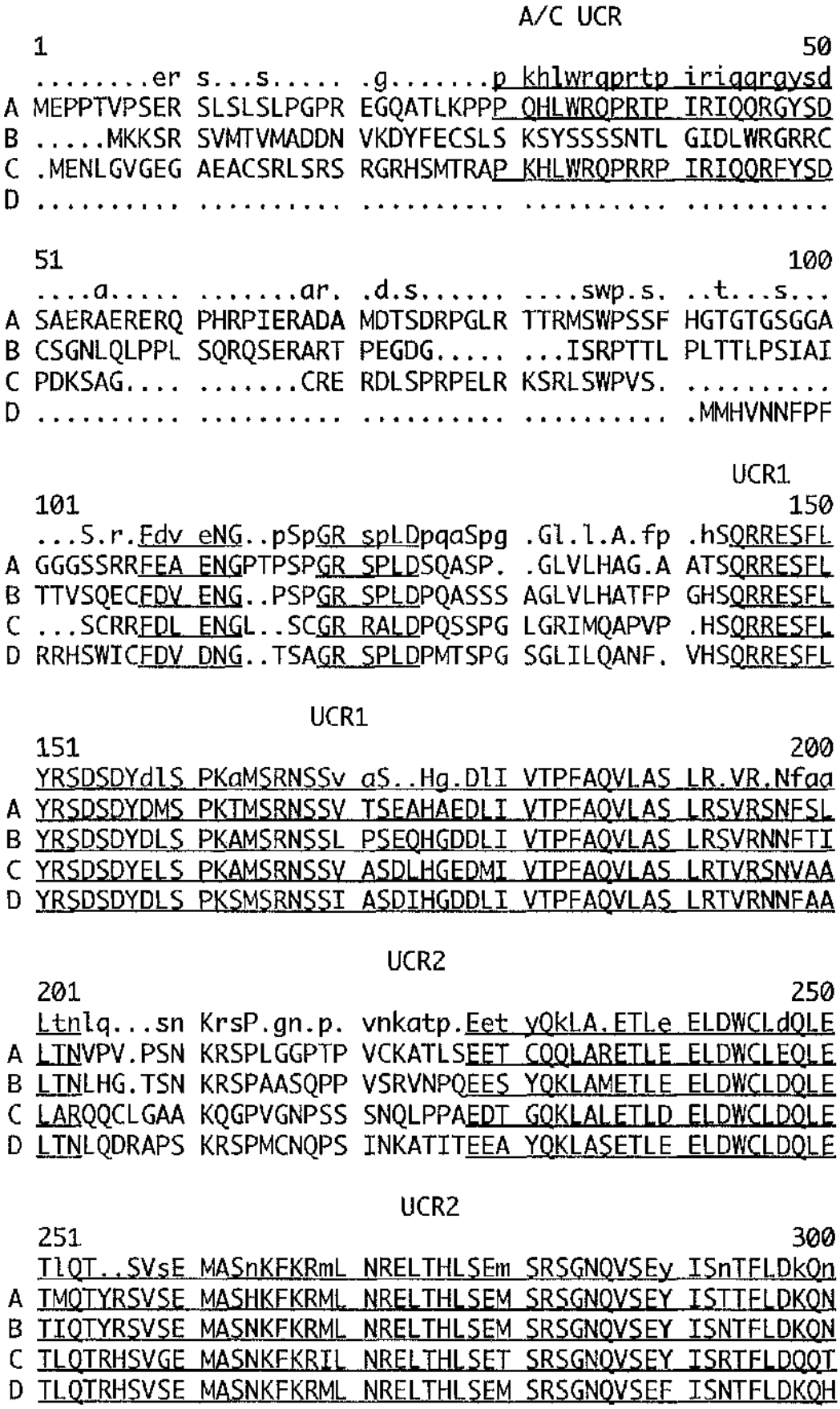
A/C UCR
1 50
.....er s...s..... .g.....p khlwrqprtp iriqqrqysd
A MEPPTVPSER SLSLSLPGPR EGQATLKPPP QHLWRQPRTP IRIQQRGYSD
B .....MKKSR SVMTVMADDN VKDYFECSLS KSYSSSSNTL GIDLWRGRRC
C .MENLGVGEG AEACSRLSRS RGRHSMTRAP KHLWRQPRRP IRIQQRFYSD
D .....
51 100
....a..... .....ar. .d.s..... ....swp.s. ..t...s...
A SAERAERERQ PHRPIERADA MDTSDRPGLR TTRMSWPSSF HGTGTGSGGA
B CSGNLQLPPL SQRQSERART PEGDG..... ...ISRPTTL PLTTLPSIAI
C PDKSAG.... .....CRE RDLSPRPELR KSRLSWPVS. .....
D .... .MMHVNNFPF
UCR1
101 150
...S.r.Fdv eNG..pSpGR spLDpqaSpg .Gl.l.A.fp .hSQRRESFL
A GGGSSRRFEA ENGPTPSPGR SPLDSQASP. .GLVLHAG.A ATSQRRESFL
B TTVSQECFDV ENG..PSPGR SPLDPQASSS AGLVLHATFP GHSQRRESFL
C ...SCRRFDL ENGL..SCGR RALDPQSSPG LGRIMQAPVP .HSQRRESFL
D RRHSWICFDV DNG..TSAGR SPLDPMTSPG SGLILQANF. VHSQRRESFL
UCR1
151 200
YRSDSDYdlS PKaMSRNSSv aS..Hg.DlI VTPFAQVLAS LR.VR.Nfaa
A YRSDSDYDMS PKTMSRNSSV TSEAHAEDLI VTPFAQVLAS LRSVRSNFSL
B YRSDSDYDLS PKAMSRNSSL PSEQHGDDLI VTPFAQVLAS LRSVRNNFTI
C YRSDSDYELS PKAMSRNSSV ASDLHGEDMI VTPFAQVLAS LRTVRSNVAA
D YRSDSDYDLS PKSMSRNSSI ASDIHGDDLI VTPFAQVLAS LRTVRNNFAA
UCR2
201 250
Ltnlq...sn KrsP.gn.p. vnkatp.Eet yQkLA.ETLe ELDWCLdQLE
A LTNVPV.PSN KRSPLGGPTP VCKATLSEET CQQLARETLE ELDWCLEQLE
B LTNLHG.TSN KRSPAASQPP VSRVNPQEES YQKLAMETLE ELDWCLDQLE
C LARQQCLGAA KQGPVGNPSS SNQLPPAEDT GQKLALETLD ELDWCLDQLE
D LTNLQDRAPS KRSPMCNQPS INKATITEEA YQKLASETLE ELDWCLDQLE
UCR2
251 300
TlQT..SVsE MASnKFKRmL NRELTHLSEm SRSGNQVSEy ISnTFLDkQn
A TMQTYRSVSE MASHKFKRML NRELTHLSEM SRSGNQVSEY ISTTFLDKQN
B TIQTYRSVSE MASNKFKRML NRELTHLSEM SRSGNQVSEY ISNTFLDKQN
C TLQTRHSVGE MASNKFKRIL NRELTHLSET SRSGNQVSEY ISRTFLDQQT
D TLQTRHSVSE MASNKFKRML NRELTHLSEM SRSGNQVSEF ISNTFLDKQH

```
                                                    Catalytic
  301                                                       350
  eVEiPspTqk erekkk.p.. ..........  ...qpMsqIs G.kkLmHSsS
A EVEIPSPTMK EREKQQAPRP RPSQPPPPPV PHLQPMSQIT GLKKLMHSNS
B DVEIPSPTQK DREKKKKQ.. ..........  ...QLMTQIS GVKKLMHSSS
C EVELPKVTAE EAP.......  ..........  ...QPMSRIS GLHGLCHSAS
D EVEIPSPTQK EKEKKKRP.. ..........  .....MSQIS GVKKLMHSSS

  351                                                       400
  LnnssipREG VkT.qE..LA kELEdlNKWG Ln.F.vadys gnRpLTcImv
A LNNSNIPREG VKTDQEELLA QELENLNKWG LNIFCVSDYA GGRSLTCIMY
B LNNTSISREG VNTENEDHLA KELEDLNKWG LNIFNVAGYS HNRPLTCIMY
C LSSATVPREG VQTDQEEQLA KELEDTNKWG LDVFKVADVS GNRPLTAIIF
D LTNSSIPREG VKTEQEDVLA KELEDVNKWG LHVFRIAELS GNRPLTVIMH

  401                                                       450
  .IFQERDLLK tFrIpvDTli TY..tLEdHY HadVAYHNsl HAADVaQSTH
A MIFQERDLLK KFRIPVDTMV TYMLTLEDHY HADVAYHNSL HAADVLQSTH
B AIFQERDLLK TFRISSDTFI TYMMTLEDHY HSDVAYHNSL HAADVAQSTH
C SIFQERDLLK TFQIPADTLA TYLLMLEGHY HANVAYHNSL HAADVAQSTH
D TIFQERDLLK TFKIPVDTLI TYLMTLEDHY HADVAYHNNI HAADVVQSTH

  451                                                       500
  VLL.TPAL.A VFTDLEILAA .FA.AIHDVD HPGVSNQFLI NTNSelALMY
A VLLATPALDA VFTDLEILAA LFAAAIHDVD HPGVSNQFLI NTNSELALMY
B VLLSTPALDA VFTDLEILAA IFAAAIHDVD HPGVSNQFLI NTNSELALMY
C VLLATPALEA VFTDLEILAA LFASAIHDVD HPGVSNQFLI NTNSDVALMY
D VLLSTPALEA VFTDLEILAA IFASAIHDVD HPGVSNQFLI NTNSELALMY

  501                                                       550
  NDeSVLENHH LAVGFKLLQe enCDIFqNL. kkQRqsLRkM VIDmVLATDM
A NDESVLENHH LAVGFKLLQE DNCDIFQNLS KRQRQSLRKM VIDMVLATDM
B NDESVLENHH LAVGFKLLQE EHCDIFMNLT KKQRQTLRKM VIDMVLATDM
C NDASVLENHH LAVGFKLLQA ENCDIFQNLS AKQRLSLRRM VIDMVLATDM
D NDSSVLENHH LAVGFKLLQE ENCDIFQNLT KKQRQSLRKM VIDIVLATDM

  551                                                       600
  SKHMnLLADL KTMVETKKVT SsGVLLLDNY sDRIQVL.Nm VHCADLSNPT
A SKHMTLLADL KTMVETKKVT SSGVLLLDNY SDRIQVLRNM VHCADLSNPT
B SKHMSLLADL KTMVETKKVT SSGVLLLDNY TDRIQVLRNM VHCADLSNPT
C SKHMNLLADL KTMVETKKVT SLGVLLLDNY SDRIQVLQNL VHCADLSNPT
D SKHMNLLADL KTMVETKKVT SSGVLLLDNY SDRIQVLQNM VHCADLSNPT
```

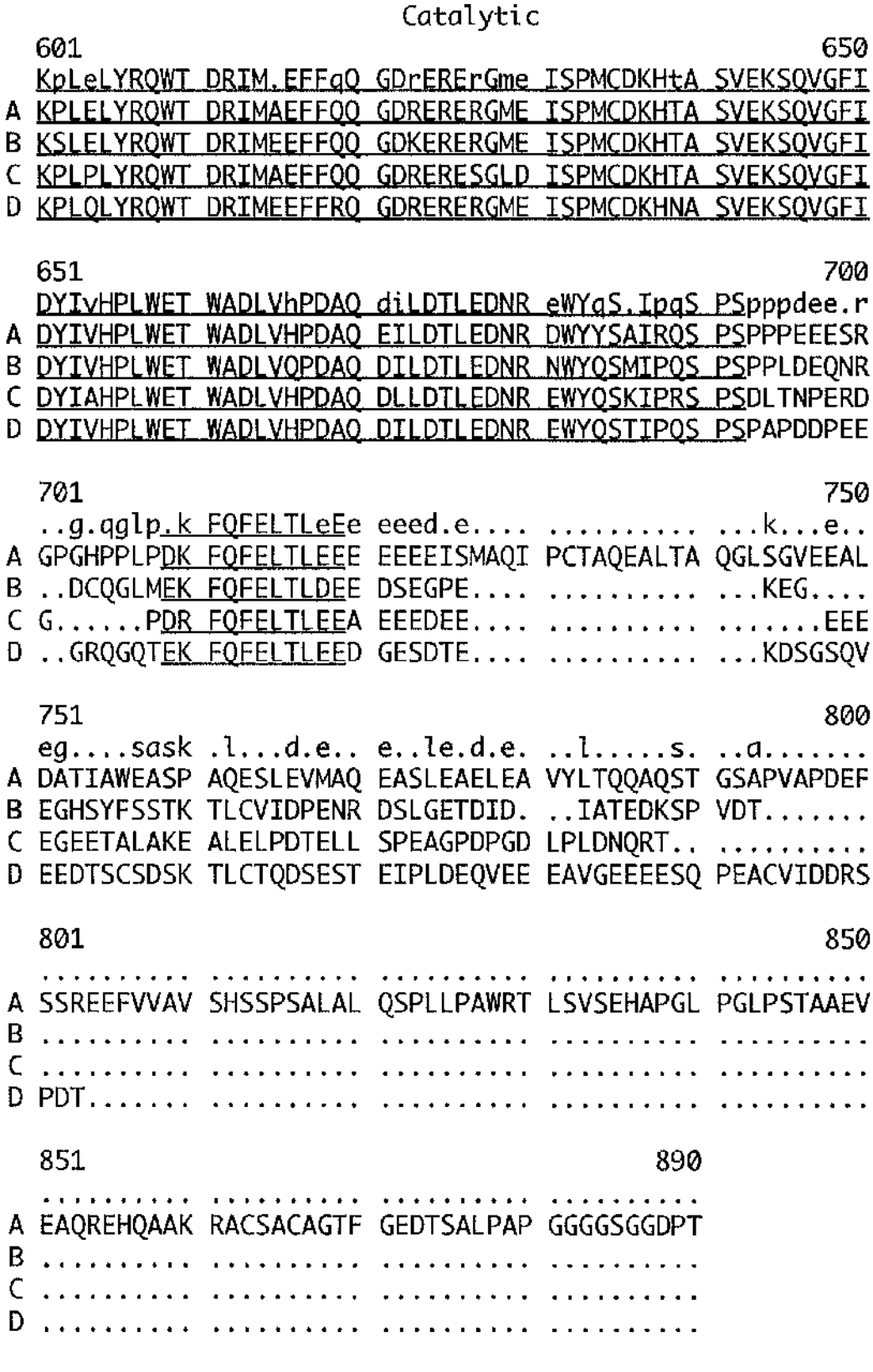
Catalytic
601 650
KpLeLYRQWT DRIM.EFFqQ GDrERErGme ISPMCDKHtA SVEKSQVGFI
A KPLELYRQWT DRIMAEFFQQ GDRERERGME ISPMCDKHTA SVEKSQVGFI
B KSLELYRQWT DRIMEEFFQQ GDKERERGME ISPMCDKHTA SVEKSQVGFI
C KPLPLYRQWT DRIMAEFFQQ GDRERESGLD ISPMCDKHTA SVEKSQVGFI
D KPLQLYRQWT DRIMEEFFRQ GDRERERGME ISPMCDKHNA SVEKSQVGFI
651 700
DYIvHPLWET WADLVhPDAQ diLDTLEDNR eWYqS.IpqS PSpppdee.r
A DYIVHPLWET WADLVHPDAQ EILDTLEDNR DWYYSAIRQS PSPPPEEESR
B DYIVHPLWET WADLVQPDAQ DILDTLEDNR NWYQSMIPQS PSPPLDEQNR
C DYIAHPLWET WADLVHPDAQ DLLDTLEDNR EWYQSKIPRS PSDLTNPERD
D DYIVHPLWET WADLVHPDAQ DILDTLEDNR EWYQSTIPQS PSPAPDDPEE
701 750
..g.qglp.k FQFELTLeEe eeed.e.... ....k...e..
A GPGHPPLPDK FQFELTLEEE EEEEISMAQI PCTAQEALTA QGLSGVEEAL
B ..DCQGLMEK FQFELTLDEE DSEGPE.... ....KEG....
C G......PDR FQFELTLEEA EEEDEE.... ....EEE
D ..GRQGQTEK FQFELTLEED GESDTE.... ....KDSGSQV
751 800
eg....sask .l...d.e.. e..le.d.e. ..l.....s. ..a.....
A DATIAWEASP AQESLEVMAQ EASLEAELEA VYLTQQAQST GSAPVAPDEF
B EGHSYFSSTK TLCVIDPENR DSLGETDID. ..IATEDKSP VDT.....
C EGEETALAKE ALELPDTELL SPEAGPDPGD LPLDNQRT.. .....
D EEDTSCSDSK TLCTQDSEST EIPLDEQVEE EAVGEEEESQ PEACVIDDRS
801 850
....
A SSREEFVVAV SHSSPSALAL QSPLLPAWRT LSVSEHAPGL PGLPSTAAEV
B ....
C ....
D PDT..... ....
851 890
....
A EAQREHQAAK RACSACAGTF GEDTSALPAP GGGGSGGDPT
B ....
C ....
D ....

Boundaries of conserved sequences (numbers refer to HSPDE4A4)

	position	% amino acid identity
A/C UCR	30-50	87
UCR1	141-200	73
UCR2	224-302	70
Catalytic	332-688	74

Figure 1.7.c. Alignment of PDE4A-D

PDE4 isoforms HSPDE4A4, HSPDE4B1, HSPDE4C1 and HSPDE4D3 were aligned on the GCG PILEUP multiple alignment software, using the default settings. HSPDE4A4 and HSPDE4C1 were chosen to present their conserved splice variant specific sequence. The other two cDNAs are arbitrarily chosen 'long' forms for the PDE4B and PDE4D genes. A/C UCR, UCR1 and UCR2 are labelled and underlined. The box provides information on the conservation of these sequence modules, with numbering for HSPDE4A4.

1.7.1. Genomic organisation of PDE4/dunce

The existence of alternatively spliced transcripts from PDE4/dunce genes suggests that the genomic structure of these genes will be complex (Figure 1.7 a,b). This is most conspicuously so in drosophila where the exons are dispersed in >135Kb of genomic sequence and where there are more than three genes contained within dunce introns (92). In terms of mammalian genes, partial genomic sequences for the rat PDE4B (94) and PDE4D genes (94,95) define in genomic sequence the extent of the 'short' forms in the gene and some promoter sequence. More recently a study has mapped the organisation of genomic sequences for 'long' forms for PDE4A (82). Nevertheless virtually all PDE4 promoter sequence remain uncharacterised. Isolation of such 5' regulatory regions of the PDE4 genes will allow analysis of the transcriptional regulation of these genes. Pertinent to this thesis, a final important point is that without exception all splice variant specific coding sequence is found together in the genomic sequence, virtually always on a single exon.

1.7.2. Primary structure of the PDE4/dunce enzymes

Analysis of the primary amino acid structure of dunce and PDE4 isoforms, deduced from the nucleotide sequences of their respective cDNAs, has revealed several highly conserved domains (19,68,96,97). The core catalytic unit is similar to all other PDE enzyme classes (97). Houslay et al attempted to map the ends of the PDE4 catalytic domain by compiling a list of all known PDE4 truncation mutants and attempting to identify the minimum requisite sequence for catalytic activity (19). The mammalian PDE4 putative catalytic domain is well conserved at its extreme N-terminal, starting at methionine 332 (MSQIT.... numbering for HSPDE4A4). However, PDE4 sequence immediately downstream of this domain is not well conserved. Furthermore, the MSQIT... motif is not essential for catalytic activity because some truncation mutants retain activity without it (19). Thus it is possible that the true PDE4 catalytic domain starts further downstream. In chapter 5 of this thesis I present some more experimental data which supports these findings.

There are two other highly conserved domains which are found further

towards the N-terminal of the catalytic region. These have been designated UCR1 and UCR2 (for Upstream Conserved Regions 1 and 2) (Figure 1.7a-c) (68). A third domain (A/C UCR in figure 1.7.c) is conserved only between PDE4A and PDE4C, found upstream of UCR1. UCR1-2 and the catalytic sequence are strongly conserved among the mammalian PDE4 isoforms, showing greater than 70% sequence identity. UCR1 is a region of ~55 residues, the first half of which is polar and the second half hydrophobic. UCR2 is a hydrophilic region of ~76 residues. The functions of UCR1 and UCR2 are not fully understood. It has been reported that they can bind to each other and suggested that this might be under dynamic regulation by phosphorylation (19). Together with the observations that PDE4 N-termini appear to alter the activity of the PDE, it has been proposed that changes in UCR1/UCR2 conformation might in turn alter the conformation of the catalytic domain either by direct interaction or by transmission of the conformational change through LR2 (see below)(19). Consistent with there being modular roles for UCR1 and UCR2 the second splice junction occurs between UCR1 and 2 and thus 'long' forms contain both UCR1 and UCR2 whereas 'short' forms delete the entire UCR1 region.

UCR1 is separated from UCR2 by LR1 (Linker Region 1) which consists of ~33 residues which show no homology between isoforms. UCR2 is in turn separated from the start of the catalytic domain by LR2 (Linker Region 2) whose length varies according to the PDE4 gene (9-34 amino acids). LR2 contains some regions of sequence, such as a proline rich region in PDE4A which are not conserved between the PDE4 genes. If LR2 does serve to transmit conformational changes in UCR1/UCR2 to the catalytic domain it is clear that gene specific regulations may be located in these sequences (19). In chapter 5 of this thesis it is shown that the N-terminal of LR2 is highly conserved in a subset of PDE4 isoforms. The significance of this is then discussed.

As well as conserved regions, various PDE4/dunce isoforms have unique regions of sequence found at their extreme N-termini, generated by alternative RNA splicing. These alter the function of specific isoforms as described below (98). In contrast, the C-terminal of PDE4 is conserved in all functional forms generated by a

particular PDE4 gene and this has enabled gene-specific antisera to be raised that are able to detect all full-length splice variants of a gene (99-102). When analysed by immunoblotting, virtually all PDE4 forms migrate more slowly than would be expected for their calculated molecular weight on the basis of their primary structure. The reason for this aberrant migration remains obscure but as with PDE3 may be due to positively charged runs of amino acid residues towards the C-terminal of the catalytic domain.

1.7.3. Drosophila *dunce*

The *dunce* mutation of *drosophila melanogaster* was the first gene isolated that specifically affected behaviour (103). At least three protein products are coded for by at least six alternatively spliced RNA transcripts. Flies with mutations in *dunce* have a complex phenotype which can include female sterility and deficits in learning and short-term memory (104). Biochemical analysis of brain extracts from *dunce* flies and subsequent studies on the dunce cDNA demonstrated that the *dunce* mutation effects the activity of a cAMP phosphodiesterase activity with properties similar to that of cyclic AMP specific mammalian PDEs (105-107), which is now unsurprising given their sequence conservation. Indeed defects in learning and memory in *dunce* flies are rescued by the overexpression of a mammalian PDE4 cDNA in drosophila (108). Nevertheless the dunce PDE is not inhibited by two mammalian PDE4 inhibitors, rolipram or Ro-20-1724. The structural reason for this remains obscure.

Analysis of *dunce* mutants has provided clues to the possible functions of the mammalian PDE4s (107). The ease and speed of genetic manipulation of drosophila (such as gene-knockout, mutational interactions) and behavioural analyses makes it an attractive system for genetic studies. Such techniques have been used to study participants in developmental pathways that modify the dunce phenotype of abnormal synaptic plasticity (107,109). As well as expected interactions with drosphila adenylyl cyclase (*rutabaga*) and PKA (*DCO*) mutations, unanticipated interactions such as that with the poorly characterised *stoned* cistronic locus are more intriguing (109). Splice variant specific exon knock-outs have allowed the individual contributions of each

splice variant to the short-term memory/learning /female sterility *dunce* phenotype to be dissected, the first demonstration of different physiological roles for different PDE splice variants (93). This is a promising precedent for studies on mammalian PDE4 splice variant sequences that seek to implicate these regions in spatio-temporal partitioning of the cAMP signal. Regrettably this system can tell us little about the roles of mammalian splice variants because little splice variant sequence is conserved between mammals and drosphila. Similar analyses in mouse will be a considerable undertaking.

1.7.4. A survey of the splicing complexity and distribution of PDE4A transcripts.

Before the work in this thesis there has been only one PDE4A splice variant for which both the human and rat homologues have been identified. This is the 'long' form HPDE46 (HSPDE4A4) and its rat homologue RPDE6 (RNPDE4A5). However this statement is unlikely to reflect the true complexity of splicing of this gene. There is evidence for two further rat and two further human splice variants, none of which are homologous to each other. RD1(RNPDE4A1) (65,76) and RPDE39 (RNPDE4A8) (77) encode, respectively, a 'short' form and a 'long' form of PDE4A. TM3 (HSPDE4A5) (68) cDNA apparently codes for a 'long' form of PDE4A though the sequence has two mismatches, three frameshifts and two larger insertions when compared to other PDE4A sequences. The existence of the unique 5' TM3 exon in PDE4A genomic sequence is nevertheless highly persuasive that a cDNA closely resembling TM3 may be transcribed (82). 2EL (HSPDE4A8A) (70,71) is a non catalytic 'short' form of PDE4A. The PDE4A 'short' forms RD1 and 2EL both have unique splice sites away from that used by other 'short' PDE4s. Two other splice variants that have been reported in the rat, RD2 (RNPDE4A2) and RD3 (RNPDE4A3) are reportedly cloning artefacts (68,76). The unique N-terminal of RD2 is spliced into the middle of an exon at a site which does not contain a consensus splice site (82). Neither of these splice variants' expression has ever been detected.

In chapters 5 and 6 of this thesis evidence is presented which adds two new

members to the list of PDE4A splice variants for which human and rat homologues have been identified

1.7.4.1. RD1 RNPDE4A1: a membrane targetted, selectively expressed phosphodiesterase.

This was the first mammalian dunce homologue to be cloned (66). Its expression is restricted to several regions of the brain (66,76,102). It has a 21 amino acid 5' exon spliced at a unique splice junction into the middle of UCR2. The first definitive evidence that alternative splicing can alter PDE enzyme properties (110,111) came from work on this splice variant. Whilst the genetic analyses of *dunce* splice variants are certainly consistent with alternative splicing leading to proteins with different properties, these results could still notionally be due simply to different promoters causing altered expression than to altered properties of the proteins themselves.

The initial studies with RD1 showed that transient expression of this isoform in COS1 cells led to the vast majority of novel PDE4 activity being found in the (high speed) particulate fraction, whereas transient expression of a recombinant PDE4A truncated form met^{26}RD1, resulted in a cytosolic location (110). Subsequent immunological detection demonstrated (112) that RD1 was exclusively associated with the membrane fraction, because the cytosolic PDE4 activity found following RD1 transfection was met^{26}RD1, apparently expressed following aberrant initiation due to a sub-optimal Kozak sequence and the use of a strong promoter. Since met^{26}RD1 is identical to RD1, apart from the unique RD1 N-terminal sequence, this N-terminal region was clearly implicated in determining membrane targeting of this splice variant. Such a notion was confirmed by conferring membrane targeting identical to RD1 on the soluble bacterial protein chloramphenicol acetyl transferase (CAT) simply by fusing this CAT to the N-terminal 25 amino acids of RD1 (111). Other segments of RD1 were unable to mimic this. As these experiments were carried out using an *in vitro* transcription/translation method, it is highly unlikely that RD1 membrane association is due to direct insertion since this is a co-translational phenomenon. Furthermore, in studies done on intact cells, then no evidence of lipid acylation of

RD1 was found, excluding such a means for membrane association (102). Deletion mutagenesis has also been done to segments of unique N-terminal RD1 structure. Deletion of the first 13 amino acids still allowed membrane association In contrast, deletion of the hydrophobic motif PWLVGWW obliterates membrane association, clearly implicating this sequence as having a key role in membrane association (113,114). Structural studies are consistent with the downstream DQFKR supporting this role (discussed below) (114).

The ^{1}H-NMR derived structure of the unique N-terminal region of RD1 has now been deduced (114). It forms two independently folding helical regions separated by a mobile 'hinge' region, Cys^{11}-Pro^{14}. An amphipathic α-helical region extends from Leu^{3}-Cys^{11}, with non-polar residues Leu^{3}, Ala^{4}, Phe^{6} and Phe^{7} found along one side of the helix. The second helical region, extending from Pro^{14}-Lys^{24}, has a distorted backbone due to the large hydrophobic residues in the motif (PWLVGWWDQFK). This irregular helix allows the rings of Pro^{14} and Trp^{15} to stack and thus the three large tryptophan rings in this domain spread out more evenly over the helical cylinder than might be expected normally, allowing Leu^{16} to form interactions with the side chains of all three tryptophans. The same interactions force Val^{17} out into the solvent at the opposite face, making this region a possible site for specific interactions with conformational freedom around both Val^{17} and Gly^{18}. The helix is apparently stabilised by an ion-pair between Asp^{21} and Lys^{24}. Nevertheless it is not clear how this domain might allow association with biological membranes and this has led to a search for RD-1 binding which might contain direct membrane binding domains (19). The nature of this species has yet to be determined. However, the ubiquitous membrane-association of native RD1 (102) and ectopically expressed RD1 in COS-1 cells (110), FTC133 cells (115) or FTC 236 cells (115) suggests that the anchor protein, or related proteins are ubiquitously expressed.

The notion that interaction of RD1 with its anchor protein may be mediated via hydrophobic interactions involving the tryptophan rich Pro^{14}-Trp^{20} motif is also consistent with solubilisation studies. These show that though RD1 is resistant to solubilisation by repeated washing or high ionic strength, it is readily susceptible to

release by very low concentrations of the non-ionic detergent Triton X-100. These concentrations are much lower than are needed to solubilise integral membrane proteins from lipid bilayers. In contrast, hydrophobic protein-protein interactions between RD1 and its putative anchor protein might easily be disturbed by such treatment.

Such a model of interaction predicts that evolutionary conservation of RD1 N-terminal sequence will be very high since sequence requirements for membrane insertion are far less stringent than for molecular recognition. That is, to be consistent with the proposed membrane association model of RD1, putative homologues of RD1 would be expected to be highly conserved in their membrane-associating N-termini. In chapter 5 of this thesis the evolutionary conservation of the putative membrane association domain of RD1 is directly analysed.

1.7.4.2. HPDE46/RPDE6

The conserved 'long' PDE isoform RPDE6 and its human homologue HPDE46 have a unique N-terminal splice region of ~110 residues. RPDE6 expression is located in many regions of the brain, including hippocampus, striatum, cortex and hypothalamus (112). Both native RPDE6 and transfected recombinant RPDE6/HPDE46 are found in soluble, low speed particulate and high speed particulate fractions of the cell (100,112). The particulate fractions are unsusceptible to solubilization with detergent or high ionic strength, implying a strong interaction with cytoskeletal components (100,112). This distribution is very different from that of RD1 (110,112) (see section 1.7.4.1), which is consistent with these differences being due to the divergent N-termini. HPDE46 localisation has also been visualised by confocal microscopy and this confirmed the earlier findings in that both cytosolic and particulate HPDE46 were identified (100). Both PDE46 and RPDE6 immunoreactivity in transfected COS cells was concentrated in foci on the margins of the cells which are enriched in specialised cytoskeletal structures. As well as this there is a more diffuse cytosolic localisation. As is the case with RD1 the determinants of the intracellular targeting are harboured in the N-terminal splice regions. Thus, the 'core' rat and

human PDE4A species met[26]RD1 and h6.1 respectively are exclusively cytosolic with a uniform, diffuse distribution (100,102)

The mechanism(s) by which HPDE46 and RPDE6 interacts with particulate fractions of the cell has not been fully characterised. Proteins are often recruited to intracellular surfaces by specific molecular recognition mediated by compact globular protein modules such as PH (pleckstrin homology), PTB (phospho-tyrosine binding), SH2 (src homology 2) and SH3 (src homology 3) domains which are integrated into many signalling proteins. An example of this is the Grb2-SOS interaction in the MAP kinase cascade and in PI 3-kinase subunit heterodimerisation. SH3 domains are unique amongst these motifs in that their recognition is exclusively based on primary protein sequence (rather than phosphorylation state of proteins or lipids for the other domains). SH3 domains interact with other proteins containing proline-rich motifs with a minimal PXXP motif which forms into a distorted 3_{10} helix. Arginines are also often found in these motifs. RPDE6 and PDE46 contain several arginine/PXXP motifs within the N-terminal splice region and LR2. RPDE6 has now been shown to interact with certain SH3 domains fused to GST (116), with a specificity indicated for SH3 domains from cytoskeletal proteins such as fodrin and cortactin and also with SH3 domains from tyrosyl kinases such as fyn, lyn and src. The physiological effects of these interactions is not known but it is clear that they could regulate not only the targeting of the PDE but also conformational changes discussed in section 1.8.1.1.

Other rat PDE4As including the 'core' species met[26]RD1 and the 'long' form RPDE39 do not interact with SH3 domains which suggests that these interactions are conferred by the N-terminus of RPDE6, not LR2. However, as discussed in chapter 5, rodent LR2s are markedly different from other PDE4A LR2 sequences and these differences include the proline rich domain which might be used in other PDE4As and might thus explain observed differences in the properties of HPDE46 and RPDE6

1.7.4.3. RPDE39

RPDE39 is the second reported 'long' form from the rat (77). It has a unique N-terminal splice region of 21 residues. The subcellular distribution of native and

recombinant RPDE39 is similar to that of RPDE6/HPDE46 in that it is located in all (S2, P2 and P1) fractions and is resistant to solubilisation with non-ionic detergent, again implying an interaction with cytoskeletal components. However, unlike the cellular distribution of RPDE6, RPDE39 appears to be highly restricted, to date having been detected only in testis.

1.7.5. A survey of the splicing complexity and distribution of PDE4B transcripts.

To date, three PDE4B splice variants have been isolated which are expressed in human and rat. These are 1) the 'long' form TM72 (HSPDE4B1) (68) and a truncated clone DPD (RNPDE4B1) (66), 2) the 'short' form PDE32 (68) /HPB106 (HSPDE4B2) (79) and rat PDE4 (67) and 3) the 'long' form HSPDE4B3 and rPDE74 (RNPDE4B3) (90). Little work has been done on the subcellular localisation of isoforms generated from the PDE4B gene. Immunological analyses done on rat brain extracts (101), using a PDE4B generic antisera, indicated the presence of both particulate and cytosolic forms. These implied that the PDE4B isoform PDE-4 was exclusively membrane associated and DPD cytosolic. However, when the three human PDE4 splice variants were expressed in COS-7 cells they all showed similar distributions between the particulate (~20%) and cytosol fractions (19,90).

PDE4B transcripts have been detected in brain, liver, lung, kidney, heart and blood (117,118). PDE4B1/3 brain expression, as measured by immunoblotting, is most abundant in the hypothalamus, cortex, , cerebellum and brain stem, whereas PDE4B2 is most abundant in cerebellum, hippocampus, striatum, cortex and hypothalamus (101).

1.7.6. A survey of the splicing complexity and distribution of PDE4C transcripts

PDE4C is the least characterised gene in the PDE4 family. Only one splice variant has been isolated with homologues in both human (HSPDE4C1 (85)) /HSPDE4C4 (91) and rat (RNPDE4C1) (76) to date, and it is possible that none of

these reflect the full open reading frame of the native protein, since HSPDE4C4 and RNPDE4C1 are incomplete reading frames and HSPDE4C1 apparently contains artefacts of cloning (85,91). HSPDE4C2 is a 'long' form which does not encode any novel amino acid sequence and HSPDE4C3 encodes a 'long' form with a reading frame open at the 5' end. HSPDE4C5 resembles HSPDE4C4 with three insertions of sequence which are not found in other PDE4 sequences. In contrast HSPDE4C6 and catalytically inactive HSPDE4C7 omit sequences found in the other PDE4 sequences.

None of the proteins encoded by any of these PDE4C splice variants, nor even endogenous PDE4C have been detected by immunoblotting and thus it is not possible to size-match the endogenous and recombinant forms as has been done for splice variants of the other PDE4 genes. HSPDE4C4, HSPDE4C5 and HSPDE4C7 have been detected as transcripts in RNA from a number of cell lines, in contrast HSPDE4C6 expression is restricted to testis (91). Generic PDE4C expression has been the subject of a number of studies. Such expression is detected in U-87 cells (78), melanoma G361, fetal lung, skeletal muscle, testis (91), brain, liver, lung, kidney, heart (117,118)

1.7.7. A survey of the splicing complexity, expression and subcellular distribution of PDE4D transcripts.

To date, three PDE4D splice variants have been identified in both human and rat. These are 1) the 'short' form Dun 11 (HSPDE4D1) (86,87) and ratPDE3.1/RPDE13 (RNPDE4D1) (67,76) 2) the 'short' form PDE82 (HSPDE4D2) (86,87) and ratPDE3.2 (RNPDE4D2) (73), 3) the 'long' form PDE43 (HSPDE4D1) and ratPDE3.3 (RNPDE4D3). Two other clones have been isolated for the human PDE4D gene. These are PDE39 (HSPDE4D4) and PDE79 (HSPDE4D5). The PDE79 reading frame is open at the 5' end.

1.7.7.1 Expression patterns and subcellular localisation of PDE4Ds

The 'short' forms RNPDE4D1 and RNPDE4D2 are expressed in sertoli cells (67,88,89) but only RNPDE4D1 is found in heart tissue (94). RNPDE4D3 is found in

the brain and FRTL-5 cell line (88,89,119). PDE4D4 was identified in rat brain cDNA(68). PDE4D forms are widely expressed in the brain (118).

Transient expression of all five human PDE4D isoforms has allowed their subcellular localisation to be examined (87). These studies demonstrated that PDE4D1 and PDE4D2 are cytosolic isoforms (For PDE4D1 ≥93% of its activity being found in the high speed supernatant fraction). In contrast to these 'short' form HSPDE4D gene products, the three 'long' forms, HSPDE4D3-5 were all partially particulate, though the degree of this varied. The molecular basis of these differences is obscure but nevertheless this data does show that as with PDE4A spliceforms, the unique N-termini clearly can alter the localisation of the PDE. No study has yet examined subcellular localisation of native PDE4D

Studies examining the solubilisation of PDE4D have also been undertaken. PDE4D3 and PDE4D5 are sensitive to solubilisation with detergent whereas only PDE4D5 is sensitive to solubilisation with high ionic strength. All three of the long PDE4D forms were completely solubilised by both such treatments combined. Such data indicate differences in the mode of anchorage of these long PDE4D isoforms and further imply that alternative mRNA splicing of the PDE4D gene produces protein products capable of different intracellular targeting.

1.8 EVIDENCE FOR DISTINCT CONFORMERS OF PDE4: REGULATION OF PDE4 CATALYTIC ACTIVITY

PDE4 enzymes specifically hydrolyse cAMP with a K_m for cAMP of between 1-5μM. This value is rarely altered in an isoform. PDE4 activity however, has been shown to be stimulated by an increase in the V_{max} following treatment with a number of extracellular stimuli including insulin (120) and TSH (88,119). The mediators which transduce these signals appear to include amongst others, kinases, phosphatidic acid and metal ions. It has been proposed that these regulate PDE4 by altering the conformation of the protein in some way (19). Initial evidence for the existence of PDE4 conformers arose from analysis of complex kinetics of cAMP hydrolysis in an uncharacterised PDE4 species in hepatocytes. This PDE exhibited a downwardly

curving Lineweaver-Burke (double reciprocal) plot. Such plots are consistent with PDE4 enzymes existing in an equilibrium between two states which bind substrate to produce a single conformer but that this, following product dissociation, releases the enzyme in only one of the original conformations, thus disturbing the equilibrium. This is the mnemonical mechanism (121) where one state of the enzyme is remembered following catalysis. If the rate constants for binding of substrate are different between the two forms then Lineweaver-Burke plots will be non-linear with either apparent negative or positive co-operativity. Conformers in a mnemonical mechanism may also have different affinities for rolipram, offering one possible explanation for the complex, apparently negatively co-operative kinetics seen in a number of PDE4 isoforms when expressed in certain cell backgrounds (see next section).

1.8.1. Inhibition of PDE4 by rolipram

Rolipram is a specific inhibitor of PDE4 isoforms. Though rolipram has anti-depressant properties, it is not used in clinical intervention. However, this compound remains of interest because it has been proposed that both its variety in its potency as an inhibitor against PDE4 and its binding affinity (19,122) may be due to the compound 'sensing' shifts in PDE4 conformation. Whatever the molecular basis of these differences (discussed below) a range of studies have shown that functional responses to rolipram correlate with either low or high binding affinity (122) and that therefore further understanding of these conformational shifts will allow production of more specific inhibitors.

1.8.1.1. Rolipram as a sensor of conformational shifts

Binding studies on brain and some other (but by no means all) tissues have identified high affinity rolipram binding sites (with K_a values in the low nM range) (122-125). These bind rolipram far more avidly than is implied by PDE4 inhibition analyses (where the IC_{50} is typically 0.1-10μM) (68,77,78,122-129). Binding is also stereoselective, with the enantiomer R-(-)-rolipram around 20 fold more potent than S-

(+)-rolipram (124). This also contrasts with rolipram inhibition of PDE activity where stereoselectivity varies (122,123,125)

The identity of the native high affinity rolipram binding site is not known. However, expression of a truncated PDE4A species in *saccharomyces cerevisiae* confers high affinity rolipram binding on homogenates from these transfected cells, indicating that PDE4 may harbour these sites (130). Interestingly, this PDE simultaneously displayed complex kinetics which diverged from linear Lineweaver-Burke plots. Instead downwardly curving double reciprocal plots of activity versus cAMP concentration were described. Aberrant kinetics such as these can arise in various ways including partial competitive inhibition, apparent negative co-operativity and multiple enzyme components differing in inhibitor sensitivity (see below) (75,130). It has been suggested that these complex kinetics may account for the apparent anomaly between directly measured rolipram binding affinity and the affinity inferred from analysis of inhibition kinetics (19). Similar kinetics have been identified when this construct is expressed in COS-1 cells (129) but, despite this, analysis of a similar N-terminally truncated PDE4A construct expressed in a second strain of *saccharomyces cerevisiae,* or in COS-7 cells, yields simple competitive inhibition by rolipram (126).

Fractionation of COS-7 cells overexpressing PDE46 (HSPDE4A4) yielded (100) two enzyme populations with similar K_m for cAMP. Cytosolic PDE4 activity observed (100) simple competitive kinetics of rolipram inhibition whereas that in the particulate fraction gave complex kinetics of a similar type to that reported by Torphy (75,130) and by Owens (129). A possible explanation for this is that PDE46 exists in two interconvertible states (122,130,131). In this case rolipram is a sensitive monitor of the different conformations of these two enzyme forms. The molecular basis of this remains unidentified but regardless of this, the finding that HPDE46 can exist in two kinetically distinguishable states indicates that there must be a means through which the conformation of this enzyme can be altered. Intriguingly, identical experiments (100) to those just described for HPDE46, done on the rat homologue RPDE6 (RNPDE4A5), identified only one state with simple kinetics. This implies that

sequence found only in HPDE46 may be necessary for multi-state switching. In chapter 5 of this thesis, analysis of novel PDE4A sequence identifies new candidates for this sequence in LR2 and the N-terminal of the catalytic domain.

1.8.1.2. The different conformations of PDE4 are associated with different signalling processes.

Rolipram and other specific inhibitors of PDE4 are powerful tools for establishing the cellular signals that PDE participates in and the pathologies associated with these signals (reviewed in (19)). The deduction that some of these inhibitors can sense conformational changes has allowed examination of the relative importance of these two conformations in a number of signalling processes that involve PDE4. Most of the CNS effects, which include emesis (132) and certain of the peripheral effects of rolipram, including bronchodilation correlate with PDE4 which has a high affinity for rolipram (122). However certain other peripheral effects correlate more closely with the PDE4 conformer which has a low affinity for rolipram. An example is suppression of TNFα generation. This protein is produced in a number of auto-immune disease states and its suppression can ameliorate symptoms. Souness et al showed that inhibition of PDE4 could suppress TNFα generation and that the effective concentrations of PDE4 inhibitors correlated more closely with low-affinity binding to PDE4 (133). The observed lack of rolipram stereoselectivity for TNFα suppression was also consistent with this notion. Similar results were obtained in suppression of a bacterial endotoxin induced release of the proliferative cytokine interleukin-2 (IL-2) in murine splenocytes. Thus, suppression correlated with rolipram inhibition of a low affinity PDE4 conformer with little stereoselectivity between rolipram enantiomers (134). Clearly, inhibitors which are specific for the low affinity conformer might be able to dissociate therapeutic effects from the undesirable side effects (such as emesis) associated with the high affinity conformer in the CNS. Thus, identification of sequences which participate in conformational shifts of PDE4 could have long-term implications for design of new therapeutics.

1.8.2. Regulation of PDE4 by vanadyl-glutathione treatment

Vanadyl-glutathione complexes (135,136) have been shown to activate an undefined PDE4 activity. This led, simultaneously, to a pronounced increase in the affinity for rolipram. In guinea-pig eosinophil membranes (123) vanadyl-glutathione treatment both increased the sensitivity of the PDE4 activity in this fraction to inhibition by rolipram and also generated high affinity rolipram binding sites. It has been speculated that thiol group modification mimics the molecular switch postulated for HSPDE4A4 and PDE4D3 (see below) and that this conformational change results in the accumulation of a conformation of a PDE4 species which is sensed by its elevated affinity for rolipram.

1.8.3. Regulation of PDE4 activity by phosphorylation

Phosphorylation sites have been analysed on the PDE4D3 (19,88,89,137) isoform and the HSPDE4B2 isoform (138). However, for the latter there is no information on the effects that this phosphorylation may have on function. There are several other less well characterised examples of PDE activities being stimulated by phosphorylation (reviewed in (19))

1.8.3.1. Regulation of PDE4D3 by phosphorylation.

Thyroid hormone (TSH) treatment of FRTL-5 thyroid cells has been shown to cause a rapid and transient elevation of intracellular cAMP levels (88,89). The transience of this response is due, at least in part, to the very rapid increase in PDE4D3 activity which can be seen within 3 min of TSH application and which returns to basal levels after ~15 min (88,89). It has been shown that native PDE4D3, and that overexpressed in Sf9 or MA10 cells ., can be phosphorylated by protein kinase A (PKA) (88,89,119,137,139). This apparently occurs at serine 54 in the UCR1 region of this isoform within a sequence motif found in common with all other PDE4 'long' forms (137). PKA-mediated phosphorylation of PDE4D3 brings about a 2 fold increase in enzyme activity and a much reduced sensitivity to stimulation by magnesium. Interestingly, such PDE4D3 shows aberrant rolipram kinetics similar to

those already described for PKA phosphorylated HSPDE4A4. The dose-response plot of rolipram inhibition implied the presence of two distinct populations of the enzyme exhibiting IC_{50} values of ~10μM and ~2μM for inhibition by rolipram. Treatment of recombinant PDE4D3 with PKA or challenge of the cells with agents which increase the concentration of cAMP appear only to be able to increase the activity of the high affinity component. This is a further indication that rolipram may be able to sense different PDE4 conformations. As with HSPDE4A4, the K_m for cAMP was unaffected (137). Again, these data indicate that PDE4 species can exist in two conformationally distinct states which can be sensed by rolipram binding affinity but in this case, the high affinity state has an identified functional correlate in that it is activated by PKA. It is not yet known whether the other PDE4 'long' isoforms can be activated by PKA phosphorylation on the conserved serine nor whether this regulation will be hierarchical in the way that it seems to be for PDE4D3.

1.8.4. Regulation of PDE4 activity by phosphatidic acid

Stimulation of lipid signalling pathways results in an elevation of the levels of plasma membrane phosphatidic acid (PA), for example following activation of inflammatory cells (59) This has been shown to cause the activation of thymocyte PDE4 activity (59). Subsequently a similar activation was seen in the PDE4 activity from U937 cells which could be activated ~2-fold by phosphatidic acid (140). Recently it has been shown that PDE4D3 and PDE4A5 are stimulated about 2 fold by PA (141). The effect on PDE4D3 resembles that of serine 54 phosphorylation in a number of ways. First, both the activation and binding of PA seen only in the 'long' form PDE4D3, not PDE4D1 or PDE4D2 which do not share the region (141), consistent with this phenomenon targeting the N-terminal of the protein. Second, PA treatment reduces the EC50 for Mg^{2+} in the same way that phosphorylation does (137,141). Finally, the PA-mediated enzyme activation of about 2-fold and the unchanged K_m for cAMP are very similar to the profile observed following PDE4D3 phosphorylation.

1.9 cGMP SPECIFIC PDE5

Within the PDE gene superfamily cGMP specific PDE5 gene is most homologous to PDE6. Only one PDE5 gene has been isolated to date. PDE5 protein has a molecular weight of ~178 kDa, indicating, by comparison with the cDNA, that the protein is expressed as a homodimer (142-144). In common with PDE6 and the more distantly related cAMP specific PDE2, PDE5 possesses a cGMP binding domain beyond the catalytic domain. Binding of cGMP to this site induces a conformational change within the N-terminal which then enables serine-92 to become a target for phosphorylation by PKG (143,144). The functional significance of these cGMP induced changes has not been elucidated.

Zinc, which binds tightly to PDE5, is necessary for its catalytic activity (145). Two zinc binding motifs have been identified in the primary sequence of the PDE5 catalytic domain. These sites are conserved in all mammalian PDEs.

The physiological roles of PDE5 are not well understood. The PDE5 selective inhibitor zaprinast, has been used to suggest a role for this PDE in modulating the effect of ANP on renal homeostasis. Thus, zaprinast treatment results in extensive loss of sodium and diuresis even under conditions of low blood volume and pressure (146,147). PDE5 inhibitors are also now used in the treatment of impotence (148).

1.10 PDE6 PHOTORECEPTOR cGMP SPECIFIC GENE FAMILY

B and

PDE6 shows most homology with PDE5 (see figure 1.2).

The PDE6 enzyme complex is composed of catalytic (α, PDE6A; α_1, PDE6C and β, PDE6B) and inhibitory gamma subunits. PDE6A and PDE6B are found in rod membranes where they form heterotetramers with two inhibitory gamma subunits. PDE6C is found in cone outer segments (12). It is not known what the stoichiometry of this enzyme complex is.

Relative to the other PDE families, the physiological role of PDE6 is well understood (see review (149)). In visual excitation, absorption of a photon by the receptor rhodopsin, leads to dissociation of the α-G subunit of the photoreceptor

coupled heterotrimeric G-protein transducin. The α-G subunit then relieves the inhibition of the PDE6 gamma subunit to liberate active PDE6. The effect of PDE6 stimulation is to rapidly and transiently decrease cGMP levels which results in closure of a cGMP gated sodium channel which in turn causes a hyperpolarisation signal to occur. All PDE6 forms contain a high affinity noncatalytic binding site for cGMP. It is thought that the cGMP binding sites in PDE6 allow modulation of the duration of PDE6 activation by transducin (12).

1.11 PDE7 IBMX INSENSITIVE PDE

Virtually all PDEs are sensitive to the non-specific phosphodiesterase inhibitor, isobutylmethylxanthine (IBMX). However, IBMX-insensitive, cAMP-specific phosphodiesterase species have been identified in both hepatocyte and liver preparations (150). More recently cDNAs have been identified which encode PDEs which show just such an insensitivity to IBMX (151,152). These cDNAs most likely reflect splice variants of the one which has been identified as PDE7A. Of the other members of the PDE gene superfamily, the PDE7 gene is most closely related to the PDE4 genes (see figure 1.2). However, beyond their insensitivity to IBMX little is known about the PDE7 isoforms, which are widely expressed, with the highest expression being in skeletal muscle (151). The earlier report does suggest that PDE7 may be insensitive to simulation by Mg^{2+} (150)

1.12 The polymerase chain reaction (PCR)

The polymerase chain reaction is a robust method for amplifying known or unknown sequence held between two known pieces of sequence from which template-specific amplification can be primed (X and Y in figure 1.13). This technique is used routinely in a variety of molecular biological protocols, which include analysis of RNA populations and design of recombinant constructs, which are both methods employed in this thesis.

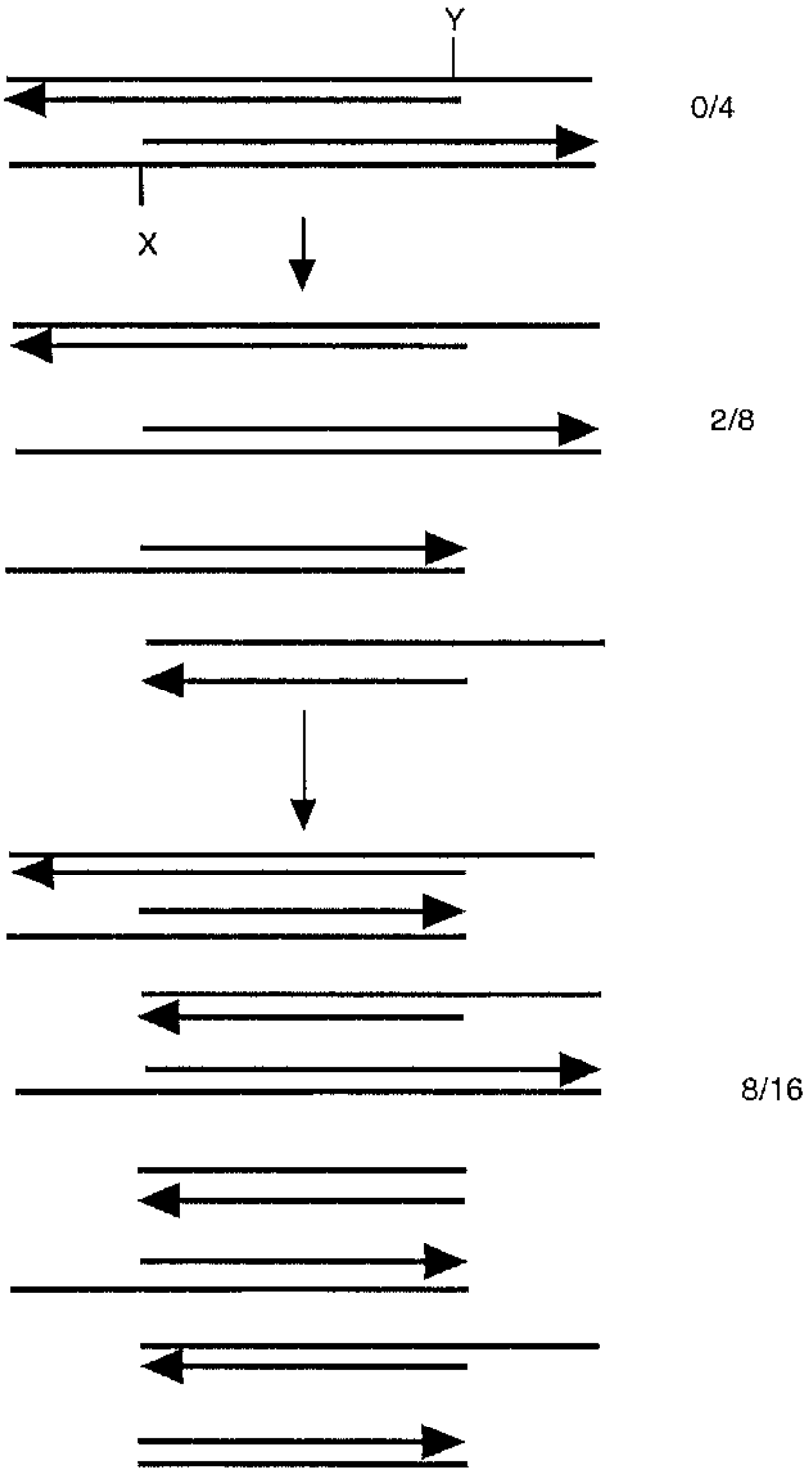

Figure 1.12 The polymerase chain reaction (PCR)

Repeated cycles of DNA polymerisation (lines with arrows) from opposed sense (X) and antisense (Y) primers results in a chain reaction amplification such that in only two cycles a single length of DNA is produced which accounts for half of the DNA molecules in the reaction mixture. After ~30 cycles this DNA molecule is virtually the only amplification product and it is usually detectable following gel electrophoresis of the reaction products.

1.12.1 Isolation of novel gene sequence by PCR: Rapid Amplification of cDNA ends (RACE)

Probing of cDNA libraries remains the major method for isolating new genes. However, cDNAs isolated from conventional dT primed libraries and even those primed with random hexamers are often incomplete. This promises to be a major bottleneck in projects that plan to sequence all human genes. As a result a number of PCR based methodologies have arisen to take over isolation of the remaining sequence following the initial cDNA library screen. Though standard RT-PCR is able readily to detect specific RNA transcripts in total RNA extracts, PCR based isolation of sequence beyond the known area of sequence is more problematic. Extra 3' sequence can be isolated by using a sequence specific sense primer with a poly dT primer which anneals to the poly A tracts commonly found at the 3' end of mature RNAs. This is not an option for isolation of extra 5' sequence and so this is even more challenging though the intrinsic topological problem remains identical: because of the uni-directional processivity of DNA synthesis (5' to 3') there must be some known sequence either side of the unknown sequence before the PCR reaction can be used to isolate that unknown sequence. A large number of protocols have arisen, all attempting to tag some known sequence on to the 5' end of the unknown sequence (see below.) (153). Such an approach has been particularly attractive in the PDE4 field (78,90) because each gene is alternatively spliced at the 5' end of a fairly large gene. Both these factors heighten the likelihood that only partial clones will be isolated from cDNA libraries as has repeatedly happened (66-68,74,75,79-81). In chapter 6 of this thesis I have attempted to use such RACE protocols to complete just such a truncated open reading frame.

TdT (terminal deoxynucleotide transferase) RACE and RLM (RNA-ligase mediated) RACE adopt an identical rationale of tagging the end of first strand cDNA and then amplifying the end of the cDNA by PCR with a tag-specific primer and a gene specific primer. The relative merits of these techniques are discussed in more detail in chapter 6. Other methods have arisen for PCR of double stranded DNA where the upstream sequence is unknown (154).

Inverse PCR can also be used to PCR amplify upstream sequence (155,156). The same topological problem as above is here answered by circularising the DNA. This can be efficiently achieved by the action of T4 RNA ligase on single stranded DNA or the action of T4 DNA ligase on double stranded DNA. This DNA circle is then amplified by primers designed to process away from each other on the known piece of sequence into the unknown piece in both directions.

In chapter 6 of this thesis I have tested a variety of PCR based methods for isolating upstream cDNA sequence. I then go on to test a new method that I devised for cloning upstream sequence. This novel method will be applicable to many other kinds of sequencing projects .

2. MATERIALS AND METHODS: BIOCHEMICAL METHODS

Except where mentioned, biochemicals were obtained from Fisons and were of analytical grade.

2.1. STANDARD POLYACRYLAMIDE GEL ELECTROPHORESIS

2.1.1. Buffers

2.1.1.1. Resolving gel buffer (Buffer A):

2M Tris/HCl, pH 8.8

0.4% (w/v) SDS

2.1.1.2. Stacking gel buffer (Buffer B):

0.5M Tris/HCl, pH 6.8

0.4% (w/v) SDS

2.1.1.3. Acrylamide mix:

30% (w/v)acrylamide N,N'methylenebisacrylamide

29:1 (3.3% cross-linking, Bio-Rad)

2.1.1.4. Resolving gel (8%):

13.9ml	distilled water
7.8ml	Buffer A
8ml	acrylamide mix (BioRad)
300µl	10% ammonium persulphate
18µl	N,N,N',N'-tetramethylethylenediamine (TEMED) (Sigma)

2.1.1.5. Stacking gel:

6.8ml distilled water

1.35ml Buffer B

1.7ml acrylamide mix (BioRad)

100µl 10% ammonium persulphate

10µl TEMED (Sigma)

2.1.1.6 Laemmli buffer (2x):

2.5ml 1M Tris/HCl, pH 6.8

5ml glycerol

8ml 10%(w/v) SDS

3.5ml distilled water

0.007% (w/v) bromophenol blue

1ml β-mercaptoethanol (added prior to use)

2.1.1.7. Electrode buffer:

192mM Glycine

25mM Tris

0. 15% (w/v) SDS

2.1.2. Preparation of Samples

Samples containing no more than 400μg of protein were added to an equal volume of 2x Laemmli buffer (157) and boiled for five minutes.

2.1.3. Protein Molecular Weight Markers

Prestained protein molecular weight markers (Bio-Rad) contain the following proteins: myosin II chain (200kDa); phosphorylase B (97.4kDa); BSA (68kDa); ovalbumin (43kDa); carbonic anhydrase (29kDa); B-lactalbumin (18.4kDa) and lysozyme (14.3kDa). The apparent molecular weights varied from batch to batch and the precise sizes of the proteins are indicated on figures.

2.1.4. Casting and Running of the Gel

Following assembly of the gel apparatus, the resolving gel was poured between the plates and 2ml of water was layered on top. When the gel set, the water was removed, a comb inserted and the stacking gel poured. When the stacking gel set, the comb was removed and the gel placed in a tank containing electrode buffer. The

samples were loaded into the wells and the gels were run at 60mA per gel until the bromophenol blue (in the loading buffer) reached the bottom of the gel.

2.2. POLYACRYLAMIDE GEL ELECTROPHORESIS FOR LOW MOLECULAR WEIGHT PROTEINS

2.2.1. Buffers

Component	Separating gel	Spacer gel	Stacking gel
acrylamide solution (49.5%)	5ml	1.25ml	1ml
gel buffer	5ml	2ml	3.1ml
water	2.5ml	2.75ml	8.4ml
glycerol 80%	2.5ml	-	-
10% APS	75µl	30µl	100µl
TEMED (Sigma)	7.5µl	3µl	10µl

2.2.2. Protein Low Molecular Weight Markers

Pre-stained low molecular weight markers (Sigma) contained differently coloured ovalbumin (yellow, 45kD), carbonic anhydrase (orange, 29kD), trypsin inhibitor (green, 20kD), α-Lactalbumin (purple, 14kD), aprotinin (blue, 6.5kD)

2.2.3. Casting and Running of the Minigel

Following assembly of the gel apparatus (BIO-RAD), the separating gel was poured 4.2cm high and spacer gel was immediately poured on top 1cm high. Water was layered on top. When the gel set, the water was removed, a comb inserted and the stacking gel poured. When this set, the comb was removed and the gel placed in a tank containing electrode buffer. The samples (prepared using Laemmli's loading buffer (157)) were loaded into the wells and the gels were run at 100 volts per gel until the bromophenol blue reached the bottom of the gel.

2.3. WESTERN (IMMUNO) BLOTTING

2.3.1. Buffers

2.3.1.1. Blotting buffer:

192mM glycine

25mM Tris 20% (v/v) methanol 80% (v/v) water

2.3.1.2. Tris buffered saline (TBS):

0.5M NaCl

20mM Tris/HCl, pH 7.4

2.3.2. Transfer to Nitrocellulose

The SDS polyacrylamide gel was placed in a cassette on top of a piece of nitrocellulose paper (Schleicher & Schuell), bound by two pieces of Whatman 3MM paper and two pieces of sponge. The cassette was assembled in a tray of blotting buffer, to exclude air bubbles. It was loaded into the transfer tank with the nitrocellulose side of the cassette towards the positive electrode. The tank was filled with blotting buffer and the proteins transferred for 2 hours at 1A.

2.4 IMMUNO-DETECTION USING ECL

The nitrocellulose was blocked using 5% dried skimmed milk (Marvel) in 100ml of TBS for 2hrs with gentle shaking. It was then washed twice with TBS containing 0.1% Nonidet P40 (NP40) (Calbiochem) for 5 minutes each. Next it was washed twice in TBS for 5 minutes each.

The primary antibody, namely that specific to the protein to be detected, was added in 10ml of TBS & 1% Marvel, sealed in a polythene bag and incubated at room temperature with vigorous shaking for 2hr.

After washing with TBS as described above, secondary antibody was added. This antibody was horse radish peroxidase (HRP) conjugated, directed against the Ig first antibody added. Secondary antibody (SAPU) was added as 40µl in 100ml TBS

plus 1% Marvel and incubated for 1 hour at room temperature with gentle shaking. The nitrocellulose was then washed four times with 100ml TBS for 5 minutes each

The membrane was incubated with ECL (Amersham) reagents as per manufacturers instructions. X-ray film (Fuji) was exposed to the nitrocellulose for 5 seconds to 10 minutes depending on the intensity of the signal. The film was then developed using a Kodak X-omat.

2.5. TRANSFORMATION OF BACTERIA

2.5.1. Medium and buffers

2.5.1.1. LB-medium:

170mM NaCl

0.5% (w/v) Bacto-Yeast Extract

1 % (w/v) Bacto-Tryptone pH 7.5

2.5.1.2. LB-Agar:

170mM NaCl

0.5% (w/v) Bacto-Yeast Extract

1% (w/v) Bacto-Tryptone

2% (w/v) Agar

2.5.1.3. Transformation buffer 1:

100mM RbCl

50mM $MnCl.4H_20$

30mM Potassium acetate

10mM $CaCl_2.2H_20$

15% (w/v) redistilled glycerol

pH 5.8, adjusted with 0.2M acetic acid.

Filter sterilise through a 0.22µ filter.

2.5.1.4.Transformation buffer 2:

10mM RbCl

10mM3-(N-Morpholino)propane sulphonic acid (MOPS)

75mM $CaCl_2.2H_2O$

15% (w/v) redistilled glycerol

pH 6.8, adjusted with 0.2M NaOH. Filter sterilise through a 0.22µ filter.

2.5.2 Procedure: Preparation of Competent E. coli JM109

A 10ml culture of JM 109 E. coli in L-broth was inoculated from a glycerol stock and grown overnight at 37°C with constant shaking. The next day 3ml of this culture was used to seed a 500ml LB medium culture which was grown at 37°C in an orbital shaker (200rpm) until the optical density at 550nm was between 0.5 and 0.55. The culture was divided equally between two sterile 250ml centrifuge bottles and cooled on ice for 30 minutes. They were then centrifuged at 2500rpm (950g) in a Beckman JA14 rotor for 15min and each pellet resuspended in 20ml of ice-cold transformation buffer 1. The cells were incubated on ice for a further 15min before centrifugation at 2500rpm for 10 minutes. The supernatant was removed and the cell pellets gently resuspended in 3.5ml of transformation buffer 2. The resuspended cells were pooled and incubated on ice for 15 minutes. The competent cells were snap-frozen in 250µl aliquots and stored at -80°C.

2.5.3. Transformation

An aliquot of frozen competent cells was thawed slowly on ice. For each transformation a 50µl aliquot of competent cells was transferred to a sterile microcentrifuge tube. To each 50µl, approximately 100ng of DNA was added and incubated on ice for 15mins. The cells were then 'heat shocked' for 60 seconds at 42°C and incubated on ice for a further 1 minute. 1ml of L-broth was then added and the transformed cells incubated at 37°C for 30-60min with shaking. 100µl of the culture was plated on a 10cm agar plate containing selection medium. Transformed colonies were picked and glycerol stocks made (section 2.5.4.)

2.5.4 Glycerol stocks

Single colonies were used to seed a 10ml LB medium culture grown overnight at 37'C. To 750µl of the overnight culture, 250µl of 80% glycerol in L-broth was added and vortexed. Glycerol stock storage was at -80°C.

2.6. PHOSPHODIESTERASE ENZYME ASSAY

Phosphodiesterase activity was measured in a cAMP hydrolysis assay. This used a modification of the two step procedure of Thomson and Appleman (158) and Rutten et al (159), as described previously by Marchmont and Houslay (160). ^{3}H-cyclic nucleotide (8 position of the adenine or guanine ring) was hydrolysed to form labelled nucleotide mono-phosphate. The nucleotide mono-phosphate ring was converted to the corresponding labelled nucleoside by incubation with snake venom which has 5'-nucleotidase activity. The conditions were such that complete conversion takes place within the incubation time. Unhydrolysed cyclic nucleotide was separated from the nucleoside by batch binding of the mixture to Dowex-1-chloride (Sigma). This removes the charged nucleotides but not the uncharged nucleosides.

2.6.1. Buffers

2.6.1.1. Assay buffer:

10mM $MgCl_2$

20mM Tris/HCl, pH 7.4

2.6.1.2 Dilution buffer

20mM Tris/HCl, pH7.4

2.6.2. Procedure

A 2x stock solution of cAMP was prepared by adding 30µl of ^{3}H-cAMP (lmCi/ml, 41.7µM) to 10ml of 2µM cAMP in assay buffer. The assay volume was 100µl consisting of 50µl 2x cAMP stock, 25µl for sample and 25µl for effector, with sample and effector prepared in dilution buffer. All tubes were kept on ice prior to

incubation at 30°C. The reaction was stopped after 10min by boiling for 2min. The tubes were cooled on ice and 25µl of 1mg/ml snake venom (Sigma) was added and incubated for a further 10 min. After cooling, 400µl of Dowex (SIgma) resin was added and incubated on ice for 15 min. The Dowex was pelleted by centrifugation in a bench-top centrifuge for 3min and 150µl of the supernatant removed for scintillation counting in 2ml scintillation fluid.

2.6.3. Use of PDE assay to profile PDE families present in various tissues

To determine the contribution of various PDE families to the overall cyclic nucleotide phosphodiesterase content of a tissue the PDE assay reaction was supplemented with various specific inhibitors. These inhibitors exploit differences between PDE families whose regulatory properties and precise form of catalytic are often unique to a family (19).

2.6.3.1. PDE3 and PDE4

The PDE3 family is specifically inhibited by the drug cilostamide (161) and the PDE4 family by rolipram (162). PDE inhibitors were dissolved in 100% DMSO as 10mM stocks and diluted in PDE assay dilution buffer (see section 2.6.1.2) for use in assay. The residual levels of DMSO do not affect PDE activity at the concentrations used (163). Measurement of PDE activity with and without cilostamide (10µM) and with and without rolipram (10µM) present gave the contribution of PDE3 and PDE4 respectively.

CELL CULTURE

2.7.1. Media

2.7.1.1. Foetal calf serum medium (FCSM)

The routine growth medium was Dulbecco's Modification of Eagle Medium (DMEM, Sigma D5671), This was supplemented with Penicillin/Streptomycin (100 units/ml, Sigma), 10mM glutamine and 10% foetal calf serum (Sigma).

2.7.1.2. New born calf serum medium (NBCSM)

This medium was Dulbecco's Modification of Eagle Medium (DMEM, Sigma D5671), this was supplemented with Penicillin/Streptomycin (100 units/ml, Sigma), 10mM glutamine and 10% new born calf serum (Sigma).

2.7.1.3. Serum free medium (SFM)

For serum starvation of cells growth medium was replaced with serum free medium (SFM) consisting of Dulbecco's Modification of Eagle Medium (DMEM, Sigma D5671) supplemented with Penicillin/Streptomycin (100 units/ml, Sigma), 10mM glutamine (Sigma)

2.7.1.4. RPMI-1640 medium

RPMI medium consists of RPMI-1640 medium (Sigma 0883) supplemented with Penicillin/Streptomycin (100 units/ml, Sigma), 10mM glutamine and 10% foetal calf serum (Sigma).

2.8. COS-7 CELL LINE

COS-7 (ATCC Number: CRL-1651) cells are a fibroblast-like cell line derived from African green monkey kidney cells. These cells have been transformed by an origin defective mutant of SV40 which codes for wild type T-antigen. They are an excellent host for transfection with vectors requiring the expression of SV40 T-antigen. They permit replication of any plasmid containing an SV40 origin of replication, thus amplifying the expression of any genes encoded by the plasmid.

2.8.1. Maintenance of COS-7 cells

Cells were grown in an atmosphere of 95% air and 5% CO_2 at 37°C in 10ml DMEM + 10% FCSM (section 2.9.1.1.). When the cells reached about 90% confluency the cells were passaged 1:3 to fresh flasks and medium.

2.8.2. Passaging COS-7 cells

The cells were washed in 10ml of PBS (section 2.5.1.1.) pre-warmed to 37°C and 3ml of trypsin were added. The cells were then returned to the incubator for 2min or until they detached from the flask. Clumps were disrupted by pipetting the cell suspension up and down ten times in a 1ml pipette. This suspension was distributed evenly to three flasks each containing 9ml of FCSM

2.9. COS-7 CELL TRANSFECTION

2.9.1. Buffers

2.9.1.1. Transfection medium

Transfection medium was Dulbecco's Modification of Eagle Medium (DMEM, Sigma D5671). This was supplemented with Penicillin/Streptomycin (100 units/ml, Sigma), 10mM glutamine, 10% new-born calf serum (Sigma) and 100µM chloroquine. This was made fresh each time.

2.9.1.2. Tris EDTA buffer (TE):

1mM Ethylenediaminetetra-acetic acid (EDTA)

10mM Tris HCl, pH 7.5

2.9.2. Procedure

Cells were grown to about 50% confluency prior to transfection. 10µg of DNA was diluted to 250µl in TE and 200µl of DEAE Dextran (10mg/ml in PBS, Sigma) were added. This was incubated for 15min at room temperature. COS-7 cell growth medium was aspirated from the cells and 5ml of transfection medium added.

The DNA solution was added dropwise to the cells and mixed by swirling. The cells were returned to the incubator for 3-4h.

The cells were shocked by first aspirating the transfection medium and 5ml of 10% DMSO in PBS were added for exactly 2 minutes. The DMSO was aspirated and the cells washed with 10ml of PBS. The cells were returned to normal growth medium, placed in the incubator for three days. Phosphodiesterase assays were then performed.

2.10 FRACTIONATION OF TRANSFECTED COS-7 CELLS: TRIETHANOLAMINE METHOD

2.10.1 Buffers

2.10.1.1 KHEM buffer

50mM KCl

10mM Ethyleneglycol-bis(P-aminoethylether)-N,N,N',N'-Tetra-acetic acid (EGTA)

50mM N-2-Hydroxyethylpiperazine-N'-2-ethanesulfonic acid (Hepes), pH 7.2

1.92mM $MgCl_2$

Added fresh:

1mM Dithiothreitol (DTT)

Protease inhibitors (These were added 1/1000 from a stock solution in DMSO. The final concentrations were 40µg/ml PMSF (Sigma), 156µg/ml benzamidine (Sigma), 1µg/ml each of aprotinin (Sigma), leupeptin (Peptide Research Foundation), pepstatin A (Sigma) and antipain (Sigma), added fresh

2.10.1.2 TEA-KCl

10mM Triethanolamine (TEA)

150mM KCl

pH 7.2 with HCl

2.10.2 Procedure

Growth medium was removed from the cells and 2ml of KHEM added. The cells were incubated at 4°C for 45min with occasional swirling. The KHEM was removed and 5ml of TEA-KCl were added and incubated for 10min at 4°C. The TEA-KCl was aspirated and the cells washed in 5ml KHEM. 1ml of KHEM was then added and the cells incubated for 2min at 4°C. The KHEM was aspirated, the cells scraped from the plate and homogenised with 20 strokes in a glass on glass dounce homogeniser. The homogenate was centrifuged at 650g for 10min to pellet debris (P1 fraction). P2 fractions were obtained by centrifugation at 75000rpm in a Beckman TL-100 ultracentrifuge. The supernatant was snap-frozen in liquid nitrogen in 100µl aliquots and stored at -80°C.

2.11 FRACTIONATION OF TRANSFECTED COS CELLS WITHOUT TRIETHANOLAMINE

2.11.1 Homogenisation Buffer

20mM 50mM N-2-Hydroxyethylpiperazine-N'-2-ethanesulfonic acid (HEPES) pH7.5

50mM NaCl

10mM Ethyleneglycol-bis(P-aminoethylether)-N,N,N',N'-Tetra-acetic acid (EGTA)

Protease inhibitors (section 2.10.1.1) and 1mM DTT added fresh

When H89 (LC laboratories) was used (see chapter 3) it was incubated over the cells as discussed in the references within (63)

2.11.2 Procedure

Growth medium was removed from the cells and the cells washed twice in homogenisation buffer. The buffer was aspirated (to leave ~500µl of buffer on the plate) and the cells scraped from the plate and then homogenised with 20 strokes in a glass on glass dounce homogeniser. The homogenate was centrifuged at 650g for 10min to pellet debris (P1 fraction). P2 fractions were obtained by centrifugation at 75000rpm in a Beckman TL-100 ultracentrifuge. These fractions were snap-frozen in liquid nitrogen in 100µl aliquots and stored at -80°C

2.12 OTHER CELL LINES

Information on these cell lines was routinely obtained from the American Type Culture Collection (ATCC) Catalogue of Cell Lines & Hybridomas (164).

2.12.1. CHO-K1, stably transfected CHO cell lines

These cells are derived from chinese hamster ovary (165). They are grown as a monolayer in Ham's F-12 medium supplemented with 10% Foetal calf serum (Sigma).

2.12.2. U-118 MG, U-87 MG and SK-N-SH cell lines

U-118 MG (ATCC Number: HTB-15) (166) and U-87 MG (ATCC Number: HTB-14) (166) cells are human glioblastoma cell lines. The SK-N-SH cell line is a human neuroblastoma. (ATCC Number: HTB-11) (167). Subculture is as shown for COS-7 cells (section 2.10) except that they were replated 1:5

2.12.3 U-937 cell line

U-937 cells are human monocyte-like cells derived from a lymphoma (ATCC Number: CRL-1593.2) (168). U937 cells are grown in suspension. Cultures were maintained by replacement of old medium with fresh medium. Cultures were maintained between 5 x 10^5 and 1 x 10^6 cells/ml

2.12.4. HeLa S3 cell line

HeLa S3 (ATCC Number: CCL-2.2) cells are derived from a human cervical carcinoma (169). Subculture is as for COS-7 (section 2.10) cells except that they are passaged 1:5

2.12.5. Jurkat J6 cell line

Jurkat J6 cells are human leukaemic T cells (170). They are grown as a suspension in continuous culture in FCSM

2.12.6. FTC133 and FTC236 cell lines

The human follicular thyroid carcinoma cell lines FTC133 and FTC236 (171) were cultured in RPMI growth medium

2.13 PROTEIN ASSAY

2.13.1. Bradford assay

A spectrophotometric standard curve of protein concentration was constructed using 0-20µg bovine serum albumin (BSA, Sigma). These concentrations of protein were dissolved in 800µl distilled water. To this, 200111 Bio-Rad reagent was added, the tubes were vortexed and the absorbance was read against a blank (as above but containing no protein), at a wavelength of 595nm. Protein concentrations of the samples were determined in a similar way, diluting 5µl of the sample in 800µl distilled water, adding Bio-Rad reagent and reading the absorbance in the spectrophotometer as before. All samples were assayed in duplicate. Protein concentrations were determined by plotting the standard curve and determining a line of best fit.

GENERAL NUCLEIC ACID MANIPULATIONS

2.14. STERILISATION OF MICRO-CENTRIFUGE TUBES, HOMOGENISERS, PIPETTE TIPS AND BUFFERS

All micro-centrifuge tubes tissue homogenisers, pipette tips and buffers used in nucleic acid manipulations were sterilised by autoclaving. Micro-centrifuge tubes and pipette tips were discarded after a single use.

2.15. CASTING AGAROSE MINIGELS

2.15.1. Buffer

2.15.1.1 Tris/Borate/EDTA (TBE) buffer 10X

1.1M Tris

0.9M boric acid

24mM EDTA

2.15.1.2. Procedure: Casting a 2% gel

200 ml 0.5x TBE was prepared for each minigel. 17ml 2% agarose in 0.5x TBE buffer was weighed in a small conical flask. This suspension was heated in microwave until the agarose dissolved. Once this occurred, the flask was reweighed and topped up with distilled water. The molten agar was poured into the gel apparatus and allowed to set. The rest of the TBE was then used to fill the tank. Samples were loaded after mixing with 6x loading dye (Promega). Ethidium Bromide (Sigma) was then added to final conc of 0.5 mg/l (add 10 µl of 10 mg/ml stock, Sigma) and the gel was run at 75V

2% gels were typically run but occasionally different percentages were used when higher molecular weight samples were run:

Range of Separation of linear DNA molecules according to agarose concentration.

Percentage gel	Size of fragment (kilobases)
0.9	0.5-7
1.2	0.4-6
1.5	0.2-3
2.0	0.1-2

2.16. EXTRACTION OF DNA FROM AGAROSE GELS WITH THE QIAEX II GEL EXTRACTION KIT

All DNA extracted from gels was purified using the QIAEX II DNA gel extraction kit according to the manufacturer's (Qiagen) instructions. Briefly, three volumes of 'QX-1' buffer and 10µl of QiaexII DNA binding beads were added to each gel plug. The plugs were dissolved by warming to 50°C during which time the beads were kept suspended by vortexing every 2min. After 10min the beads were pelleted by a 20s centrifugation in a benchtop centrifuge. The supernatant was removed and the pellet washed in 500µl 'QX-1' buffer, resuspended, and then pelleted in the same manner as above. The pellet was then washed, resuspended and pelleted similarly in an ethanolic wash 'PE' buffer. The pellet was then allowed to dry for 10 min and then eluted in 20µl of water. This DNA was typically contaminated with ethanol and so was subsequently purified by ethanol precipitation.

2.17. RESTRICTION ENZYME DIGESTS

All restriction enzyme digestswere performed on pure plasmid DNA using restriction enzymes supplied by Promega or New England Biolabs. Incubation conditions were 37°C for a minimum of 1 hour using the appropriate buffer supplied by Promega. Following digestion DNA was run on an agarose gel and gel extracted using QiaexII gel extraction kit (Qiagen)

2.18. ETHANOL PRECIPITATION

To the volume of DNA to be ethanol precipitated, 0.1 volume 3M sodium

acetate was added and 2 volumes of 100% ethanol. The vial was mixed and incubated at -80°C for 30 minutes. The precipitated suspension was centrifuged at 11000rpm in a Jouan (MR1812) refrigerated centrifuge for 10min to pellet the DNA. The supernatant was aspirated and 1ml of 70% ethanol added. The DNA was pelleted again by centrifugation at 11000rpm in the refrigerated centrifuge for 5min, the supernatant aspirated and the pellet allowed to air-dry for 5-10 minutes. The DNA was resuspended in TE buffer and the purity of the DNA checked by UV absorption at 260nm and 280nm where A260/A280=1.8 for pure plasmid DNA.

2.19. PHENOL/ CHLOROFORM EXTRACTION OF DNA

The DNA solution had an equal volume of phenol:chloroform:isoamyl alcohol (25:24:1) added to it. It was then vortexed. The phases were separated by centrifugation for 15s at full speed in a benchtop microcentrifuge. The aqueous (upper) clear phase was transferred to a new microcentrifuge tube leaving behind the organic (lower) yellow phase and the interphase layer (with proteins). This phase separation was repeated until no protein was detectable at the interface

Next an equal volume of chloroform was added to the aqueous solution in a new microcentrifuge tube. This was vortexed into an emulsion. Phase separation was repeated by centrifugation in a benchtop centrifuge. The aqueous phase was the top layer again. This upper phase was transferred to a new microcentrifuge tube. Following phenol/ chloroform extraction the DNA was ethanol precipitated.

2.20. GENERATION OF PLASMID DNA

Plasmid DNA was prepared using maxiprep and miniprep kits (Promega). Cosmid DNA was isolated by similar means (Qiagen midiprep and maxiprep kits). A brief protocol for a Promega maxiprep kit is given below.

2.21.1 Promega maxi-prep

A culture was set up by stabbing a toothpick into frozen glycerol stocks and adding it to 400ml of ampicillin (50µg/ml, Sigma) LB medium. The culture was

incubated overnight at 37°C in a rotating incubator at 200rpm

2.21.2. Preparation of Cleared Lysate

The culture was then poured equally into 250ml Beckman centrifuge tubes and pelleted at 9500g for 10min at room temperature in a JA-14 rotor. Each pellet was resuspended in 7.5ml 'Resuspension solution' using a heat-sealed 5ml pipette to manually disrupt the pellet. These suspensions were combined. To the combined 15ml, 15ml 'Cell Lysis' solution was added and mixed by inversion. Lysis was allowed to complete (up to 20 min) and then 15ml of 'Neutralisation solution' was added and immediately mixed by inversion.

The suspension was centrifuged at 14,000g for 15min at room temperature. The cleared supernatant was transferred to a new container

2.21.3. Plasmid DNA precipitation.

0.6 volumes of isopropanol was now added and mixed by inverting several times. The DNA was pelleted by centrifugation at 14,000g for 15 mins at room temperature. The supernatant was discarded and the DNA pellet resuspended in 2ml TE

2.21.4. Plasmid Purification

One Maxicolumn was inserted into a vacuum manifold. 10 ml of well-shaken pre-warmed 'DNA purification resin' was added to the DNA/TE solution and then this slurry was added to the maxicolumn. A vacuum was applied to draw the slurry through. The DNA/resin container was rinsed with 13ml of 'Column wash solution' and immediately added to the column under vacuum. A final wash of 12ml of 'Column wash solution' was then added to the column. The resin was rinsed with 5ml of 80% isopropanol under vacuum.

The resin was dried by centrifuging the column in its 50ml conical tube in a bench-top clinical centrifuge at 2,500 rpm (1300 g) for 5min. It was then transferred to a new 50ml conical centrifuge tube. 1.5 ml pre-heated water (65-70°C) was applied

to the tube. After 1 minute this water was centrifuged out of the column using the conditions above

DNA solution was stored-20°C

NUCLEIC ACID ISOLATION

2.22. ISOLATION OF RNA FROM TISSUE OR CELLS USING TRI-REAGENT

Pre-weighed tissue was homogenised in Tri-Reagent (Sigma) (1ml per 50-100mg tissue) using a sterilised glass homogeniser (sample volume not to exceed 10% of vol of Tri-Reagent used). Alternatively one flask of a cell monolayer was scraped into 1ml of Tri-Reagent and resuspended with a pipette. Cells grown in suspension were lysed by addition to pelleted cells and resuspension with a pipette. The homogenate was stored at room temperature for 5 min. It was then transferred, 1ml to each 1.5ml microcentrifuge tube. Cell membranes, polysaccharides and high molecular weight DNA were then pelleted out of the homogenate by centrifugation at 11000 rpm for 10min at 4°C. The supernatant was transferred to another microcentrifuge tube. The RNA and DNA were now phase separated by addition of 0.2ml RNAase-free chloroform per 1ml of Tri-Reagent. The solution was vortexed for 15s then stored at room temp for 3min. Phase partition was brought about by centrifugation at 12 000g (11 000 rpm) for 15 min at 4°C. For DNA isolation the interphase and organic phase were taken (see 2.27). For RNA isolation the aqueous phase was transferred to a new microcentrifuge tube and the RNA precipitated by addition of isopropanol (propan-2-ol): 0.5ml per 1ml of T-R used initially. Precipitation was allowed to continue for 5-10 min at room temperature. RNA was then pelleted by centrifugation at 12 000g (11 000 rpm) for 10 min at 4°C. RNA forms a white pellet on the side and bottom of the tube. The supernatant was aspirated and the pellet washed in 1ml 75% ethanol. In this state the RNA can be stored for up to a year at -20°C.

RNA was prepared for use by centrifugation at 7500g (9000 rpm) for 5min at 4°C in a refrigerated Jouan (MR1812) centrifuge. Most of the supernatant was

aspirated and the RNA pellet dried under vacuum for 5-10 min (not to completion). RNA was re-solubilised in di-ethyl pyrocarbonate (DEPC) treated water. Pellets which do not solubilise immediately were incubated at 55-60°C for 10 min. Typical yield was 6-10µg RNA/mg liver

2.23. ISOLATION OF GENOMIC DNA FROM RAT LIVER USING TRI REAGENT

This used the interphase and organic phase of the Tri-reagent when it was partitioned by chloroform treatment (see previous section). The DNA in these fractions was then precipitated by addition of 300µl of ethanol per ml of Tri-reagent initially used. The samples were stored at room temperature for 3 min then the DNA sedimented by centrifugation at 4200rpm in a Jouan (MR1812) refrigerated centrifuge. The supernatant was then removed and the DNA was washed twice in 0.1M sodium citrate in 10% ethanol. 1ml was used per ml of Tri-reagent initially used. At each wash the DNA pellet was washed for 30min at room temperature with occasional mixing and then centrifuged as above. Following these two washes, the DNA pellet was suspended in 75% ethanol (1.5ml-2ml per 1ml of Tri-reagent used initially), stored at room temp for 20 min then centrifuged as above. Under ethanol the DNA could be stored for months at 4°C. DNA was dried for 5-10 min in a vacuum then resuspended in 8mM sodium hydroxide by passing gently through a pipette. Insoluble material (cell membranes) was then removed by sedimentation at 11000rpm in a Jouan (MR1812) refrigerated centrifuge. DNA was quantitated by it absorbance at 260nm. Samples in 8mM NaOH could be stored overnight.

2.24. SYNTHESIS OF FIRST-STRAND COMPLEMENTARY DNA (cDNA)

2.24.1. Procedure.

5 µg of total RNA was made up to 20µl with DEPC H_2O, heated to 65° C in a thermal cycler for 10min then immediately chilled on ice

The "Bulk 1st strand cDNA mix" (Pharmacia) has its particulate matter gently

suspended and then collected with a brief centrifugation. The cDNA synthesis reaction was prepared on ice and contains:

11 µl of "Bulk 1st strand cDNA mix"

1 µl of "DTT" solution

1 µl of a 1/25 dilution of "Not1-d(T)18" (0.2 µg/µl) primer

20 µl heat-denatured RNA from 1st tube

The cDNA synthesis reaction was incubated at 37° C for 1 hour

2.25. POLYMERASE CHAIN REACTION

2.25.1. PCR Reaction mix

50mM KCl (Supplied 10x in Taq polymerase buffer, Promega)

10mM Tris HCl (pH9) (Supplied 10x in Taq polymerase buffer)

200µM of each dNTP (Promega)

0.5µM of each primer (Genosys), (except for 1.5µM of GR18 and GR19)

1.5mM $MgCl_2$ (Promega)

3-5µl first strand cDNA mix

5U of Taq DNA polymerase (Promega)

2.25.1.1. 'Hot Start' PCR

Taq processes at 4°C albeit very slowly. This activity can reduce specificity of the PCR reaction. This is remedied by 'hot start' methodologies which reversibly inhibit Taq polymerase in a variety of ways. In cases where 'hot start' was used, Taq was first mixed with 'Taq Start' antibody (Clontech) for 'hot-start' PCR according to the manufacturer's instructions.

2.25.1.2. "Perfect Match" PCR additive

The PCR additive "Perfect Match" (Stratagene) is designed to increase specificity in complex backgrounds (such as cDNA derived from total RNA) by destabilising mismatch annealing. When it was used, the PCR additive "Perfect Match" was added last (0.5µl), to a total volume of 50µl

2.25.2. Procedure

Amplification of sequence fragments was performed in 1x PCR buffer (see above). After amplification a 10µl aliquot from each reaction was typically resolved by electrophoresis on a 2% agarose gel (section 2.20) and visualised with ethidium bromide under UV light.

2.25.2.1 Typical amplification protocol

- •Denaturation for 60s at 94°C
- •Annealing for 60s at a temperature 7°C below the melting temperature of the primer
- •Extension for 60s at 72°C

METHODS USED IN PCR-BASED RAPID AMPLIFICATION OF cDNA ENDS (RACE) PROTOCOLS

2.26. REVERSE TRANSCRIPTION FOR RAPID AMPLIFICATION OF cDNA ENDS

First strand cDNA syhthesis of RNA for RACE used Superscript II enzyme (Gibco). This is the Moloney Murine Leukaemia Virus reverse transcriptase (MMuLV RTase) but it is a recombinant protein that has had its RNAse activity removed. As a result it synthesises more full length cDNAs than the wild type. It is also active at a higher temperature. Used at these higher temperatures less cDNA will be synthesised by mis-priming events.

5µg of RNA to be used in this protocol was diluted to 10µl using DEPC water. It was then denatured at 70°C for 5min in a thermal cycler which was programmed to heat the solution at the annealing temperature of the primer. 1pmol of a gene specific primer was now added along with 10x hybridisation buffer. For intramolecular ligation (circularisation) reactions a phosphorylated oligonucleotide was used. After this annealing step the reaction was heated at 42°C for 2min before addition of 1µl SuperscriptII enzyme. The cDNA synthesis reaction was incubated at

42°C for 1h. Then 1µl of RNAse H (Promega) was added and the reaction incubated at 55°C for 10 min.

ANCHORING REACTIONS IN RACE TECHNIQUES.

2.27. ANCHORING OF cDNA ENDS BY HOMOPOLYMERIC TAILING WITH TERMINAL DEOXYNUCLEOTIDYL TRANSFERASE (TdT)

Homopolymeric tailing of cDNA ends was done using the '5' RACE System for Rapid Amplification of cDNA Ends' (GibcoBRL) kit.

First strand cDNA was separated from enzymes and buffer components by GLASSMAX spin cartridge (GibcoBRL). TdT tailing was then performed in the following reaction mix:

DEPC water

10X reaction buffer

(20mM Tris-HCl (pH 8.4), 50mM KCl)

25mM $MgCl_2$

2mM dCTP

cDNA sample

The mixture was incubated for 2min at 94°C then placed on ice. 1µl TdT (10 units/µl) was added and incubated for 10 min at 37°C. The TdT was now heat inactivated for 10 min at 65°C

2.28. ANCHORING OF cDNA ENDS BY T4 RNA LIGASE MEDIATED (RLM) SINGLE STRANDED INTRAMOLECULAR OR INTERMOLECULAR LIGATION OF PHOSPHORYLATED OLIGONUCLEOTIDES

First Strand cDNA was purified from primer by phenol/chloroform extraction followed by centricon 30 filtration (Amicon). Then 1pmol (1pmol/µl) of 5'

phosphorylated oligonucleotide was added to 16µl cDNA, 2µl 10x buffer (50mM Tris-HCl, pH7.8, 10mM $MgCl_2$, 10mM β–mercaptoethanol) and 1µl T4 RNA ligase (New England Biolabs.). In cases where intramolecular ligations were attempted, the phosphorylated oligonucleotide was omitted. This ligation was incubated at 24°C overnight.

CLONING DNA

2.29. PHOSPHATASE TREATMENT OF DNA

Prior to ligation of an insert into a vector, the plasmid DNA should be treated with calf intestinal alkaline phosphatase (CIAP, Promega) if the vector has been digested with a single restriction enzyme. The CIAP removes the 5' phosphate groups and thus prevents recircularization of the vector during ligation.

2.29.1 Reaction mix

Add the following in a microcentrifuge tube:

vector DNA

CIAP 10x buffer

CIAP

dH_2O

Mix gently and incubate for 1 hour at 37°C. CIAP must be removed prior to ligation by phenol/chloroform extraction.

2.30. DOUBLE STRANDED DNA LIGATION

Double stranded DNA with cohesive ends was ligated into 100ng vector by adding 1unit of T4 DNA ligase (Promega) to 1:1 and 1:3 ratios of vector and insert DNA in 19.5µl 1x Ligase buffer (10X T4 DNA ligase buffer is 30mM Tris-HCl, pH7.8, 100mM $MgCl_2$, 100mM DTT, 10mM ATP). This reaction was incubated at 14°C overnight. The ligase buffer was aliquoted to prevent degradation of ATP.

2.31. TA CLONING

2.31.1 Sample preparation

PCR samples were used directly in ligations (see below). Cosmid digests were heated to 65°C for 10min to inactivate the restriction enzyme, then concentrated by ethanol precipitation. The precipitates were then redissolved and incubated with Taq polymerase for 10min to give 3' A-overhangs. The sample was collected again by ethanol precipitation. The precipitate was resuspended in a volume such that the ratio of concentration of the average sized insert to vector would be 3:1 in the ligation.

2.31.2. Ligation

TA cloning depends on a property which certain polymerases possess in transferring single adenines onto the 3' end of blunt-ended DNAs. Vectors carrying complementary T overhangs can ligate with these DNAs very efficiently because neither molecule can circularise thus promoting intermolecular reactions. TA cloning was performed using the Original TA cloning kit (Invitrogen) or the Eukaryotic TA cloning kit (Bidirectional) as required. The ligation reaction is carried out essentially as above, using the supplied precut vector containing the T overhang. The PCR reaction DNA was not quantified but instead 1µl of PCR reaction was added as advised in the manual notes.

2.31.3. TA cloning: transformation

An aliquot of frozen competent cells (The strain invαF was supplied with Original TA cloning kit. The strain TOP10F was supplied with Eukaryotic Bidirectional TA cloning kit, both from Invitrogen) was thawed slowly on ice. 2µl of ligation reaction and 2µl of 0.5Mβ-Mercaptoethanol was added to the tube, mixed with the pipette tip and incubated on ice for 30min. The cells were then heat shocked for 30s at 42°C and incubated on ice for a further 2min. 250µl of SOC broth was then added and the transformed cells incubated at 37°C for 60min with shaking (225rpm) . 100µl of the culture was plated on a 10cm agar plate containing 50µg/ml ampicillin. Transformed colonies were identifiable in the 'Original' TA cloning vector (pCR2.1)

using blue/white colour selection because insertion was into the β-Galactosidase gene. Colour selection was not possible in the eukaryotic TA cloning expression vector (pCR3.1). In either case white colonies were picked, PCR screened (2.31.4) and glycerol stocks made of positive colonies (section 2.5.4.)

2.31.4. TA cloning: PCR screen

PCR screens were usually done with one vector primer and one insert specific primer used in the PCR, to select for recombinants. The template for PCR screens were colonies, which were picked onto a master plate before being placed into the reaction tube. In very large screens where very few positives were anticipated (such as the screens of cosmid digestion fragment subclones), the initial PCR screens were done with one tube for each row and column to reduce the number of tubes. The PCR mix was as normal (see section 2.29) except for Taq polymerase, where only 1Unit was added per reaction. The final volume of each reaction was 30µl. The cycling times were:

Cycles (30)	Denaturation	96°C for 30s
	Annealing*	47°C for 30s
	Extension	72°C for 1min

Positive PCR reactions were detected by gel electrophoresis

2.32. DNA SEQUENCING WITH THE ABI SEQUENCER

2.32.1. Protocol for cycle sequencing

Samples for sequencing taken from maxi-preps or mini-preps were mixed with the Taq DyeDeoxy Terminator (ABI) reaction premix.

Reaction mix:

Reaction premix	
(contains buffer, polymerase, dNTPs, magnesium)	8µl
ds DNA template	400ng
primer (for ds DNA)	3.2pmol
H_2O	to 20µl

Sequencing reactions so prepared were subjected to thermal cycling using the following conditions

Cycles (25)	Denaturation	96°C for 30s
	Anncaling*	47°C for 15s
	Extension	60°C for 4min

* This segment temperature was variable according to the primer used. The temperature shown was that used for the T7 sequencing primer (taatacgactcactataggg) and the pCR2.1 upstream primer (agctatgaccatgattacg)

Reaction products were concentrated by ethanol precipitation and the pellets sent to the Glasgow University Molecular Biology Support Unit for gel electrophoresis.

2.33 SEQUENCE ANALYSIS

Routine DNA sequence handling and analysis was performed on the Gene Jockey II program (BIOSOFT), though some alignments (see figure legends) were then transferred to the DNA STAR program for presentation. Protein analysis was also done on DNA STAR. The GCG suite of software was used for similarity searching of the nucleotide and protein databases.

3. STUDIES ON THE MEMBRANE ASSOCIATION AND REGULATION OF PDE3B.

3.1 INTRODUCTION: MEMBRANE ASSOCIATION OF PDE3B

The intracellular localisation of PDE3 derived from different sources varies (58). PDE3 activity in adipocytes, which is thought to be predominantly PDE3B (54), is almost exclusively particulate (56,172). A hydrophobic sequence between amino acid 73 and 251 of rat PDE3B has been proposed to confer membrane association upon the protein. This was suggested on the basis that this region displayed hydropathic periodicity which resembled that of integral trans-membrane helices (54). However, many soluble proteins have hydropathic periodicities which might otherwise be used to justify membrane association (173). Therefore this measure is in itself insufficient and, in any case, would not exclude other regions of the protein having membrane association determinants. To date, the most detailed studies characterising deletions of PDE3B have not addressed the issue of intracellular localisation (174,175), however a picture of the membrane association of PDE3 is beginning to emerge from other sources.

Membrane association of PDE3A has been studied, with targeting of both full-length and N-terminal truncations of PDE3A being examined (52,56). It has been suggested, on the basis of sequence similarity (see figure 1.6.1.), that this work is also applicable to PDE3B (58). The susceptibility of full length PDE3B to solubilisation with high ionic strength or detergent has also been examined (56). All of this work is summarised below.

According to Leroy et al (56), in low ionic strength and the absence of detergent, full length recombinant PDE3B expressed in NIH3006 fibroblast is almost exclusively particulate, confirming data from adipocytes (172). Detergent was shown to be able to solubilise partially this enzyme, as was treatment with high ionic strength. The combined effects of these treatments was at least additive, consistent with there being more than one means of membrane association. Similar results were obtained with full-length PDE3A expressed in Sf9 cells (52). In the absence of high ionic strength or detergent, N-terminally truncated forms, with deletion of either 483 amino

acids (52) or 511 amino acids (56) of PDE3A, were found in both cytosolic and particulate fractions (52). In contrast, an N-terminally truncated construct with a deletion of 611 amino acids of PDE3A was entirely cytosolic (56). It therefore seems that the PDE3A membrane association determinants may be manifest in the first ~600 amino acids of the PDE. Taken together, these findings hint at a complexity of PDE3 membrane association which is difficult to reconcile with the single integral membrane binding domain originally proposed by Taira et al (54). Indeed there is a possibility that PDE3B may have more than one membrane association domain. Thus cytosolic localisation would only be conferred when all such binding determinants are removed.

Wild-type rat PDE3B has two in-frame Sac II restriction digestion sites which, if digested (the short fragments removed) and religated, would delete 85% of the putative membrane association domain suggested by Taira et al (54). This construct, which is generated in this study and called PDE3BΔ1, might be considered an attractive first step to address the question of whether the membrane association domain proposed by Taira et al (54) does indeed harbour membrane binding determinants or not.

3.2 INTRODUCTION: INVESTIGATIONS INTO THE PATHWAY BY WHICH INSULIN SIGNALS TO PDE3B.

The evidence for insulin stimulation of PDE3B as a key step in insulin-mediated anti-lipolysis was discussed in the Introduction. The increase in activity of adipocyte PDE3B, due to either insulin or isoprenaline treatment, coincides with an increase in the level of phosphorylation of this enzyme (176), an effect which is also seen in cell free stimulation of PDE3B (49). Furthermore, okadaic acid, an inhibitor of protein phosphatases 1 and 2A, is able to block reversal of the insulin stimulation of PDE3B (177). Thus the stimulation of PDE3B by insulin is apparently due to a reversible phosphorylation of PDE3B.

The identity of the kinase (designated variously in the literature as cGIPDEISK for Cyclic GMP Inhibited PDE Insulin Stimulated Kinase or PDE3IK for PDE3 Insulin Stimulated Kinase (58)) responsible for this phosphorylation is still

unknown. The PDE3IK activity appears to be located in the cytosolic fractions of liver, adipocytes and human platelets (178-180). The kinase is only insulin stimulated in the pH range 7-8 (178). PDE3IK activity is rapidly lost if cell lysis is not carried out in the presence of phosphatase inhibitors, consistent with the notion that the PDE3IK itself is also sensitive to phosphorylation (178-180). Since PDE3IK is not adsorbed by anti-tyrosine antibodies this suggests that PDE3IK is sensitive to serine/threonine phosphorylation (180). Insulin stimulation of PDE3B is resistant to treatment with the PKC & PKA inhibitor H7 (177,178) and the protein kinase A inhibitory peptide (49,178), indicating that these kinases are not involved in insulin-mediated stimulation of PDE3 (177-179). To date, attempts to purify this protein to homogeneity have failed (63). However, inhibitor studies suggest that the kinase is not p70 S6 kinase, casein kinase II, PKA, PKC, Mn^{2+} specific protein kinase or protease-stimulated protein kinase (63,180). Despite contrary evidence from *in vitro* studies (181) serine 302 appears to be the sole site for physiological PDE3B phosphorylation following either insulin or isoprenaline treatment (182).

Insulin mediated activation of PDE3IK and the phosphorylation and activation of PDE3B are blocked by treatment with wortmannin at concentrations which inhibit phosphatidyl inositol-3 kinase (PI 3-kinase) (183). On this basis it has been postulated that the PDE3IK kinase lies downstream of PI 3-kinase (183). Three kinases, p70S6 kinase (p70 S6K) (184,185), glycogen synthase kinase-3 (GSK-3) (186) and protein kinase B (PKB, also known as RAC and akt, but not related to the small ras like GTPase rac) (187) are known to provide downstream effectors of PI 3-kinase. Of these kinases, two can most likely be discounted as putative PDE3B kinase. p70S6K is unlikely to be the PDE3B kinase since rapamycin, a specific inhibitor of p70S6K, has been reported to be ineffective at inhibiting insulin mediated PDE3B stimulation (63). Furthermore, GSK-3 is inactivated by insulin in the pathway downstream of PI3K (186). On this basis it is not possible that GSK-3 could mediate directly PDE3B phosphorylation and activation due to insulin. It thus seems likely that neither p70S6K or GSK-3 will participate in insulin signalling to PDE3B. In contrast there are two lines of circumstantial evidence that suggest that PKB might be involved

in PDE3B stimulation due to insulin. First, the insulin mimetic pervanadate produces an insulin-like stimulation of PDE3 activity in adipocytes (61). This compound is also the most potent activator of recombinant PKB (186). Second, the observation that PKA and insulin synergistically activate PDE3B by phosphorylation on a single site (182) has led to postulation that PDE3IK might contain one PKA and one insulin mediated activation site, both of which would need to be activated for maximal activity (182). PKB is a candidate for this convergence of signals since it contains two phosphorylation sites, both of which need to be phosphorylated for maximum activity (188).

With these considerations in mind, co-transfection experiments were planned with kinase active and kinase dead forms of PKB. It was hypothesised that if PKB was able to signal to PDE3B, then following stimulation with pervanadate one would observe an increase in PDE3 activity in cell lysates. An important control would be that pervanadate was unable or at least significantly less able to have the same effect if kinase-active PKB was replaced with kinase-dead PKB since this would suggest that the pervanadate effect was due to a specific effect on PKB rather than a generalised effect on the cell or a specific effect on PDE3B itself (61).

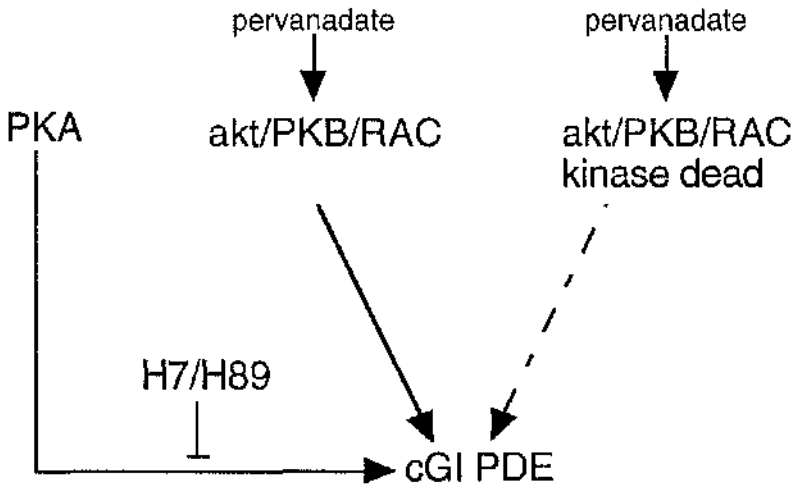

Figure 3.2 Schematic of planned experiment to test PKB signalling to PDE3B.

If PKB is capable of signalling to PDE3B in COS-7 cells, pervanadate treatment of cells should stimulate PKB which will then stimulate PDE3B. A negative control which should detect direct pervanadate stimulation of PDE3B is to repeat the cotransfection with kinase-dead PKB. PKA activity is acutely blocked with H89 which does not effect insulin-mediated stimulation of PDE3B (63).

3.3. SYNTHESIS OF PDE3B CONSTRUCTS

3.3.1. Construction of PDE3B/pSV SPORT

The cDNA for rat PDE3B (rcGIP-1) (54) was excised from the blue/white colour screen cloning vector pBluescript, where it was cloned into the Spe I site. For mammalian expression PDE3B was subcloned into the eukaryotic expression vector pSV SPORT on the basis that PDE3B liberated from pBluescript by Spe I digestion could be ligated directly into identically digested pSV SPORT. Greater than 50 colonies were obtained in two ligations of PDE3B and pSV SPORT digested with Spe I. Six colonies from each were mini-prepped for further study. DNA was subjected to BamH I digestion. pSV SPORT containing PDE3B ligated in the correct orientation should give fragment sizes of 6, 0.9 and 0.6 Kb (see figure 4.3.1.a), whilst pSV SPORT with PDE3B in the wrong orientation and pBluescript with PDE3B in either orientation will give different banding patterns. 12/12 colonies gave a BamH I digest pattern corresponding to pSV SPORT containing PDE3B in the correct orientation except that the expected 0.9Kb band did not appear. This corresponds to the 3' untranslated region of PDE3B and was therefore confirmed by a new digestion where Spe I and Xba I co-digestion should give digestion fragments of 3.2, 2.6 and 1.8 Kb (see figure 4.3.1.b). The same 10/12 colonies contained these bands with the shared exception that the lightest band, which corresponds to the 3' untranslated region of PDE3B, was considerably shorter than expected (~0.9Kb versus 1.8Kb). Since this is in the area of the 3' end of the ORF sequencing of the plasmid was used to confirm that the reading frame was intact. This showed that the Spe I site had in fact been engineered to cut out the 3' UTR (see figure 4.3.1.c) and this finding fully explains the aberrant banding patterns observed.

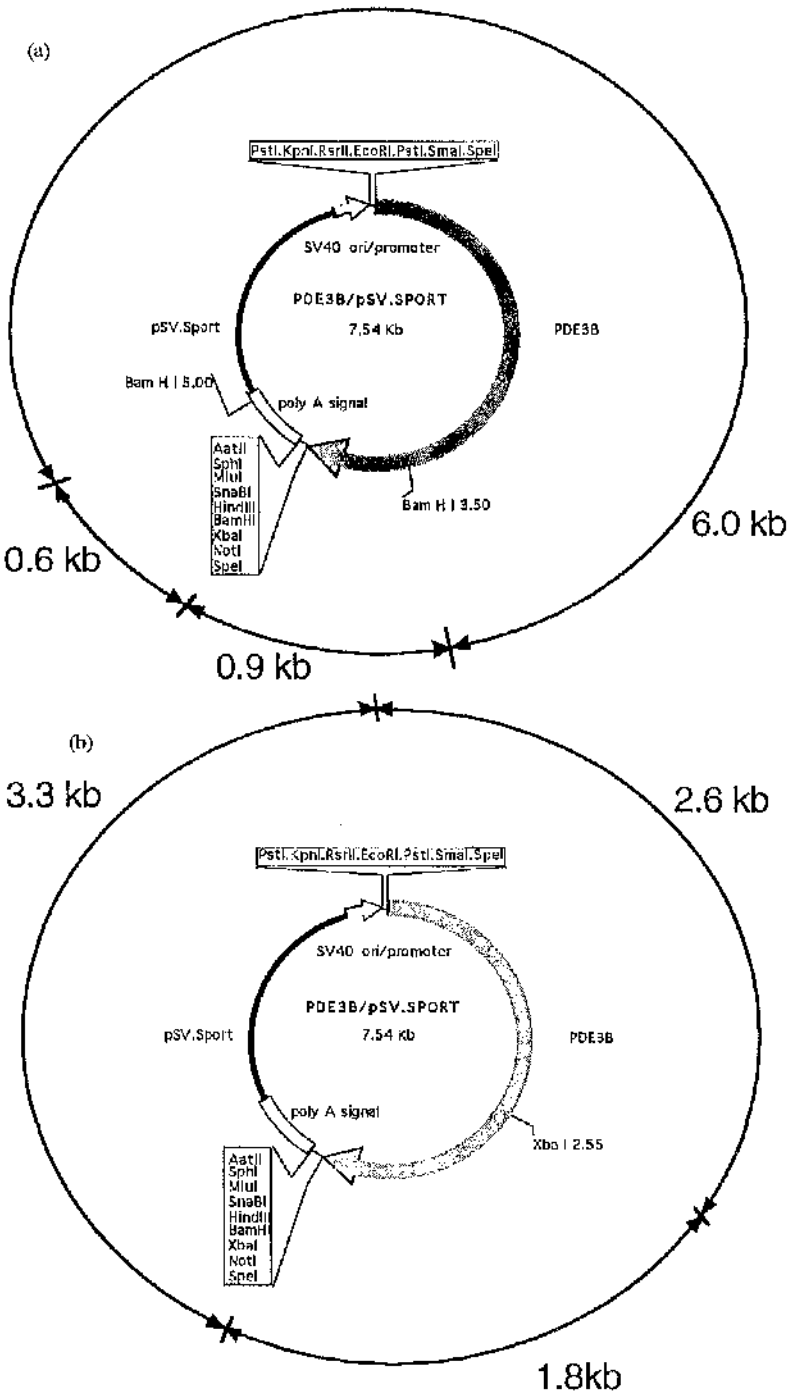

Figure 3.3.1.a,b Expected restriction digestion pattern of PDE3B/pSV SPORT following digestion with BamH I or Spe I and Xba I

Shown above is the plasmid map of PDE3B/pSV SPORT with PDE 3B cloned into the Spe I linker site in the correct orientation. The digestion pattern is that shown (a) when the plasmid is digested with BamH I, or (b) when it is digested with Spe I and Xba I. These patterns were different from those expected for pSV SPORT with PDE3B in the wrong orientation and for pBluescript in either orientation.

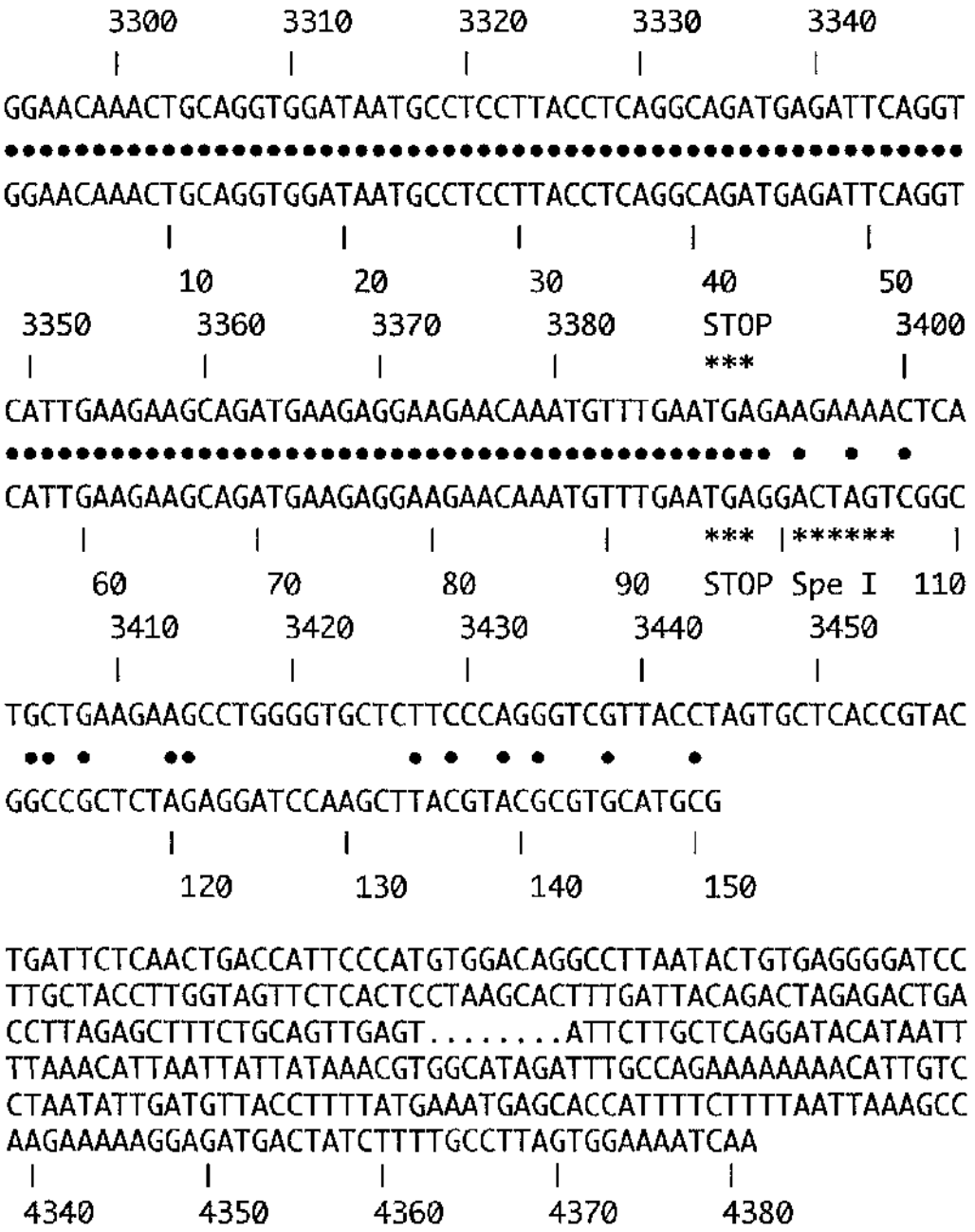

Figure 3.3.1.c A Spe I site is found immediately following the stop codon in PDE3B/pSV SPORT construct

PDE3B/pSV SPORT construct was analysed by sequencing using the 3' T7 sequencing primer (see methods). This DNA sequence was then compared to the published PDE3B ORF sequence (numbered as in (54)). The coding sequence is conserved but just downstream of the stop codon (STOP in diagram), a Spe I site is found. The sequence beyond this is vector sequence. That is, the remaining ~900bp of 3' UTR was removed at some point in the cloning of PDE3B

3.3.2. Construction of PDE3BΔ1: an internally deleted mutant of PDE3B/pSV SPORT which lacks 151 out of 178 amino acids of a putative membrane association domain.

PDE3B pSV/SPORT was digested with Sac II, to remove the putative membrane association domain of PDE3B (figure 3.3.2.a). Nar I, which digests one of the short deleted fragments at a unique site was also used to reduce the numbers of short fragments which would have double-ended Sac II sites and therefore be able to religate with the large linearised PDE3BΔ1/pSV SPORT. To reduce further the risks of intermolecular religation, the small digested fragments were removed by gel electrophoresis. The linearised PDE3BΔ1/pSV SPORT was then recircularised with T4 DNA ligase. Ten colonies were taken from the subsequent transformation and screened by cycle sequencing from an N-terminal primer used in the construction of PDE3BΔ2 (see below). This primer gave reads long enough to determine whether the internal truncation had been made. All colonies for which sequence was obtained contained the PDE3B sequence with the membrane association domain removed. One of these colonies, (number 2) was taken for use in all further studies. Figure 3.3.2.c is a hydropathy plot of PDE3B which shows the hydrophobicity of the sequences deleted to make PDE3BΔ1.

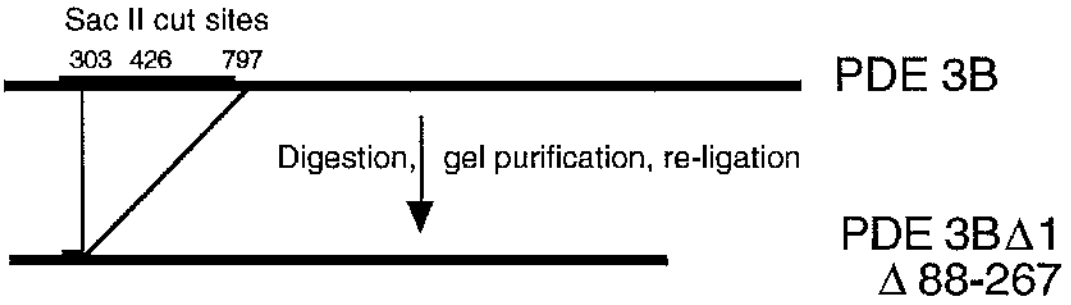

Figure 3.3.2.a Schematic of PDE3BΔ1 construction

PDE3B and PDE3BΔ1 are shown. The thick line represents the putative membrane association domain and the thin line represents the rest of PDE3B. PDE3B was subjected to Sac II digestion which cuts in PDE3B three times at the positions shown but not in the vector (not shown). Purification of this longest fragment by gel electrophoresis followed by recircularisation would yield a plasmid with an in frame deletion of nearly 500 nucleotides

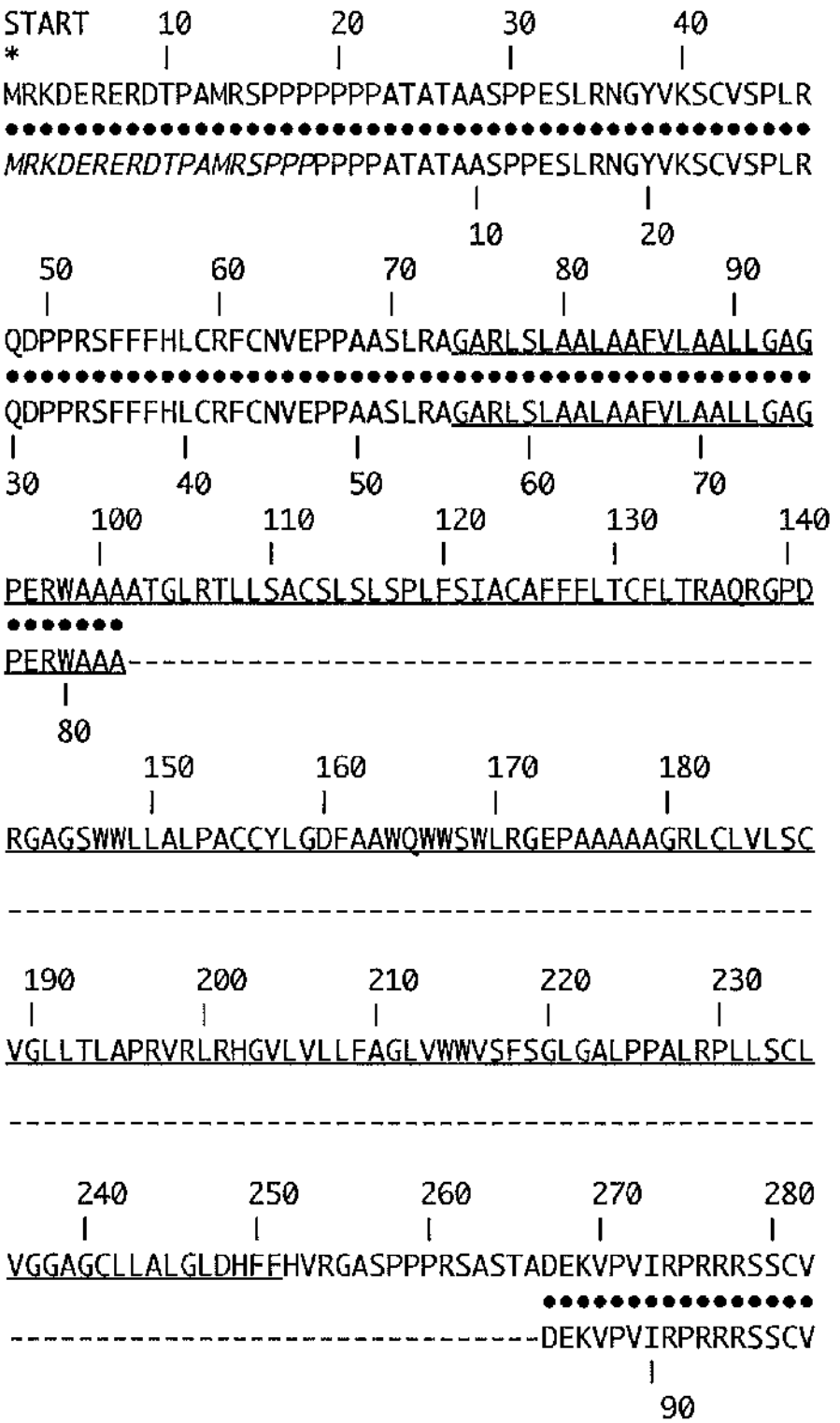

Figure 3.3.2.b Sequencing analysis of the N-terminal of PDE3BΔ1.
A candidate PDE3BΔ1 clone (2) was sequenced using a primer designed to the 5' end of PDE3B. The inferred amino acid sequence (bottom; the sequencing primer starts at the ATG of PDE3B so the reads start further downstream, unread sequence is shown in italics) was aligned to the N-terminal region of PDE3B itself (top). The PDE3B putative membrane association domain (54) is underlined.

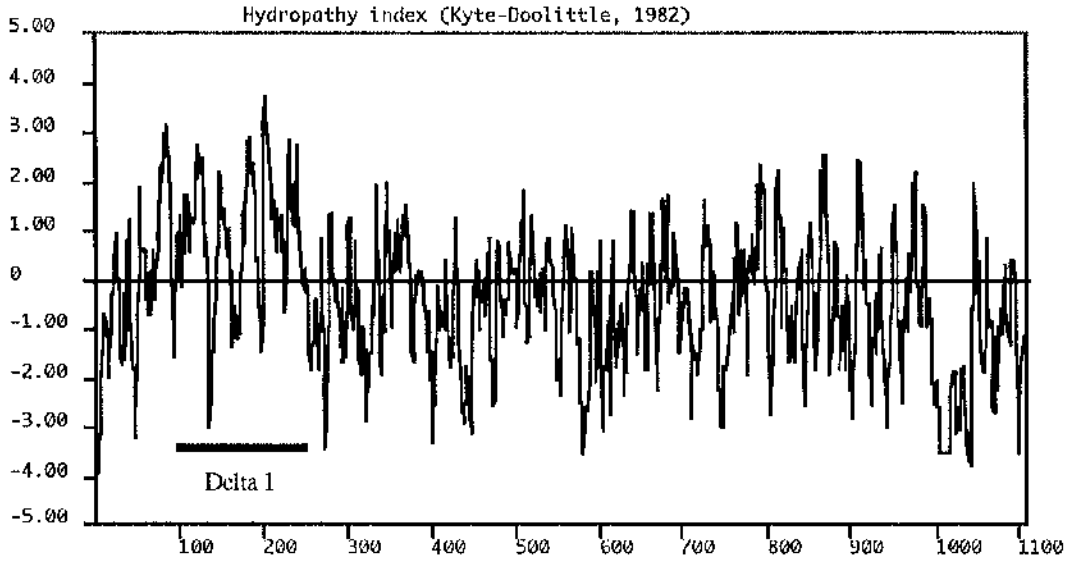

Figure 3.3.2.c Kyte and Doolittle hydropathy plot of PDE3B. PDE3BΔ1 lacks hydrophobic PDE3B sequences

The hydropathy of PDE3B is presented (**189**). The sequence marked delta 1 is that deleted in PDE3BΔ1

3.3.3. Construction of PDE3BΔ2: The first 72 amino acids of PDE3B tagged to the vesicular stomatitis virus (VSV) epitope YTDIEMNRLGK

The construction of PDE3BΔ2 was done using a PCR based procedure. Three primers were designed for amplification of the N-terminal 72 amino acids.

(1) A sense primer was designed to the N-terminal of PDE3B taking care to include the Kozak initiation sequence (190).

Sense PDE3B N-terminal + KOZAK sequence GCTATGAGGA AGGACGAGC (GR88)

(2) An antisense primer was designed to the vesicular stomatitis virus (VSV) epitope YTDIEMNRLGK (with codons selected for mammalian preference) and then continuing with the PDE3B region leading up to amino acid 72.

Antisense VSV tag fused to PDE3B sequence. CTACTTGCCC AGCCTGTTCA TCTCGATGTC GGTGTAGCGG AGCGAGGCCG CCGG (GR87)

(3) For amplification a second antisense primer was designed to the VSV epitope.

VSV amplification primer CTACTTGCCC AGCCTGTTC (GR89).

A PCR reaction was set up using a glycerol stab of PDE3B/pSV SPORT as template (figure 3.3.3.a). The N-terminal of PDE3B is GC rich (PDE3BΔ2 sequence is 76% G+C). Perhaps, because of this, a fragment of the correct size (~256bp) was obtained only when DMSO or a 96°C melting temperature was used. Cycling conditions were 25 cycles of 96°C for 60s, 53°C for 60s (37°C in the first cycle) and 72°C for 60s. The PCR product was directly cloned into the bi-directional eukaryotic expression TA cloning vector pCR 3.1. 60 clones were screened (as described in the methods but again with a 96°C melt step) by a unidirectional PCR to identify clones only if they are in the correct orientation. The screen used the T7 upstream (on the vector) sequencing primer and the antisense primer used in the PCR. 9 positive clones were cycle sequenced in both strands. All 9 sequences displayed the correct sequence in every position in one or other read, but one colony, number 66, was taken for further experiments because it reads perfectly on both strands (figure 3.3.3.b)

In figure 3.3.3.c, all three of the PDE3B constructs amino acid sequences are presented for comparison

(a)

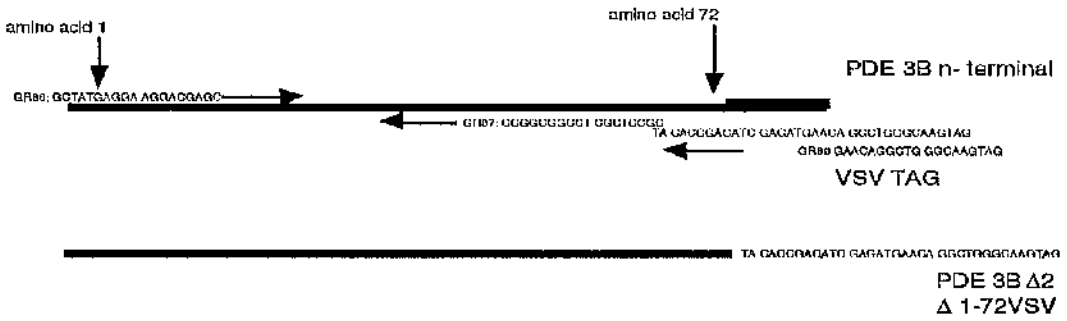

(b)

```
          10         20         30         40
          |          |          |          |
MRKDERERDTPAMRSPPPPPPPATATAASPPESLRNGYVKSCVSPLR
••••••••••••••••••••••••••••••••••••••••••••••••••
MRKDERERDTPAMRSPPPPPPPATATAASPPESLRNGYVKSCVSPLR
          |          |          |          |
           10         20         30         40

  50         60         70         80
  |          |          |          |
QDPPRSFFFHLCRFCNVEPPAASLRYTDIEMNRLGK•
••••••••••••••••••••••••••••
QDPPRSFFFHLCRFCNVEPPAASLRAGARLSLAALAAFVLAALLGAG
  |          |          |          |          |
   50         60         70         80         90
```

Figure 3.3.3.a,b Construction of PDE3BΔ2.

(a) Schematic of the PCR mediated fusion of the N-terminal of PDE3B with the VSV epitope YTDIEMNRLGK. PCR was carried out using primers GR88 & GR89 with a lower concentration of primer GR87. (b) As PDE3BΔ2 was constructed by PCR based methodologies it was sequenced in both directions along its full length. The predicted amino acid sequence from clone 66 is shown (top) aligned with the first 90 amino acids of PDE3B (bottom). The YTDIEMRNLGK motif is the VSV tag.

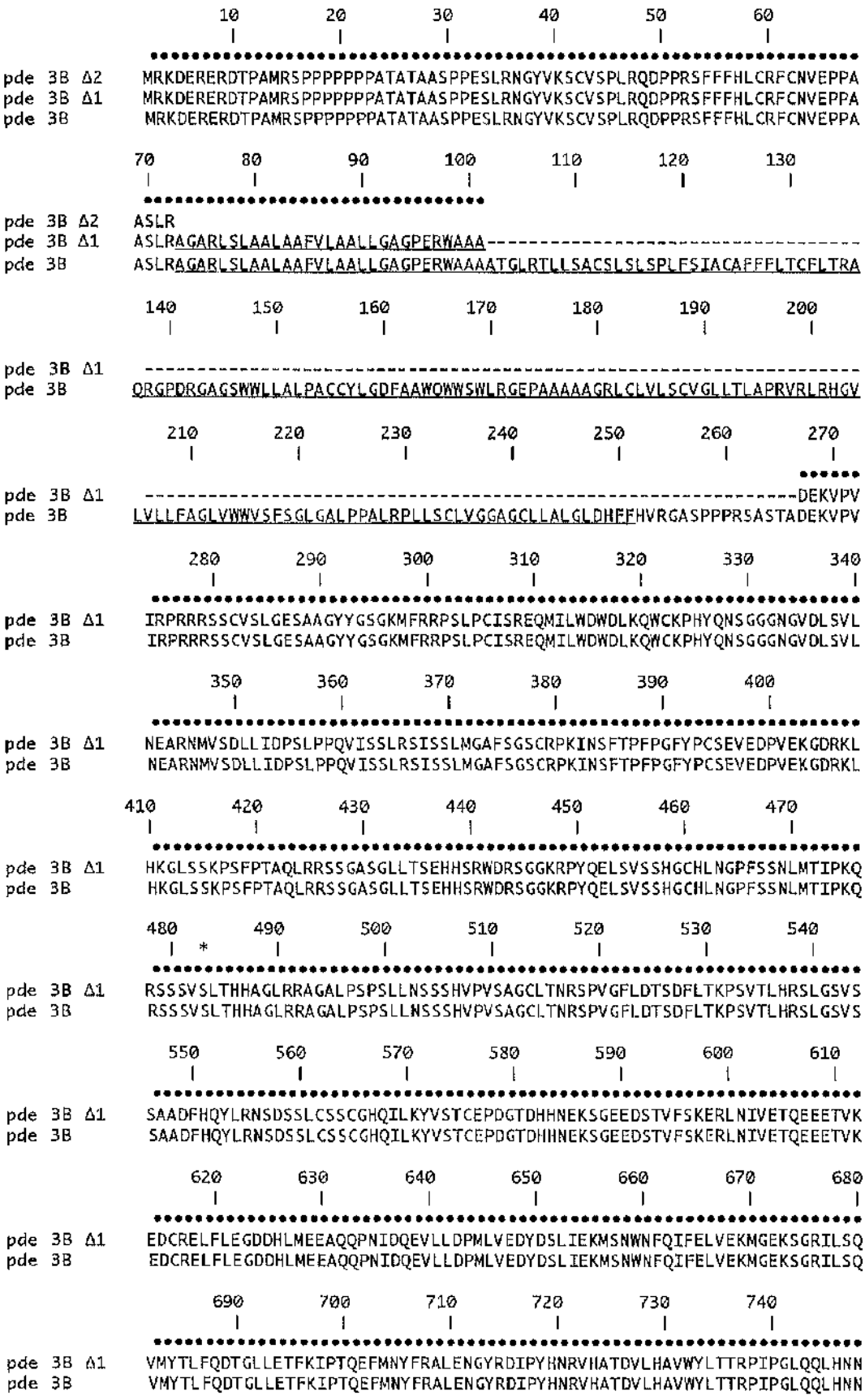
10 20 30 40 50 60
pde 3B Δ2 MRKDERERDTPAMRSPPPPPPPATATAASPPESLRNGYVKSCVSPLRQDPPRSFFFHLCRFCNVEPPA
pde 3B Δ1 MRKDERERDTPAMRSPPPPPPPATATAASPPESLRNGYVKSCVSPLRQDPPRSFFFHLCRFCNVEPPA
pde 3B MRKDERERDTPAMRSPPPPPPPATATAASPPESLRNGYVKSCVSPLRQDPPRSFFFHLCRFCNVEPPA
70 80 90 100 110 120 130
pde 3B Δ2 ASLR
pde 3B Δ1 ASLRAGARLSLAALAAFVLAALLGAGPERWAAA----------
pde 3B ASLRAGARLSLAALAAFVLAALLGAGPERWAAAATGLRTLLSACSLSLSPLFSIACAFFFLTCFLTRA
140 150 160 170 180 190 200
pde 3B Δ1 ----------
pde 3B QRGPDRGAGSWWLLALPACCYLGDFAAWQWWSWLRGEPAAAAAGRLCLVLSCVGLLTLAPRVRLRHGV
210 220 230 240 250 260 270
pde 3B Δ1 ----------DEKVPV
pde 3B LVLLFAGLVWWVSFSGLGALPPALRPLLSCLVGGAGCLLALGLDHFFHVRGASPPPRSASTADEKVPV
280 290 300 310 320 330 340
pde 3B Δ1 IRPRRRSSCVSLGESAAGYYGSGKMFRRPSLPCISREQMILWDWDLKQWCKPHYQNSGGGNGVDLSVL
pde 3B IRPRRRSSCVSLGESAAGYYGSGKMFRRPSLPCISREQMILWDWDLKQWCKPHYQNSGGGNGVDLSVL
350 360 370 380 390 400
pde 3B Δ1 NEARNMVSDLLIDPSLPPQVISSLRSISSLMGAFSGSCRPKINSFTPFPGFYPCSEVEDPVEKGDRKL
pde 3B NEARNMVSDLLIDPSLPPQVISSLRSISSLMGAFSGSCRPKINSFTPFPGFYPCSEVEDPVEKGDRKL
410 420 430 440 450 460 470
pde 3B Δ1 HKGLSSKPSFPTAQLRRSSGASGLLTSEHHSRWDRSGGKRPYQELSVSSHGCHLNGPFSSNLMTIPKQ
pde 3B HKGLSSKPSFPTAQLRRSSGASGLLTSEHHSRWDRSGGKRPYQELSVSSHGCHLNGPFSSNLMTIPKQ
480 * 490 500 510 520 530 540
pde 3B Δ1 RSSSVSLTHHAGLRRAGALPSPSLLNSSSHVPVSAGCLTNRSPVGFLDTSDFLTKPSVTLHRSLGSVS
pde 3B RSSSVSLTHHAGLRRAGALPSPSLLNSSSHVPVSAGCLTNRSPVGFLDTSDFLTKPSVTLHRSLGSVS
550 560 570 580 590 600 610
pde 3B Δ1 SAADFHQYLRNSDSSLCSSCGHQILKYVSTCEPDGTDHHNEKSGEEDSTVFSKERLNIVETQEEETVK
pde 3B SAADFHQYLRNSDSSLCSSCGHQILKYVSTCEPDGTDHHNEKSGEEDSTVFSKERLNIVETQEEETVK
620 630 640 650 660 670 680
pde 3B Δ1 EDCRELFLEGDDHLMEEAQQPNIDQEVLLDPMLVEDYDSLIEKMSNWNFQIFELVEKMGEKSGRILSQ
pde 3B EDCRELFLEGDDHLMEEAQQPNIDQEVLLDPMLVEDYDSLIEKMSNWNFQIFELVEKMGEKSGRILSQ
690 700 710 720 730 740
pde 3B Δ1 VMYTLFQDTGLLETFKIPTQEFMNYFRALENGYRDIPYHNRVHATDVLHAVWYLTTRPIPGLQQLHNN
pde 3B VMYTLFQDTGLLETFKIPTQEFMNYFRALENGYRDIPYHNRVHATDVLHAVWYLTTRPIPGLQQLHNN

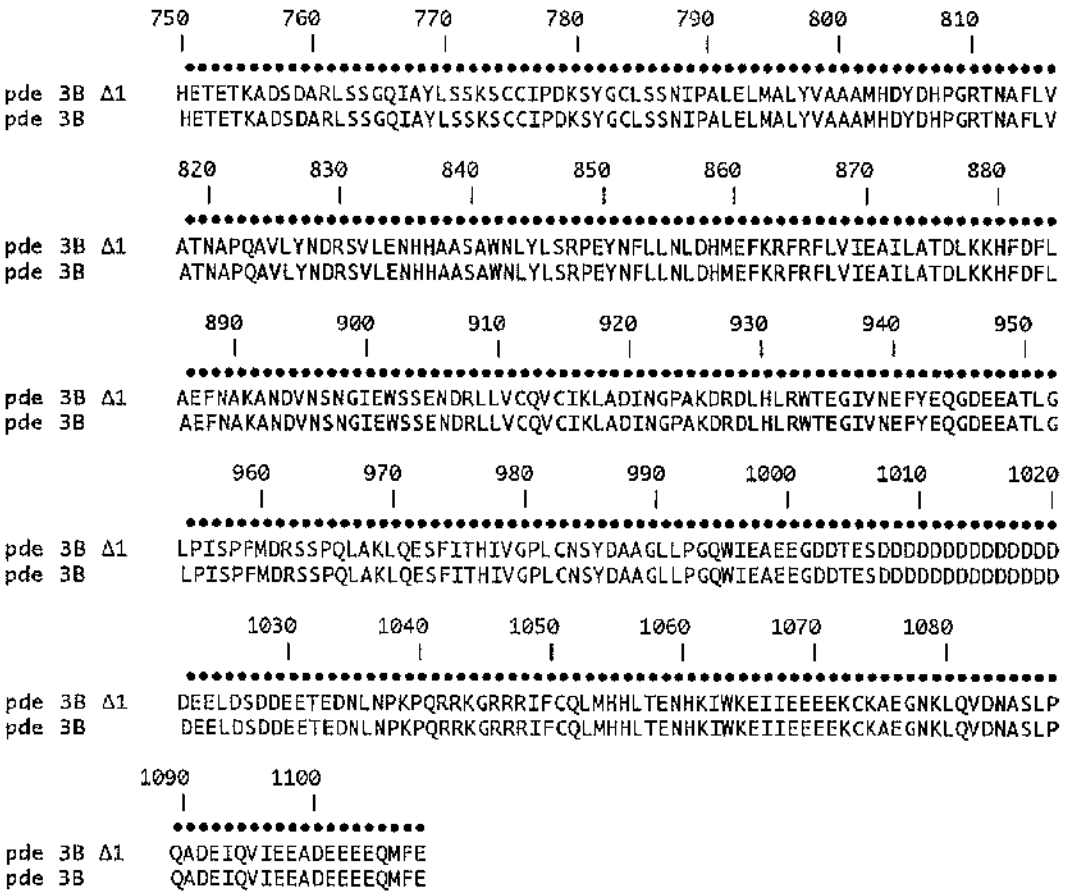

Figure 3.3.3.c Comparison of PDE3BΔ1 and PDE3BΔ2 sequence with PDE3B

PDE3BΔ1 and PDE3BΔ2 are shown compared to PDE3B. Note that PDE3BΔ2 also contains a VSV tag, but for simplicity the sequence is not shown here. The putative membrane association domain identified by Taira et al is underlined (54). The asterisk marks the start of a partially cytosolic construct made by Kasuya at al (52).

3.4. USE OF PDE3B AND VSV-G SPECIFIC ANTIBODIES TO STUDY THE MEMBRANE ASSOCIATION OF PDE3B, PDE3BΔ1 AND PDE3BΔ2

Lysates of COS cells transfected with PDE3B/pSV SPORT subjected to Western blotting by two different antibodies revealed an immunoreactive band of the same weight (~135kD) in both P1 and P2 fractions but not in the S2 fraction (figure 3.4.a.). There was no such immunoreactivity in lysates of mock transfected cells. Lysates of COS cells transfected with PDE3BΔ1 produced a ~120 kD band when they were immunoblotted with the same antibody (figure 3.4.a.). This protein was also exclusively particulate. In order to determine the relative detergent solubilities of PDE3B and PDE3BΔ1, particulate fractions from transfected COS cell lysates were subject to washes in 1% triton X-100 (figure 3.4.b,c). For both PDE3B and PDE3BΔ1 the P1 fraction could be partially solubilised (to about the same degree) but the P2 fraction was resistant to this. In contrast, PDE3B and PDE3BΔ1 particulate fractions from transfected COS cell lysates showed different sensitivity to washing with high ionic strength. Thus, PDE3B in either P2 or P1 fractions appeared to be insensitive to washing with buffer containing 2M NaCl (figure 3.4.1.d). In contrast, PDE3BΔ1 in either P2 or P1 fractions could be removed from particulate association by washing with high ionic strength (figure 3.4.1.e).

Mock transfected and PDE3BΔ2 transfected COS cell lysates were immunoblotted with a VSV specific monoclonal antibody. This antibody detected an immunoreactive species of the correct size in transfected whole cell lysates. This species was not apparent in mock transfected lysates. Immunoblots performed on fractionated PDE3BΔ2 transfected COS cell lysates demonstrated that this construct was found exclusively in the cytosolic fraction (figure 3.4.1.f).

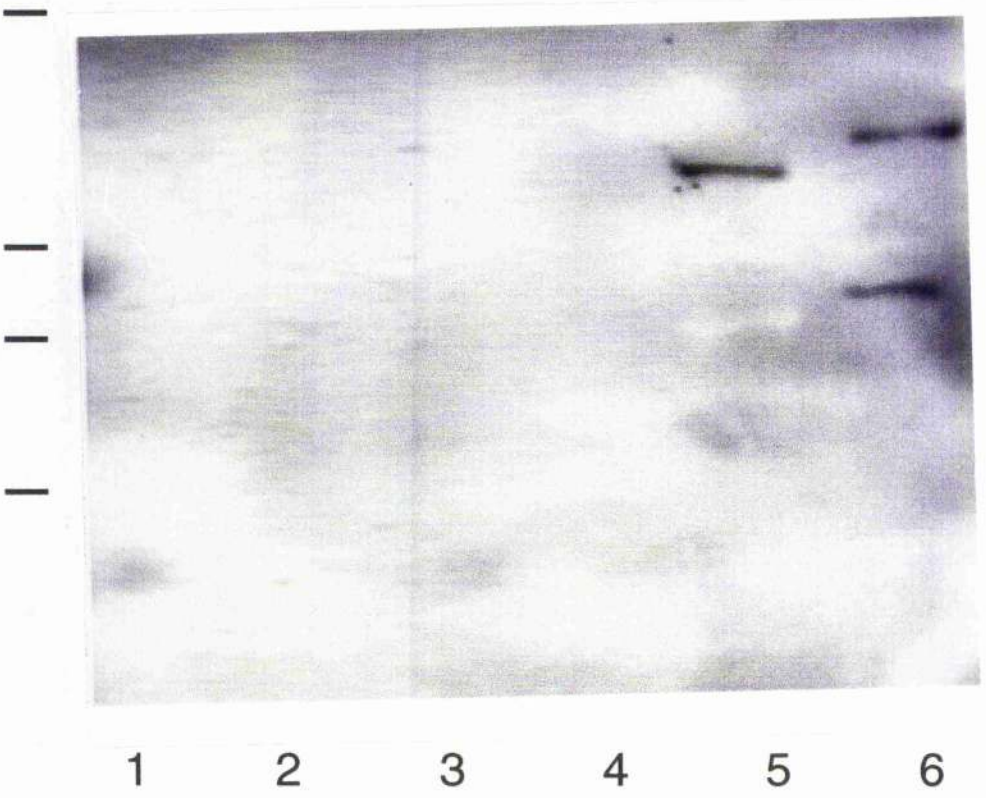

Figure 3.4.a. PDE3B specific antibodies detect PDE3B and PDE3BΔ1 in transfected COS cell lysis fractions.

S2 (lanes 1-3) and P2 (lanes 4-6) fractions were prepared from various COS-7 cell lysates. These fractions, from COS-7 cells which were mock-transfected (lanes 1 and 4), transfected with PDE3BΔ1/pSV SPORT (lanes 2 and 5), or transfected with PDE3B/pSV SPORT (lanes 3 and 6) were subject to immunoblotting with a PDE3B specific antibody. This was an IgG purified polyclonal antibody raised to the C-terminal of PDE3B. This antibody does not cross-detect PDE3A (56). Primary antibody was used at a concentration of 1/500. Secondary antibody was used at a concentration of 1/2500. For each sample, the same amount of S2 protein was loaded and the proportionate amounts of P2 sample were loaded. The positions (from the top) of the 200kD, 100kD, 75kD and 43kD markers are shown

Buffer		1% TRITON		NO TRITON			1% TRITON		NO TRITON	
Fraction	S2	P2	WASH	P2	WASH	M	P1	WASH	P1	WASH

Figure 3.4.b. Detergent solubilisation of PDE3B from P1 and P2 particulate fractions of transfected COS cell lysates

Particulate fractions of lysates of COS cells transfected with PDE3B/pSV SPORT were washed with various buffers prior to immunoblotting with a PDE3B specific antibody. Lanes are labelled P1, P2 or S2 to denote the lysate fraction and the solubilisation treatment is also shown. PDE3B is marked with an arrow. Immunoblotting of PDE3B is with an N-terminal PDE3B specific polyclonal antibody. This antibody does not cross-detect PDE3A (56). Primary antibody was used at a concentration of 1/2000. Secondary antibody was used at a concentration of 1/2500. For each sample, equal amounts of S2, P2 and P1 samples were loaded. M denotes a marker lane.

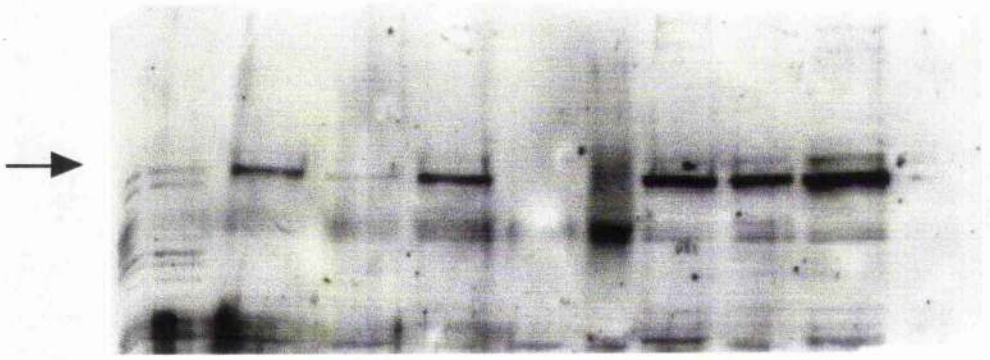

Buffer		1% TRITON		NO TRITON			1% TRITON		NO TRITON	
Fraction	S2	P2	WASH	P2	WASH	M	P1	WASH	P1	WASH

Figure 3.4.c. Detergent solubilisation of PDE3BΔ1 from P1 and P2 particulate fractions of transfected COS cell lysates

Particulate fractions of lysates of COS cells transfected with PDE3BΔ1/pSV SPORT were washed with various buffers then subject to immunoblotting with a PDE3B specific antibody as in figure 3.4.1. Lanes are labelled P1, P2 or S2 to denote the lysate fraction and the solubilisation treatment is also shown. PDE3BΔ1 is marked with an arrow. Immunoblotting of PDE3BΔ1 is with the C-terminal PDE3B specific antibody which was used as in figure 3.4.a. Primary antibody was used at a concentration of 1/500. Secondary antibody was used at a concentration of 1/2500. For each sample, equal amounts of S2, P2 and P1 fraction were loaded. M denotes a marker lane.

Buffer	No Na Cl		1M Na Cl		No Na Cl		1M Na Cl	
Fraction	P2	WASH	P2	WASH	P1	WASH	P1	WASH

Figure 3.4.d. Treatment of particulate PDE3B with high ionic strength buffers: use on P1 and P2 particulate fractions from transfected COS cell lysates

Particulate fractions of lysates of COS cells transfected with PDE3B/pSV SPORT were washed with various buffers then subject to immunoblotting with the C-terminal PDE3B specific antibody as in figure 3.4.1. Lanes are labelled P1, P2 or S2 to denote the lysate fraction and the solubilisation treatment is also shown. Immunoblotting of PDE3B is with the N-terminal PDE3B specific antibody which was used as in figure 3.4.b. Primary antibody was used at a concentration of 1/500. Secondary antibody was used at a concentration of 1/2500. For each sample, equal amounts of P2 and P1 fraction was loaded.

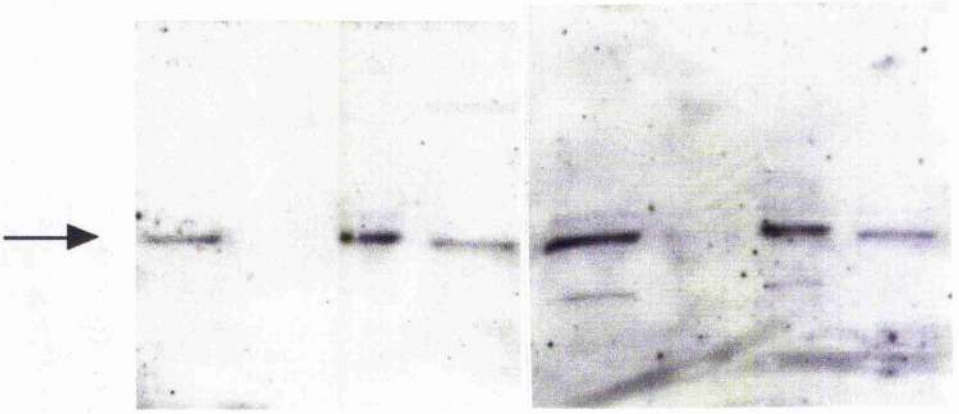

Buffer	No Na Cl		1M Na Cl		No Na Cl		1M Na Cl	
Fraction	P2	WASH	P2	WASH	P1	WASH	P1	WASH

Figure 3.4.e. Treatment of P1 and P2 particulate fractions of transfected COS cell lysates with high ionic strength to evaluate the solubilisation of PDE3BΔ1.

Particulate fractions of lysates of COS cells transfected with PDE3BΔ1/pSV SPORT were washed with various buffers then subject to immunoblotting with a PDE3B specific antibody. Lanes are labelled P1, P2 or S2 to denote the lysate fraction and the solubilisation treatment is also shown. Immunoblotting of PDE3BΔ1 is with the C-terminal PDE3B specific antibody which was used as in figure 3.4.a. First antibody was used at a concentration of 1/500. Second antibody was used at a concentration of 1/2500. For each sample, equal protein concentrations of P2 were loaded. P1 fraction was loaded at an amount 1:3 lower than the P2 fraction.

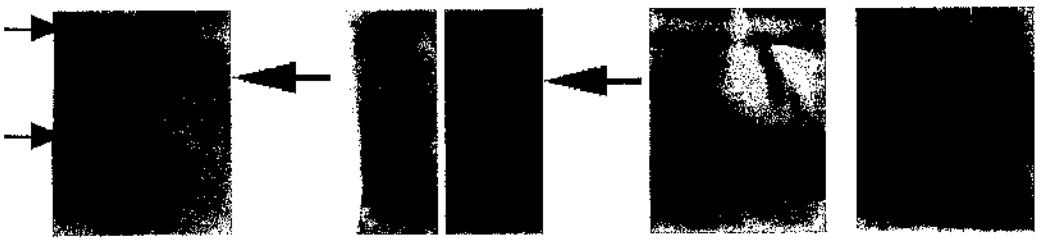

SAMPLE:									
WHOLE CELL			S2			P1			P2	
MOCK	Δ2		MOCK	Δ2		MOCK	Δ2		MOCK	Δ2
FRACTION:										

Figure 3.4.f. PDE3BΔ2 localisation in fractions of transfected COS cell lysates

COS-7 cells were transfected with PDE3BΔ2/pCR3.1. Whole cell lysates and P1, P2 and S2 fractions of lysates of these cells were immunoblotted with a VSV specific monoclonal antibody. Fractions from mock transfected cells were immunoblotted for comparison. First antibody was added at 1/250 dilution. Second antibody dilution was 1/500. The small arrows on the left show the positions of the marker for 16kD (top arrow) and 6.5kD (bottom arrow). The larger arrows denote a band of the predicted size which is not found in untransfected COS-7 cells. For each sample, the same amount of P1 protein was loaded and the proportionate amounts of P2 sample was loaded. Whole cell lysates and S2 fractions are 4 times more dilute than these fractions.

3.5 STUDIES ON PDE3B ACTIVITY: A NOVEL, CILOSTIMIDE-INHIBITABLE PDE ACTIVITY OBSERVED IN COS-7 CELLS TRANSFECTED WITH PDE3B/pSV SPORT

Cilostamide inhibitable (PDE3) activity in untransfected COS cells is 18 ± 3 pmol cAMP hydrolysed/min/mg of protein (n=3 separate transfections). All of this activity was restricted to the S2 fraction. When PDE3B/pSV SPORT was transfected into COS-7 cells a novel, cilostimide inhibitable PDE3 activity was observed. The amount of extra PDE3 activity observed varied between transfections and was 5-15 fold greater than the endogenous PDE3 activity such that the observed cilostamide-inhibitable activity was 96-270 pmol cAMP hydrolysed/min/mg of protein (n=6 separate transfections). Replicate transfections performed side by side had much less variation in the amount of PDE3 activity they exhibited. Transfection of PDE3B/pSV SPORT into COS-7 cells did not increase non-PDE3 activity.

3.5.1. Triethanolamine/KCl treatment partially solubilises PDE3B

COS cells transfected with PDE3B/pSV SPORT, were washed with triethanolamine/KCl buffer prior to homogenisation in KHEM buffer. The lysates were fractionated and the activity in high speed particulate (P2) and supernatant (S2) determined. It was found that approximately equal amounts of PDE3 activity was present in the S2 and the P2 fractions (The ratio of activities S2:P2 was 57:43). Furthermore, immunoreactivity was now detectable in soluble fractions, albeit less than that detected in the P2 fraction (figure 3.5.1.).

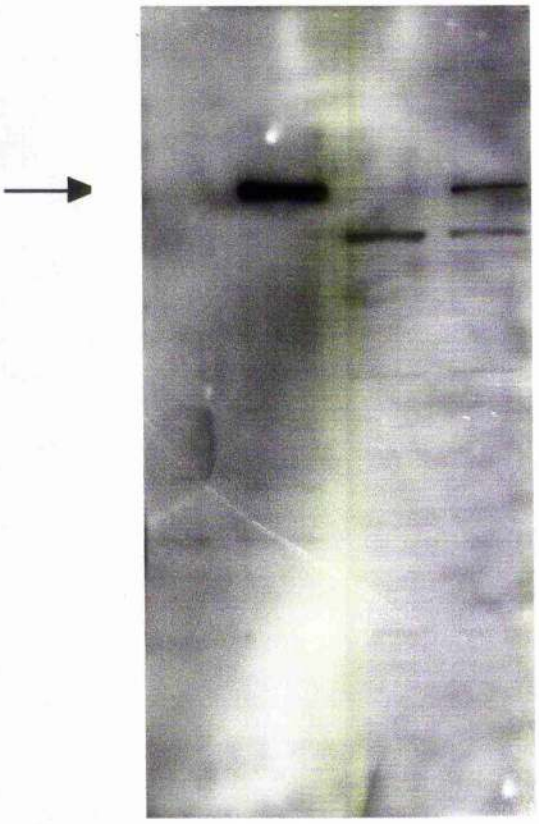

Fraction	P2		S2	
Transfection	Mock	PDE3B	Mock	PDE3B

Figure 3.5.1. Solubility of PDE3B protein in lysates of COS-7 cells washed in TEA/KCl prior to homogenisation

COS-7 cells were incubated in TEA/KCl at 4°C for 10min. They were then washed twice and fractionated. P2 and S2 fractions from these cells and from mock transfected cells were immunoblotted. Immunodetection was performed using PDE3B specific N-terminal antibody (see figure 3.4.b.) PDE3B is identified with an arrow

3.5.2. The insulin mimetic pervanadate cannot stimulate total phosphodiesterase activity in serum-starved TEA/KCl treated PDE3B/PKB cotransfection bulk fractions.

The effect of pervanadate was determined on the total PDE activity in S1 fractions of COS-7 cells cotransfected with PDE3B/pSV SPORT and plasmids containing either kinase-active PKB (PKB+) or kinase-dead PKB (PKB-). The reaction and lysis buffers contained phosphatase inhibitors and cells were serum starved for 12 hours prior to treatment for 15 min with pervanadate and subsequent lysis. On five separate occasions no significant effect of pervanadate treatment on total PDE activity (figure 3.5.2.) was observed. However, the active PKB cotransfections had significantly more PDE activity than kinase dead PKB transfections (see figure 3.5.2.)

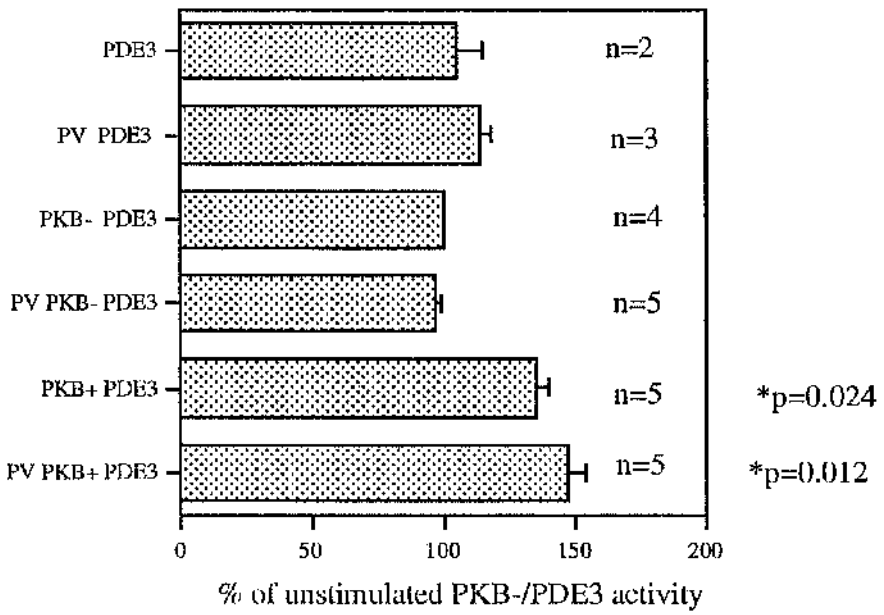

Figure 3.5.2. Effect of pervanadate treatment on total PDE activity of COS-7 cells.

COS-7 cells were transfected with PDE3B alone (PDE3) or co-transfected with PDE3B (PDE3) and kinase active PKB (PKB+ PDE3) or PDE3B with kinase dead PKB (PKB- PDE3). Cells were then treated with pervanadate (PV) prior to lysis. Total PDE activity of lysates was measured. Student's paired T-test was performed to assess significance of the increased activity in PKB+ co-transfections compared to PKB- co-transfections.

3.5.3. Pervanadate up-regulates PDE3 phosphodiesterase in COS-7 cells cotransfected with PDE3B and PKB+ but not in COS-7 cells cotransfected with PDE3B and PKB-

The protocol detailed in section 3.5.2. was now modified in a number of ways.

1. Since PDE3B is found only in particulate fractions of adipocytes (172) and TEA/KCl apparently released PDE3B from COS-7 particulate fractions, the TEA/KCl step in cell lysis was omitted because this apparently resulted in non-physiological release of PDE3 protein. This may have effected its regulation (see below).

2. P2 fractions were taken for study instead of S1 fractions. In adipocytes, the P2 fraction is the only insulin sensitive subset of PDE3 activity (172). In addition, PDE3B western blots and activity data suggest that the P2 population of PDE3B is less active than the solubilised S2 population. This could be taken to imply, although it does not necessarily follow, that the membrane bound fraction has a greater capacity to be activated.

3. Based on the assumption that transfected PDE3B is active without any treatment, the PKA inhibitor H89 was added at concentrations which have been shown to block PKA mediated activation of PDE3B in other systems (63). This was done to prevent any unquantifiable PKA-mediated stimulation of PDE 3B occurring under basal conditions (see figure 3.2). For the same reason, phosphatase inhibitors were omitted from the reaction buffer, so as to heighten the threshold of kinase activation required to stimulate PDE 3B;

4. Cilostimide inhibitable activity was measured instead of total PDE activity. There is apparently no endogenous PDE3 activity expressed in P2 fractions. This suggests that all the cilostamide-inhibitable P2 PDE activity measured in COS-7 cells transfected with PDE3B/pSV SPORT is due to the recombinant PDE 3B. Any effects in this subset of PDE activity should thus become more obvious.

Using this protocol a ~2-3 fold up-regulation of the P2 fraction of PDE3 activity due to pervanadate was observed in co-transfections with kinase-active PDE3B. This did not occur in co-transfections with kinase-dead PKB (figure 3.5.3).

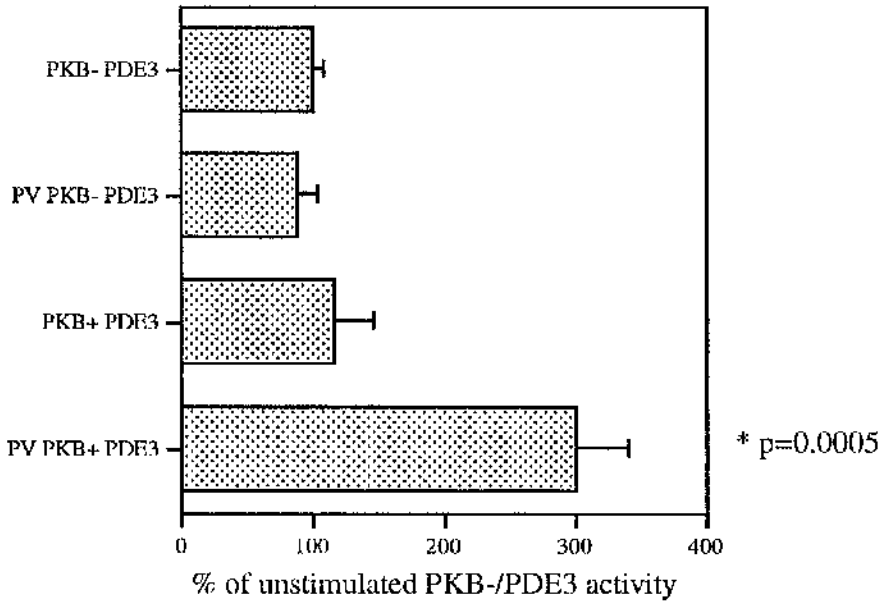

Figure 3.5.3. Pervanadate treatment of P2 fractions of mechanically lysed COS-7 cell transfections

Serum starved COS-7 cells were treated with pervanadate (PV) and the effect on cilostamide inhibitable activity measured in the P2 fraction. COS-7 cells were mock co-transfected with PDE3B (PDE3) and kinase active PKB (PKB+ PDE3) or PDE3B with kinase dead PKB (PKB- PDE3). Student's paired T-test was performed to assess significance.

CONCLUSION

3.6. PARTICULATE FULL-LENGTH PDE3B CAN BE SOLUBILISED IN COS-7 CELLS

In this study I have characterised three constructs made from the rat PDE3B cDNA rcGIP-1. The complete cDNA was subcloned into the mammalian expression vector pSV SPORT and the integrity of the open reading frame verified. Two more constructs, PDE3BΔ1 and PDE3BΔ2, were made which lack certain regions of the reading frame. On transfection of these plasmids into COS-7 cells the proteins encoded by these plasmids can be detected by immunoblotting with specific antibodies. PDE3B has also been detected as PDE3 activity.

In conditions of low ionic strength and absence of detergent similar to those used here, others (56,172) have reported that PDE3B was exclusively particulate and the data presented here concurs with this. Thus I was unable to detect any soluble PDE3B under similar conditions.

Under conditions of high ionic strength or in the presence of non-ionic detergent, PDE3B activity has been shown to be solubilised from the particulate fractions, albeit to varying degrees depending on the cell type (56) (see table 3.6). Immunoblotting of two membrane fractions from COS-7 cells showed that the solubility of PDE3B within these fractions varied too. Thus particulate fractions which sediment at 3500g (P1, leaving a soluble S1 fraction) contained PDE3B which could be readily solubilised by detergent but not by high ionic strength. This solubilisation probably does not reflect detergent-mediated release of soluble PDE3 from unbroken cells because, in the conditions used, there was little or no cytosolic PDE3B. On this basis it can be assumed that this PDE activity reflects a genuine release of full length PDE3B from the COS-7 cell low speed particulate fraction, rather than release of entrapped cytosolic enzyme.

A second particulate fraction was obtained by centrifugation of the S1 fraction at 100000g (P2). In contrast to the data obtained in the P1 fraction, PDE3B in the P2 fraction was not solubilised in detergent nor in high ionic strength. This is the first evidence that pools of PDE3B may associate differently with different membranes in

the same cell. Thus the partial solubilities of whole cell particulate PDE3B (all the data from Leroy et al and Kasuya et al (52,56) in table 3.6 used single particulate fractions) may in part be due to them containing heterogeneous pools of particulate PDE3B which associate with the membrane in different ways, as has been proposed to explain the differences in PDE3B solubilities between cells (56). The differences in the P1 and P2 PDE3B solubilisation are consistent with the notion that membrane bound PDE3 exists in at least two states as has been suggested by others (52,56). Pertinent to this finding, adipocyte fractionation showed that adipocyte PDE3 is found in both the plasma membrane and in the endoplasmic reticulum (ratio 20:80) (191). It would be interesting to see whether the two states of membrane binding and of targeting (191) reflect the same division of PDE3B and if so, to pursue the mechanism by which alternative targeting of these conformers alters membrane association.

Data was also obtained which was consistent with the notion that extracellular addition of triethanolamine can partially solubilise PDE3B from membranes. Though there is evidence that triethanolamine can enter cells through channels (192) and that triethanolamine can alter cytoskeletal structure (193), the molecular bases of these phenomena are not yet well understood and therefore the solubilisation effect on PDE3B was not pursued.

The data presented in this chapter are the first presentation of immunoblots of solubilised full-length PDE3B because the two previous studies presented activity data only (52,56). The use of immunoblots is an important refinement, inspired by previous studies that were only able to establish the unequivocal membrane association of the PDE4A RD1 by immunoblotting in place of activity measurements (110,112). The previous works on PDE3 membrane association are open to two criticisms that solubilised PDE3 activity may not be due to solubilised full length PDE3. (1) The soluble activity may represent truncated forms of PDE3A or PDE3B which are known to exist in real cells by alternative splicing (174) and which are likely to be present also in recombinant systems due to aberrant translation initiation events at methionines downstream of the true initiator methionine (56). These forms are known to be partially particulate (52,56) but are more readily solubilised than the full length forms

(56). By weight on the immunoblot, release of full-length PDE3B could be studied in isolation. The soluble activity measured could also be due to full-length or truncated PDE3A species but again, the immunoblot analyses employed in this study used antibodies specific for PDE3B (56) and thus PDE3B solubility was studied in isolation. (2) The release of activity from particulate fractions probably overestimates the amount of PDE3 mobilised because the activity data obtained here, and that presented in previous work (52,56), supports the notion that solubilised PDE3 activity is ~2 times more active than when it is associated with the membrane and therefore a calculation of solubilisation due to activity release will overestimate the amount of PDE3 protein released.

Thus, by use of immunoblotting this work is the first unequivocally to demonstrate mobilisation of full-length PDE3B or indeed any full-length PDE3 from a particulate fraction. By finer fractionation of cells than previously, novel intracellular variations in the membrane association of PDE3B have been demonstrated. The significance of these findings is discussed below.

Material Source	Fraction Examined	Solubility in detergent	Solubility in Na Br	Solubility in Detergent & Na Br	Reference
Adipocyte[1]	100000g P1	38%	16%	89%	(56)
NIH3006 Fibroblast[1]	100000g P1	23%	10%	64%	(56)
NIH3006 Fibroblast[1]	whole cell	71-87%	18-23%	n.d.	(56)
Sf9 cells[1,2]	whole cell	n.d.	n.d.	20-30%	(52)
COS-7	3500g P1	~50%	none detected[3]	n.d.	This study
COS-7	100000g P2	<5%	none detected[3]	n.d.	This study

[1] These studies use activity measurements and so are only a guide to the true proportions of soluble PDE3B since soluble PDE3 is more active than particulate PDE3 (52,56) (see section 3.6)

[2] These studies were on PDE3A but on the basis that regions of the N-terminal of PDE3A and PDE3B are conserved it has been suggested that these results may also apply to PDE3B

[3] In the experiments in this chapter 1000mM Na Cl was used in place of 500mM Na Br

n.d. = not determined

Table 3.6. Summary of effects of detergent and high ionic strength on the membrane association of full length PDE3

3.7. DELETION OF THE PUTATIVE INTEGRAL MEMBRANE BINDING DOMAIN EFFECTS SOLUBILITY OF PDE3B.

The particulate nature of full length PDE3B in conditions of low ionic strength and low detergent has already been discussed as has the fact of increasing solubility with greater N-terminal truncations of PDE3 (52,56). A new truncation construct, PDE3BΔ1, which removes 150 amino acids (amino acid residues 101 to 266) of the hydrophobic putative N-terminal integral membrane binding domain, also altered some aspects of PDE3 solubility. Similarly to PDE3B all of the PDE3BΔ1 was particulate in low ionic strength and the absence of detergent. The P1 and P2 fractions also showed the same differences in detergent solubility that were seen for the full length PDE3B. On this basis the truncation did not eliminate the triton soluble membrane-association domain. This could either be because PDE3BΔ1 has a large enough remnant of the putative domain's amino acids for an integral membrane helix (173) or because a triton soluble domain resides elsewhere in the N-terminal 600 amino acids of PDE3B. Yet, despite these similarities between PDE3B and PDE3BΔ1, the latter was found to be soluble in high ionic strength, in contrast to the resilience of PDE3B to this treatment.

3.7.1. Central sequences of PDE3B harbour a membrane association domain which is sensitive to ionic strength.

As shown in figure 3.3.3.c, PDE3BΔ1 contains extra N-terminal sequences on either side of the putative membrane association domain when it is compared to the truncations used by Kasuya et al (52) or by Leroy et al (56) (the beginning of the largest of the largest construct used by Kasuya et al (52) or Leroy et al (56) is marked with an asterisk in figure 3.3.3.c.) PDE3BΔ2 was designed to express the 73 amino acids preceding the putative membrane association domain (see figure 3.3.3.c.) to test whether this sequence could associate with the membrane. It was found that this sequence is entirely soluble.

These studies on PDE3B, PDE3BΔ1 and PDE3BΔ2 in COS-7 cells are consistent with the existence of a novel membrane association domain sensitive to

ionic strength. This domain is located towards the middle of PDE3B, beyond the sequence already proposed and also outside of the first 73 residues of PDE3B. It is therefore likely to be present between residues 267 and around 600 (since 613 is the start point of the longest totally soluble PDE3 (56)). This triton insoluble domain is evident in all PDE3B association with the P2 fraction but not all association with the P1 fraction PDE3B because a component of this fraction is triton soluble. Such a domain is implicit in previous data (52,56) and could explain why detergent treatment solubilises particulate PDE3 from different sources incompletely and variably (see table 3.6) (52,56). The ion-strength soluble domain at least does not coincide with the putative integral membrane binding domain (54) or with the extreme N-terminal of PDE3B. With the caveats given in the previous section (section 3.7) this may be true of the membrane association functioning through hydrophobic interactions ablated by triton. It is possible that the two putative domains are both found within residues 267-600. This region of PDE3B is in fact the next best conserved between PDE3A and PDE3B after their catalytic domains, with conservation exceeding that of Taira's putative membrane association domain (27% amino acid identity versus 22% for the Taira's putative membrane association domain and 8% for the extreme N-terminal sequence which contains all the sequence of PDE3BΔ2 (58), see figure 1.6.1). This conservation may be in part due to the existence of a conserved membrane binding determinant.

3.7.2. Future work

This work was discontinued as a result of a collaboration breaking down. Future work to show the distribution of the ionic-strength sensitive domain should involve reassessment of the solubility of finer fractions of PDE3B activity in cell types already examined, NIH3006 and adipocytes. These studies should use immunoblots, not activity readings as a measure of the amount of PDE3B solubilised. Existing nested N-terminal deletion constructs (174) could then be used to map more precisely the position of the domain in PDE3B. Once it is known which parts of the protein are responsible for which components of the membrane association, it should be easier to

study these functions exhaustively. The figure (3.7.2) below summarises the effects of this work in this mapping.

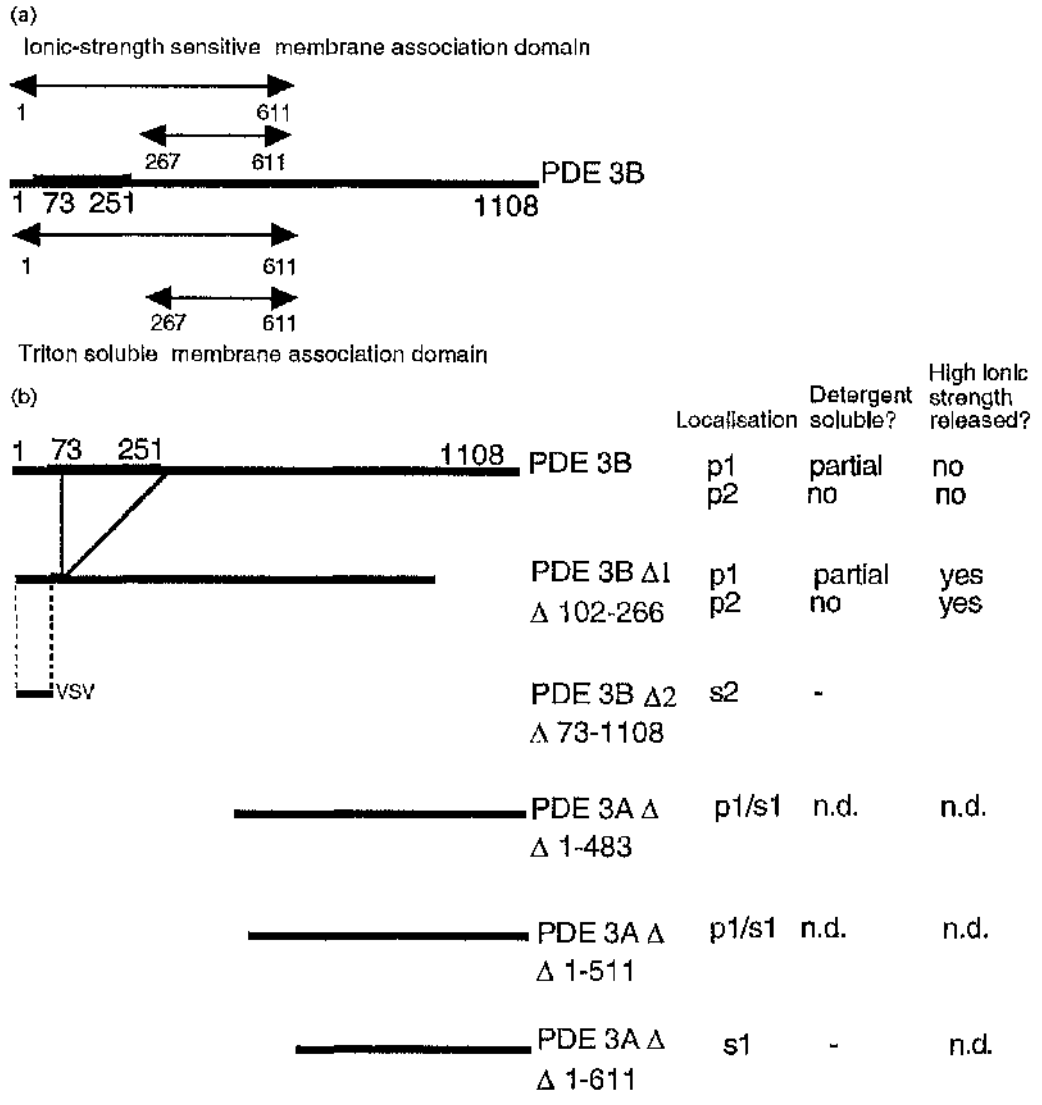

Figure 3.7.2. Schematic summary of membrane binding determinants in PDE3

(a) Above full length PDE3, with its putative membrane association domain shown in thick line (54), are the limits for the triton insoluble membrane association domain before (top) and after (bottom) the data presented in this chapter. Arrows beneath PDE3B show the same information for the triton soluble component of membrane association. (b) The schematic constructs summarise localisation and solubility information for PDE3 constructs; those for PDE3B are from this chapter, those from PDE3A are from (52,56).

3.8 PERVANADATE TREATMENT ACUTELY ACTIVATES PDE3B ACTIVITY FOLLOWING COTRANSFECTION WITH PKB+

Following treatment of cells with pervanadate, PDE3B/PKB+ cotransfections show a 2-3 fold increase in PDE3 activity in the particulate fraction P2. This effect is apparently specifically due to PKB because identical cotransfections of PDE3B which replace PKB+ with PKB- did not show a similar increase in PDE3 activity. Previous studies on P2 fractions which have shown a similar up-regulation of PDE3B activity have claimed it as an activation. The increased total PDE activity in S1 samples of kinase active PKB/PDE3B cotransfections versus kinase dead PKB/PDE3B cotransfections is certainly consistent with an overall up-regulation of PDE activity due to kinase active PKB transfections compared to kinase-dead. The activation in P2 compares favourably with other stimulations of PDE3 (49,172,177-179,182,183,191,194). This preliminary result suggests that PKB is capable of activating PDE3B under the regulation of the insulin mimetic pervanadate. My finding is therefore consistent with the notion that insulin signals to PDE3B in a kinase cascade which includes PKB. Recent published data supports this finding. Thus, Wijkander et al (195) have shown that PKB and the PDE3IK, whose activity was measured by *in vitro* assay, have the same chromatographic properties. It has also been shown that PKB and PDE3IK translocated to the membrane in response to pervanadate (195), this is the same stimulus as I used.

3.8.1 Future experiments

Now that PKB has been implicated in PDE3B signalling, it is important to reproduce these experiments in adipocytes or an adipocyte cell line. An additional tool which would be very useful for examining *in vivo* PKB signalling would be a specific inhibitor for this kinase. Demonstration of this putative signalling pathway in the correct physiological context may allow other crucial questions to be answered.

First, the inhibitor H7 is a potent inhibitor of PKA and PKC but several papers purport that this is not the case for PDE3IK (177-179). PKB is most closely conserved with PKA and PKB amongst the kinases and thus it is probable that PKB is

also a target for H7. Thus, if the data of Shibata et al (177-179) were true it would argue that PKB does not lie in the true physiological path of signalling from insulin to PDE3B. However, when Shibata et al used very high concentrations of H7 (178,179) they obtained it from Sigma and this supply was subsequently shown to be considerably less potent than advertised (196). It might therefore now be worthwhile reassessing the potency of H7 in inhibiting PDE3IK. The inhibitor H89 used in this study is more specific for PKA and thus it is less likely that this inhibitor will inhibit PKB

Second, the single site of activation and phosphorylation of PDE3B is at serine 302. This site is not likely to be a PKB site and thus there would have to be at least one other step between PKB and PDE3B in this scheme. Indeed, PKB appears not to phosphorylate PDE3B at serine 302 (195). The existence of a specific inhibitor for PKB might facilitate identification of this new PKB target.

USE OF DEGENERATE REVERSE TRANSCRIPTION POLYMERASE CHAIN REACTION TO IDENTIFY A PROTEIN KINASE C-INDUCED Ca^{2+}/CaM STIMULATED CYCLIC NUCLEOTIDE PHOSPHODIESTERASE FOR WHICH NO SEQUENCE WAS AVAILABLE

INTRODUCTION

4.1. A PROTEIN KINASE C MEDIATED INDUCTION OF PDE1 ACTIVITY

The cyclic AMP and lipid signalling pathways both provide major routes for controlling cellular function (20,197,198). Recently it has become established that interplay between these systems modulates the functioning of regulatory pathways, which has given rise to the notion of 'cross-talk' (10). Protein kinase C appears to play a key role in mediating such interactions between the lipid and cyclic AMP signalling system.

Protein Kinase C (PKC) activity is provided by a multi-gene family, the protein products of which are grouped on the basis of their distinct structural and biochemical properties (199,200). 'Conventional' PKCs (α, βI, βII and γ) are calcium and diacylglycerol (DAG) sensitive whereas 'non-conventional' PKCs (ε, δ, θ, μ and η) are calcium-insensitive. There are also atypical PKCs (ζ,λ,τ) which are structurally related to the other PKCs but whose activities are not regulated by either DAG or phorbol esters (201). There is evidence that particular PKC isoforms may have discrete functional roles, which is consistent with their exhibiting distinct biochemical characteristics and tissue distributions (199,200). This is seen in the various cell specific effects of PKC on cAMP signalling (10)

PKC regulates cAMP concentrations in many ways. It can modulate the functioning of stimulatory and inhibitory receptors (10), the inhibitory G protein G_{i-2} (5,10,202) and adenylate cyclase itself (10,203-205). An example of selectivity in such processes is that both PKCζ and PKCα can selectively activate a specific adenylyl cyclase isoform, namely adenylyl cyclase V (203). Additionally, the ability of

PKC to attenuate the action of the inhibitory G-protein G_i appears to show cell specificity (5,10,202). There is also evidence that PKC may effect the activity of PDEs in certain cells (10,206).

The presented study originated from an observation made by Dr S. Spence in this laboratory, namely, that PMA and ligands able to activate lipid signalling processes can generate a rapid induction of calcium/calmodulin stimulated phosphodiesterase (PDE1) activity in chinese hamster ovary cells. This appeared to be a novel PDE activity because wild-type chinese hamster ovary cells (CHO-K) and chinese hamster cells which had been stably transfected to overexpress the insulin receptor (CHO-T cells), demonstrated cAMP phosphodiesterase activity which was insensitive to Ca^{2+}/CaM (50μM 20ngml^{-1}), indicating an absence of PDE1 activity (163). However, when CHO-K or CHO-T cells were challenged for 6h with the protein kinase C activator PMA (10 nM), the actinomycin D attenuable appearance of PDE1 activity was detected (163). This is consistent with a novel PDE1 activity being produced de novo by induced transcription. This novel PDE1 activity was apparent within 25min, reached a maximum after a number of hours and then declined, thus being transient in nature. Additionally CHO-T cells stably expressing PKC α or PKC ε exhibited elevated PDE activity which is entirely attributable to Ca^{2+}/CaM- stimulated PDE1 activity, whereas CHO-T cells stably transfected with PKC βI or PKC γ exhibited PDE activity similar to untransfected CHO-T cells (163). This was taken to suggest that transcriptional control of this PDE gene may be regulated by specific PKC isoforms in CHO cells. Such an ability to induce novel PDE1 enzyme is not restricted to PMA but could also be seen with occupancy of endogenous receptors which are known to be coupled to lipid-signalling processes which produce DAG. These include agonists for endogenous P_2-purinoreceptors, lysophosphatidic acid receptors and thrombin receptors (207).

4.2. DESIGN OF MOLECULAR PROBES FOR USE IN GENETICALLY UNDER-CHARACTERISED SYSTEMS

The identity of the PDE1 isoform involved in the PDE1 induction in chinese

hamster ovary cells was not known. Therefore I set out to identify which of the three PDE1 genes (see Introduction) was involved. As with any system which is not a major genetic model such as human and rat, the problem here is one of molecular probe design. Antisera able to detect PDE1 in a species independent fashion are unavailable. Furthermore, when this work was initiated, there was no published PDE1 sequence from chinese hamsters. The absence of these data precluded analysis of protein by Western blotting or of transcripts by Northern blotting. By a rigorous rational application of information from the model species I was able to design low degeneracy PCR probes able to detect PDE1 forms in a range of species.

It is usual to design primers for unknown genes to the sequences of known homologues, using conserved sequence containing several low redundancy codons, for example, those that code for phenylalanine. Then degeneracy can be minimised using codon usage tables for the particular organism. However, the final primer design is still often highly degenerate and the effectiveness of such primers in RT-PCR may be reduced because of this. This is presumably because of the dual effects of more non-specific reactions occurring and a lower effective concentration of cognate primer. Furthermore, low degeneracy codons on which this approach depends, code for rare amino acids such as tryptophan, histidine, cysteine and this, necessarily, seriously restricts sequences which can be used for such an approach (figure 4.2).

To circumvent these problems I adopted a modified rationale in probe design. Selection of sequence conserved between two PDE1 genes (PDE1A & PDE1B) from various species but differing from other closely related genes, aimed to identify very highly conserved regions of sequence since it is to be expected that sequences well conserved between genes will also be conserved between species. Having identified such sequences, probes for use in RT-PCR analyses could be designed to detect the lowest redundancy codons in this conserved gene sequence. Primers designed in this way would thus be far less degenerate. Using such an approach I was able to selectively detect PDE1 transcripts in a range of species. This was despite the absence of enough published information to identify phylogenetically conserved PDE1A

specific sequence.

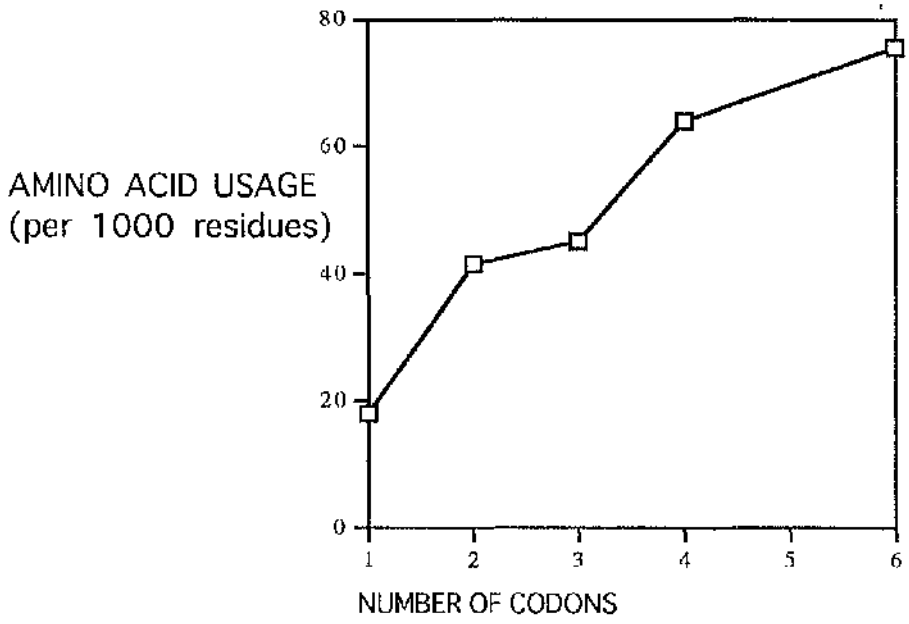

Figure 4.2. Amino acid usage increases as a function of the number of codons that code for the amino acid.

The graph shows the average number of times an amino acid is expressed per 1000 residues (Y axis) against the number of codons that code for that amino acid (X axis). All but one of these values is the mean for all of the amino acids that have that number of codons. Thus: x=1 is a mean of met and trp; x=2 a mean of phe, tyr, his, gln, asn, lys, asp, glu, cys; x=3 the value for ile; x=4 a mean of val, pro, thr, ala, gly and x=6 is a mean of leu, ser and arg. Raw data taken from a National Center for Biotechnology Information codon usage table derived from 1,697,109 mouse (mus musculus) codons.

RESULTS

4.3. DESIGN OF PROBES TO PHYLOGENETICALLY STABLE SEQUENCES OF PDE1

4.3.1. Design of primers GR18 & GR19 to phylogenetically conserved PDE1A and PDE1B specific sequence.

Several sequences for PDE1 forms were available at the start of this study. These sequences were (with GenBank accession numbers in brackets) for PDE1A from bovine (M90358) (32) and PDE1B from bovine (M94867) (34), rat (M94537) (36), mouse (M94538) (36) and human (M94539) (36) sources. The existence of only one species' PDE1A sequence (accessions L34069 and M90358 (32)) made it impossible to identify phylogenetically conserved PDE1A specific sequences. The next best option was to identify phylogenetically conserved sequences in all PDE1 forms. I thus set out to see if I could identify a stretch of sequence conserved between PDE1 genes but which was not found in other PDE genes. The ability to locate such a region would enable primers to be designed which, when used in RT-PCR, would be expected to detect the presence of PDE1 in a species-independent fashion. This would allow detection of the presence of transcripts for PDE1 in RNA from CHO cells using RT-PCR.

To attempt this I first performed a multiple gap alignment of the complete and partial PDE1 nucleic acid sequences listed above. This revealed substantial homology across the whole reading frame (52% identity among four complete sequences). I then analysed in detail a ~1250 base pair stretch of sequence (nucleotides 440-1700 in mouse) which contains sequence encoding the putative catalytic domain (19) which showed >56% identity between the sequences. This region exhibited homology with the central domain of various PDE types other than PDE1 (including PDE2, PDE3 and PDE4). However, three stretches (figure 3.3.1.a; regions X, Y & Z) appeared to show high similarity between PDE1 forms from various sources but were not present in other PDE subtypes. These were nucleotides 669-699 (region X; numbering for mouse PDE1B), which showed 77-96% identity, nucleotides 1243-1261 (region Y) which showed 88-100% identity and nucleotides 1330-1369 (region Z) which showed

83-98% identity in pairwise alignments between different PDE1s. In contrast, for example, in alignment analyses done with four PDEs then region X showed only 3% identity, region Y 19% identity and region Z 49% identity. Similar results were evident for PDE2, PDE3 and PDE7. Therefore the alignments had exposed three phylogenetically stable sequences which appeared to be uniquely conserved in PDE1 genes. In order to amplify a manageable fragment, degenerate primers (GR18 and GR19) were designed to regions X and Y. The sequences used for the primers were chosen so that degeneracy could be minimised. The primers were thus designed in the expectation that they would specifically amplify a 601 base pair fragment in PDE1 in a range of species given the apparent phylogenetic stability of the sequences I identified.

The conserved sequences so identified were recently, subsequent to this study, shown to be conserved in a new PDE1 gene. However the functional roles which presumably underlie this PDE1-specific conservation remain obscure. The sequences identified outside the catalytic domain do not converge with PDE1 functional domains identified to date. These domains are a calmodulin binding domains and an inhibitory domain, both identified by Sonnenburg et al (33) (figure 4.3.1.b).

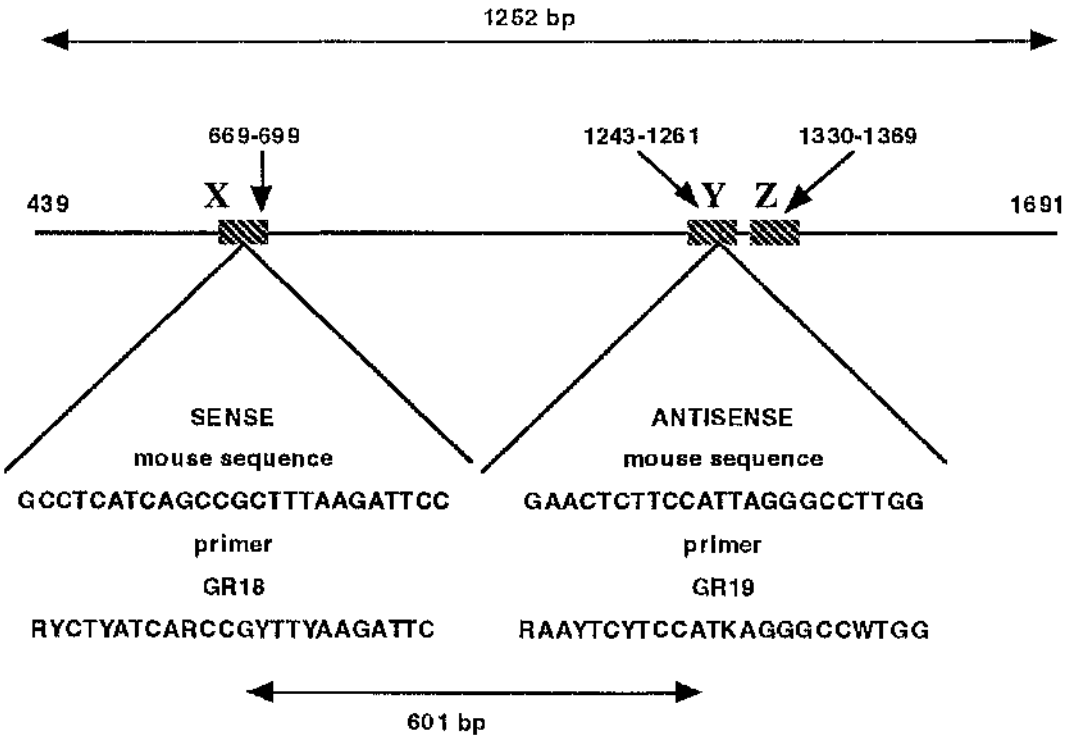

Figure 4.3.1.a. Design of primers GR18 & GR19 to phylogenetically conserved PDE1A and PDE1B specific sequence.

As described in the text, pairwise alignments of PDE1 cDNAs exposed >1.2Kb of highly conserved sequence. Within this region, three shorter stretches were identified which were highly conserved between PDE1 cDNAs but not other phosphodiesterases (hatched boxes X-Z). These were nucleotides 669-699 (region X; numbering for mouse PDE1B), which showed 77-96% identity, nucleotides 1243-1261(region Y) which showed 88-100% identity and nucleotides 1330-1369 (region Z) which showed 83-98% identity in pairwise alignments between different PDE1s but negligible identity with other PDEs (163). Sequences were selected for primers in regions A and B (mouse sequence shown and actual primer sequence with degeneracy allowing perfect matching with every known PDE1A and PDE1B sequence). The predicted fragment size, 601 base pairs, is also shown.

1 MGSSATEIEE LENTTFKYLT GEQTEKMWQR LKGILRCLVK QLERGDVNVV

51 DLKKNIEYAA SVLEAVYIDE TRRLLDTEDE LSDIQTDSVP SEVRDWLAST

101 FTRKMGMTKK KPEEKPKERS IVHAVQAGIF VERMYRKTYH MVGLAYPAAV

151 IVTLKDVDKW SFDVFALNEA SGEHSLKFMI YELFTRYDLI NRFKIPVSCL
X

201 ITFAEALEVG YSKYKNPYHN LIHAADVTQT VHYIMLHTGI MHWLTELEIL

251 AMVFAAAIHD YEHTGTTNNF HIQTRSDVAI LYNDRSVLEN HHVSAAYRLM

301 QEEEMNILIN LSKDDWRDLR NLVIEMVLST DMSGHFQQIK NIRNSLQQPE

351 GIDRAKTMSL ILHAADISHP AKSWKLHYRW TMALMEEFFL QGDKEAELGL
Y

401 PFSPLCDRKS TMVAQSQIGF IDFIVEPTFS LLTDSTEKIV IPLIEEASKA
Z

451 ETSSYVASSS TTIVGLHIAD ALRRSNTKGS MSDGSYSPDY SLAAVDLKSF

501 KNNLVDIIQQ NKERWKELAA QEARTSSQKC EFIHQ

Figure 4.3.1.b. The amino acid sequences of regions X, Y and Z do not coincide with PDE1 specific conserved features with defined functions

The amino acid sequence of Human PDE1A (U40370) is shown. Regions X, Y and Z are shown double underlined. A conserved PDE1 inhibitory domain is shown with a single dashed underline (33). The calmodulin binding domain of PDE1 is shown with a single underline (33). Serine 120 (bold) can be phosphorylated by PKA and this alter the affinity of the PDE for calmodulin. Regions X-Z do not coincide with these motifs.

4.3.2. Design of PCR primers GR45 and GR46 to a phylogenetically conserved PDE1C specific sequence.

A third PDE1 gene, PDE1C, was described recently (29-31). This was reported subsequent to the design, use and publication of the PDE1A and PDE1B specific probe already discussed (163). Although the PDE1-specific sequences already identified are partially conserved in PDE1C, the changes in PDE1C are sufficient that probes GR18 & GR19 will be unlikely to be able to detect transcripts from this gene. Therefore, in an attempt to design PDE1C specific probes, primers were designed to low-degeneracy codon, phylogenetically stable PDE1C specific sequence. This was done using the conventional method already described in section 3.1. Such an approach was possible here because, unlike PDE1A, PDE1C sequence was available from more than one species. By performing pairwise gap alignments of human and rat PDE1C sequences and other PDE1 forms I could identify 500 base pairs of species-independent PDE1C specific sequence. This was located between the putative PDE1C catalytic domain and the 3' splice junction. Primers were designed to amplify this region (figure 3.3.2.).

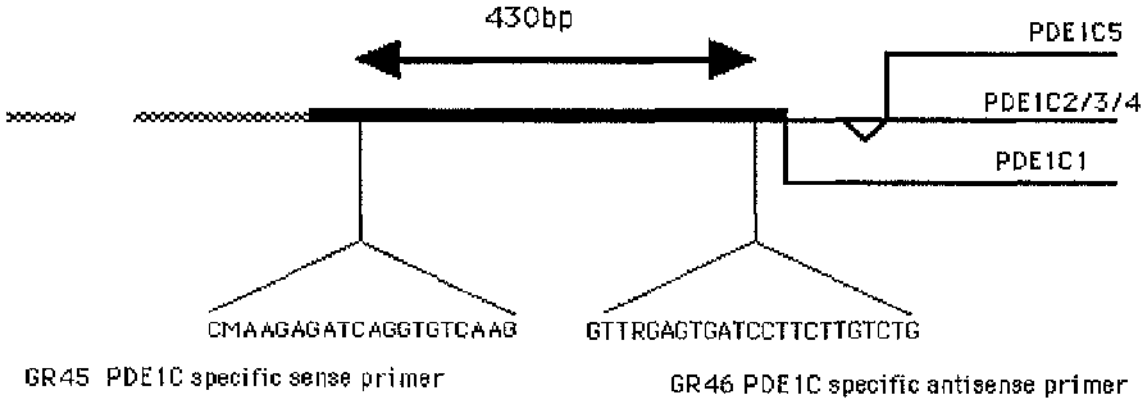

Figure 4.3.2. Design of PCR primers GR45 and GR46 to a phylogenetically conserved PDE1C specific sequence directly downstream of the PDE1C catalytic domain.

Schematic of PDE1C genes is shown. Thin solid line is splice variant specific sequence. Hatched line is catalytic domain and upstream sequence, which is homologous to sequence in other PDE1 genes. The length of this sequence is larger than is shown in this schematic. 5' splicing of the PDE1C forms is not shown. Thick line is PDE1C specific sequence found between the end of the catalytic domain and the 3' end splice junctions. Primers GR45 and GR46 were designed to the PDE1C specific sequence between the catalytic domain and the splice junctions, as shown. The primer sequences and expected fragment size are shown.

4.4. USE OF PROBES DESIGNED TO PHYLOGENETICALLY STABLE SEQUENCES OF PDE1

4.4.1. Use of PDE1A and PDE1B specific primers GR18 and GR19 and the PDE1C specific primers GR45 and GR46 in a range of genetic backgrounds

The primers GR18 and GR19 were first used in RT-PCR on RNA extracted from rat brain. This is known to provide a good source of PDE1 mRNA (32,34,36). Subsequently RNA from cat brain was used. This allowed for fragment of the correct-size (~600 base pair) to be amplified, consistent with the notion that these primers could amplify PDE1 sequences from more than one species (figure 4.4.1).

The primers GR45 & GR46 also allowed amplification, by RT-PCR of RNA from rat brain to identify a fragment of the expected size (~430 bp).

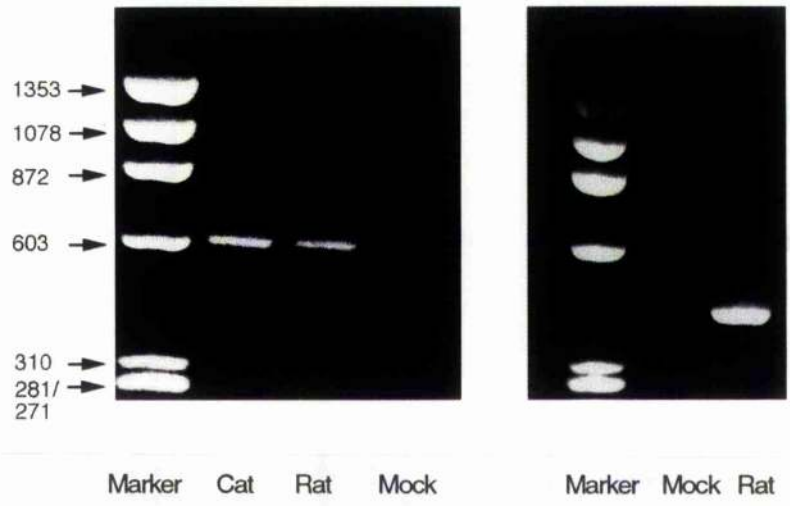

Figure 4.4.1. Detection of PDE1A, PDE1B and PDE1C specific RT-PCR primer pairs

Total RNA was first isolated from tissues and cells and then RT-PCR carried out as described in the Method chapter. (a) Using primers GR18 & GR19, designed to PDE1A both and PDE1B, I was able to amplify a 600bp band from cat brain and rat brain, a tissue in which these forms are known to be expressed (32,34,36). No product was evident in a mock reaction with no cDNA. The PCR conditions were 40 cycles of 94°C for 60s, 50°C for 80s and 72°C for 70s, with 'hot start' and PCR additive 'Perfect Match' added

Using primers GR45 and GR46 designed to detect PDE1C transcripts, I was able to amplify a band of the correct size in RNA from in rat brain cells, where PDE1C is expressed (31). No fragment was amplified in a mock reaction containing no cDNA. PCR conditions were 40 cycles of 94°C for 60s, 51°C for 70s and 72°C for 70s, with 'hot start' and PCR additive 'Perfect Match' added

4.4.2. The PDE1 specific primers GR18 & GR19 anticipate exactly the relevant sequence of human PDE1A

The sequence of a human PDE1A form has now been published (29) (GenBank accession U40370). The sequence homologous to that which primers GR18 & GR19 were designed to is contained within the modest degeneracy encoded within these primers (36x per primer), with no mismatches in either primer. Given the fact that the only PDE1A sequence in the data set was the evolutionarily distant bovine form and given that this single sequence precluded identification of PDE1A specific phylogenetically conserved sequence, this adds further support to the contention that the primer sequences identified here using a deductive approach are capable of identifying PDE1A in RNA from a range of species.

4.4.3. Use of PDE1 specific primers to monitor the induction of PDE1 by PMA in chinese hamster ovary (CHO) cells.

The PDE1 specific primers GR18 & GR19 were used to monitor the induction of PDE1 in chinese hamster ovary (CHO) cell lines. Attempts to amplify PDE1 from RNA extracted from untreated wild type (CHO-K) or from chinese hamster cells stably transfected to overexpress the insulin receptor (CHO-T), were unsuccessful. This is consistent with CHO-K and CHO-T PDE having activity profiles which suggest that there is no PDE1 activity present (163). However, RT-PCR using primers GR18 & GR19 on RNA extracted from CHO-K or CHO-T cells that had been challenged with PMA (6h; 10nM) detected a single band of the anticipated size, consistent with there having been an induction of transcripts. This concurs with biochemical data which showed that when CHO-K or CHO-T cells were treated with PMA, an actinomycin D-inhibitable appearance of PDE1 activity was detected (163).

Conversely, I was singularly unable to detect transcripts using PDE1C specific primers, consistent with the notion that PDE1C was not expressed in these cells even following PMA treatment.

4.4.4. Use of PDE1A and PDE1B specific primers to monitor the effect of stable transfection of PKC isoforms on the presence of PDE1 transcripts in chinese hamster ovary cells.

When the presence of PDE1 transcripts was determined in RNA taken from CHO-T cells stably transfected with PKC isoforms it was found that transcripts could be detected in RNA from cells expressing PKC α or PKC ε but not PKC βI or PKC γ. This is consistent with the observed biochemical data where CHO-T cells stably expressing PKC α or PKC ε exhibited up-regulated PDE1 activity compared to PKC βI or PKC γ which failed to exhibit such activity (163).

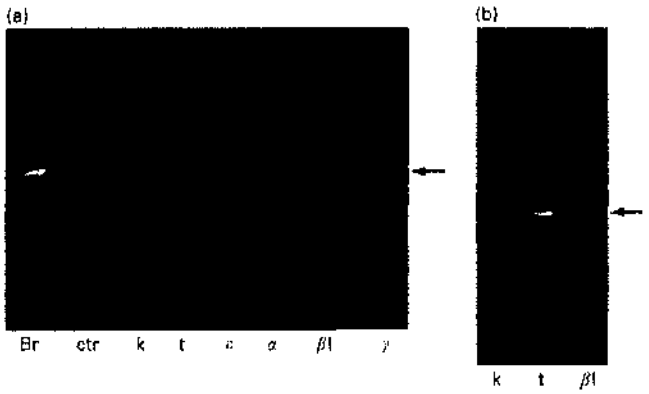

Figure 4.4.3. RT-PCR analyses on PDE1 transcripts in CHO cells.

This was done as described in Methods with precise conditions as described in figure 4.4.1. These experiments probed for PDE1A and PDE1B using primers GR18 and GR19. An arrow denotes a band of the correct size.

In (a) are shown analyses done on rat brain (Br), control blank (ct), CHO-k cells (k), CHO-t cells (t), CHO-ε cells (ε), CHO-α cells (α), CHO-βI cells (βI) and CHO-γ cells (γ).

In (b) are shown analyses done on cells which had been treated with PMA (10nM) for 6h prior to harvesting. These are for CHO-k cells (k) CHO-t cells (t) and CHO-βI cells (βI). Data show typical experiments performed at least three times with different cell preparations.

4.4.5. Use of PDE1 specific primers to monitor the induction of PDE1 transcripts in chinese hamster ovary cells stimulated with ATP, a ligand for an endogenous lipid signalling receptor

CHO cells express endogenous P_2-purinoceptors (208) which are able to stimulate inositol phospholipid metabolism and increase intracellular Ca^{2+} (209). Thus one might expect that the DAG produced would be able to activate endogenous PKC identified in these cells (199) and thence to activate PDE1. Employing a concentration of ATP (100μM) which has been shown to activate maximally inositol phospholipid metabolism in CHO cells (209), I identified a PDE1 transcript by RT-PCR using primers GR18 and GR19 able to detect PDE1A and PDE1B (see figure 4.4.5.). This was consistent with the observed ability of ATP to cause an actinomycin D inhibitable up-regulation of PDE1 activity (207).

As with the experiments on cells challenged with PMA, no transcripts for PDE1C were detected in the RNA from CHO cells either before or following stimulation with ATP.

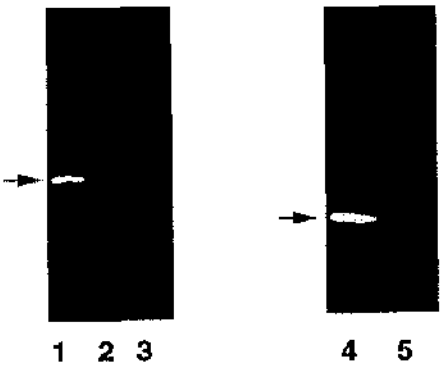

Figure 4.4.5. RT-PCR analyses of PDE1 transcripts in CHO cells

This was done as described in the methods with the conditions used as described in the legend to figure 4.4.1. An arrow denotes bands of the correct size. Lane 1-3 shows the result of PCR reactions using the primer pair GR18 & GR19 for detection of PDE1A or PDE1B transcripts. Lane 4 & 5 shows reactions using primer pair GR45 and GR46 for the detection of PDE1C transcripts. Shown are data using RNA from CHO cells treated with 100μM ATP (lanes 1&5), FTC-133 cells* (lanes 2&4) and blank (track 3).

*These are a thyroid carcinoma cell line (115), see section 4.4.7.

4.4.6. The Ca^{2+}/CaM-stimulated PDE1 enzyme in CHO cells is PDE1B

The RT-PCR analyses done on RNA from stimulated CHO cells supports the notion that either PDE1A or PDE1B but not PDE1C was induced by treatments which caused an increase in PKC activity (section 4.4.5). Since primers GR18 & GR19 were designed to identify transcripts for PDE1A and PDE1B, it was necessary to clone and sequence bands from RT-PCR to discriminate between these two possibilities. Sequences of six separate clones of the 601 bp band amplified from PDE1 induced CHO cells from either PMA or ATP treated cells were identical. Pair-wise alignments found that the three existing PDE1B sequences shared 91-95% nucleotide identity with the chinese hamster sequence whereas the PDE1A and PDE1C sequences were only 68-69% identical with the new sequence (figure 4.4.6.a). As might be expected, most of the mismatches occur at 'wobble' positions, such that the conservation between the chinese hamster sequence and the homologous PDE1B sequences was even more marked at the amino acid level. Thus, the chinese hamster sequence had 99% amino acid identity when compared to the other PDE1B sequences, but only 65-69% when compared to the non-homologous PDE1A and PDE1C sequences (figure 4.4.6.b.). I am thus able to assign my sequences as PDE1B forms (207) (figure 4.4.6.c).

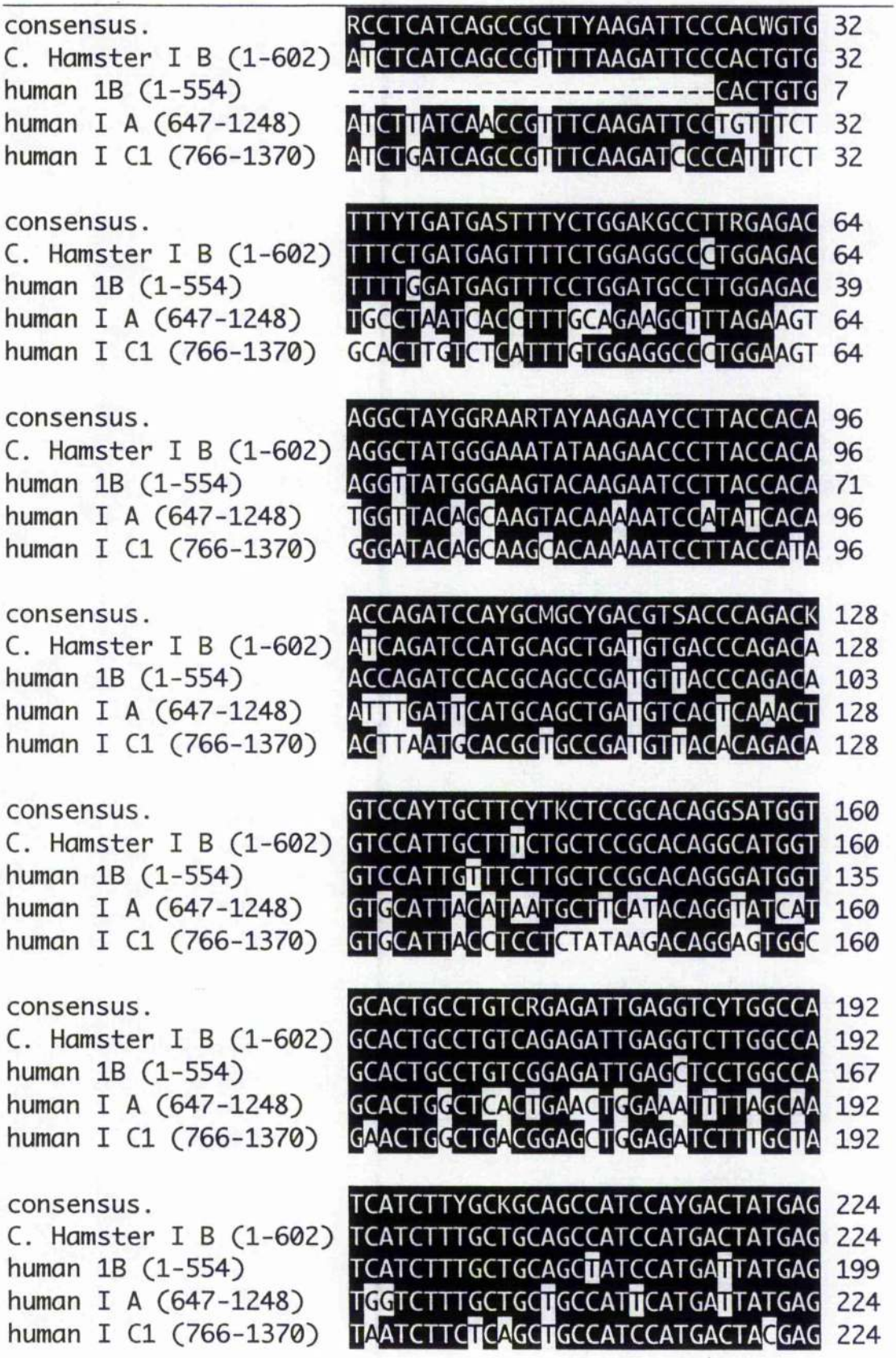
consensus. RCCTCATCAGCCGCTTYAAGATTCCCACWGTG 32
C. Hamster I B (1-602) ATCTCATCAGCCGTTTTAAGATTCCCACTGTG 32
human 1B (1-554) ----------CACTGTG 7
human I A (647-1248) ATCTTATCAACCGTTTCAAGATTCCTGTTTCT 32
human I C1 (766-1370) ATCTGATCAGCCGTTTCAAGATCCCCATTTCT 32
consensus. TTTYTGATGASTTTYCTGGAKGCCTTRGAGAC 64
C. Hamster I B (1-602) TTTCTGATGAGTTTTCTGGAGGCCCTGGAGAC 64
human 1B (1-554) TTTTGGATGAGTTTCCTGGATGCCTTGGAGAC 39
human I A (647-1248) TGCCTAATCACCTTTGCAGAAGCTTTAGAAGT 64
human I C1 (766-1370) GCACTTGTCTCATTTGTGGAGGCCCTGGAAGT 64
consensus. AGGCTAYGGRAARTAYAAGAAYCCTTACCACA 96
C. Hamster I B (1-602) AGGCTATGGGAAATATAAGAACCCTTACCACA 96
human 1B (1-554) AGGTTATGGGAAGTACAAGAATCCTTACCACA 71
human I A (647-1248) TGGTTACAGCAAGTACAAAAATCCATATCACA 96
human I C1 (766-1370) GGGATACAGCAAGCACAAAAATCCTTACCATA 96
consensus. ACCAGATCCAYGCMGCYGACGTSACCCAGACK 128
C. Hamster I B (1-602) ATCAGATCCATGCAGCTGATGTGACCCAGACA 128
human 1B (1-554) ACCAGATCCACGCAGCCGATGTTACCCAGACA 103
human I A (647-1248) ATTTGATTCATGCAGCTGATGTCACTCAAACT 128
human I C1 (766-1370) ACTTAATGCACGCTGCCGATGTTACACAGACA 128
consensus. GTCCAYTGCTTCYTKCTCCGCACAGGSATGGT 160
C. Hamster I B (1-602) GTCCATTGCTTTCTGCTCCGCACAGGCATGGT 160
human 1B (1-554) GTCCATTGTTTCTTGCTCCGCACAGGGATGGT 135
human I A (647-1248) GTGCATTACATAATGCTTCATACAGGTATCAT 160
human I C1 (766-1370) GTGCATTACCTCCTCTATAAGACAGGAGTGGC 160
consensus. GCACTGCCTGTCRGAGATTGAGGTCYTGGCCA 192
C. Hamster I B (1-602) GCACTGCCTGTCAGAGATTGAGGTCTTGGCCA 192
human 1B (1-554) GCACTGCCTGTCGGAGATTGAGCTCCTGGCCA 167
human I A (647-1248) GCACTGGCTCACTGAACTGGAAATTTTAGCAA 192
human I C1 (766-1370) GAACTGGCTGACGGAGCTGGAGATCTTTGCTA 192
consensus. TCATCTTYGCKGCAGCCATCCAYGACTATGAG 224
C. Hamster I B (1-602) TCATCTTTGCTGCAGCCATCCATGACTATGAG 224
human 1B (1-554) TCATCTTTGCTGCAGCTATCCATGATTATGAG 199
human I A (647-1248) TGGTCTTTGCTGCTGCCATTCATGATTATGAG 224
human I C1 (766-1370) TAATCTTCTCAGCTGCCATCCATGACTACGAG 224

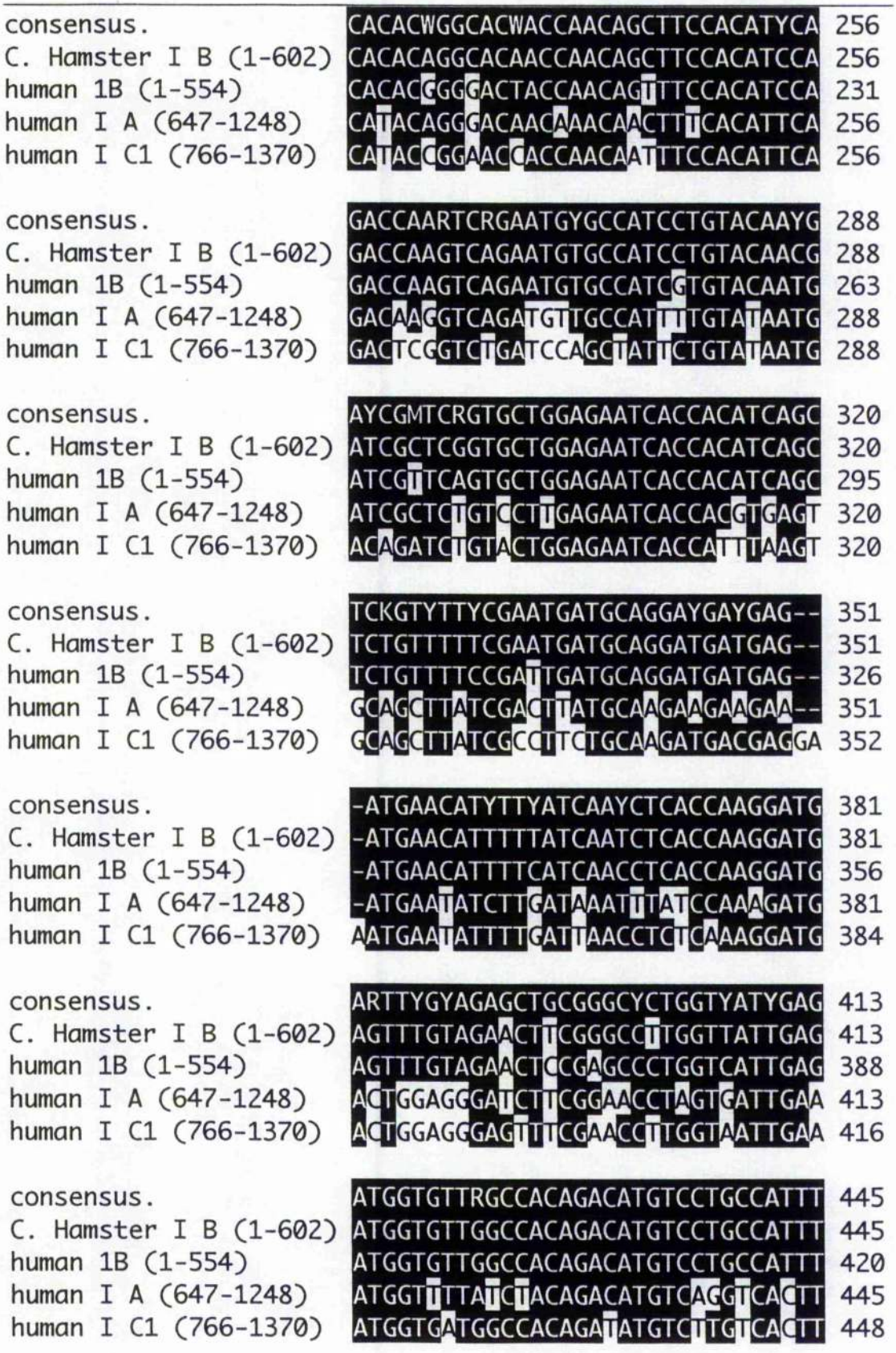
consensus. CACACWGGCACWACCAACAGCTTCCACATYCA 256
C. Hamster I B (1-602) CACACAGGCACAACCAACAGCTTCCACATCCA 256
human 1B (1-554) CACACGGGGACTACCAACAGTTTCCACATCCA 231
human I A (647-1248) CATACAGGGACAACAAACAACTTTCACATTCA 256
human I C1 (766-1370) CATACCGGAACCACCAACAATTTCCACATTCA 256
consensus. GACCAARTCRGAATGYGCCATCCTGTACAAYG 288
C. Hamster I B (1-602) GACCAAGTCAGAATGTGCCATCCTGTACAACG 288
human 1B (1-554) GACCAAGTCAGAATGTGCCATCGTGTACAATG 263
human I A (647-1248) GACAAGGTCAGATGTTGCCATTTTGTATAATG 288
human I C1 (766-1370) GACTCGGTCTGATCCAGCTATTCTGTATAATG 288
consensus. AYCGMTCRGTGCTGGAGAATCACCACATCAGC 320
C. Hamster I B (1-602) ATCGCTCGGTGCTGGAGAATCACCACATCAGC 320
human 1B (1-554) ATCGTTCAGTGCTGGAGAATCACCACATCAGC 295
human I A (647-1248) ATCGCTCTGTCCTTGAGAATCACCAGGTGAGT 320
human I C1 (766-1370) ACAGATCTGTACTGGAGAATCACCATTTAAGT 320
consensus. TCKGTYTTYCGAATGATGCAGGAYGAYGAG-- 351
C. Hamster I B (1-602) TCTGTTTTTCGAATGATGCAGGATGATGAG-- 351
human 1B (1-554) TCTGTTTTCCGATTGATGCAGGATGATGAG-- 326
human I A (647-1248) GCAGCTTATCGACTTATGCAAGAAGAAGAA-- 351
human I C1 (766-1370) GCAGCTTATCGCCTTCTGCAAGATGACGAGGA 352
consensus. -ATGAACATYTTYATCAAYCTCACCAAGGATG 381
C. Hamster I B (1-602) -ATGAACATTTTTATCAATCTCACCAAGGATG 381
human 1B (1-554) -ATGAACATTTTCATCAACCTCACCAAGGATG 356
human I A (647-1248) -ATGAATATCTTGATAAATTTATCCAAAGATG 381
human I C1 (766-1370) AATGAATATTTTGATTAACCTCTCAAAGGATG 384
consensus. ARTTYGYAGAGCTGCGGGCYCTGGTYATYGAG 413
C. Hamster I B (1-602) AGTTTGTAGAACTTCGGGCCTTGGTTATTGAG 413
human 1B (1-554) AGTTTGTAGAACTCCGAGCCCTGGTCATTGAG 388
human I A (647-1248) ACTGGAGGGATCTTCGGAACCTAGTGATTGAA 413
human I C1 (766-1370) ACTGGAGGGAGTTTCGAACCTTGGTAATTGAA 416
consensus. ATGGTGTTRGCCACAGACATGTCCTGCCATTT 445
C. Hamster I B (1-602) ATGGTGTTGGCCACAGACATGTCCTGCCATTT 445
human 1B (1-554) ATGGTGTTGGCCACAGACATGTCCTGCCATTT 420
human I A (647-1248) ATGGTTTTATCTACAGACATGTCAGGTCACTT 445
human I C1 (766-1370) ATGGTGATGGCCACAGATATGTCTTGTCACTT 448

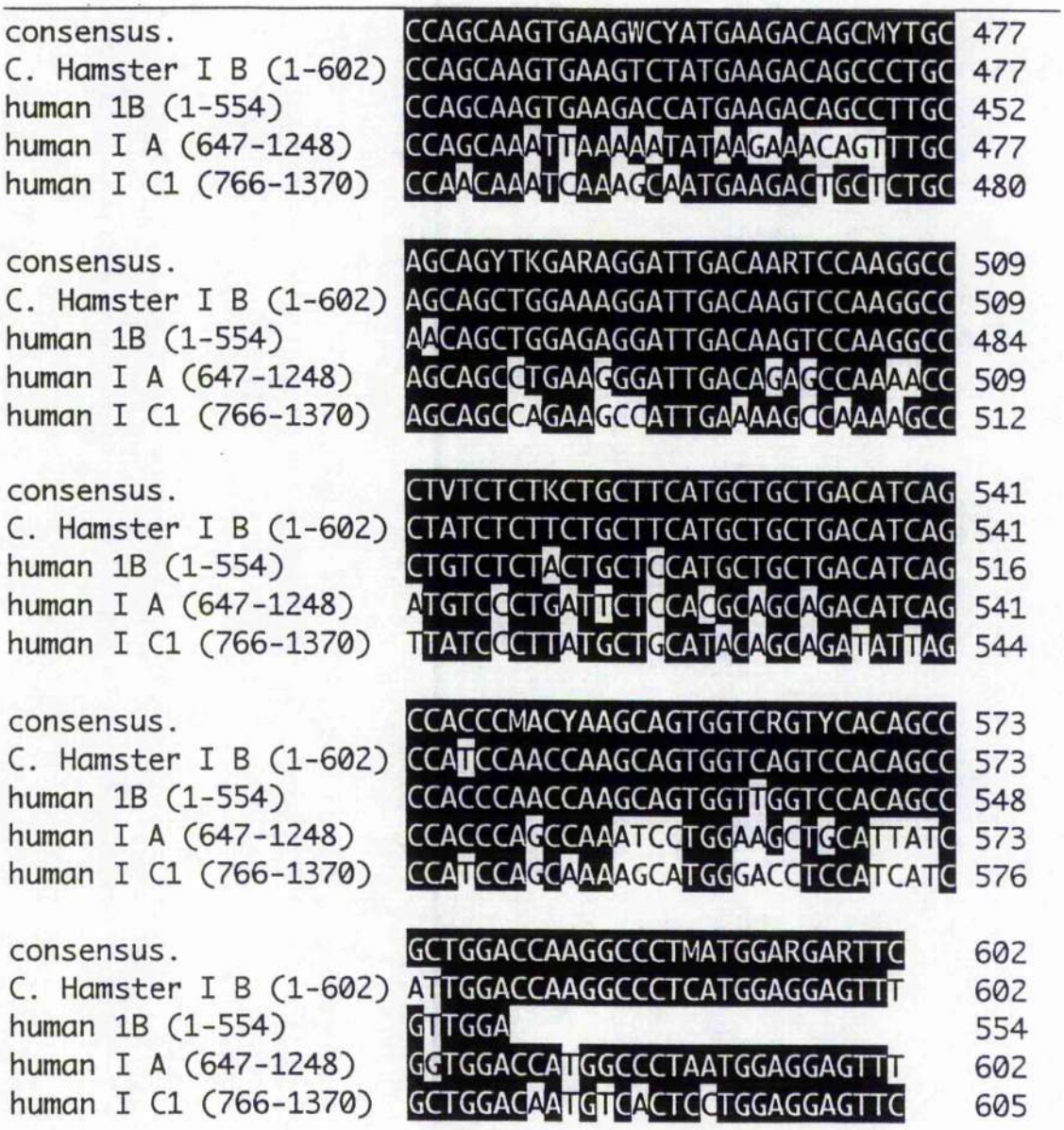

Figure 4.4.6.a Sequences of PDE1 transcript PCR products.

Sequences of PCR products amplified using the PDE1A/B species-independent primers from PMA treated CHO cells and from human Jurkat T-cells (GenBank accession numbers U40585 & U40584 respectively) are shown compared with the equivalent region of human PDE1A and PDE1C sequences. Alignment mismatches (black on white) are shown with respect to a degenerate consensus of three PDE 1B sequences: mouse, rat and bovine (GenBank accession M94538, M94537 & M94867 respectively). This shows that the novel sequences share a higher degree of homology with PDE1B forms than do PDE1A or PDE1C forms (human PDE1C and human PDE1A (GenBank accession U40370 and U40371 respectively) are shown in this alignment). Note that these PCR fragments were TA cloned by Dr Michael Sullivan

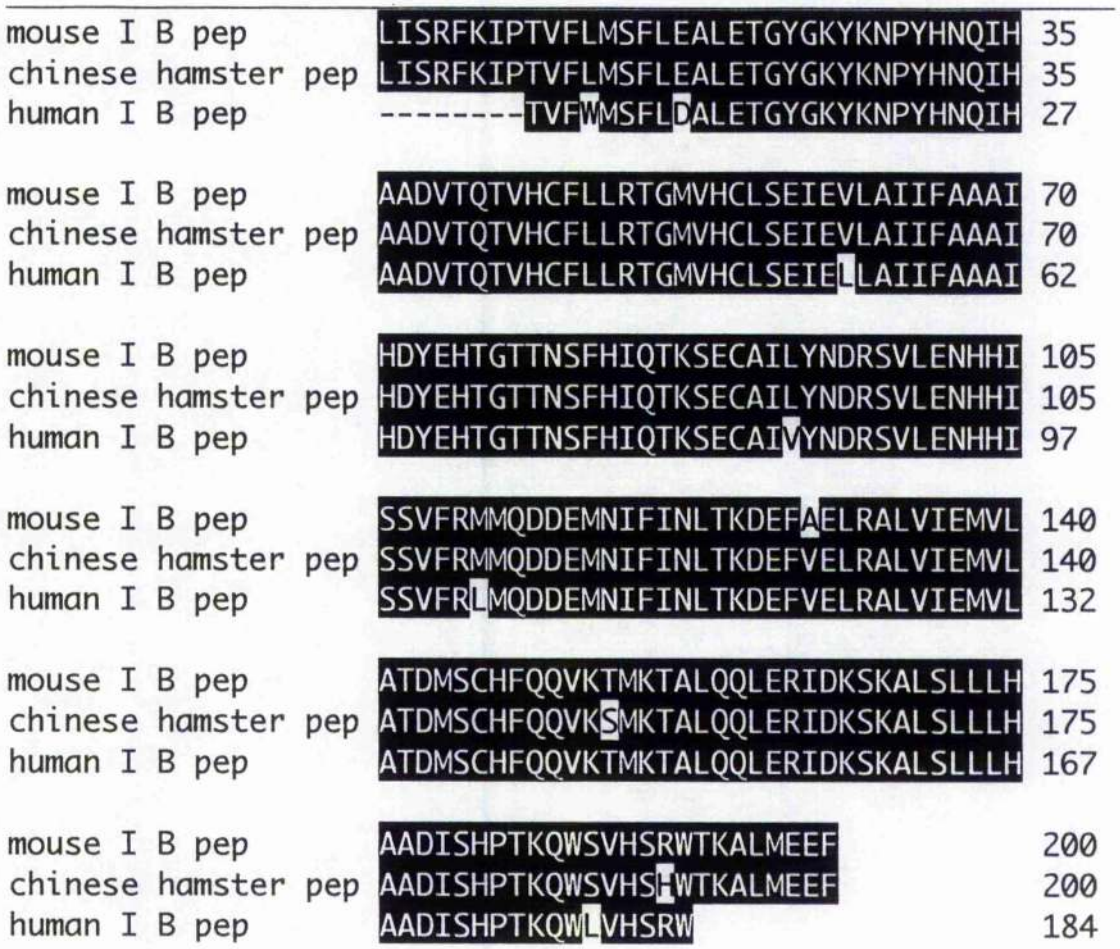

Figure 4.4.6.b Amino acid sequence alignment of mouse PDE1B and novel chinese hamster ovary PDE1 forms from this study.

Amino acid sequences of PCR products amplified using the PDE1A/B species-independent primers from PMA treated CHO cells (GenBank accession number U40585) and from human Jurkat T-cells (GenBank accession number U40584) are shown aligned with mouse PDE1B (GenBank accession M94538). The large number of matches to the simple majority (white on black) demonstrate that these sequences are even more closely conserved at the amino acid level as would be expected in evolutionarily conserved sequences since many of the mutations in such proteins will occur at silent or wobble positions. Furthermore, the majority of substitutions are conservative (for example E to D, V to L, S to T)

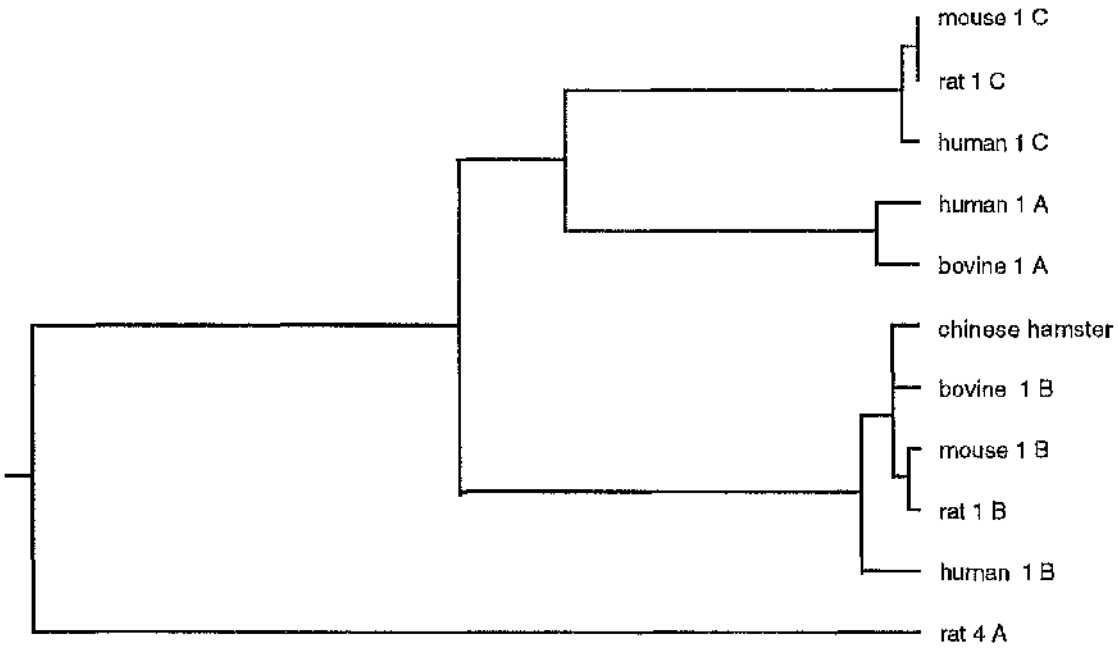

Figure 4.4.6.c The novel PDE1 sequences cluster with PDE1B sequences on a phylogenetic tree of PDE1 forms.

The sequences homologous to the 601bp fragment were identified in all published PDE1 forms. These sequences then had their distances calculated and a tree constructed in the MegAlign program of the DNAstar suite of programs, using the default settings. This tree shows quite clearly that the chinese hamster and human sequences isolated here are highly related to PDE1B sequences but not to either PDE1A or PDE1C sequences. The rat PDE4A sequence is included as a less related "control" sequence.

4.4.7. The Ca^{2+}/CaM-stimulated PDE1 enzyme in human thyroid carcinoma cell line FTC133 is a PDE1C form

The human thyroid carcinoma cell line FTC133 (210-214) is known to contain PDE1 activity which can be attenuated when the PDE4A form RNPDE4A1 (RD1) is stably transfected into them (115). Using primers GR18 and GR19 however, we were singularly unsuccessful in detecting transcripts for either PDE1A or PDE1B in RNA preparations made from native FTC133 cells, FTC133G cells and the RD1-expressing FTC133A cells. However, when I used PDE1C specific primers GR45 and GR46 I was able to amplify a fragment (431 bp) of the expected size, indicating the presence of PDE1C in the native FTC133 cell line. Whilst no attempt was made to perform quantitative studies, the magnitude of this signal was similar using identical amounts of RNA from both the native FTC133 cells and the 'control' transfected FTC133G cells but was dramatically reduced in the RD1-expressing FTC133A cell line (figure 4.4.7). This trend is consistent with the decrease in PDE1 activity observed in FTC133G cells and the lack of observable PDE1 activity in RD1 transfected FTC133A cells (115).

4.4.8. The Ca^{2+}/CaM-stimulated PDE1 enzyme in the mouse neuronal cell line AtT 20 cells is a PDE1C form.

The mouse neuronal cell line AtT 20 is known to contain PDE1 activity (F. Antoni unpublished). Yet using GR18 and GR19, I was singularly unsuccessful in detecting transcripts for either PDE1A or PDE1B in RNA. However, when I used PDE1C specific primers GR45 and GR46 we were able to amplify a fragment (431 bp) of the expected size, indicating that the PDE in AtT 20 cells is a PDE1C form

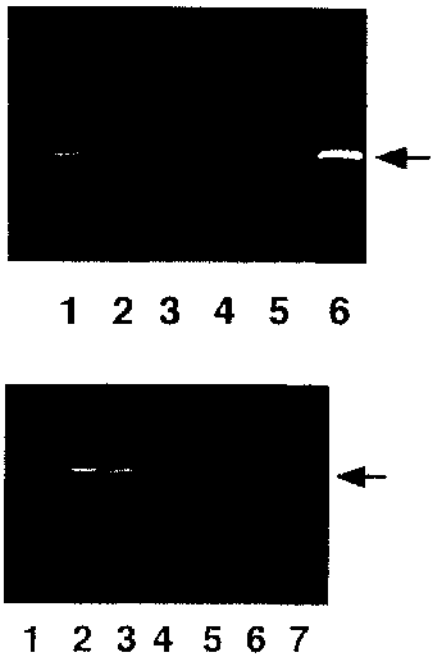

Figure 4.4.8. Detection of PDE1 transcripts in human FTC133 cell lines and mouse AtT20 cell lines

RT-PCR was carried out using primer pairs GR18 & GR19 or GR45 & GR46 to detect PDE1A/B and PDE1C, respectively. An arrow denotes a band of the correct size.

(a) Using primers GR45 & GR46, which are specific for PDE1C analyses were done on RNA (track number is in brackets) (1) rat brain; (2) FTC133A cells; (3) FTC133G cells; (4) FTC133 wild-type cells; (5) no DNA control lane and (6) AtT20 cells

(b) Using primers GR18 & GR19 to detect both PDE1A and PDE1B in RNA from (1) no DNA control; (2) rat brain; (3) rat brain; (4) FTC133A cells; (5) FTC133 wild type cells; (6) FTC133G cells (7) AtT20 cells.

4.5. CONCLUSION

4.5.1 Use of primers which are able to amplify select PDE1 forms

RT-PCR was used to identify the nature of the PDE1 isoform which was rapidly induced in CHO cells in response to a number of stimuli including PMA, PKC α and ε isoform overexpression and latterly exposure to ligands for endogenous receptors which stimulate lipid signalling processes. This was achieved even though there was no sequence information available for PDE1 or indeed any PDE form, for chinese hamster.

Probes for non-homologous systems are normally designed to conserved gene sequences containing several low redundancy codons. Then, in order to minimise degeneracy further, species specific codon usage tables are employed. However, the final primer design is often still highly degenerate and thus the effectiveness of such primers in RT-PCR can be reduced. The rationale adopted in this study for the design of PDE1A/B specific primers serves to ameliorate these problems and may be more generally applicable. Thus, by selecting sequence conserved between two genes, rather than just one, and between species but differing from other closely related genes, one can rigorously apply conservation information from genetic model systems such as rat and human to genetically uncharacterised systems. Here I have done this for the analysis of PDE1 isoforms in chinese hamster. Once such stretches of sequences are identified, then probes can be designed to them in the usual way, to amplify sections containing low redundancy codons. These primers will be far less degenerate whilst still able to selectively detect transcripts in a range of species. As has been shown, the primer sequences chosen were published before and correctly anticipated the human PDE 1A (Gen Bank accession; U40371) sequence exactly (no mismatches in either primer). The primers were also able to amplify PDE1 forms from a variety of species and as such should provide an invaluable tool for the detection of transcripts for these isoforms.

4.5.2. Induction of PDE1B by PKC subtypes

By RT-PCR analyses I have been able to show amplification of a PDE1A/B,

but not PDE1C form in CHO cells under conditions of PKC stimulation where novel PDE1 activity has been shown to be induced (163,207). Sequencing of the PCR fragments revealed that the induced PDE was a PDE1B form (207). On the basis that induction of PDE1B could be elicited by the phorbol ester PMA it is reasonable to assume that protein kinase C provides the basis for induction by the endogenous receptor systems in CHO cells which are coupled to lipid signalling processes. That overexpression of PKC-α or PKC-ε, but not overexpression of PKC-β or PKC-γ, can also induce PDE1 activity and transcript production, suggests that the transcriptional regulation of the PDE1B gene may show a distinct specificity as regards the action of protein kinase C isoforms. Identification of the molecular basis of this remarkably rapid induction may shed light on the functional roles of protein kinase C isoforms and 'crosstalk' between the lipid and cyclic nucleotide signalling pathways.

Though this study was the first to show an induction of PDE1B, such an effect has now been reported by others (35) following mitogenic stimulation of several types of lymphoblastoid and leukaemic cells. It was suggested by Jiang et al (35) that the PDE activity might be contributing towards a 'survival' signal, since antisense and vinpocetine blocking of the PDE1 activity led the lymphocytes to undergo apoptosis. This is a very interesting result, although the mechanism for this 'survival' signal has still to be determined.

4.5.3. Identification of two cell lines which express PDE1C

The PDE1A/B primers designed here were unable to identify PDE1 transcripts in FTC 133 and AtT20 cell lines which are known to express PDE1 activity. I have now determined that the reason for this is that these express PDE1C forms which are not detectable with GR18 and GR19. These are the first cell lines shown to express PDE1C and in the case of FTC 133 cells, the first examination of PDE1 forms in thyroid cell RNA. In FTC 133 cells the data reported (115) is consistent with the notion that the loss of PDE1 activity in the RD1 (PDE4A)-expressing transfected cell line FTC133A, is likely to have been due to a marked

reduction in the amount of PDE1 enzyme protein. If this is the case, this cell line might be of use in determining the molecular mechanism of the interplay between expression of PDE4A and PDE1C forms. This may involve an effect at the level of the of the PDE1C form.

One possible explanation for why the PDE1C RT-PCR signal did not disappear completely is that PDE1C spliceforms might be alternatively regulated (Five PDE1C forms have been reported so far (29-31)). Some of these could be constitutively expressed in the FTC cell line, whilst others were regulated, similar to the differing regulation of PDE4D splice variants (84,119).

5. USE OF LOW STRINGENCY REVERSE TRANSCRIPTION POLYMERASE CHAIN REACTION TO DEMONSTRATE UNIVERSAL EXPRESSION OF MAMMALIAN HOMOLOGUES OF THE RAT SHORT FORM PDE4A TRANSCRIPT RD1 (RNPDE4A1)

INTRODUCTION

5.1. RAT SPLICE VARIANT RD1 (RNPDE4A1)

The splice variant RD1 was the first mammalian dunce PDE homologue to be isolated, being identified in a rat brain cDNA library (65). Since this time, the biochemical characteristics endowed by RD1's unique N-terminal 21 amino acids have been the subject of intensive study (see introduction). However, parallel to this effort, little was known about expression of native RD1 forms. Despite data which indicated the existence of endogenous RD1 (76,102), the continuing lack of any data on RD1 homologues in other species raised the possibility that RD1 might be a rat specific splice variant and therefore a curiosity of little relevance to man. The molecular layout of RD1 and the published literature of the time did nothing to dispel this notion: (1) the RD1, PDE4A 'short' form splice junction is apparently unique, being distinct from the 'short' form splice junction which is conserved between the other mammalian PDE4 genes and that found in drosophila (see introduction); (2) the other cDNAs reported alongside RD1 and suggested to be splice variants, namely RD2 (RNPDE4A2) and RD3 (RNPDE4A3) have now convincingly been shown to be cloning errors (68,76,82). This accounts for the subsequent inability of various investigators to detect these species; (3) human homologues of RD1 have not, to date, been identified, although human homologues have been identified for many of the other rat splice variants. These include human homologues of all three rat PDE4D splice variants, (RNPDE4D1-3) (86), the two rat PDE4B splice variants, (RNPDE4B1 and RNPDE4B2) (68) and the 'long' form rat PDE4A splice variant RNPDE4A5 (68); (4) rat RD1 RNA has never been shown to be expressed in a rat cell line or any rat tissue other than rat brain by any technique. Nevertheless, in rat brain it has been detected by RNAse protection assay (76) which is in accord with the isolation of RD1 from a rat

brain cDNA library in the original study of Davis et al (65). RD1 protein has, to date, only been suggested to be expressed in rat brain (102).

In view of these difficulties, there is a pressing need to determine whether homologues of RD1 occur in humans and other species and thus whether conservation of biochemically identified motifs within RD1 occur. Additionally, given the brain specific expression of RD1 and the wealth of human brain cell lines compared to the lack of rat brain cell lines, identification of a human homologue of RD1 and a cell line which expresses RD1 endogenously would be a powerful tool for studying regulatory processes controlled by this PDE4A isoform.

Given my success using RT-PCR, in identifying novel PDE species in mRNA from a chinese hamster cell line using sequence information from other species (163,207), I decided to search for a human RD1 homologue by RT-PCR. To do this I used primers designed to sequences found within known human PDE4A sequence and rat RD1 sequence

5.2 THE PRIMARY STRUCTURE OF PDE4A LR2

The structure of the LR2 region of PDE4A is currently of intense interest given its apparent role in species specific differences in the biochemistry of PDE4A splice variants. These include proposals that it may contain conformational 'switches' (see Introduction) (19). Alignment of human and rat PDE4A sequence using default settings in alignment programs including Gene Jockey 2 and GCG PILEUP produces an alignment such as that shown in figure 5.2. In this alignment, a proline rich putative SH3 binding domain appears to occur only in the human form of LR2 (19,79). This deletion represents the major primary structural difference between human and rat PDE4A. Sequence information from the LR2 region of other species, which is presented in this chapter, deepens this understanding of the sequence differences between human and rodent PDE4A LR2. The new data is consistent with an alternative alignment which suggests that a form of a proline rich domain is retained in both human and rat PDE4A, although individual residue positions are not well conserved. In this chapter I demonstrate the true identity of the deletion in rat PDE4A LR2 and the

significance of this is discussed with respect to the altered biochemical properties of human and rat PDE4A splice variants.

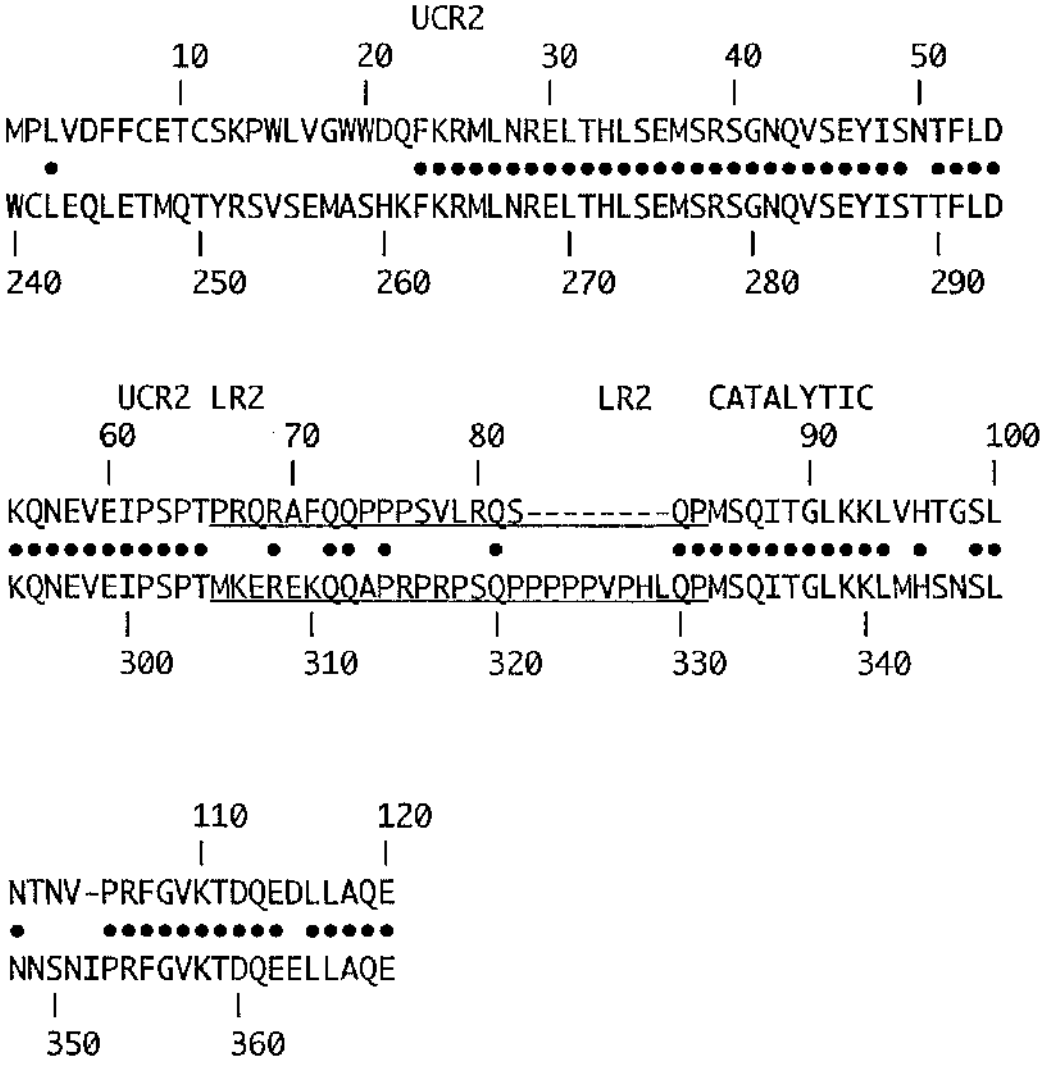

Figure 5.2. Typical peptide alignment of rat (top) and human (bottom) PDE4A.

This figure shows a typical alignment of rat (RNPDE4A1) and human (HSPDE4A4) PDE4A sequence around the RD1 splice junction and LR2 (underlined) (after (79)). This alignment clearly indicates that a proline rich domain is deleted in rat PDE4A. The positions of UCR2, LR2 and the putative catalytic domain are shown for orientation.

RESULTS

5.3. USE OF PRIMERS DESIGNED TO RAT RD1 ON HUMAN CELL LINES 293, FTC133, HeLa, SK-N-SH, U-87, U-118

In order to amplify specifically a fragment of rat RD1, I designed one primer (GR73) to sequence found within the unique 5' region of RD1. The second primer was designed to a region of human PDE4A sequence common to all splice variants known to date and which would be expected to appear in a human homologue of RD1 (see appendix). Thus only one primer contained sequence uncertainty with respect to human PDE4A, namely the rat 5' RD1 sequence. These primers readily detected a product in rat brain RNA of the expected size (372 bp) despite the three mismatches in the antisense primer with respect to the rat sequence. A similarly sized product was seen in RNA from various human brain cell lines, namely U-118 cells, SK-N-SH cells and also the human thyroid cell line FTC133 but not in cervical cell line HeLa, human brain cell line U-87 or human kidney cell line 293 (cell-line accession numbers are in the Materials and Methods chapter). TA cloning and sequencing of the 372 bp product from the rat brain RNA source showed that the sequence of the amplified species reflected that of RD1. However sequencing of clones from the human sources did not identify any RD1-like species; all of the colonies reflected single primer artefacts, with no homology to RD1. Indeed, a putative "human RD1" PCR fragment is expected to migrate more slowly because of a deletion of rat PDE4A in LR2 which is part of the region amplified by these primers (figure 5.4.1.). Later results concur with this prediction (section 5.4.1). This is highly persuasive that the band seen here is artefactual and therefore that none of these cell lines express an RNA homologous to RD1. This preliminary failure forced me to reconsider the strategy employed.

Given that RD1 has not yet been detected in any cell line I decided to screen RNA directly extracted from brain tissue. Since I could not discriminate whether any potential lack of signal could be because there was no RD1 expressed in these cell lines or because my probes were unable to amplify human RD1, in the first instance I elected to screen mouse brain because the mouse is more closely related to the rat.

```
1    GGGACTCGGC CAAACCTACC TTACCTGTGC GCCAGCCCAG AGCTAAGCTT
                                     CAGGCG   GGCTAAGTCT
                                     GR5'HRD1
51   CCATCATGCC TCTGGTTGAC TTCTTCTGCG AGACCTGCTC CAAGCCCTGG
     CCAAG                TTCTTCTGCG AGACCTGCTC CAAG
                          GR73                    GR73
101  CTGGTGGGCT GGTGGGACCA GTTCAAAAGG ATGCTGAACC GTGAGCTCAC
151  ACACCTGTCG GAAATGAGCA GGTCAGGAAA CCAGGTCTCA GAGTACATTT
201  CCAACACATT CCTGGACAAG CAGAATGAAG TGGAGATCCC CTCACCCACA
251  CCTCGGCAGA GAGCCTTCCA GCAGCCCCCG CCGTCAGTGC TGCGACAGTC
301  CCAGCCCATG TCTCAGATCA CAGGGCTGAA AAAGCTGGTA CACACTGGAA
351  GCTTGAACAC CAACGTCCCA CGGTTTGGAG TCAAGACAGA TCAAGAGGAC
401  CTCTTAGCAC AAGAACTGGA GAACTTGAGC AAATGGGGCC TGAACATCTT
                       CCT CTTGGACTTG TTCACCCCGG AC
                       GR36                    GR36
451  TTGTGTGTCG GAGTACGCTG GAGGCCGCTC ACTCAGCTGT ATCATGTATA
501  CGATATTCCA GGAGCGGGAC CTACTGAAGA AATTCCACAT CCCTGTGGAC
551  ACCATGATGA TGTACATGCT GACCCTGGAG GACCACTACC ATGCCGACGT
601  GGCCTACCAC AACAGCCTGC ACGCAGCGGA TGTGCTGCAG TCCACACACG
651  TGCTGCTGGC CACGCCCGCA CTGGACGCTG TGTTCACAGA CCTGGAGATT
701  CTTGCTGCCC TCTTCGCTGC TGCCATCCAC GATGTGGACC ACCCTGGCGT
                                GGTG CTACACCTRG TGGGAC
                                GR29                 GR29
```

Figure 5.3 Primers used in this chapter.

The sequence shown is that for RD1 (M26715). The initiator methionine of RD1 is underlined. Sense primers are underlined once, antisense primers are double underlined. GR29 is designed to both rat and human sequence, GR36 is designed to human sequence, hence there are a few mismatches when aligned to the rat sequence. GR37 is designed to rat sequence. Primer GR5' hRD1 is designed to the recently identified human RD1 5' exon (see section 5.7).

5.4. RT-PCR USING PRIMERS DESIGNED TO RAT RD1 ON MOUSE BRAIN IDENTIFIES A MURINE RD1-LIKE SPECIES: A NEW RAT AND MOUSE SPECIFIC DELETION IS REVEALED

In order to examine whether the RD1 transcript is unique to rat, low stringency RT-PCR was done on mouse RNA. By cloning and sequencing, partial sequence of a mouse homologue of RD1 was obtained.

5.4.1. Alignment of mouse RD1 to rat and human PDE4A LR2 indicates that a hydrophilic MKEREKQQA motif forms the major primary structure difference between human and rodent PDE4A LR2

The previous alignment of human and rat LR2 (figure 5.2) is not supported by the extra sequence information derived from the partial sequence of mouse RD1. In a multiple alignment of the mouse, human and rat LR2 regions, the deletion of a hydrophilic motif from the two rodent PDE4As is indicated (figure 5.4.1).

This tentative new alignment prompted me to attempt to isolate RD1-like signals from brains of a range of species. It was anticipated that the sequence information so obtained would be useful in two ways. Firstly, one would be able to identify RD1 specific sequence conservation, so that primers could be designed to phylogenetically stable sequences (as shown in chapter 3 (163,207)) and tested on human RNA. Secondly, one would accumulate more sequence information to test the proposed new alignment and at the same time the sequence information would allow a preliminary survey of the evolutionary history of the newly identified rodent PDE4A deletion (see section 5.7.7.)

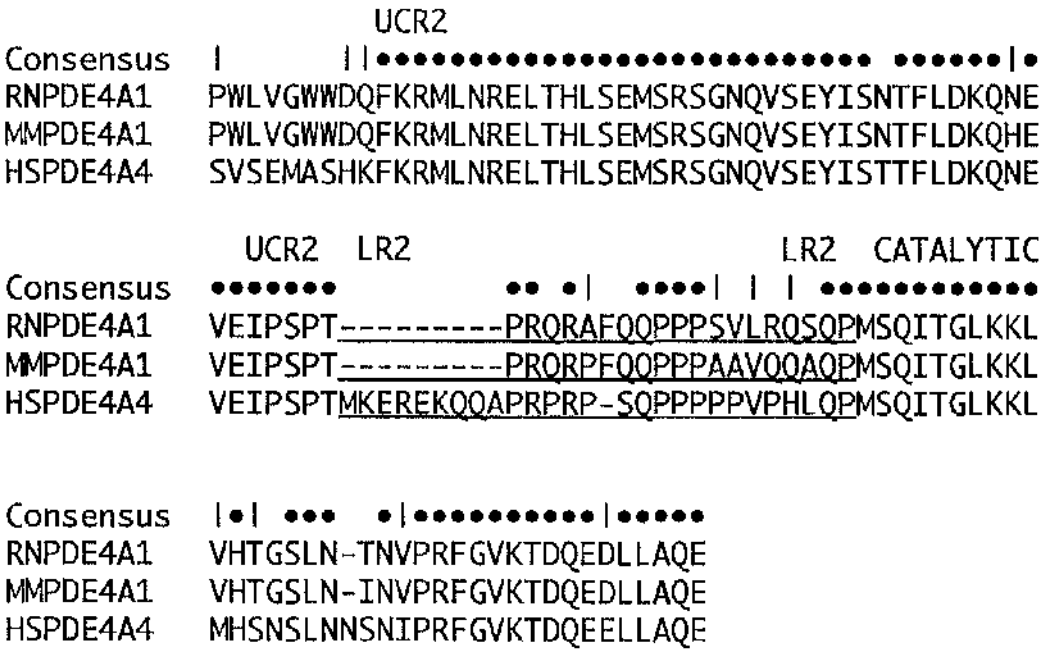

Figure 5.4.1. New alignment of PDE 4A LR2 when mouse PDE4A LR2 is include in the alignment.

Sequences from PCR fragments of rat (RNPDE4A1) and mouse (MMPDE4A1) PDE4A are aligned with human PDE4A (HSPDE4A4) sequence. LR2 sequence is underlined. The mouse sequence information exposes an alternative alignment where the human PDE4A LR2 specific motif is MKEREKQQA. LR2 and other PDE4 domains are marked to allow orientation.

5.5. IDENTIFICATION OF RD1-LIKE TRANSCRIPTS IN BRAIN RNA FROM A RANGE OF MAMMALS: DEMONSTRATION THAT RD1 IS HIGHLY CONSERVED

RT-PCR of RNA from the brains of various mammalian species detected RD1-like transcripts. This was done in RNA of cat, pig, rabbit, guinea pig and human. No signal was obtained from chicken, though this may simply reflect the longer evolutionary distance rather than an absence of an RD1-like transcript. Concerning the accuracy of the PCR data, each sequence represents data from six PCR clones. In every species, bar pig, all six colonies had identical sequence. In pig there was a 2/6 'silent' substitution in the DNA region coding for UCR2. The rat and human sequence in this chapter could, in part, be tested against existing sequence from rat and human PDE4A splice variants. I found no mismatches in the sequences of any of the clones.

The extra sequence found in human, pig, cat, guinea-pig and rabbit makes their bands slightly greater in size (~400bp). This agrees with the contention, put forward above (section 5.2), that the ~370bp band observed in RT-PCR on human cell lines with RD1 primers is an artefact. The sequences I have isolated are the first data which demonstrate that RD1-like species of RNA are conserved in mammals including human (human RD1 is henceforward designated hRD1)

5.5.1. Alignment of mammalian RD1 forms demonstrates that a hydrophilic MKEREKQQA motif forms the major primary structure difference between human and rodent PDE4A LR2

The extra DNA sequence and inferred peptide sequence confirms the new alignment suggested in the section 5.4.1. Thus, when all of the peptide sequences are aligned, the rat and mouse sequences skip the same sequences as was predicted by the mouse, rat and human alignment (compare figure 5.4.1. with 5.5.1.a). Furthermore, the DNA sequence alignments skip the same sequences (figure 5.5.1.b). Therefore, explicitly stated, the new alignment is favoured over the old one for two main reasons. Firstly, the alignment programs give the new alignment when as more sequence

information is supplied to them. Thus, a multiple alignment of mouse, rat and human PDE4A gives the new alignment. In contrast, a pair-wise alignment of rat and human PDE4A gives the old alignment. Secondly, the DNA alignment concurs with the new peptide alignment, not the old peptide alignment.

The new alignment clearly demonstrates that it is the deletion of the hydrophilic sequence, MKEREKQQA, which forms the major difference in primary structure between the LR2 regions of human and rodent PDE4A. LR2 regions of PDE4A which contain these hydrophilic regions (cat, pig, human and guinea-pig), are henceforth designated LR2HP (linker region 2 containing hydrophilic and proline components) to discriminate them from rodent PDE4A LR2P (linker region 2 containing proline component) regions which lack the hydrophilic domain. PDE4 LR2 regions categorisation is outlined in table 5.5.1. It is argued below (section 5.6.3.) that the hydrophilic component of LR2HP is an (otherwise) anciently conserved sequence.

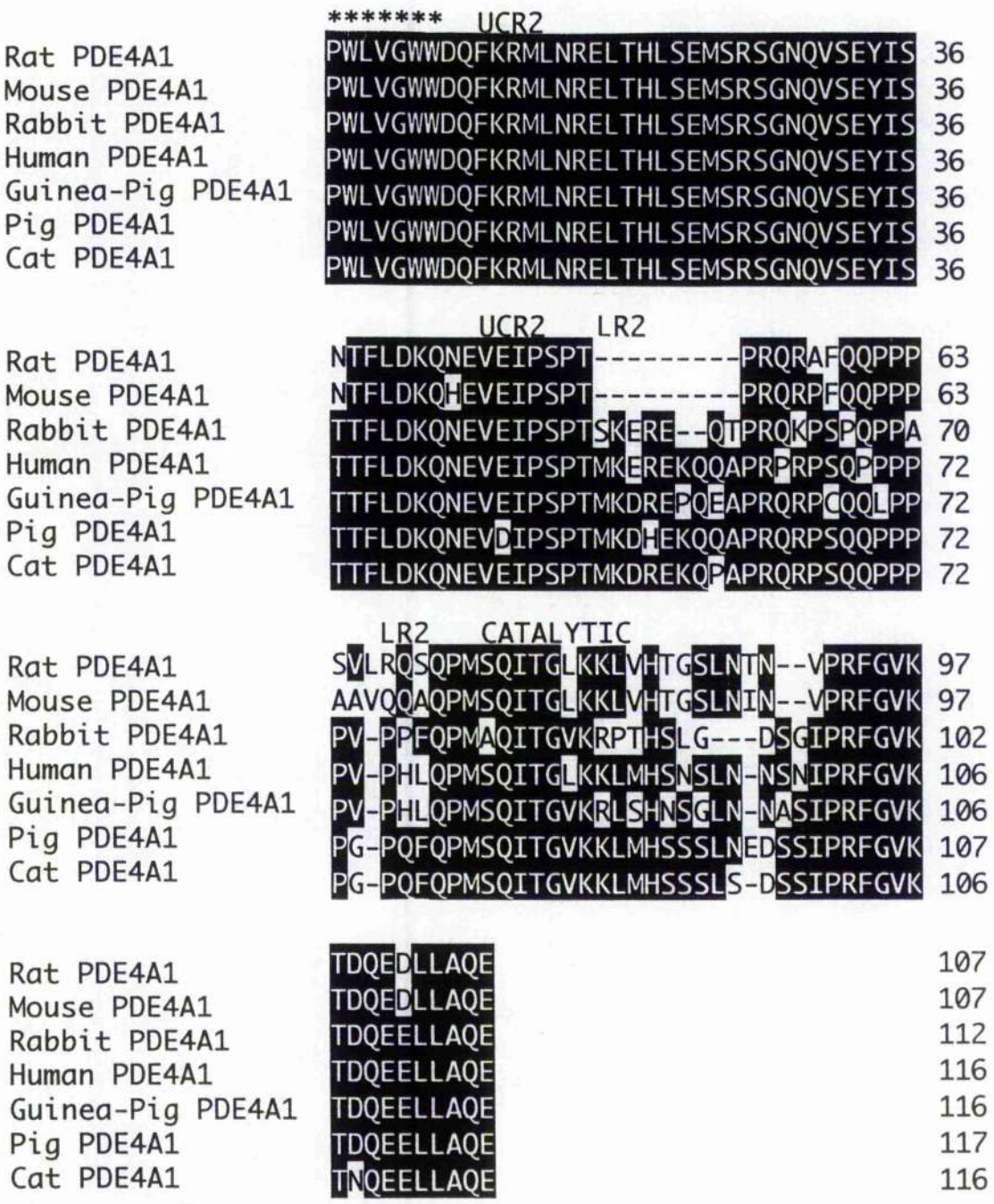

Figure 5.5.1.a. Peptide alignment of all seven mammalian RD1 like transcripts exposes the MKEREKQQA-like motif as a rat and mouse specific deletion. One RD1-specific and two PDE4 modules are conserved to differing degrees

All the mammalian RD1 like peptide sequences were aligned using a GeneJockey2 multiple alignment. Consensus matches are white on black, mismatches black on white. The MKEREKQQA-like motif is deleted in rat and mouse, with some disturbance also in the rabbit form. section (see 5.6.3.1.)

The RD1 PWLVGWW putative membrane association motif is perfectly (asterisked) and the UCR2 domain almost perfectly conserved in all species (section 5.6.1 and 5.6.2.). In comparison the N-terminal of the putative catalytic domain is poorly conserved with substitutions accepted at over 40% of the positions with one gap (section 5.6.3).

```
                          10        20        30
                          |         |         |
Consensus                 CCGTGGCTGGTGGGCTGGTGGGACCAGTTCAAGAGGATG
Human PDE4A1              CCTTGGCTGGTGGGCTGGTGGGACCAGTTCAAAAGGATG
Pig PDE4A1                CCGTGGCTGGTGGGCTGGTGGGACCAGTTCAAGAGGATG
Cat PDE4A1                CCGTGGCTGGTGGGCTGGTGGGACCAGTTCAAGAGGATG
Guinea-pig PDE4A1         CCGTGGCTGGTGGGCTGGTGGGACCAGTTCAAGAGGATG
Rabbit PDE4A1             CCGTGGCTGGTGGGCTGGTGGGACCAGTTCAAGAGGATG
Mouse PDE4A1              CCCTGGCTGGTGGGCTGGTGGGACCAGTTTAAAAGGATG
Rat PDE4A1                CCCTGGCTGGTGGGCTGGTGGGACCAGTTCAAAAGGATG

                     40        50        60        70
                     |         |         |         |
Consensus            CTGAACCGTGAGCTCACACACCTGTCAGAAATGAGCAGG
Human PDE4A1         TTGAACCGTGAGCTCACACACCTGTCAGAAATGAGCAGG
Pig PDE4A1           CTAAACCGTGAACTCACACACCTGTCAGAGATGAGCAGG
Cat PDE4A1           TTAAACCGTGAACTCACACACCTGTCAGAGATGAGCAGG
Guinea-pig PDE4A1    CTAAACCGGGAGCTCACACACCTGTCAGAAATGAGCAGG
Rabbit PDE4A1        CTGAACCGGGAGCTCACGCACCTGTCAGAAATGAGCAGA
Mouse PDE4A1         CTGAACCGGGAACTCACACACCTGTCGGAAATGAGCAGG
Rat PDE4A1           CTGAACCGTGAGCTCACACACCTGTCGGAAATGAGCAGG

                     80        90        100       110
                      |         |         |         |
Consensus            TCAGGAAACCAGGTCTCAGAGTACATTTCCACCACATTC
Human PDE4A1         TCCGGAAACCAGGTCTCAGAGTACATTTCCACAACATTC
Pig PDE4A1           TCAGGAAACCAGGTCTCTGAGTACATCTCCACTACATTC
Cat PDE4A1           TCAGGAAACCAGGTCTCTGAGTACATCTCCACCACATTC
Guinea-pig PDE4A1    TCGGGAAACCAGGTCTCAGAGTACATTTCCACGACATTC
Rabbit PDE4A1        TCAGGAAACCAAGTGTCAGAGTACATCTCCACCACGTTC
Mouse PDE4A1         TCAGGAAACCAGGTCTCAGAGTACATTTCCAACACGTTC
Rat PDE4A1           TCAGGAAACCAGGTCTCAGAGTACATTTCCAACACATTC

                     120       130       140       150
                       |         |         |         |
Consensus            CTGGACAAGCAGAATGAAGTGGAGATCCCATCACCCACG
Human PDE4A1         CTGGACAAACAGAATGAAGTGGAGATCCCATCACCCACG
Pig PDE4A1           CTGGATAAGCAGAATGAAGTGGACATCCCATCACCCACA
Cat PDE4A1           CTGGACAAGCAGAATGAAGTGGAGATTCCATCACCCACG
Guinea-pig PDE4A1    CTCGACAAACAGAATGAAGTGGAGATCCCGTCACCAACG
Rabbit PDE4A1        CTGGACAAACAGAATGAAGTGGAGATCCCCTCACCCACG
Mouse PDE4A1         CTAGACAAGCAGCACGAAGTGGAGATCCCATCGCCCACG
Rat PDE4A1           CTGGACAAGCAGAATGAAGTGGAGATCCCCTCACCCACA
```

```
                          M  K  E  R  E  K  Q  Q  A
                         160       170       180       190
                          |         |         |         |
Consensus                 ATGAAGGANCGAGANAAACAGCAAGCNCCNCGVCAGAGA
Human PDE4A1              ATGAAGGAACGAGAAAAACAGCAAGCGCCGCGACCAAGA
Pig PDE4A1                ATGAAGGATCATGAAAAACAGCAAGCACCACGGCAGAGA
Cat PDE4A1                ATGAAGGATCGAGAAAAACAGCCAGCTCCCCGCCAGAGA
Guinea-pig PDE4A1         ATGAAAGACCGAGAGCCCCAAGAAGCACCCCGACAAAGG
Rabbit PDE4A1             TCGAAGGAACGAGAG------CAGACGCCACGGCAGAAA
Mouse PDE4A1              --------------------------CCGCGACAGAGA
Rat PDE4A1                --------------------------CCTCGGCAGAGA

                           200       210       220       230
                            |         |         |         |
Consensus                 CCCTCCCAGCAGCCCCCACCCCCDGTVNNNCCVCAGTTC
Human PDE4A1              CCCTCCCAGCCGCCCCCGCCCCCTGTA---CCACACTTA
Pig PDE4A1                CCTTCCCAGCAGCCCCCACCCCCTGGA---CCACAGTTC
Cat PDE4A1                CCTTCCCAGCAGCCCCCGCCCCCTGGG---CCGCAATTC
Guinea-pig PDE4A1         CCCTGCCAGCAGCTTCCACCCCCAGTG---CCGCATTTG
Rabbit PDE4A1             CCCTCCCCGCAGCCCCCAGCCCCGGTC---CCCCCGTTC
Mouse PDE4A1              CCCTTCCAGCAGCCCCCACCAGCAGCAGTGCAGCAGGCC
Rat PDE4A1                GCCTTCCAGCAGCCCCCGCCGTCAGTGCTGCGACAGTCC

                           240       250       260       270
                            |         |         |         |
Consensus                 CAGCCCATGTCTCAGATCACAGGGGTGAAAAAGCTGATG
Human PDE4A1              CAGCCCATGTCCCAAATCACAGGGTTGAAAAAGTTGATG
Pig PDE4A1                CAGCCCATGTCACAGATCACCGGGGTGAAAAAGCTGATG
Cat PDE4A1                CAGCCCATGTCTCAGATCACGGGGGTGAAGAAGCTGATG
Guinea-pig PDE4A1         CAGCCCATGTCCCAGATCACGGGGGTGAAGAGGCTGTCG
Rabbit PDE4A1             CAGCCCATGGCTCAGATCACAGGGGTGAAAAGGCCCACA
Mouse PDE4A1              CAGCCCATGTCTCAGATCACAGGGCTGAAAAAGCTGGTA
Rat PDE4A1                CAGCCCATGTCTCAGATCACAGGGCTGAAAAAGCTGGTA

                           280       290       300       310
                            |         |         |         |
Consensus                 CACAGCAGCAGCCTGAACNNNNACTCCAGCATCCCCCGC
Human PDE4A1              CATAGTAACAGCCTGAAC---AACTCTAACATTCCCCGA
Pig PDE4A1                CATAGCAGCAGCCTGAATGAGGATTCCAGCATTCCCCGC
Cat PDE4A1                CATAGCAGCAGCCTGAGT---GACTCCAGCATCCCCCGC
Guinea-pig PDE4A1         CACAACAGCGGCCTGAAC---AACGCCAGCATCCCACGC
Rabbit PDE4A1             CACAGCCTCGGC---------GACTCTGGCATCCCCCGC
Mouse PDE4A1              CACACCGGAAGCTTGAAC------ATCAATGTCCCACGA
Rat PDE4A1                CACACTGGAAGCTTGAAC------ACCAACGTCCCACGG
```

```
                          320        330        340        350
                           |          |          |          |
Consensus                 TTTGGGGTGAAGACCGATCAAGAGGAGCTCCTGGCCCAA
Human PDE4A1              TTTGGGGTGAAGACCGATCAAGAAGAGCTCCTGGCCCAA
Pig PDE4A1                TTTGGGGTGAAGACCGATCAAGAGGAGCTCCTGGCCCAA
Cat PDE4A1                TTTGGGGTGAAGACCAACCAAGAAGAGCTCCTGGCCCAA
Guinea-pig PDE4A1         TTCGGGGTGAAGACGGATCAGGAGGAGCTCCTGGCCCAA
Rabbit PDE4A1             TTTGGCGTGAAGACCGACCAGGAGGAGCTCCTGGCACAG
Mouse PDE4A1              TTTGGAGTCAAGACAGATCAGGAGGACCTCTTAGCACAA
Rat PDE4A1                TTTGGAGTCAAGACAGATCAAGAGGACCTCTTAGCACAA
```

```
Consensus                 GAACT
Human PDE4A1              GAACT
Pig PDE4A1                GAACT
Cat PDE4A1                GAACT
Guinea-pig PDE4A1         GAGCT
Rabbit PDE4A1             GAACT
Mouse PDE4A1              GAACT
Rat PDE4A1                GAACT
```

Figure 5.5.1.b DNA alignment of mammalian RD1 like transcripts

DNA sequence from PCR fragments of (Genbank accession numbers in brackets) cat (U97589), pig (U97587), human (U97584), guinea-pig, rabbit (U97585), mouse (U97586) and rat are aligned by clustal alignment on the Gene Jockey 2 program, using the default settings. The rat and mouse nucleotide sequence clearly skip exactly the nucleotides that code for MKEREKQQA (this peptide sequence is shown). Small adjustments were made to the short insertions at ~220 and ~290 in order that they would match the peptide alignment as well. PCR conditions used to isolate the RD1 fragments: 34 cycles of 1 minute 94°C, 1 minute 49°C, 1 minute 72°C

SPECIES	GENE	HYDROPHILIC DOMAIN	PROLINE-RICH DOMAIN	
RAT	RNPDE4A	none	PRQRAFQQPPPSVLRQSQP	LR2P
MOUSE	MMPDE4A	none	PRQRPFQQPPPAAVQQAQP	LR2P
RABBIT	OCPDE4A	SKERQT	PRQKPSPQPPAPV-PPFQP	LR2P
HUMAN	HSPDE4A	MKEREKQQA	PRPRPSQPPPPPV-PHLQP	LR2HP
PIG	SSPDE4A	MKDHEKQQA	PRQRPSQQPPPPG-PQFQP	LR2HP
CAT	FCPDE4A	MKDREKQPA	PRQRPSQQPPPPG-PQFQP	LR2HP
GUINEA-PIG	CPPDE4A	MKDREPQEA	PRQRPCQQLPPPV-PHLQP	LR2HP

Table 5.5.1. Classification of PDE4A LR2 domain types

To facilitate discussion of the results of this chapter, two sub-classifications of PDE4A LR2 domain are designated as in the table above. SPECIES IDENTIFICATION KEY: CP cavia porcellus (guinea-pig), FC felis catus (cat), HS homo sapiens (human) MM mus musculus (mouse), OC oryctolagus cuniculus (rabbit), RN (rattus norvegicus), SS sus scrofa (pig)

5.6. ANALYSIS OF THE SEQUENCE CONSERVATION OF THE MODULES CONTAINED IN THE N-TERMINAL REGION OF SEVEN RD1-LIKE SPECIES

As anticipated, sequence analysis of the fragments of RD1 homologues has provided information on the conservation of the various modules included within the fragment, as well as allowing the evolutionary history of the rodent specific deletion to be examined (section 5.8.5.).

5.6.1. Conservation of the RD1 membrane association domain and PDE4A UCR2 in seven mammals

The most striking conservation of sequence is that of the RD1-specific, putative membrane-association determinant PWLVGWW (114) which is perfectly conserved with no residue mismatches between all species examined (figure 5.4.b). Indeed, the entire PWLVGWWDQFK (see section 1.7.4.1) putative membrane association helix is perfectly conserved between all seven RD1 homologues. The C-terminal 43 amino acids of UCR2 contained within these RD1-like species is also very highly conserved. There is only one non-conservative substitution, where threonine-289 (numbering for HSPDE4A4) is switched to an asparagine in rat and mouse. There are two conservative substitutions: these are asparagine-296 to histidine in mouse and glutamate-299 to aspartate in pig (figure 5.5.1.a).

5.6.2. The hydrophilic component of PDE4A LR2HP domain is conserved in two other PDE4 genes, PDE4B and PDE4D

As has already been described, LR2 is the region of PDE4 which connects UCR2 to the catalytic domain. In rodents, the LR2 region of PDE4A consists of a unique PDE4A proline-rich domain, LR2P. In human, cat, pig and guinea-pig PDE4A this proline-rich domain is juxtaposed with a hydrophilic domain and this type of LR2 region is termed LR2HP. These types of LR2 regions are thus very different from each other.

As well as being conserved between most PDE4A species, the hydrophilic

component of PDE4A LR2HP region is more widely conserved, with homologous regions found in PDE4B and PDE4D genes (figure 5.6.2.) I have termed these domains LR2H (Linker region 2 containing a hydrophilic component) regions. The PDE4B and PDE4D LR2H region is larger than the hydrophilic component of PDE4A LR2HP but there is charge conservation in the shared regions (figure 5.6.2). Thus there is a reversal of the normal situation where sequences are typically better conserved between species' homologues of a gene than between different genes. Deletion of this sequence correlates with a restructuring of the N-terminal of the catalytic domain. (see section 5.6.4.). Finally, not all PDE4s conform to the patterns so far described such that neither hydrophilic or proline-rich regions are found in PDE4C nor the *dunce* gene. I have termed these regions LR2A (Linker region 2 with atypical sequence).

```
          UCR2
Cons.                                FKRmL NRELTHLSEm SRSGNQVSEy ISnTFLDkQn
PDE4A  TMQTYRSVSE MASHKFKRML NRELTHLSEM SRSGNQVSEY ISTTFLDKQN
PDE4B  TIQTYRSVSE MASNKFKRML NRELTHLSEM SRSGNQVSEY ISNTFLDKQN
PDE4C  TLQTRHSVGE MASNKFKRIL NRELTHLSET SRSGNQVSEY ISRTFLDQQT
PDE4D  TLQTRHSVSE MASNKFKRML NRELTHLSEM SRSGNQVSEF ISNTFLDKQH

          301                                          Catalytic    350
Cons.  eVEiPspTqk erekkk.p.. .......... ...qpMsqIs G.kkLmHSsS
PDE4A  EVEIPSPTMK EREKQQAPRP RPSQPPPPPV PHLQPMSQIT GLKKLMHSNS
PDE4B  DVEIPSPTQK DREKKKKQ.. .......... ...QLMTQIS GVKKLMHSSS
PDE4C  EVELPKVTAE EAP..... .......... ...QPMSRIS GLHGLCHSAS
PDE4D  EVEIPSPTQK EKEKKKRP.. .......... .....MSQIS GVKKLMHSSS

          351                                                   400
Cons   LnnssipRFG VkT.qE..LA kE
PDE4A  LNNSNIPRFG VKTDQEELLA QELENLNKWG LNIFCVSDYA GGRSLTCIMY
PDE4B  LNNTSISRFG VNTENEDHLA KELEDLNKWG LNIFNVAGYS HNRPLTCIMY
PDE4C  LSSATVPRFG VQTDQEEQLA KELEDTNKWG LDVFKVADVS GNRPLTAIIF
PDE4D  LTNSSIPRFG VKTEQEDVLA KELEDVNKWG LHVFRIAELS GNRPLTVIMH
```

Figure 5.6.2. The hydrophilic component of the PDE4A LR2HP domain is conserved in other PDE4 genes

Alignment of partial sequences of PDE4 genes (human PDE4A, 4B, 4C & 4D are shown, there are similar sequences in rat PDE4B and 4D). The C-terminal of UCR2 and the N-terminal of the putative catalytic domain are underlined. The intervening section is the LR2 region. In the text the PDE4A LR2 regions which contain a hydrophilic motif (human, cat, pig and guinea-pig) are designated LR2HP regions and this sequence is in italics. The hydrophilic component of LR2HP which is conserved between PDE 4A, 4B and 4D (double underline) is shown within this sequence. This is a reversal of the normal situation as these sequences are not conserved between PDE 4A from different species, as has already been shown (rat, mouse vs human, rabbit, cat and pig; figures 5.5.1.a).

GENE	HYDROPHILIC LR2 REGION	PROLINE-RICH LR2 REGION	
HSPDE4A	MKEREKQQA	PRPRPSQPPPPPV-PHLQP	LR2HP
RNPDE4A	none	PRQRAFQQPPPSVLRQSQP	LR2P
HSPDE4B	QKDREKKKKQQL	none	LR2H
RNPDE4B	QKDREKKKKQQL	none	LR2H
HSPDE4D	QKEKEKKKRP	none	LR2H
RNPDE4D	QKEKEKKKRP	none	LR2H
HSPDE4C	none	none	LR2A
RNPDE4C	none	none	LR2A
DMPDE	none	none	LR2A

Table 5.6.2. Classification of PDE4 LR2 domain types compared with the two PDE4A LR2 subtypes.

To facilitate understanding of the results of this chapter, PDE4B, PDE4D and PDE4C and *dunce* PDE LR2 regions are classified based on their similarity to the hydrophilic component of the PDE4A LR2HP domain. SPECIES IDENTIFICATION KEY: CP cavia porcellus (guinea-pig), DM drosophila melanogaster (fruit fly), FC felis catus (cat), HS homo sapiens (human) MM mus musculus (mouse), OC oryctolagus cuniculus (rabbit), RN (rattus norvegicus), SS sus scrofa (pig)

5.6.3. Secondary structure analysis of LR2HP compared with LR2P

The hydrophilic sequences in the LR2HP and LR2H regions are exceptional in that they are the most hydrophilic sequence found in PDE4A outside of the putative catalytic domain. LR2HP is one of two hydrophilic proline-rich motifs found within HPDE46/RPDE6. The other hydrophilic-proline motif (UHP in figure 5.6.4.a) found in these splice variants is in their unique N-terminal (figure 5.6.4.a) (116). The functional significance, if any, of these hydrophilic proline motifs remains to be identified. So far, most of the allowed PDE 4A substitutions of LR2HP regions (excluding the rodent lineage-specific transition to LR2P) conserve charge, consistent with there being a functional role for this sequence. As a preliminary examination of the possible role of LR2HP/LR2P regions I have performed secondary structure analyses on all of the known LR2HP and LR2P sequences. Doing this I obtained three broad patterns from the data set of seven LR2 regions. For the LR2HP, as seen in human, pig, cat, and guinea-pig then using two secondary structure algorithms and a surface probability plot all suggest that MKEREKQQA like motif forms a surface alpha helix (figure 5.6.4.b). The rabbit form is intermediate between this form and LR2P forms (mouse and rat) where no secondary structure is predicted in the area of the deletion and the LR2 is much less hydrophilic (figure 5.6.4.c). A similar profile of secondary structure to that seen for the LR2HP (figure 5.5.4.2.b.) is seen in a UHP (data not shown) but there is not the same degree of charge conservation between the hydrophilic regions of the two sites as there is between different examples of the same site. Thus, the current consensus for the hydrophilic sections in all PDE4A UHP & LR2HP is (D/E)rE(k/r)q, (where capitals represent the only residues found at that position and non-capitals represent residues where there is 1/6 substitution). Yet there is a higher degree of consensus between genes for the LR2HP when it is compared to the homologous LR2H regions in PDE4B and PDE4D. Here the consensus is K(D/E)(K/R)EK(K/Q)(k/q) (where non-capitals represent residues where there is a 1/9 substitution).

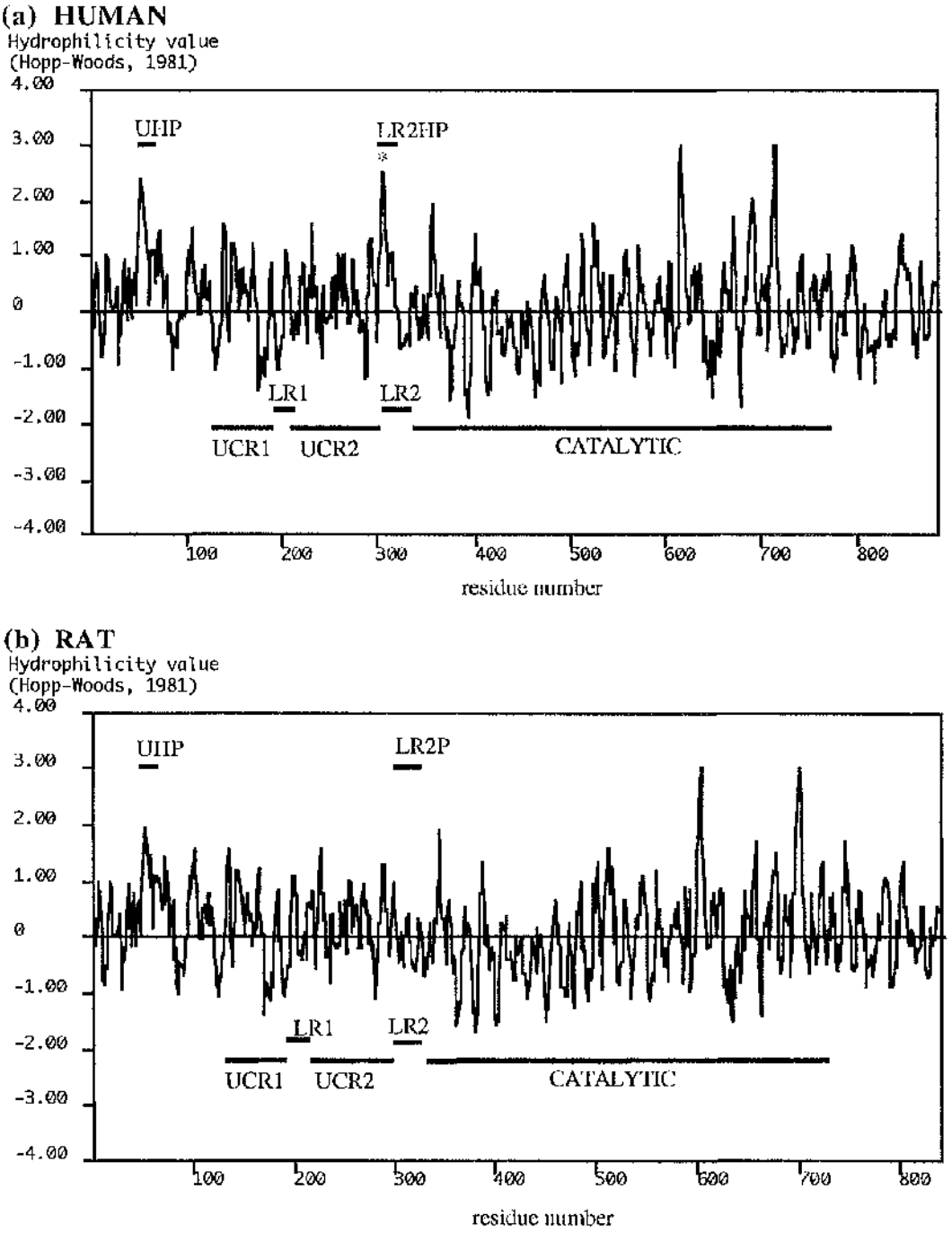

Figure 5.6.4.a Hopp-Woods hydrophilicity plots of HSPDE4A4 and RNPDE4A5: Missing hydrophilic MKEREKQQA section of LR2HP in the rat LR2P

MKEREKQQA corresponds to the asterisked 'spike' in HSPDE4A4 (HUMAN) which is missing from the otherwise identical plot of RNPDE4A5 (RAT) hydrophilicity. This domain forms part of a PDE4A hydrophilic-proline LR2 (LR2HP), as shown, which is therefore missing in rat (LR2P). There is another hydrophilic-proline rich domain which is shared between PDE46 and rPDE6 (UHP). UCR1, UCR2, LR1, LR2 and the catalytic domain are shown to allow orientation

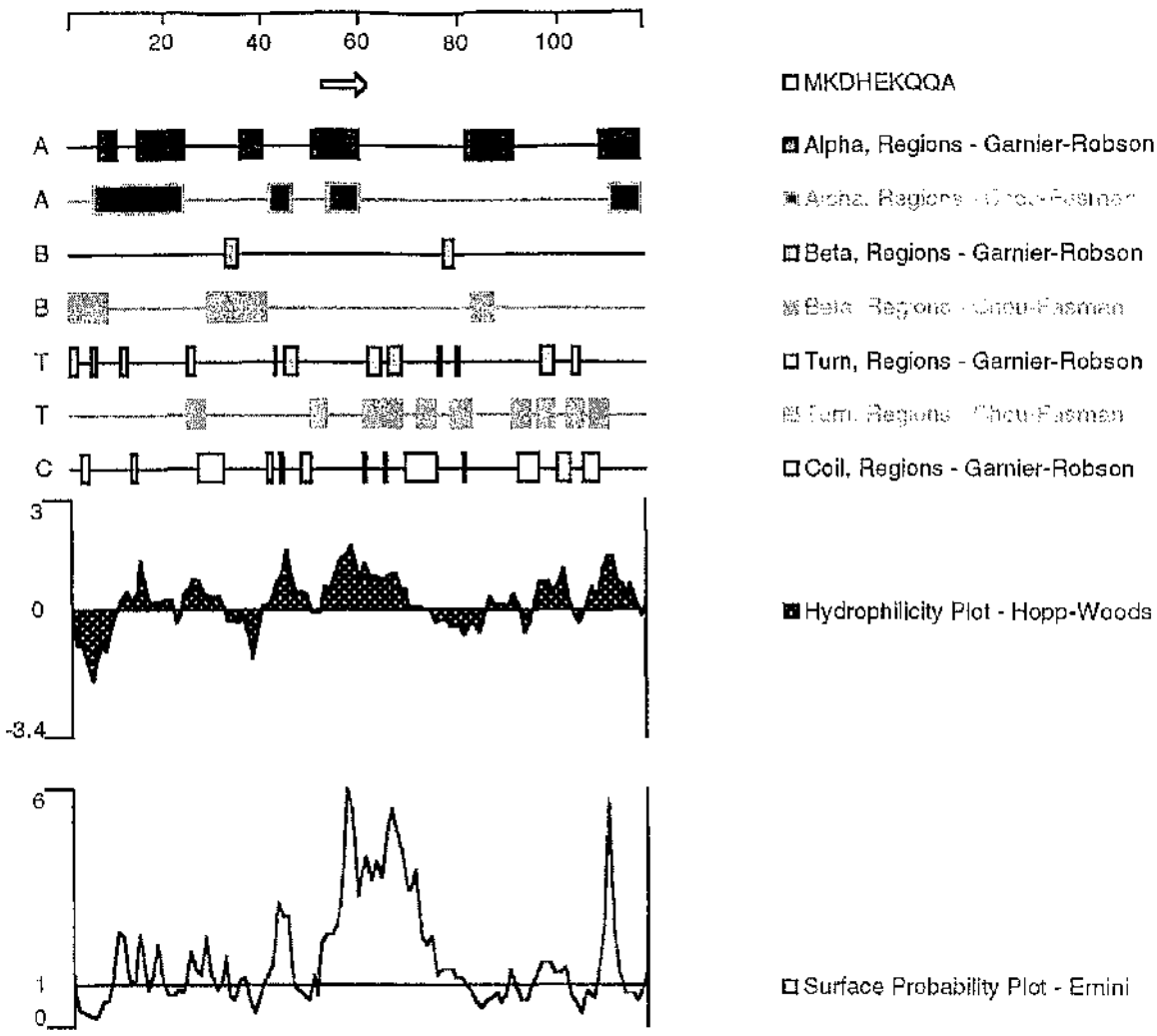

Figure 5.6.4.b Predictive Peptide Analysis of LR2HP Region

The partial peptide sequences (~110 amino acids) of PDE4A that I have obtained (see figure 5.5.1.a) were analysed using a number of predictive algorithms. This plot is typical of those when human, guinea-pig, cat or in this case pig are subjected to Hopp-Woods hydrophilicity, Emini surface probability and Chou & Fasman and Garnier & Robson secondary structure analyses. These species' PDE4A contain the LR2HP type of LR2 domains. The position of the hydrophilic component of LR2HP is marked on the first line. The two secondary structure algorithms agree and are consistent with LR2HP regions forming a surface alpha helix in PDE4A. The sequence in the region of the deletion in rat and mouse PDE4A is not predictive of alpha helix, is much less hydrophilic and is less likely to be present at the surface (compare with figure 5.6.4.c)

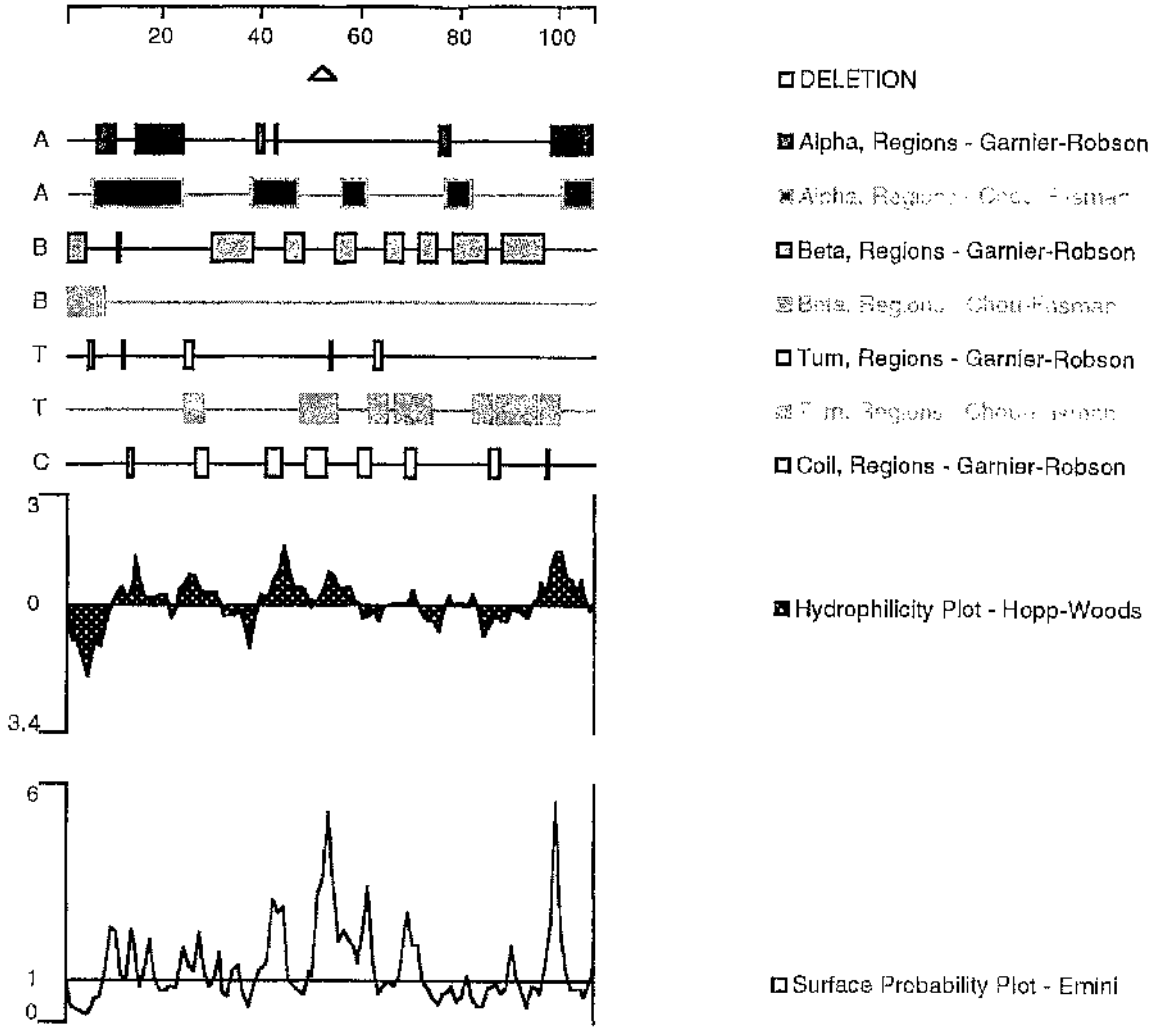

Figure 5.6.4.c Predictive Peptide Analysis of LR2P Region

The complete partial peptide sequences (~110 amino acids) of PDE4A that I have obtained (see figure 5.5.1.a) were analysed using a number of predictive algorithms. This plot is typical of those when mouse or in this case rat are subjected to Hopp-Woods hydrophilicity, Emini surface probability and Chou & Fasman and Garnier & Robson secondary structure analyses. These species' PDE4A **do not contain** the hydrophilic component of LR2HP and are termed LR2P. The deletion relative to LR2HP is marked in the first line above. In contrast to LRHP2, in LR2P the two secondary structure algorithms predict random coil structure in the region around the deletion and this sequence is less likely to be presented at the surface.

5.6.5. Conservation of the N-terminal of the putative catalytic domain: conservation of an octapeptide occurs only in PDE genes with LR2H or LR2HP regions

The PDE4A sequences I have obtained extend into the catalytic domain. The maximum N-terminal extent of the putative catalytic domain is marked in figure 5.6.2. This N-terminal catalytic sequence was not as well conserved as UCR2 in the RD1 homologues I isolated. Nearly 40% of the positions are substituted and one gap is inserted (figure 5.5.1.a). I have found that the lack of conservation is concentrated in an octapeptide following the well conserved putative start of the PDE4 catalytic domain (see Introduction). Thus, the region between 332 and 344 (numbering for HSPDE4A4, as in figure 5.6.2.) is highly conserved between all PDE4 genes with a consensus of MsQITGvKklmHs (where capitals represent invariant residues and non-capitals residues with an absolute majority at that position). In contrast, the next eight residues, between positions 345 and 352, are found conserved only in a subset of PDE4 sequences. Thus, this octapeptide has a consensus of ssLnnssI (case significance as above) in PDE4 genes which contain LR2HP or LR2H but is unconserved in PDE4 genes which lack a hydrophilic domain in LR2 (see figure 5.6.5.a and 5.6.5.b). As a control, I compared LR1 sequences from PDE4 forms and found that conservation of LR1 sequence was not linked to any particular LR2 subtype. Instead LR1 sequences are most closely conserved between homologues of the same gene from different genes, as would be expected.

Percent Similarity

Percent Divergence

	1	2	3	4	5	6	7	8	9	10	11	12	13	14		
1		33.3	11.1	11.1	0.0	0.0	11.1	11.1	11.1	11.1	11.1	11.1	0.0	11.1	1	DMPDE
2	75.0		44.4	22.2	22.2	22.2	44.4	44.4	44.4	44.4	44.4	44.4	33.3	44.4	2	RNPDE4C
3	100.0	62.5		11.1	33.3	22.2	33.3	33.3	33.3	33.3	33.3	44.4	22.2	33.3	3	HSPDE4C
4	100.0	83.3	100.0		0.0	0.0	33.3	33.3	22.2	22.2	33.3	44.4	33.3	33.3	4	OCPDE4A
5	100.0	66.7	50.0	100.0		77.8	33.3	33.3	44.4	44.4	33.3	22.2	33.3	44.4	5	MMPDE4A
6	100.0	66.7	66.7	100.0	28.6		33.3	33.3	44.4	44.4	33.3	22.2	33.3	44.4	6	RNPDE4A
7	100.0	62.5	75.0	66.7	50.0	50.0		88.9	66.7	66.7	55.6	66.7	55.6	66.7	7	RNPDE4D
8	100.0	62.5	75.0	66.7	50.0	50.0	12.5		77.8	77.8	66.7	77.8	66.7	66.7	8	HSPDE4D
9	100.0	62.5	75.0	83.3	33.3	33.3	37.5	25.0		100.0	77.8	66.7	66.7	66.7	9	RNPDE4B
10	100.0	62.5	75.0	83.3	33.3	33.3	37.5	25.0	0.0		77.8	66.7	66.7	66.7	10	HSPDE4B
11	100.0	62.5	75.0	66.7	50.0	50.0	50.0	37.5	25.0	25.0		55.6	55.6	55.6	11	CPPDE4A
12	100.0	62.5	62.5	50.0	66.7	66.7	37.5	25.0	37.5	37.5	50.0		77.8	55.6	12	FCPDE4A
13	100.0	62.5	75.0	50.0	57.1	57.1	37.5	25.0	25.0	25.0	37.5	12.5		55.6	13	SSPDE4A
14	100.0	62.5	75.0	66.7	33.3	33.3	37.5	37.5	37.5	37.5	50.0	50.0	37.5		14	HSPDE4A
	1	2	3	4	5	6	7	8	9	10	11	12	13	14		

Figure 5.6.5.a Conservation of an octapeptide of sequence within the catalytic domain correlates with conservation of the hydrophilic domain of LR2 in PDE4 forms.

The matrix above shows the similarity of sequences in the octapeptide towards the beginning of the putative start of the catalytic domain. The octapeptide follows on from the start of the putative PDE4 consensus from (numbering for HSPDE4A4) amino acids 332 and 344 MsqIsGvkklmHs which is at the beginning of the putative catalytic domain (19) (see Introduction). Thirteen PDE4 sequences and dunce were compared in this region using the default settings on the DNAstar program. Percentage similarity is shown in the top right half, dissimilarity in the bottom left half. The diagram is quartered with two bold lines. The 'south-east' quadrant shows that this octapeptide is conserved between PDE4s which contain LR2HP or LR2P. These sequences are cat, guinea-pig, pig and human PDE4A, human and rat PDE4B and human and rat PDE4D. Sequences which lack hydrophilic LR2 regions (dunce, rat and human PDE4C rabbit, rat and mouse PDE4A) do not conserve their own separate sequence in this region, 'north-west', yet neither are their sequences in this part of the catalytic domain similar to those conserved between PDEs that contain the hydrophilic domain in LR2, ('north-east' & 'south-west')

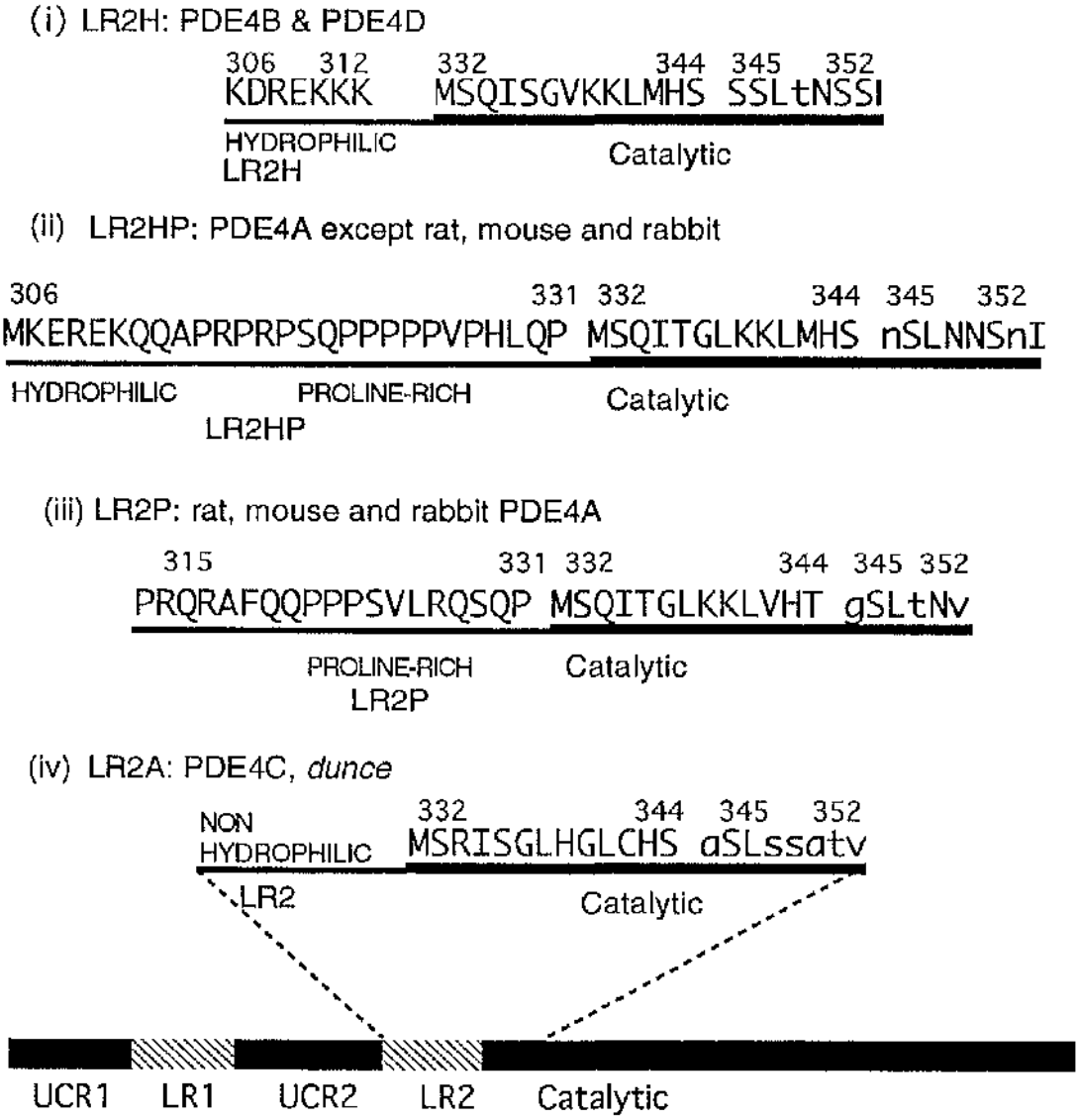

5.6.5.b. Schematic of LR2/catalytic conservation for PDE4 genes

The conservation data of 5.6.5.a is summarised in the schematic above. The LR2 domain and the furthest extent of the putative catalytic domain (19), are shown respectively with thin and thick line. Numbering of residues is for HSPDE4A4. Sequences are human PDE4A for (i), human PDE4D for (ii), rat PDE4A for (iii) and human PDE4C for (iv). A schematic PDE4 gene structure is added to allow orientation.

(i) Conservation of a hydrophilic domain in LR2 (LR2H) correlates with conservation of the SSLNNSSI (matches to this consensus are shown in capitals) domain which lies just within the putative catalytic domain. The intervening sequence is conserved in all PDE4 forms, as shown. (ii) The hydrophilic domain and SSLNNSSI conservation correlation is also seen in PDE4A LR2HP domains (LR2 region which contains hydrophilic and proline motifs.). (iii) In rat, mouse and rabbit PDE4A the hydrophilic LR2 sequence is deleted. The 8mer whose conservation is linked with LR2H and LR2P is similarly unconserved. (iv) In LR2A subtypes there is no LR2 hydrophilic sequence with less hydrophilic sequences substituted. Again, the SSLNNSSI-like motifs are not conserved.

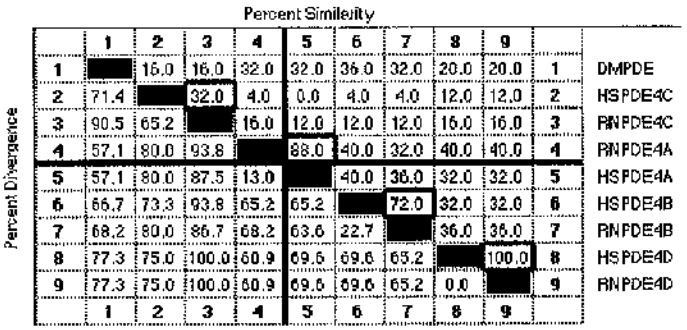

Figure 5.6.5.c Sequences are typically conserved better in homologues of the same gene than in different genes.

The matrix above shows the similarity of sequences in PDE4 LR1. Eight PDE4 LR1 sequences and dunce were compared using the default settings on the DNAstar program. Percentage similarity is shown in the top right half, dissimilarity in the bottom left half. The diagram is quartered with two bold lines as in figure 5.6.5.a. The 'south-east' quadrant shows the conservation of LR1 in PDE4s which contain LR2HP or LR2P. These sequences are human PDE4A, human and rat PDE4B and human and rat PDE4D. In the 'north-west' quarter of the diagram the conservation of LR1 sequence between PDE4 with LR2A regions which lack hydrophilic LR2 component (dunce, rat and human PDE4C rabbit, rat and mouse PDE4A) is shown. The 'north-east' and 'south-west' quarters of the diagram compare LR1 sequences from PDE4 which contain LR2A with LR1 sequences from PDE4 which contain LR2H and LR2HP.

Unlike figure 5.6.5.a, no clear pattern emerges in the quadrants described. This indicates that LR1 conservation is not linked with conservation of the hydrophilic domain of LR2. Instead, LR1 sequences are most closely related to the homologue of the same gene (bold bordered boxes.)

SPECIES	GENE	LR2 TYPE	LINKED CATALYTIC SEQUENCE
HUMAN	HSPDE4A	LR2HP	nSLN-NSnI
PIG	**SSPDE4A**	LR2HP	SSLNedSSI
CAT	FCPDE4A	LR2HP	SSLs-dSSI
GUINEA PIG	CPPDE4A	LR2HP	SgLN-NaSI
HUMAN	HSPDE4B	LR2H	SSLN-NtSI
RAT	RNPDE4B	LR2H	SSLN-NtSI
HUMAN	HSPDE4D	LR2H	SSLt-NSSI
RAT	RNPDE4D	LR2H	SSLt-NScI
RAT	RNPDE4A	LR2P	gSLNtN--n
MOUSE	MMPDE4A	LR2P	gSLNiN--v
RABBIT	OCPDE4A	LR2P	lg---dSgI
HUMAN	HSPDE4C	LR2A	aSLs-satv
RAT	RNPDE4C	LR2A	tSLp-taaI
DROSOPHILA	DMPDE	LR2A	tnSf-tger

Table 5.6.5. Conservation of an octapeptide of sequence within the catalytic domain is linked with conservation of LR2H and LR2HP regions

This table recapitulates the information in figure 5.6.5.a-c. An octapeptide of putative catalytic sequence is apparently only conserved in PDE forms which conserve a hydrophilic domain in LR2. The type of LR2 for each PDE is listed (LR2HP, LR2H, LR2P and LR2A) and the conservation of the SSLNNSSI motif in the putative catalytic domain (matches are in upper case, mismatches in lower case. LR2H and LR2HP domains are linked with conservation of SSLNNSSI, these PDE forms are highlighted in bold. SPECIES IDENTIFICATION KEY: CP cavia porcellus (guinea-pig), DM drosophila melanogaster (fruit fly), FC felis catus (cat), HS homo sapiens (human) MM mus musculus (mouse), OC oryctolagus cuniculus (rabbit), RN (rattus norvegicus), SS sus scrofa (pig)

5.7. Human RD1 RNA shares homology with rat RD1 upstream of the putative initiator methionine.

The full length sequence of hRD1 has now been deduced from cosmid clones of human genomic DNA (82). It is homologous to the rat form RD1 over the coding sequence for its unique 5' alternative splice region and also further upstream than the initiator ATG. RT-PCR of primers designed to this sequence were able to amplify a fragment from human brain. TA cloning and sequencing demonstrated that this sequence was the result of amplification of the hRD1 transcript. This result confirms that the initiator methionine is present in the hRD1 like transcript, along with conserved sequence further upstream.

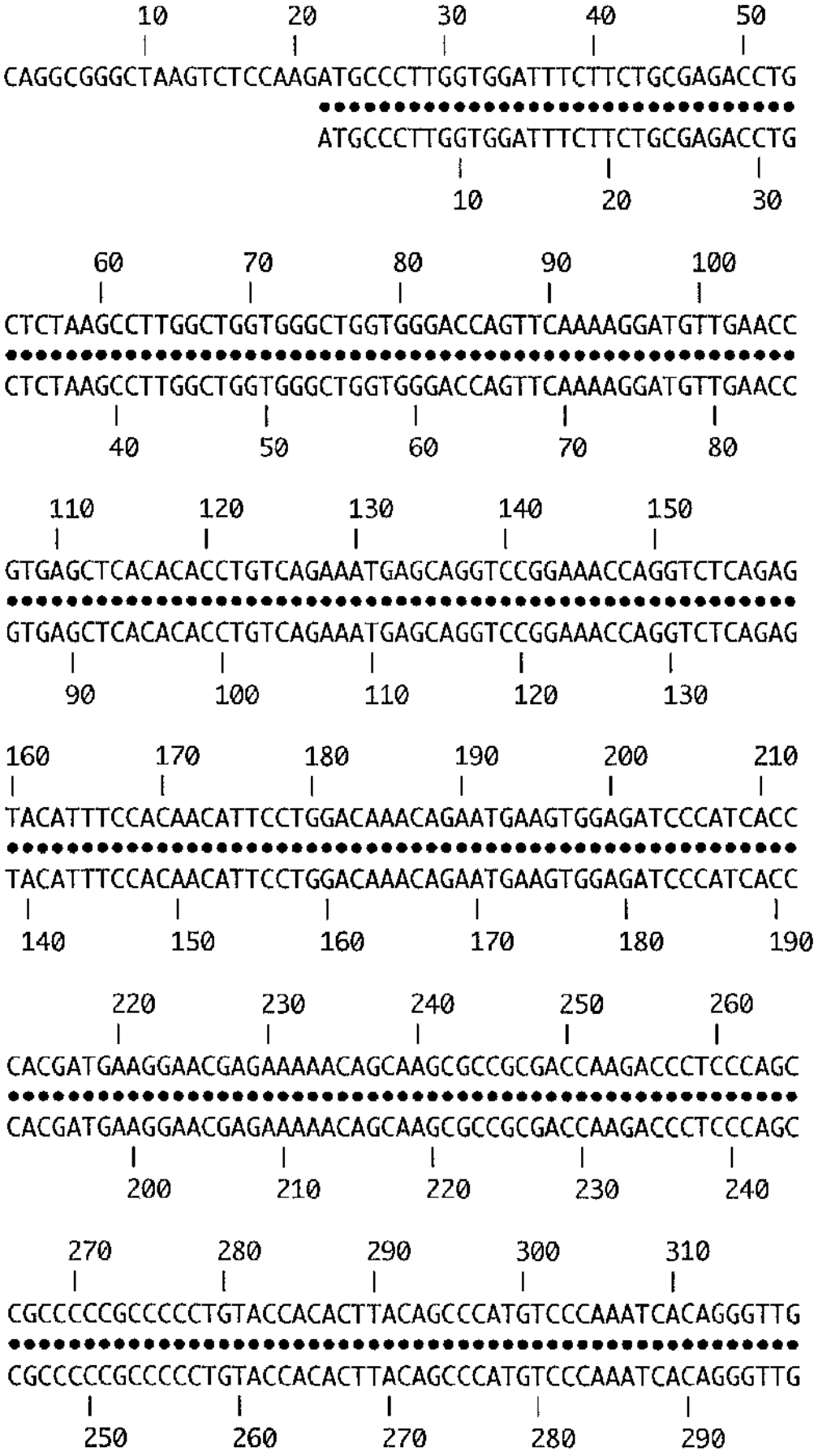
10 20 30 40 50
CAGGCGGGCTAAGTCTCCAAGATGCCCTTGGTGGATTTCTTCTGCGAGACCTG
ATGCCCTTGGTGGATTTCTTCTGCGAGACCTG
10 20 30
60 70 80 90 100
CTCTAAGCCTTGGCTGGTGGGCTGGTGGGACCAGTTCAAAAGGATGTTGAACC
CTCTAAGCCTTGGCTGGTGGGCTGGTGGGACCAGTTCAAAAGGATGTTGAACC
40 50 60 70 80
110 120 130 140 150
GTGAGCTCACACACCTGTCAGAAATGAGCAGGTCCGGAAACCAGGTCTCAGAG
GTGAGCTCACACACCTGTCAGAAATGAGCAGGTCCGGAAACCAGGTCTCAGAG
90 100 110 120 130
160 170 180 190 200 210
TACATTTCCACAACATTCCTGGACAAACAGAATGAAGTGGAGATCCCATCACC
TACATTTCCACAACATTCCTGGACAAACAGAATGAAGTGGAGATCCCATCACC
140 150 160 170 180 190
220 230 240 250 260
CACGATGAAGGAACGAGAAAAACAGCAAGCGCCGCGACCAAGACCCTCCCAGC
CACGATGAAGGAACGAGAAAAACAGCAAGCGCCGCGACCAAGACCCTCCCAGC
200 210 220 230 240
270 280 290 300 310
CGCCCCCGCCCCCTGTACCACACTTACAGCCCATGTCCCAAATCACAGGGTTG
CGCCCCCGCCCCCTGTACCACACTTACAGCCCATGTCCCAAATCACAGGGTTG
250 260 270 280 290

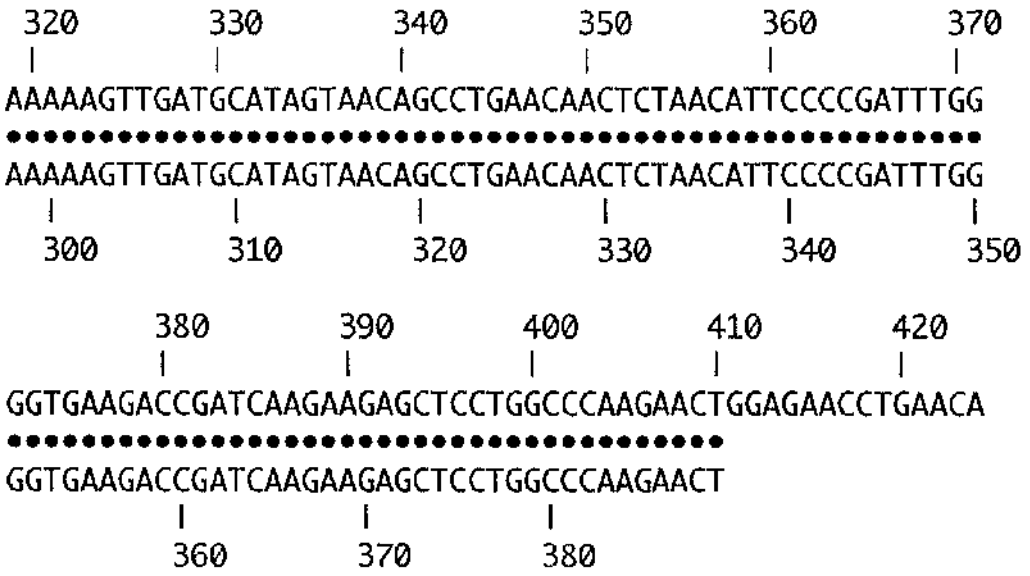

Figure 5.7. RD1-like transcript in human brain RNA

Human brain RNA was probed for RD-1 like transcripts by RT-PCR using GR36 and a GR5'hRD1. Sequence of one of ten TA clones (clone h3) from this PCR reaction (bottom) is shown aligned to the expected transcript that would be produced if the RD1 exon isolated from human genomic DNA was spliced in the same manner as rat RD1 (82). This sequence starts at the conserved initiator methionine (underlined).

5.8. CONCLUSION

5.8.1. RD1(RNPDE4A1)-like PDE4A splice variants transcripts are expressed in brains from various mammals.

In this chapter one of the longest standing questions of PDE molecular biology has been answered, namely: do homologues of RD1 exist in other species? By using primers designed to rat RD1, then using a low stringency RT-PCR procedure on brain RNA I have been able to demonstrate that RD1-like transcripts are expressed in a variety of mammals. Thus RD1 has become only the second PDE4A splice variant, after HPDE46 (HSPDE4A4)/RPDE6 (RNPDE4A5) which has been unequivocally identified in more than one species. Since rat RD1 has been shown to date only to be expressed in the brain it is reasonable to anticipate that this may be the case in human. It will thus be of interest to see if a neuronal cell line can be found which expresses hRD1. The lack of availability of rat brain cell lines has meant that studies on RD1 were hampered because the only sources from which RD1 could be obtained were native brain tissue or recombinant protein. RT-PCR screening of the large number of human brain cell lines holds out the possibility that a cell line expressing hRD1 may yet be found, which will make possible studies on regulation and targeting of endogenous protein.

5.8.2. The importance of functional domains identified in RD1 and in other PDE4 species is underscored by their conservation in mammalian RD1-like homologues.

My finding that the putative membrane association domain of RD1, PWLVGWW, is perfectly conserved in mammals emphasises the importance of a number of papers which have established this motif as a novel membrane association determinant which is primarily responsible for the membrane association of rat RD1 (see Introduction) through a protein-protein hydrophobic interaction (102,110,111,113,114). The next residues are also perfectly conserved which is consistent with the notion that the DQFKR motif is needed to stabilise the PWLVGWW motif as was suggested by Smith et al (114). Given the conservation of

the unique RD1 motifs which is implied in the data presented here, it would seem likely that this region is conserved across all mammals, underscoring its importance. Further, the conservation of the N-terminus of RD1 is certainly consistent with membrane association being due to a conserved molecular recognition involving the N-terminal of RD1 (as proposed in (19)), rather than it being due to a less stringently conserved membrane insertion. This data makes it imperative that the molecular mechanism by which PWLVGWW attaches to membranes be elucidated and the physiological importance of this event defined.

The finding that the C-terminal of UCR2 is almost invariant between seven species of mammals (40/43 invariant residues) further confirms the conclusions drawn from the previous dunce/human/rat comparisons which first established the existence of UCR 2 conservation in PDE4 forms **(68,81)**. The function of UCR2 remains poorly defined

5.8.3. Sequence conservation analyses of the mammalian PDE4 LR2 regions and putative catalytic domain suggest two correlated variations of "ancient" PDE4 sequence in PDE4C, *dunce*, and in rat, rabbit and mouse PDE4A

I have identified a short stretch of hydrophilic sequence which appears to be deleted from rat, mouse and rabbit PDE4A LR2P, which is not conserved in dunce and PDE4C LR2A but which is present in all other mammalian PDE4A, B and D forms. This deletion is predicted to alter radically the secondary structure of the LR2 region. Comparison of my PDE4A partial clones with other PDE4 sequences also allowed identification of a second sequence which is apparently variable in a subset of PDE4. Interestingly, this variation correlates with deletion of the hydrophilic domain of LR2. Thus there is a reversal of the normal situation, where sequences are typically conserved more between homologues of a gene from various species than between different genes in the same species. I have shown, for example, that the latter is the case for conservation patterns in LR1.

Regardless of whether the LR2 hydrophilic motif and its linked octapeptide

reflect 'ancient' mammalian sequence which has been duplicated in three of the four genes, or evolutionary molecular parallelism, a clear inference that can be drawn is that these sequences interact in some way because their conservation is linked.

Such sequence conservation analyses may now provide a means to derive the function of LR2HP. Whilst it is clear that the rat and mouse species are able to function without LR2HP and the linked 8mer within the putative catalytic domain, there may be nevertheless, alterations in function due to these changes. Thus mouse and rat PDE4A splice variants will provide 'null' controls against which putative functions of the domain can be tested. These may be powerful tools in experiments that aim to elucidate the role of LR2HP. Functional differences between rat PDE4A splice variants and their human homologues have already been observed. As discussed at length in the introduction, HPDE46 (HSPDE4A4) is able to switch between two states as sensed by rolipram, whereas the rat homologue of this isoform, RPDE6 (RNPDE4A5), does not exhibit this ability (77,100). The unequivocal test of whether this property can be attributed to the newly identified sequences would thus be to engineer LR2HP and/or the linked catalytic 8 mer domains into the rat PDE4A in an attempt to recover a PDE with rolipram inhibition kinetics that resemble those of the human PDE4A. (figure 5.7.4). The converse approach would be to attempt to knock-out conformation shifting in human PDE4A by deleting the hydrophilic domain in LR2 and/or the linked octapeptide in the catalytic domain.

The interaction between LR2HP/LR2H and the linked 8mer, suggested above, could be regulated in PDE4A forms by binding to SH3 domains by virtue of the intervening sequence being proline rich. SH3 binding to the PDE4A specific LR2 proline motif could sterically interfere with this interaction. This notion is consistent with functional differences between RPDE6 and HPDE46 which have been observed in COS cells. Thus, both RPDE6 and HPDE46 could bind to SH3 domains because their respective LR2 domains, LR2P and LR2HP, have proline-rich regions. Therefore, both HPDE46 and RPDE6 would bind to membranes. Only in HPDE46 could this be expected to effect the interaction between LR2HP and the linked 8mer peptide in the catalytic domain, leading to conformational change. Evidence for such a

mechanism could be obtained by trying to mimic the apparent effects of SH3 domain interaction on HPDE46 by saturating cell lysates with peptides designed to the hydrophilic section of LR2HP or the linked 8mer peptide sequence. This would be expected to produce a conformer with a high affinity of rolipram binding in the absence of SH3 containing proteins.

Data is now also needed to define whether switches in other PDEs occur due to the sequence motifs identified here. Thus, based on the assumption that switching is caused by some interaction between LR2H/LR2HP and the linked 8mer, it is predicted that isoforms which contain this sequence, PDE4A, B and D, will have multi-state conformations. To date, this switching has only been shown for PDE4A and PDE4D forms, as discussed in the introduction. PDE4B forms all show complex kinetics of rolipram inhibition (83,90). Although various IC_{50} (varying by up to 10 fold) values have been obtained for subcellular fractions of PDE4B, switching between these different kinetics of rolipram inhibition has not yet been observed.

Dunce PDE and PDE4C, which lack both LR2H/LR2HP and the linked 8mer, are predicted not to be able to exhibit switching between multi-state conformations. In this regard, Dunce PDE is not susceptible to inhibition by rolipram which in itself is consistent with the notion that LR2H and the linked 8mer may have a role in rolipram binding. PDE4C does retain rolipram binding however. So, clearly, even if LR2H and the linked 8mer play a role in rolipram binding, other conserved domains must exist in the rest of the protein. Intracellular switching of rolipram kinetics has not been observed in PDE4C. However, different patterns of rolipram inhibition have been detected for PDE4C from different sources. Rolipram inhibition which observed simple kinetics was detected in yeast whereas in COS-7 cells a complex inhibition was observed (78). Importantly however, these two PDEs showed a major (4-fold) alteration in the K_m for cAMP and thus are qualitatively different from the conformers sensed by rolipram in PDE4A, B and D where the K_m for cAMP is always unchanged (90,100,137).

To recapitulate, the conformational shifts sensed by alterations of rolipram inhibition kinetics in PDE4C are also detected by an altered affinity of cAMP. Since

the conformational shift detected in PDE4A, B and D is not sensed by cAMP, the underlying molecular basis for the alteration in PDE4C kinetics is probably not the same as that for PDE4A, B and D. Neither has PDE4C been shown to switch conformations in a single cell type, as is the case for PDE4A and PDE4D.

The form of the interaction that takes place between the LR2H/LR2HP and the linked 8mer peptide remains obscure. The LR2H/LR2HP hydrophilic sequence is, generally, positively charged but the linked catalytic octapeptide is uncharged. From the point of view of regulation one of the most attractive possibilities is that one or more of the four serines in the octapeptide could be phosphorylated and that this incorporation of negative charge would then allow a conditional charge interaction with the LR2 as has been suggested previously for UCR1 association with UCR2 (19) but unlike the former case there are no obvious consensus sites for known kinases in this region (215).

5.8.4. Sequence variations in the N-terminal of the catalytic domain are consistent with the shortest previous estimation of the range of the catalytic domain

The finding here that the N-terminal of the putative catalytic domain is not very well conserved also concurs with the existing dunce/human/rat conservation data (see section 1.7.2.) but this appears to be accentuated in my data set. My data shows that the mammalian PDE4A putative catalytic domain is well conserved at its extreme N-terminal, starting at methionine 332 with a consensus of MsQITGvKklmHs, in good agreement with existing data (19). In the PDE4A sequences that I have isolated there is then the 8mer of sequence variation (residues 345-352) which was discussed above. Finally, there is a highly conserved sequence starting iPRFGVKT... This sequence, starting at position 352, is close to the starting positions of truncation mutants hyb1 (starts at 365) and ΔG212-P342 (which starts at 342) (19,129), which are the most radically truncated PDE constructs which still retain catalytic activity. The truncation data therefore indicates that the catalytic domain proper commences at the iPRFGVKT... motif (19). The lack of sequence conservation that I have identified in

the 8mer linked peptide (345-352) concurs with this notion. Nevertheless, the position of the MsQITGvKklmHs motif and its conservation means that though it is unnecessary for PDE catalytic activity its position makes it highly likely that it will have some role in catalysis or catalytic regulation in native PDE4.

5.8.5. The PDE4A LR2 hydrophilic motif deletion may be suitable for delineating the true extent of the order rodentia.

Establishing ancestry by molecular means depends on finding genetic lesions which have occurred and been consolidated in a branch of evolution but not in others. This allows closely related species to be assigned (or not) to this branch. The single most difficult problem in such analysis is deciding whether a shared taxonomic character is due to common ancestry or one that appeared independently due to convergence, parallelism or reversion to an ancestral state. Mitochondrial genomes are often used in these studies because of their maternal inheritance, lack of recombination and insulation from species-specific evolutionary constraints in preference to nuclear genes which are open to such variations. Recently, phylogenies have been constructed using mammalian L1 retrotransposons which promise to revolutionise this field (216-218). These undergo periodic amplifications in which multiple copies of the elements are interspersed in the genome. Since these elements are transmitted only by inheritance and are retained in the genome, a shared L1 amplification event can only be an inherited ancestral character. These two methods, combined with phylogenetic analyses on nuclear genes, do not agree with a number of phylogenetic orthodoxies regarding the validity of the taxonomic order Rodentia. First, they have challenged the validity of the proposed monophyletic superordinal grouping of Glires (219-221) which unites the orders lagomorpha (rabbits) and rodentia (rodents) (that is, these two orders were proposed to share a common ancestor which was not shared with any other order and this has now been challenged). Second, the monophyletic validity of the order rodentia itself has been questioned (220-224), with a proposal that the sub-order hystricomorpha (guinea-pigs and porcupines) or at least the family caviomorpha (guinea-pigs) should be conferred an independent ordinal status, distinct from the

other suborders, which include myomorpha (rats and mice.)

The radical restructuring of a conserved sequence of apparently ancient sequence that I have detected in the myomorphic PDE4A gene may yet be a useful taxonomic character in solving the refractory problems of rodent phylogenies discussed above. Once the extent of the LR2P motif amongst species assigned as rodents is known, it may be possible to address one or both of the above problems. This would be done by performing RT-PCR on brains from a range of rodent species to determine whether or not they contain the deletion in PDE4A. In principle this could be done without sequencing since the LR2P motif is distinguishable from LR2HP as altered mobility of DNA fragments on an agarose gel. Species containing the LR2P could then form a true monophyletic grouping of rodents. An important prerequisite for such a rationale would be to establish that the deletion seen is not more generally prevalent than my preliminary survey of five non-rodent species suggests (which would imply parallelism or convergence). This would be done by performing RT-PCR on brains from non-rodent species. For the deletion to be a reliable marker of rodent monophyly these fragments should not contain the LR2P region. Given the apparent ancient nature of the hydrophilic sequence in LR2HP, there is clearly a possibility that the LR2 deletion could be a reliable marker for a true monophyletic grouping based around rodents. This would be of considerable interest in the field of molecular taxonomy. In the meantime, based on the assumption that the deletion I have identified is rodent-specific, the preliminary data I have obtained certainly concurs with the notion that caviomorphs (guinea-pigs) and lagomorphs (rabbits) are not part of a monophyletic rodent grouping because neither of them share the deletion conserved in the myomorphs (rat and mouse).

6. USE OF A NOVEL CLONING STRATEGY TO CLONE THE FULL OPEN READING FRAME OF A NOVEL HUMAN PDE4A SPLICE VARIANT, PDE4A10

INTRODUCTION

6.1 PDE4A10, A NEW PDE4A SPLICE VARIANT.

This section of work follows on from the discovery of a rat cDNA library clone which apparently encodes partial sequence for a novel PDE4A splice variant (M.D. Houslay, unpublished) which I have designated PDE4A10. This cDNA has ~90 base pairs of novel sequence upstream of the splice junction shared between all PDE4 'long' forms and the reading frame is open at the 5' end. It was decided to use the skills developed through the work of the two previous chapters to attempt to identify this partial clone in total RNA to confirm that it was not an artefact. Then PCR based methodologies would be employed to isolate the remaining sequences.

6.2. PCR BASED METHODOLOGIES FOR ISOLATING 5' END GENE FRAGMENTS: RAPID AMPLIFICATION OF cDNA ENDS (RACE).

Probing of cDNA libraries is still the major method for isolating new PDEs. However, PDE cDNAs isolated by such means are often incomplete (66-68,74,75,79-81). The robust nature of the PCR reaction makes it an obvious choice for isolating the remaining sequence but there are practical difficulties in applying PCR to cDNA end isolation. The abstract problem is that because of the uni-directional processivity of DNA polymerisation (5' to 3') there must be some known sequence on either side of the unknown sequence before the PCR reaction can be used to isolate that unknown sequence. A number of PCR based methodologies are now available to allow isolation of the remaining sequence. These methods are often termed RACE (for Rapid Amplification of cDNA Ends). RACE strategies are theoretically particularly attractive in the PDE4 field because each gene is alternatively spliced at the 5' end of a large G/C rich gene. This means that the splice variant specific sequence is not propitiously placed for identification in cDNA libraries as is manifest in the literature (see Introduction). The use of PCR

based methods for isolating new PDE4 sequence has rarely been reported although it has been used successfully to generate new PDE4B and PDE4C forms (78,90). A reliable PCR-based method for isolating PDE4 5' ends was sought.

6.2.1.Terminal deoxyribonucleotidyl transferase (TdT) mediated RACE (see figure 6.2.1.)

This was the first protocol developed for PCR mediated isolation of 5' ends (225-227). cDNA is synthesised using a recombinant reverse transcriptase which lacks RNAse H activity. This is done in order to maximise synthesis of long cDNAs by eliminating reverse transcriptase mediated digestion of the template RNA. The cDNA primer is then removed to prevent competition for the tagging process, which uses the activity of terminal deoxynucleotidyl transferase to add a homopolymeric tail of nucleotides to the 3' end of first strand cDNA (see figure). An inosine containing primer designed to anneal specifically to this sequence is then used in PCR with a gene specific primer.

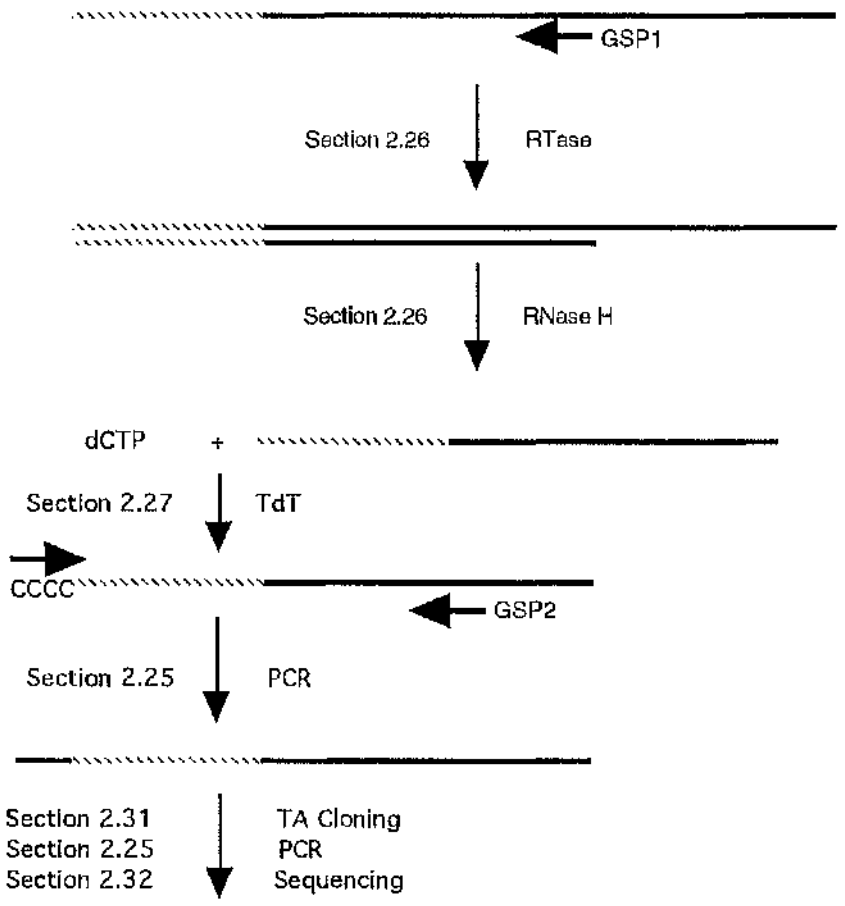

Figure 6.2.1. Terminal deoxynucleotidyl Transferase (TdT) RACE
The figure above is a schematic of TdT RACE. cDNA is first transcribed from RNA by reverse transcriptase (RTase) (sections in figure relate to methods sections), using a gene specific primer (GSP1). Then TdT is used to 'tail' the 3' end of the first-strand cDNA with a homopolymeric stretch of nucleotides (CCCC). An inosine containing primer optimised for amplifying such homopolymers can then amplify the unknown sequence (hatched), in a PCR with a nested gene specific primer (GSP2)

PRIMER KEY: 5' end; Primers are unphosphorylated.
3' end: Primers unblocked at the 3' end have an arrow-head.

6.2.2. T4 RNA ligase mediated (RLM) RACE (see figure 6.2.2.)

This protocol uses a different reaction for tagging the cDNA than TdT mediated RACE (above). Following cDNA synthesis the cDNA primer is removed. As in the TdT RACE protocol above this is to prevent competition for the subsequent tagging step. T4 RNA ligase which catalyses single stranded oligonucleotide ligations is used to ligate a phosphorylated oligonucleotide onto the cDNA 3' end (228-233). The concentration of primer added in this step is intentionally low so that PCR can be carried out directly on an aliquot of the ligation, using a primer complementary to the phosphorylated oligonucleotide and a primer complementary to the gene of interest.

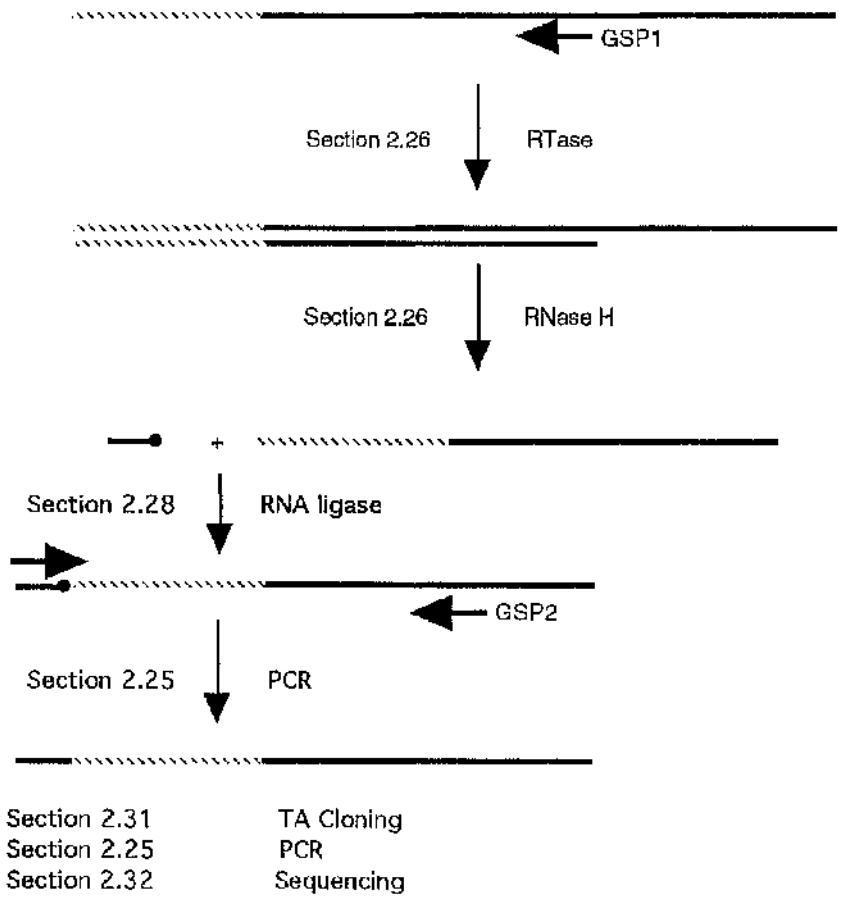

Figure 6.2.2. RNA Ligase Mediated (RLM) RACE.

The diagram above is a schematic of RLM RACE. cDNA was transcribed from RNA by reverse transcriptase (RTase) using a gene specific primer (GSP1). A single-stranded phosphorylated deoxyriboligonucleotide (•–) was then ligated to the 3' end of the first-strand cDNA. A complementary primer would then be able to amplify unknown sequence (hatched) as shown, in a PCR with a gene-specific primer (GSP2).

PRIMER KEY: 5' end; Primers phosphorylated at the 5' end are shown thus (•) whereas unphosphorylated primers are undecorated.

3' end: Primers unblocked at the 3' end have an arrow-head. Blocked primers are undecorated at this end of the primer

6.2.3. Intramolecular RACE: T4 DNA ligase mediated isolation of gene fragments by inverse PCR (see figure 6.2.3.)

Intramolecular RACE is a variation on the theme of standard RLM RACE. This uses a phosphorylated oligonucleotide in the cDNA synthesis to create cDNAs with a phosphorylated 5' end. T4 RNA ligase was used to circularise these, a reaction which it carries out more efficiently than intermolecular ligations of standard RLM RACE (234,235). New sequence would then be isolated by inverse PCR (where primers polymerise away from each other on the known piece of DNA but because the cDNA is circularised, the unknown DNA is then PCR amplified, see figure 6.2.3.)(156). This rationale has been used successfully with an RNA viral genome (236). However it has not been reported for cDNAs derived from complex RNA populations.

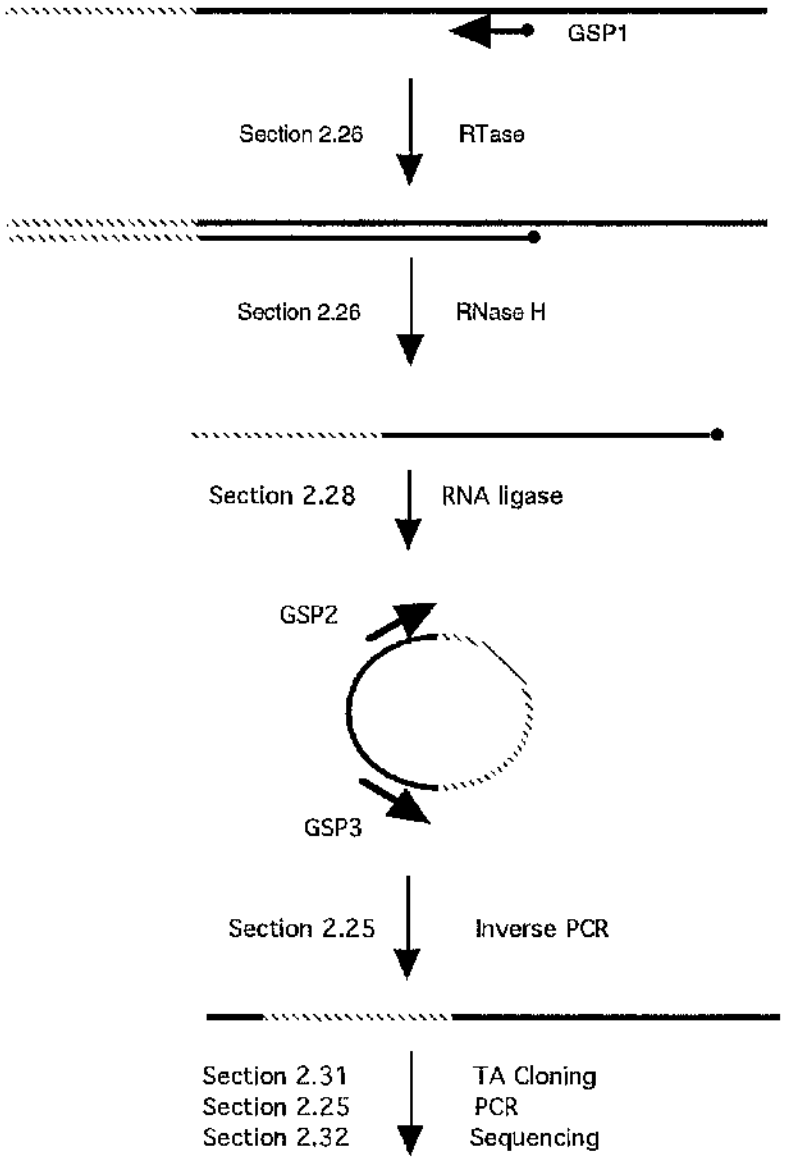

Figure 6.2.3. Intramolecular RACE

The figure above is a schematic of intramolecular RACE. cDNA is transcribed from RNA by reverse transcriptase using a phosphorylated primer (GSP1). The cDNAs can then be circularised by T4 RNA ligase **(234,235)**. The unknown sequence (hatched) can then be isolated by a standard inverse PCR **(156)** with a nested gene-specific primer (GSP2).

PRIMER KEY: 5' end; Primers phosphorylated at the 5' end are shown thus (●) whereas unphosphorylated primers are undecorated.
3' end: Primers unblocked at the 3' end have an arrow-head.

6.3. SPLICE VARIANT ISOLATION FROM GENOMIC COSMID CLONES

PDE4 splice variants typically have only one 5' end exon alternatively spliced. Thus, each splice variant specific sequence will be found all together in one place in the genome. This makes genomic screening a realistic alternative, one where partial clones are not a problem. Indeed, with the recent mapping of a 210Kb contig of overlapping cosmid clones which covers all of the known PDE4A locus, screening of two or three of these ~40Kb clones at the 5' end of the contig by PCR becomes a simple proposition (82), which allows probing of large amounts of sequence highly likely to harbour the splice variant specific sequence. The genomic organisation of PDE4s has allowed the use of a novel cloning technique that I have devised to isolate DNA sequence from large clones of DNA such as cosmids. This system has two major advantages over RACE: (1) The PCR reaction in the screen is a conventional one where the diagnostic band is of a known size; (2) Since there is no PCR step in the isolation itself, concerns regarding fidelity of thermal polymerases do not apply.

The major problem concerned with handling genomic DNA is processing the large amounts of DNA to get at the sequence of interest. The next sections outline a new method for production, alignment and restriction mapping of contiguous clones.

6.4. TA SHOTGUN CLONING: MORE EFFICIENT CLONING

Cutting a large DNA insert (such as cosmid or library inserts) sequence into smaller pieces (so called shotgun cloning) is a common procedure in molecular biology. The smaller insert is easily sequenced and more manageable for downstream cloning. This is typically done by digesting the DNA that is to be the insert with a frequent cutting enzyme such as Sau3A I and digesting the vector with a rarer cutting enzyme which will give complementary ends to the frequent cutting enzyme. A suitable example in this case would be BamH I. Since Sau3A I fragments ligating into BamH I sites will mostly not regenerate the BamH I site (7/8 chance for all inserts), BamH I can be added to the ligation to prevent vector recircularisation. The small size of Sau3A I fragments sometimes makes the use of less frequently cutting enzymes

such as Xho II more attractive for cloning into the BamH I site because this will produce larger inserts. However BamH I should not be added in ligations with Xho II because in this case half of all inserts will regenerate the BamH I insert at one or other end. Thus recircularisation of the vector will be promoted and ligation of Xho II fragments will be lower unless time consuming steps such as alkaline phosphatase treatment of vector or insert are adopted in place of the use of BamH I in the ligation.

Regardless of the above considerations, 'classical' ligation efficiency is still reduced by circularisation of inserts. TA cloning is more efficient than this because neither insert nor vector can circularise and thus intermolecular ligations are favoured. This is because TA cloning makes use of the property of certain DNA polymerases to add a single base overhang (usually an A) to DNA ends (237). This can then be ligated to a vector containing complementary single T overhangs and since neither vector nor insert have self-cohesive ends, intramolecular ligation is less probable. The efficiency of TA cloning was harnessed for subcloning. In principle the conventional 5' to 3' polymerase activity of Taq polymerase should be able to polymerise DNA digested by any enzyme which leaves recessed 3' ends (such as Xho II/ BamH I/ Sau3A I). This DNA should then also have the non-template-directed A added onto its 3' end (237), allowing conventional TA cloning. I sought to establish whether this protocol would work by TA shotgun cloning cosmid DNA containing PDE4 unique exons.

6.5. OVERLAPPING TA SHOTGUN CLONING ALLOWS RAPID CONTIG ASSEMBLY AND SINGLE ENZYME RESTRICTION MAPS.

As a protocol for long distance sequencing classical shotgun cloning is not attractive (even as modified above) because the ends of the DNA fragments are identical and so it is not easily possible to order them without resorting to restriction mapping. This problem could be solved by making use of enzymes that cut away from their recognition sites. An example of such an enzyme is Hga I. If these digestion fragments are filled in as described above, then they could be formed into a contig without restriction digestion on the basis of the resulting unique overlaps (see figure 6.5.) As will be shown in this chapter, the ease of this approach could make it the

method of choice for sequencing and/or restriction mapping projects using all but the largest pieces of DNA.

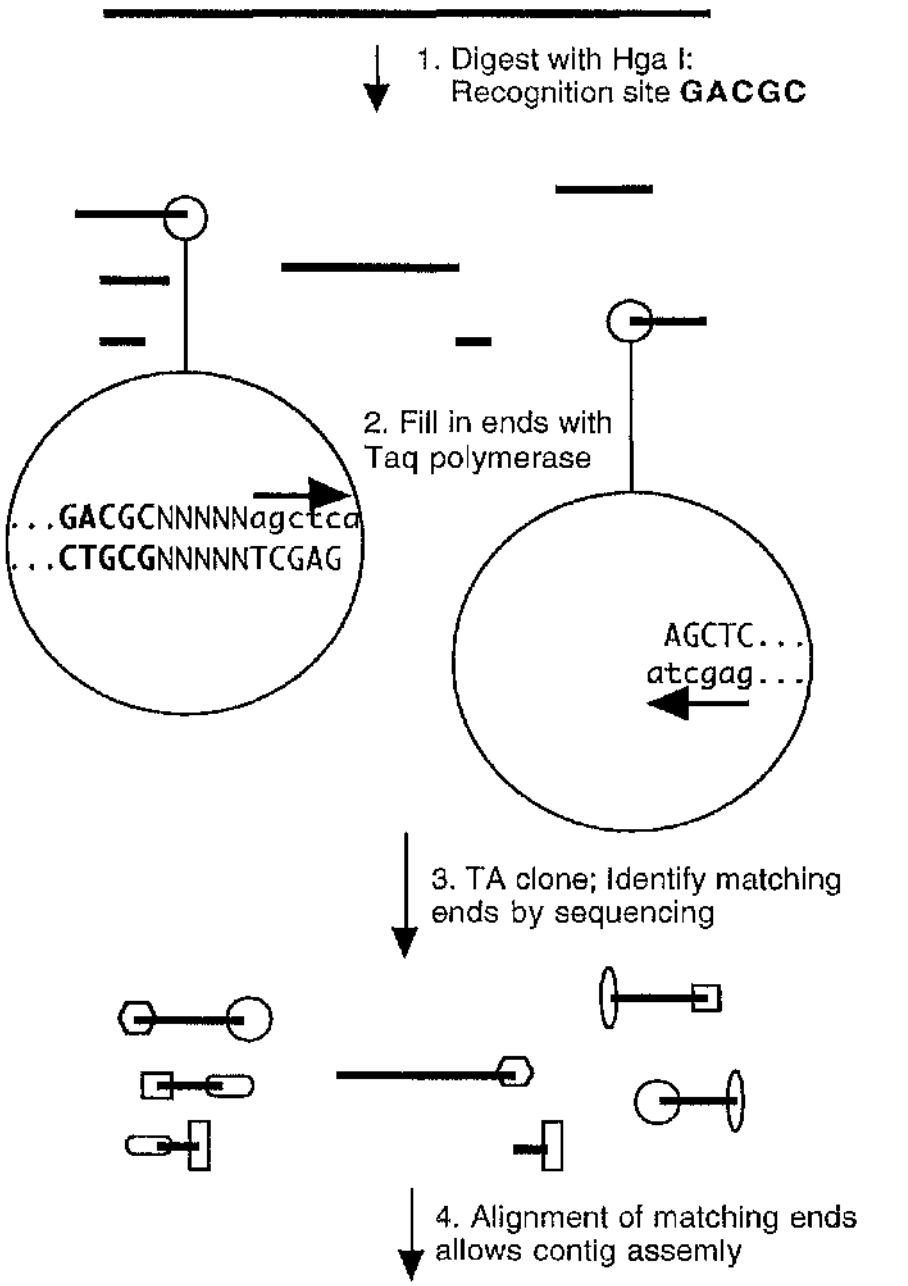

Figure 6.5. Assembly of a contig by overlapping shotgun TA cloning

(1) The target DNA is digested with an enzyme which digests at a site beyond its recognition site (e.g. Hga I recognition site is shown in bold.) to give a unique 5' overhang (circles). (2) This can be filled in by Taq polymerase to give two copies of the unique cut sequence, one in each of the restriction fragments. Taq polymerase also adds a non-template directed A. (3) The A overhang allows TA cloning and then the unique fragment ends (paired shapes) can be identified by sequencing. (4) Unique fragment ends (paired shapes) allow the fragments to be ordered into a contig and restriction map.

6.6. IDENTIFICATION OF TRANSCRIPTS FOR RNPDE4A10 IN RNA EXTRACTED FROM THE OLFACTORY BULB OF RATS AND IN RAT GENOMIC DNA.

Primers GR10 and GR11 (see figure 6.6) were designed to the ends of the 86 base pairs of unique RNPDE4A10 sequence in order to detect a band this size in RT-PCR on olfactory bulb RNA with reverse transcription primed by generic PDE4A primer GR29. Primer GR36, designed to sequence shared between all PDE4As, was also used in conjunction with GR10 (figure 6.6). When the two sets of PCR primers were used in RT-PCR both amplified bands of the expected size, consistent with the notion that rat olfactory bulb RNA does indeed express this RNA. PCR of genomic DNA using the same conditions with the two PDE4A10 specific primers GR10 and GR11 (the antisense primer GR36 could not be used here because that sequence is on a different exon) also produced a correct size band. This was further evidence that the clone was not an artefact. Thus it was decided to attempt to isolate the rest of the PDE4A10 open reading frame.

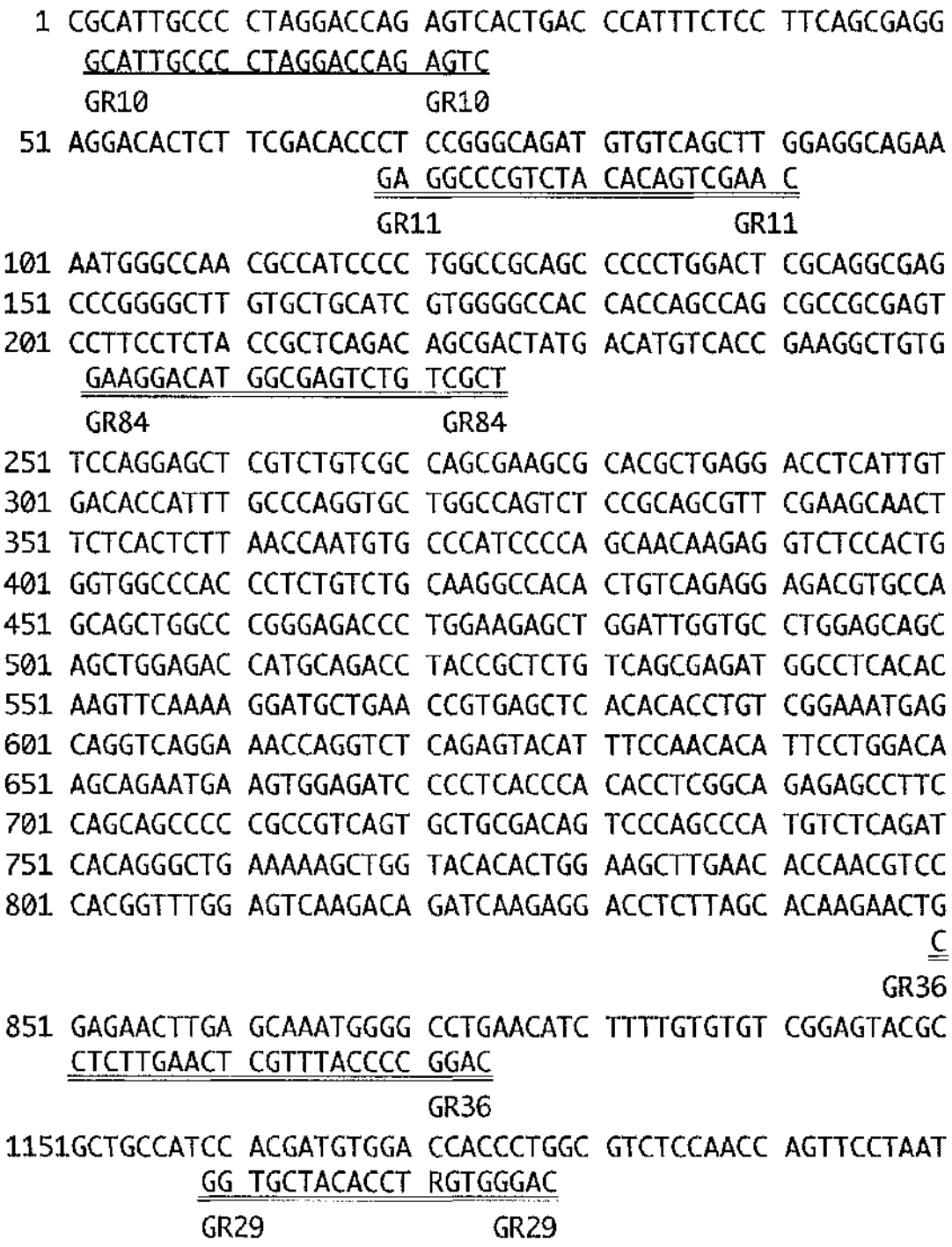

Figure 6.6. Primers designed for RT-PCR of the 5' end of PDE4A10 forms.

Above is shown the 5' sequence of the original cDNA clone of rat PDE4A10.

GR29 is designed to human and rat sequence. Primers were used in ligations and PCR as described in the text. Primer sequences are as presented, underline is sense, double underline is antisense.

6.7. PCR-BASED ATTEMPTS TO ISOLATE THE 5' END OF PDE4A10

6.7.1. TdT RACE fails to produce any amplification products

PDE4A10 specific cDNA was primed with GR38. PCR with the gene specific primer GR39 and the anchor primer failed to produce a PCR band on three separate occasions.

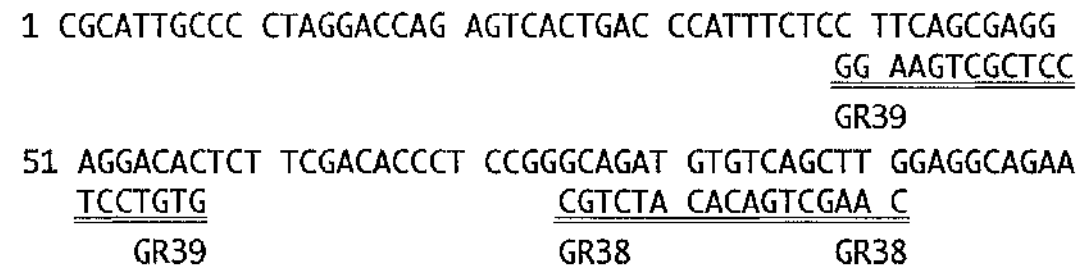

ADAPTORS

GR39 CAUCAUCAUCAUGTGTCCTCCTCGCTGAAGG
ANCHOR CUACUACUACUAGGCCACGCGTCGACTAGTACGGGIIGGGIIGGGIIG
AMPLIFICATION CUACUACUACUAGGCCACGCGTCGACTAGTAC

Figure 6.7.1. Primers used in TdT mediated RACE

The diagram above shows the 5' end of rat PDE4A10 and the primers used in TdT RACE. Primer GR38 was used for reverse transcription. Anchor primer, Amplification primer and GR39 (the full sequence is shown beneath rat PDE4A10) were used in a PCR reaction to try to isolate new PDE sequence. The inosines in the anchor primer are designed to specifically bind to the polyC tail added to the cDNAs by TdT. The uracil containing 5' ends of the adaptors were to allow a ligase free ligation of any PCR products obtained

6.7.2. RNA ligase mediated (RLM) RACE produces no PDE4A amplification products.

A series of experiments attempted to isolate upstream PDE4A10 sequence using RNA ligase mediated RACE (228). Though these experiments differed in fine detail, often simply modified PCR conditions, the results presented here are typical of those obtained.

6.7.2.1 Experimental outline

PDE4A10 specific cDNA was primed with GR11. This cDNA was ligated to the 5' end with one of two phosphorylated oligonucleotides, GR85 or GR100 as shown in figure 6.2.2. GR85 and GR100 are designed to reduce non-specific reactions. Thus, GR85 is truncated so that it is not an effective priming site for GR54 amplification but gene specific polymerisation on the antisense strand then creates these sites. It is amine blocked at the 3' end so that if GR54 does bind to it, Taq cannot fill-in the overhang to create perfect competing GR54 binding sites. Amine blocking should also prevent intramolecular or intermolecular self-ligation reactions which would compete with intermolecular ligation to cDNAs. GR100 is longer than GR85 which allows nested PCR of the anchor as well (see below). As with GR85, GR100 was blocked at its 3' end to prevent self-ligation.

Both of the ligations were then subjected to two rounds of nested PCR. For the GR85 ligation, only the gene specific primer was nested, with the GR85 anchor-specific primer GR54 used in both PCR reactions. GR100 is a longer anchor so in PCRs of this ligation nesting of anchor primers was possible too, thus the first PCR of this ligation used anchor-specific primer GR79 and the second PCR used anchor-specific primer GR54.

The gene-specific primer in the first PCR was always GR52. However, nested PCRs were done in parallel with different primers, GR51 & GR50. The different positions of these primers on PDE4A10 should cause authentic PDE4A10 RACE amplifications to be differently sized in each reaction and for fragments up to ~400 base pairs this would be readily observable on an agarose gel.

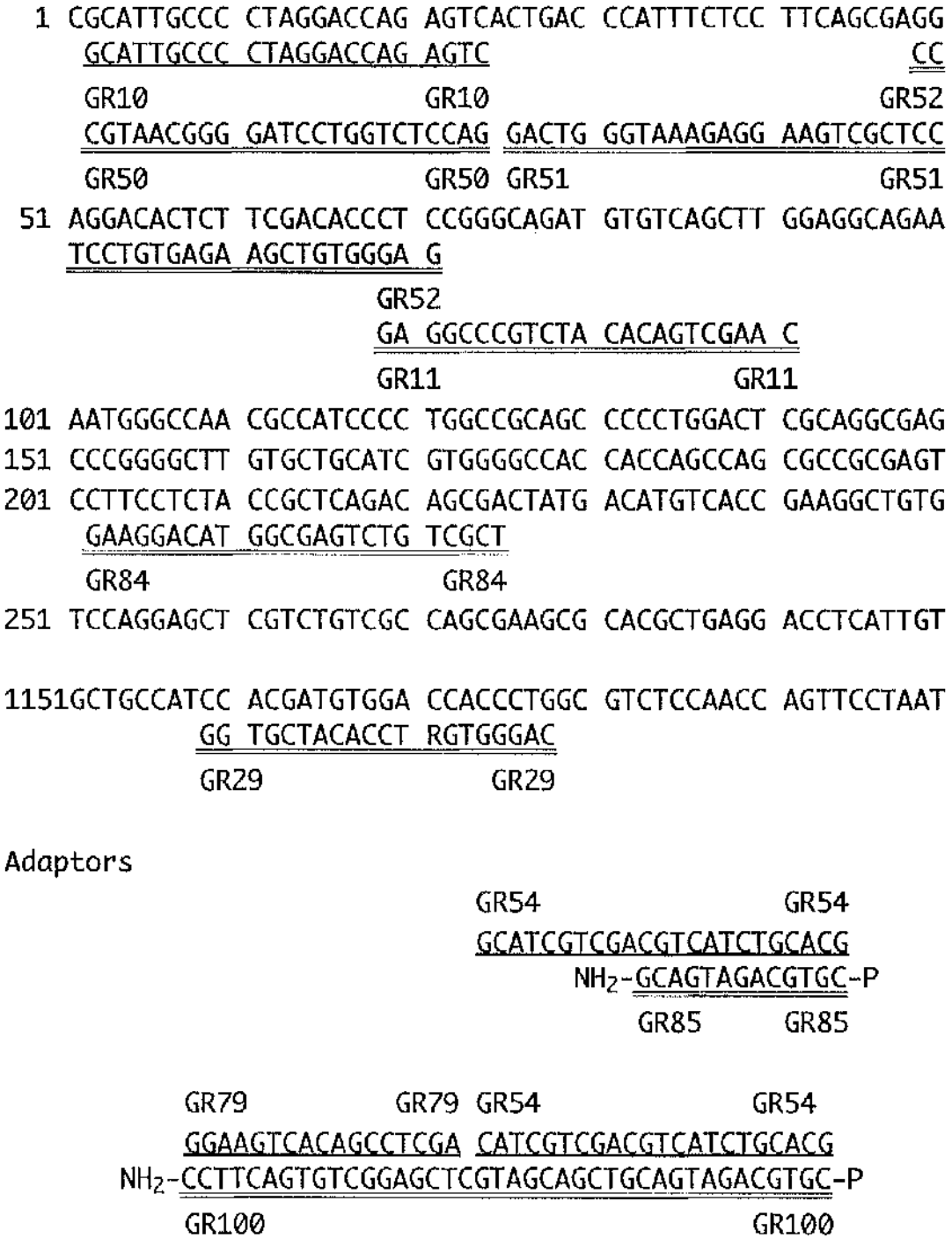

Figure 6.7.2.1. Primers used in RLM RACE

Above is shown the 5' sequence of the original cDNA clone of rat PDE4A10.
GR84 is designed to the human sequence. Primers were used in ligations and PCR as described in the text. Primer sequences are as presented, underline is sense, double underline is antisense.

6.7.2.2 Most bands obtained in the RACE reaction are RNA ligase specific but not gene-specific.

When T4 RNA ligase was omitted from the ligation reaction then subjected to two rounds of PCR as described above, very little amplification was detected. In contrast, when the same PCR was carried out on a ligation reaction which contains ligase, large amounts of amplification is detected in the nested PCR. However, there was little evidence of the expected shifting of band size in PCRs containing GR50 against those containing GR51. Furthermore, most amplification was consistently seen in lanes where the second PCR only contained GR54 and no gene-specific primer. There were also discrete bands in PCR nested reactions which only contained gene specific primers GR50 or GR51. These could notionally be genuine PDE4A amplification products if they had been formed with miniscule amounts of primer carried over from the first nested reaction and indeed it has been suggested that use of such low concentrations can improve the specificity of RACE PCR (153). Therefore, a variety of the bands and whole PCR reactions which came from amplifications with GR51 were TA cloned. The resulting clones were screened with GR50 and a flanking TA vector primer. Very few TA clones were positive in this test and these clones were false positives in that they were not homologous to PDE4A10 when they were sequenced.

6.7.3. Intramolecular RACE produces artefacts apparently caused by intermolecular ligation of the phosphorylated cDNA primer

cDNA circularisation was attempted in the expectation that inverse PCR of these circles would yield upstream cDNA sequence. cDNA was synthesised with phosphorylated GR109 (figure 6.7.3.) This cDNA was then circularised by T4 RNA ligase. Nested inverse PCR was performed using GR51 and GR108 followed by GR50 and GR107. When PCR products were TA cloned, most were sequences of varying lengths which resembled a number of GR109 oligonucleotides joined together.

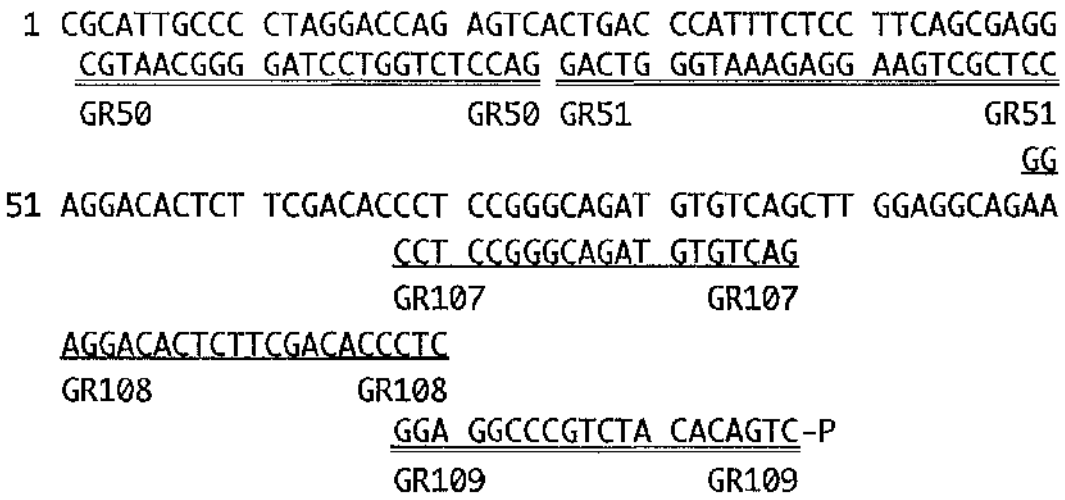

Figure 6.7.3. Inverse PCR RACE of rat PDE4A10

Above is shown the 5' sequence of the original cDNA clone of rat PDE4A10. Primers were used in ligations and PCR as described in the text. Primer sequences are as presented, underline is sense, double underline is antisense.

6.8 PCR SCREENS FOR HUMAN HOMOLOGUES OF RAT PDE4A SPLICE VARIANTS.

6.8.1. Identification of the human homologue of rat PDE4A10 but not the putative human homologues of RPDE66 or rat PDE4A8 in human cell lines.

To attempt to isolate human sequence equivalent to the rat sequence for the unique exon of PDE4A10, PCR was attempted using the sense exon-specific primer successfully used on rat DNA and RNA (GR10, see section 6.6) and also an alternative antisense primer designed to human sequence (GR84, see section 6.6) found in all 'long-form' PDE4A splice variants. The same approach was attempted for the other two rat PDE4A splice variants for which no human sequence has been isolated:

(1) RPDE66/ RNPDE4A9 (Graeme Bolger, unpublished) used unique exon specific primers

GR665 (sense ATGGAAGAGTGTTACCTTCAAGGAC;) and

GR663 (antisense TCCAGTGGTCCATACTTCCAC;) or GR84;

(2) RNPDE4A8 (RPDE39) used exon specific primer

GR395 (sense ATGCCAAGTCGCAAGAGGCTGACAC;) with GR84.

For PDE4A10, a correct size band was identified in U-118, SK-N-SH and 293 cells but not in U-87 or Jurkat cells (see figure 6.8.1.a). The band from RT-PCR on U-118 cells was TA cloned. Sequence obtained from these clones revealed sequence highly homologous to that for the rat PDE4A10 sequence (See figure 6.8.1.b. The 5' extent of this sequence is marked in figure 6.10.d.). This short amount of sequence information is nevertheless important for a number of reasons. First, the sequence is conserved (and unlike the RD1 conserved untranslated region (82), without frameshifts) which strongly suggests that it will code for protein (see figure 6.8.1b). Second, the human sequence crosses the exon boundary into PDE4A shared sequence (see figure 6.8.1.b), further confirming the notion that rat PDE4A10 is a genuine splicing variant. The alternative possibility, that the unique rat PDE4A10 sequence

represents unspliced intronic sequence, is simultaneously undermined because such sequence would not be conserved between humans and rats. Third, the human PDE4A10 RNA has been shown to be expressed in human cells, only the third human splice variant for which this proof exists. The others being HSPDE4A4 (68) and HSPDE4A1 (chapter 5 and (82)).

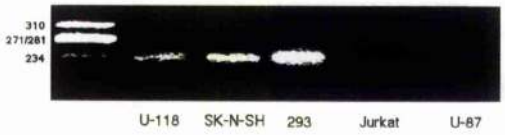

Figure 6.8.1.a. RT-PCR of human cell lines with PCR probes designed to rat PDE4A10

RT-PCR was carried out on RNA from human cell lines using probes to rat PDE4A10. These different cell lines are labelled below the tracks.

The RT-PCR conditions used were 30 cycles of 96°C 1min, 55°C 1min, 72°C 1min. An arrow denotes fragments of the correct size (220bp). The fragment amplified from U-118 cells was cloned and sequenced (see section 6.8.1.b).

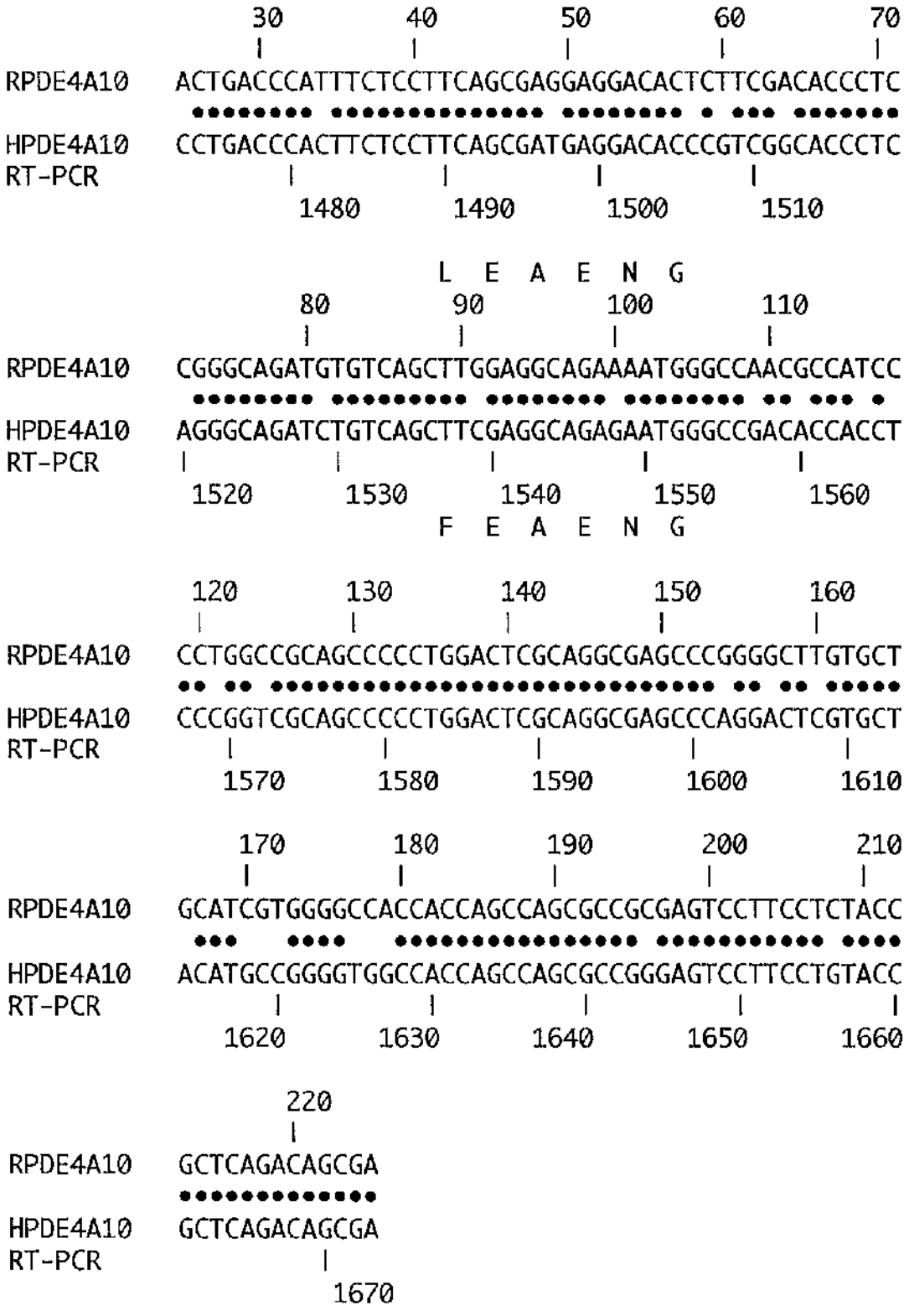

Figure 6.8.1.b. Identification of a fragment of human PDE4A10

The full extent of the RT-PCR fragment obtained from human U 118 cells is compared with the 5' end of the incomplete rat PDE4A10 clone. Note that HPDE4A10 is numbered identically to figure 6.10.d. The conserved peptide sequence which follows the 'long' form splice junction is shown. The human sequence crosses this boundary.

6.8.2. Identification of the unique exon of rat PDE4A10 but not the putative human homologue of rat PDE4A9 in three cosmids in the 210Kb cosmid contig which contains the PDE4A locus

The identification and sequencing of a partial clone of human PDE4A10 combined with the recent mapping of a 210Kb cosmid contig of PDE4A genomic sequence (82) allowed isolation of the remaining 5' sequence of PDE4A10 by a PCR screen of the cosmids. Thus three cosmids, R31069, R29158 and R27270, between them containing all the sequence from the 5' extreme of the PDE4A contig to the 5' end of the first commonly used PDE4A exon, were screened with the primers (brackets) specific to the rat forms of the unique PDE4A10 (GR10 & GR11) or PDE4A9 (GR665 & GR663) exon. The PDE4A10 primers readily detected a PCR fragment of the expected size (~90 base pairs) in all three cosmids whereas the primers designed to PDE4A9 did not amplify a PCR fragment from these cosmids. A human homologue for RPDE39 (RNPDE4A8) was not searched for by these means because the coding sequence for the unique exon of this splice variant is only 63 bp which is too small to be visualised on an agarose gel.

Attempted direct sequencing of the human PDE4A cosmids with the rat specific primers GR10, GR11, GR50, GR51 & GR52 or with a primer designed to the human specific sequence (primer GR HOLF was used which is a humanised version of part of GR11 (figure 6.7.2.1), with the sequence ACAGATCTGCCCTGAGG) was unsuccessful. Given that this may be due to the size of the cosmids (~50Kb per clone), it was decided to 'shotgun' clone a digestion of one cosmid and screen the subclone library for clones which contain the PDE4A10 sequence.

6.9. SUBCLONING OF THE UNIQUE EXON OF HUMAN PDE4A10 BY A NOVEL RAPID, EFFICIENT CLONING PROTOCOL.

The partial sequence of human PDE4A10 obtained by RT-PCR showed that there was a Xho II site at the 3' end of the PDE4A10 unique exon. This site is not found in the rat sequence. This enzyme will cut an unbiased, random sequence of

DNA with an average frequency of 1/1024 which is a rare and useful property for subcloning. The average size of an insert from a digestion with a restriction enzyme with a six base pair identification sequence such as BamH I is 1/4096 and this presents difficulties in the efficient ligation of the insert, where efficiency decreases proportionally to insert size. Furthermore, sequencing reads are typically 400-600bp. This means that such large inserts have either to be 'walked' along with primers designed to the insert, or subjected to further subcloning. In contrast, the average size of an insert from a digestion with an enzyme with a four base pair identification sequence (such as Sau3A I) is 1/256 and this causes difficulties because the screens must be larger (~200 colonies assuming 100% ligation efficiency and equal ligation efficiency for all inserts) such that a straightforward PCR screen is no longer so attractive. Also, with such small inserts there is an increased possibility that not all of the exon sequence will be in a single digestion fragment. In such a case, where the sequence which was used in the PCR screen was dispersed amongst more than one subclone, then no single colony would show up positive, so an alternative screen would be required. Thus, the ~1Kb average size of Xho II fragments is attractive because it is small enough to ligate efficiently and sequence rapidly yet it is large enough that one might reasonably expect to find all the sequence for an exon in one insert.

The positioning of the Xho II digestion site also facilitated subcloning. It is at the 3' end of the exon which meant that my existing PDE4A10-specific primers (GR10 &GR11) should identify the Xho II fragment in a PCR screen. Xho II digestion would place all PDE4A10 subclones at the ends of the inserts, thus eliminating completely the risk of subcloning the human PDE4A10 sequence in an inaccessible site placed in the middle of a large insert. To ensure a high efficiency of ligation of digestion fragments a novel subcloning strategy was used which harnesses the high efficiency TA ligation normally used for PCR products.

6.9.1. TA cloning and PCR screening of Xho II fragments of cosmid R27270 for the human homologue of the unique exon of RNPDE4A10.

The Xho II digest of cosmid R27270 was TA cloned and 80 white colonies subject to PCR screen with GR10 and GR11. This was performed in place of a PCR screen done with either GR10 or GR11 together with a flanking vector primer because such a screen would be directional and this would have to be done twice; namely once in each direction. Since there was no PCR step in this cloning strategy, there was no risk of GR10 and GR11 amplifying contaminating, unrecombined template from a previous PCR. A single positive colony, 67, was obtained and taken for further study. PCR with GR10 and T7 or pCR2.1 reverse primer (see Methods section for vector primer sequences) revealed that the exon was ligated to the pCR2.1 reverse primer vector arm. The insert of colony 67 could not be sized by PCR with the two vector primers. Digestion with the EcoR I sites which flank the multiple cloning site excises a ~2.5Kb fragment.

6.10. NOVEL TA CLONING STRATEGY PRODUCES OVERLAPPING FRAGMENTS OF THE 5' END OF PDE4A10 CLONE

Sequencing with the T7 sequencing primer of colony 67 reveals a reading frame still open at the 5' end. The novel cloning strategy used in section 6.9. was repeated but this time a restriction enzyme was used which cuts away from its recognition site (see section 6.5) in order that clones with overlapping ends could be isolated. Using this protocol, fragments of the entire Xho II insert of clone 67 have now been sequenced and ordered into a contig. This contig order has been confirmed by two partial digests (see figure 6.10.b) and by PCR analysis (see figure 6.10.c.). Fragments 3 and 4 of this contig have now been sequenced fully and this sequence is presented in 6.10.d

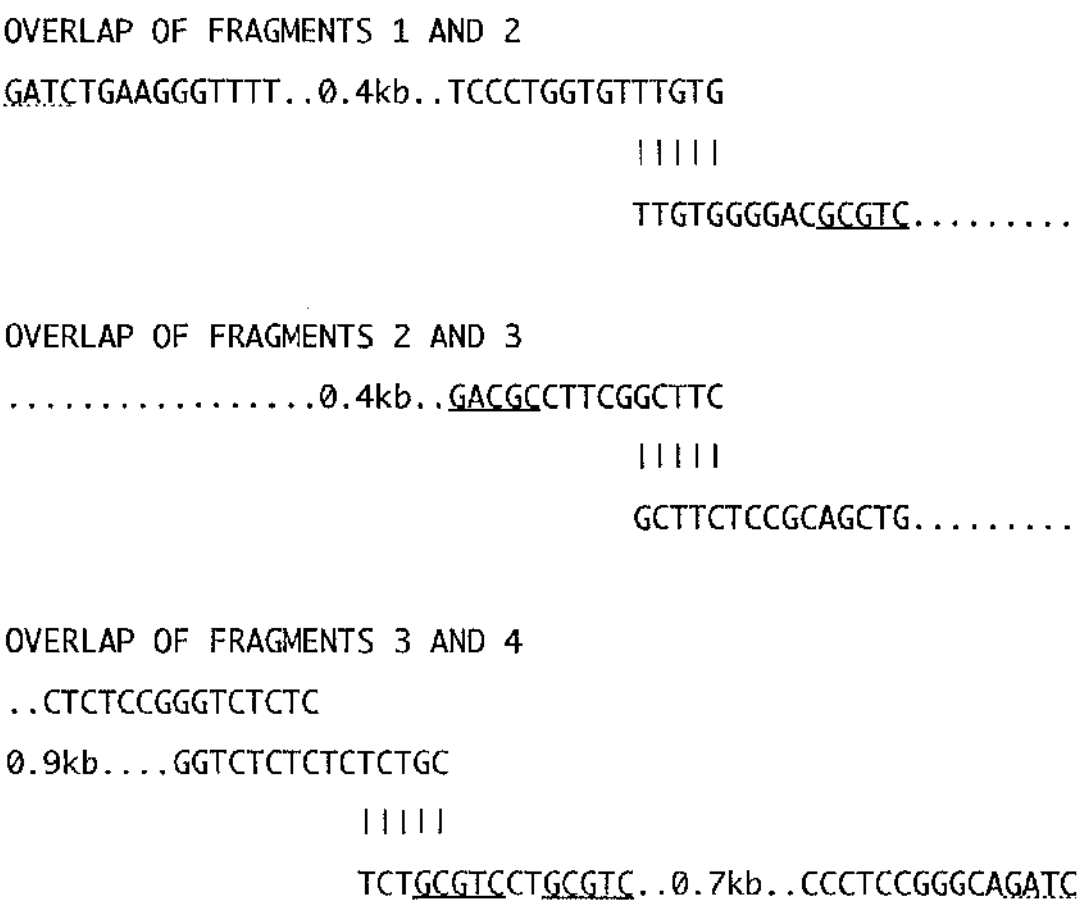

Figure 6.10.a. Deduction of a Contig from Short Overlaps of DNA sequence.

The short unique overlaps (l) introduced into the PDE4A10 digestion fragments allowed the fragments to be correctly orientated and ordered. This in turn allowed immediate deduction of a contig equivalent to the original sequence digested (see figures 6.10.b and 6.10.c). Inspection of the sequence surrounding the overlaps identified Hga I recognition sites (underlined) consistent with these overlaps being due to filling-in of an Hga I digestion, as was intended. As discussed in section 6.10, the fragments at the junction between fragments 3 and 4 were more complex due to two Hga I recognition sites being close together in the DNA sequence. However, in such a situation, digestion at one site destroys the other, such that the overlap can still be identified in some clones. The dotted underlined GATC motif at the ends of fragments 1 and 4 are the ends of the Xho II fragment following TA cloning (Recognition sequence RGATCY where R=G/A and Y= C/T)

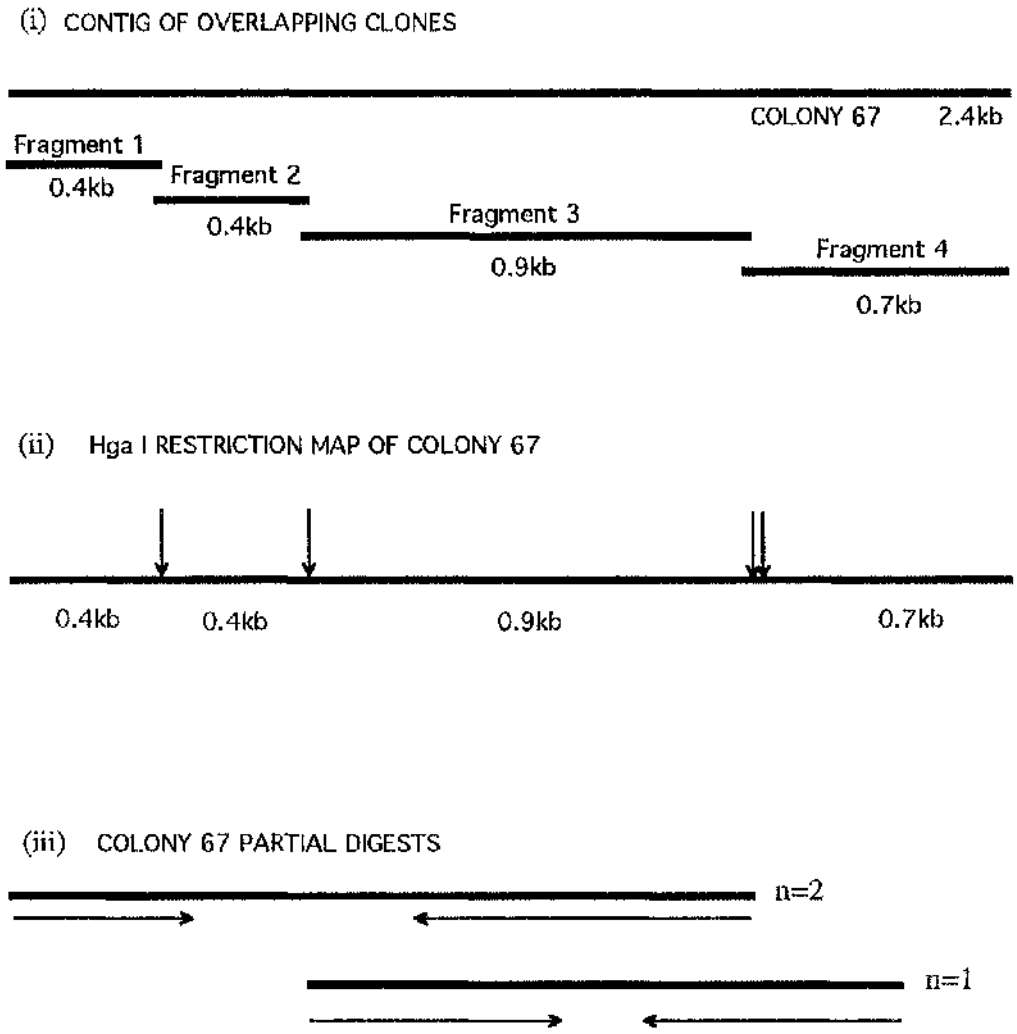

Figure 6.10.b. Analysis of Partial Digestion Fragments to Verify the Authenticity of a Contig deduced from Overlapping Sequence Information

(i) A schematic of a contig, deduced from introduced sequence overlaps, is shown.

(ii) Hga I restriction map based on the deduced contig.

(iii) Two kinds of partial digestion fragments were obtained from colony 67. Partial sequencing of these fragments (extent of sequencing depicted by the arrows) is consistent with the order and orientation of fragments 1-4 in the deduced contig.

(i)

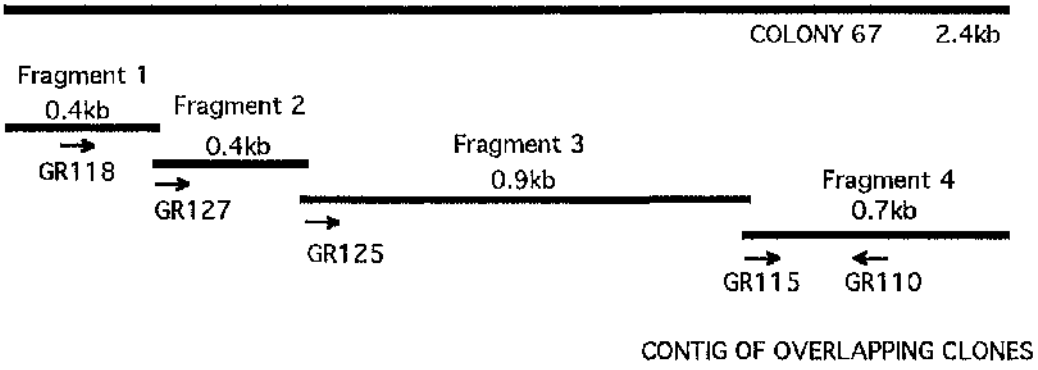

(ii)

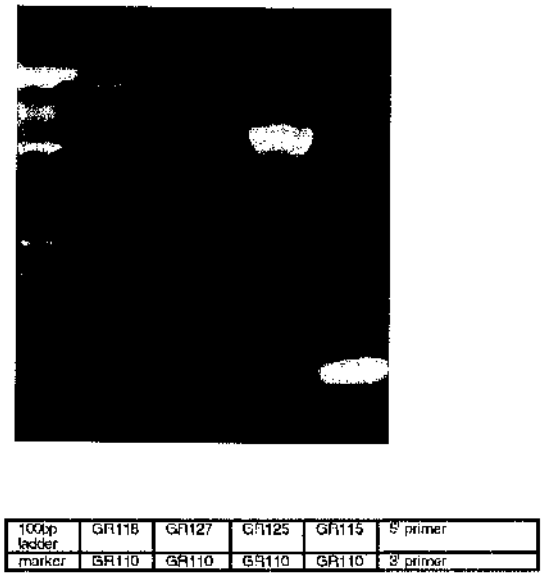

Figure 6.10.c. PCR Analysis to Verify the Authenticity of a Contig deduced from Overlapping Sequence Information

(i) A schematic of a contig, deduced from introduced sequence overlaps, is shown. Primers were designed to these sequences in order to confirm this order and orientation by PCR. (ii) PCR analysis of colony 67 indicates that the orientation and order of the deduced contig are authentic. Thus, sense primers designed to fragments 1-4 were able to amplify a fragment when PCR was performed with an antisense primer from fragment 4, indicating that the deduced fragment orientations are correct. Moreover, the sizes of the amplified fragments are consistent with the order of the fragments in the deduced contig. PCR conditions were 34 cycles of 98°C 1min, 47°C 1min and 72°C 2min.

PCR primer sequences:

GR118 GCATCTGGAGAGCTATG
GR127 TTGTGGGGACGCGTCCGG
GR125 GCAGCTGCCAGGATTTGG
GR115 ATCAGCGATCAGAGACCT
GR110 GCAGGACCCCTGCAGG

1GCTTCTCCGC AGCTGCCAGG ATTTGGGCCG CCAGGCTTGG GCTGGGGCTG
Sp1 Sp1
51GGTAAGTGCA GCGCTGGTGG CCGTGGGTTC AAGTCGCCCC TGGCCACCTG

101GCGCACTCCA GGGTCTAGGG TTCGTGGCTC ACTCTCTCCA GCCTCACTTT

151CCTCTTCTGT CACATAGCAG CGATCAAAAT CATCCCTGAC CGCCAGGGTT

201GCCCTGGAGA CCTCTGATAG GGCATGCAGT AGACGTTTAA TAAATGTTGC

251ATCCTTCCCA CTTCCTGTGC AAACCTGAAG CTGCGGTCAC GCTTTGGAGG

301AGTGAGGGCG ACCTGCCATC CAGGTCATGT GTTCATCCTG GGGTATGTGT

351TCAGTTCTGT CAGCCTCAGT CTACTGGCCT GTGAAATGGG GCCAGTCATG

401CCTTCTGTGG GTGGCCTTGC GGTGAGGCTT GGTGTCACTC C*TAG*TACCGG
Sp1 Sp1 Sp1 Sp1

451GCCACAGAGG GCAAATGGAA GTTCCCTTTC TGGCCAGACG GGGTGGGCTG
Sp1

501CGGGGGCTTG AAGTCTGGGA GTGACAGGCC CCGAGGCCAC ATCCAGTCTG
Sp1 Sp1
551GCTTTCTAAT GTCCTTATAT CCTGGAGGCA GAAGTTGGCA GCCCGGAGTT

601GGGCACTGGC TGGCCCTGGG GGCTTCTCCG GGTCCTCAGC CTCCCCCTCT

651TCCACCTACT TTCCACGTGC AATTGAGGCA CAGACTGAAG GAGGGCACGG

701CGGGGCAGGA CCGGGCCCAG CGACTGGCCC CAGGAACGAA ATGGGGCGGG
Sp1

751GACAGAAGAG GAAGAGGGGC CAGGGCCTTT GGGAGCCCCG CGTGGGGTCC
Sp1
801GCAGGGTGTG TGTAGGGAAA TCGTTGCTTC TCTCCGGGTC TCTCTCTCTG
Sp1 Sp1

851CGTCCTGCGT CTCTGTCTCC ACTTCTGTCT CTTCTGTCTC TGTTTTGTTT

901CTCCTTCCCA CCGCTGAGCT GCACCTTCCC CTCCCCTGGG TTTATGTCAC

951CCGGCCCCAC ACTCGAGTCC CGTTTCCCCG GGGGCGCACG GCGATCAGCG

1001ATCAGAGACC TCGAGCGGGC CCAGCTCGAC GTCAGGGCGG GGAGGGGGGA
CRE

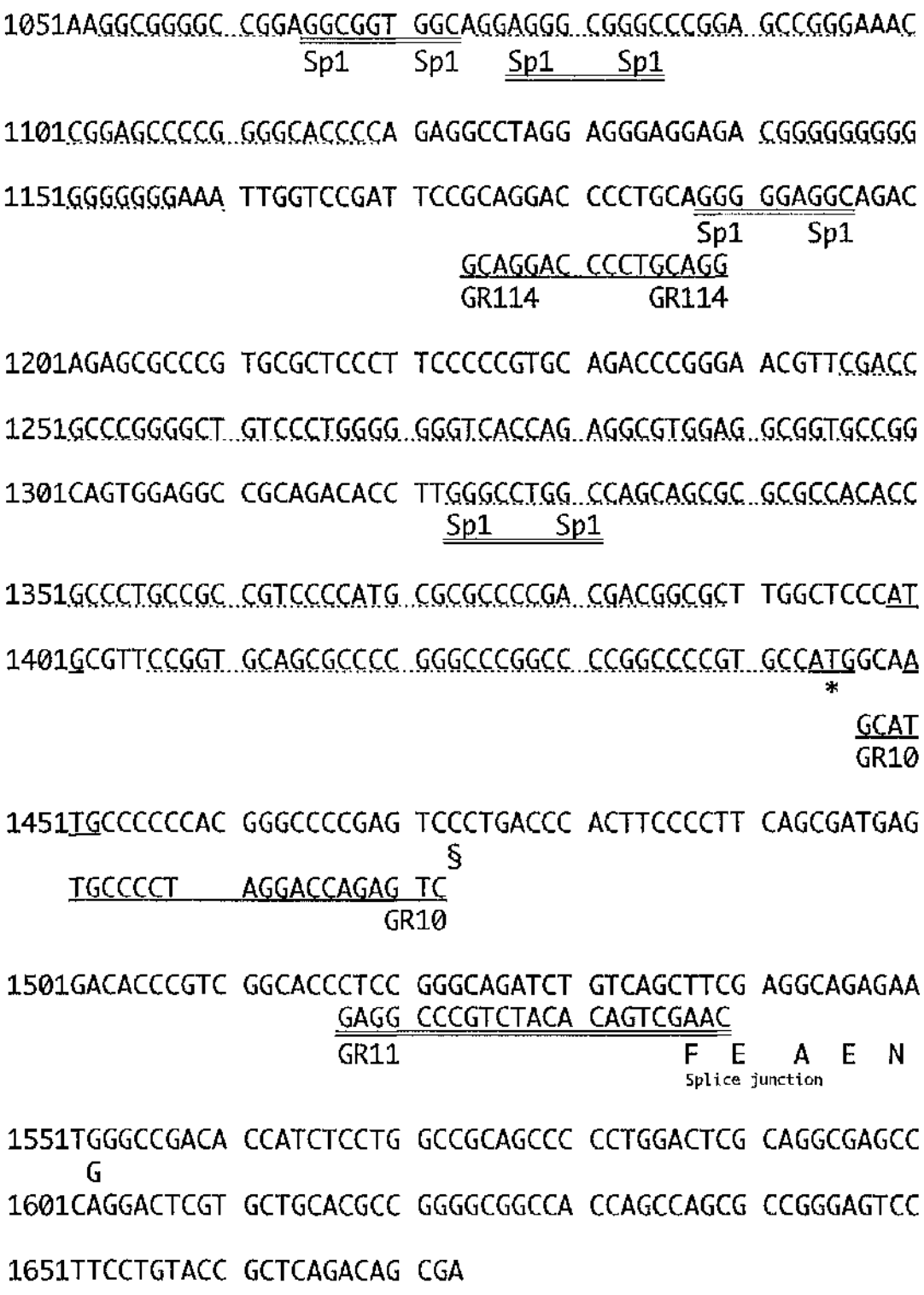
1051AAGGCGGGGC CGGAGGCGGT GGCAGGAGGG CGGGCCCGGA GCCGGGAAAC
Sp1 Sp1 Sp1 Sp1
1101CGGAGCCCCG GGGCACCCCA GAGGCCTAGG AGGGAGGAGA CGGGGGGGGG
1151GGGGGGGAAA TTGGTCCGAT TCCGCAGGAC CCCTGCAGGG GGAGGCAGAC
Sp1 Sp1
GCAGGAC CCCTGCAGG
GR114 GR114
1201AGAGCGCCCG TGCGCTCCCT TCCCCCGTGC AGACCCGGGA ACGTTCGACC
1251GCCCGGGGCT GTCCCTGGGG GGGTCACCAG AGGCGTGGAG GCGGTGCCGG
1301CAGTGGAGGC CGCAGACACC TTGGGCCTGG CCAGCAGCGC GCGCCACACC
Sp1 Sp1
1351GCCCTGCCGC CGTCCCCATG CGCGCCCCGA CGACGGCGCT TGGCTCCCAT
1401GCGTTCCGGT GCAGCGCCCC GGGCCCGGCC CCGGCCCCGT GCCATGGCAA
*
GCAT
GR10
1451TGCCCCCCAC GGGCCCCGAG TCCCTGACCC ACTTCCCCTT CAGCGATGAG
§
TGCCCCT AGGACCAGAG TC
GR10
1501GACACCCGTC GGCACCCTCC GGGCAGATCT GTCAGCTTCG AGGCAGAGAA
GAGG CCCGTCTACA CAGTCGAAC
GR11 F E A E N
Splice junction
1551TGGGCCGACA CCATCTCCTG GCCGCAGCCC CCTGGACTCG CAGGCGAGCC
G
1601CAGGACTCGT GCTGCACGCC GGGGCGGCCA CCAGCCAGCG CCGGGAGTCC
1651TTCCTGTACC GCTCAGACAG CGA

Figure 6.10.d. Human Genomic Sequence Encompassing the 5' end of PDE4A10.

The sequence shown above encodes the 5' end of the PDE4A10 open reading frame including all of the unique splice variant specific sequence. The sequence is that of fragments 3 and 4 as depicted in figure 6.10.a, with extra 3' end sequence derived from RT-PCR. KEY:

TAG The first in-frame stop codon in the PDE4A10 genomic clone

§ The furthest 5' extent of sequence obtained by RT-PCR using primers designed to rat PDE4A10 (primer GR10 was used, see section 6.8.1.)

dotted underline: GC rich regions

ATG: In frame putative initiator methionine (*=most likely initiator methionine, see next section)

Named sense primers are shown single underlined. Named antisense primers are shown double underlined.

Named putative promoter elements are shown double underlined. These are the putative cAMP response element (238) and putative Sp1 regulatory sites. (239).

6.10.1. Expression of PDE4A10 as RNA in cells and identification of the initiator methionine of PDE4A10 by RT-PCR analyses.

There are four candidate initiator methionines (i-iv, figure 6.10.1.a) downstream of the first in-frame stop codon in the PDE4A10 genomic sequence. Authentic initiator methionines are found in the context of a Kozak consensus. The Kozak consensus sequence is CC(A/G)CCATGG (the methionine triplet is in bold)(190). Point mutations of this sequence indicated that the bases at +4 and -1 (underlined) are the only bases that are essential if initiation is to be enabled at the site (190). Kozak showed that the critical positions in the consensus were -3 and +4 (where the A of the ATG triplet is 1). The optimum sequence at these sites is a purine (A or G) at -3 and a G at -4. When these two requirements are met, Kozak showed that translational initiation is >15 fold more efficient from that ATG than an ATG which does not conform to the Kozak consensus (190). On these criteria, only sites (iii) and (iv) are within a Kozak sequence and likely to be effective initiators of translation. This sequence information strongly indicates that translation will initiate at the first of these sites, which is site (iii). The lack of conservation of the site (iv) ATG in rat is also consistent with the notion that site (iii) is the initiator ATG because the PDE4 initiation sites are apparently always conserved between species (19). However, it remains to be seen whether sites (i)-(iii) are conserved.

Further experiments were carried out to provide further evidence that translation initiates at site (iii). Primer GR114 was designed to sequence upstream of sites (iii) and (iv) and primer GR10 is designed to sequence around sites (iii) and (iv) (see figure 6.10.1.b). RT-PCR was carried out on a number of human cell lines and rat and mouse brain using these primers with antisense primers GR10 and GR84 (see section 6.7.2.1). RT-PCR using primers designed to sites (iii) and (iv) produced correct-sized bands in RNA from mouse, rat and a range of human cell lines. In contrast, RT-PCR of sequence upstream of this position produces a signal in human U118 and SK-N-SH RNA samples but not in the rat or mouse RNA (figure 6.10.1.b and c).

The shorter band (A) is the same size as the human RT-PCR fragment already

sequenced. The longer RT-PCR band (C) obtained in U118 and SK-N-SH cells was now sequenced. Both these fragments were found to encode the expected segment of human PDE4A10 sequence (The sense primer in this reaction is GR114. This fullest extent of human PDE4A10 RNA sequence is marked in both figure 6.10.d and 6.10.1.c). As I could only amplify this sequence from RNA from human cell lines, this result is consistent with the notion that sequence upstream of sites (iii) and (iv) is an unconserved UTR and that the ATG with surrounding Kozak sequence is indeed the initiator methionine. The experiments of Kozak (190) showed that upstream sub-optimal Kozak sequences do not interfere with initiation from a downstream ATG which is in a Kozak consensus. This suggests that the presence of the site (ii) in the human PDE4A10 UTR should not perturb initiation from site (iii).

The DNA structure upstream of site (iii) contains a number of putative promoter elements, as reported below. These findings are consistent with the findings presented in this section. The full peptide sequence of the ORF of human PDE4A10 is shown in figure 6.10.1.d

SITE	CONTEXT OF PUTATIVE INITIATION CODON	POSITION OF ATG IN PDE4A10
KOZAK SITE CONSENSUS	CCACC ATG G G	-
(i)	TTCTA ATG T	559
(ii)	CTCCC ATG C	1398
(iii)	GTGCC ATG G	1444
(iv)	TGGCA ATG C	1450

Figure 6.10.1.a In-frame putative initiator methionines for human PDE4A10

The putative initiator methionines for PDE4A10 are compared to the Kozak consensus (190). Underlines represent matches with the consensus at the crucial +4 and -3 positions.

(a)

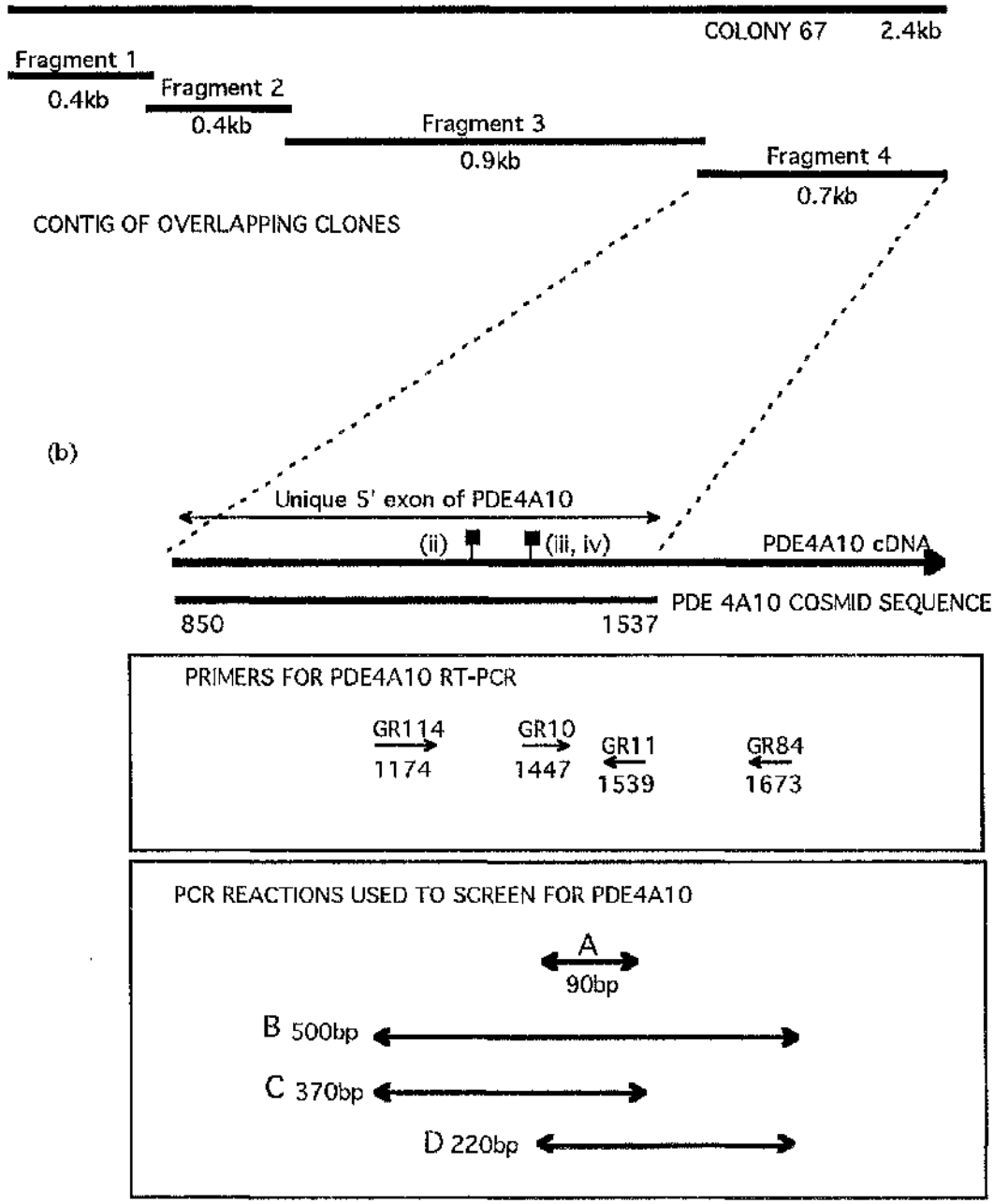
COLONY 67 2.4kb
Fragment 1
0.4kb
Fragment 2
0.4kb
Fragment 3
0.9kb
Fragment 4
0.7kb
CONTIG OF OVERLAPPING CLONES
(b)
Unique 5' exon of PDE4A10
(ii)
(iii, iv)
PDE4A10 cDNA
PDE 4A10 COSMID SEQUENCE
850
1537
PRIMERS FOR PDE4A10 RT-PCR
GR114
1174
GR10
1447
GR11
1539
GR84
1673
PCR REACTIONS USED TO SCREEN FOR PDE4A10
A
90bp
B 500bp
C 370bp
D 220bp

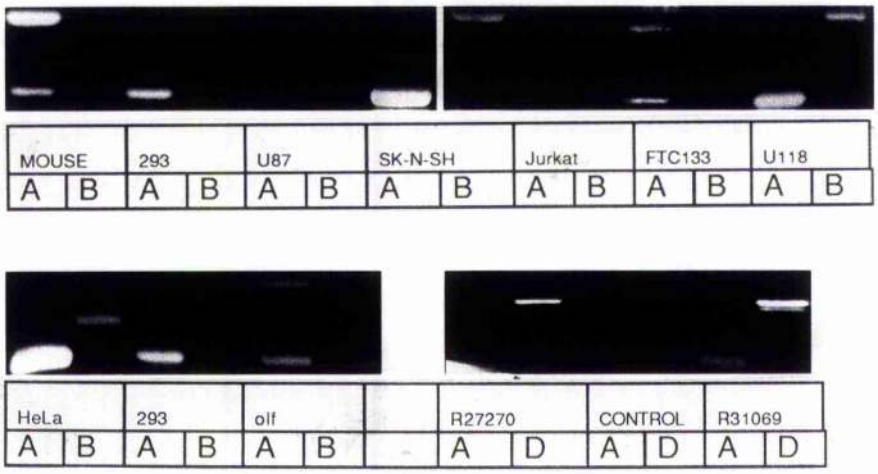

Figure 6.10.1.b. RT-PCR screen for PDE4A10 expression

(i) and (ii) Orientation of primers for PDE4A10 PCR screen. RNA screens were performed with PCR reactions with GR10 and GR11 (Reaction A) or GR114 and GR84 (Reaction B). These primers are shown aligned to the PDE4A10 cDNA (the arrowhead indicates that there is more 3' sequence) and the PDE4A10 cosmid sequence. Since the PDE4A10 cosmid sequence is only the PDE4A10 specific exon, this could not be screened with GR84 which is designed to generic PDE4A sequence. For a PDE4A10 screen of cosmids, PCR reaction B was replaced with one using GR114 and GR11 (Reaction C). Primer GR114 sequence is GCAGGACCCCTGCAGG, the other primer sequences are listed in figure 6.7.2.1. Reaction D is that used in the initial RT-PCR analysis of human PDE4A10 (see figure 6.8.1.a)

(iii) PCR screen of human cell lines, rat brain, mouse brain and cosmids. For reactions A, C and D, cycling conditions were 34 cycles of 96°C for 1min, 50°C (C) or 55°C (A and D) for 1min, 72°C for 1min. Reaction C was supplemented with 5% DMSO. For reaction B, cycling conditions were 34 cycles of 98°C for 1min, 50°C for 1min, 72°C for 1min. This was supplemented with 5% DMSO

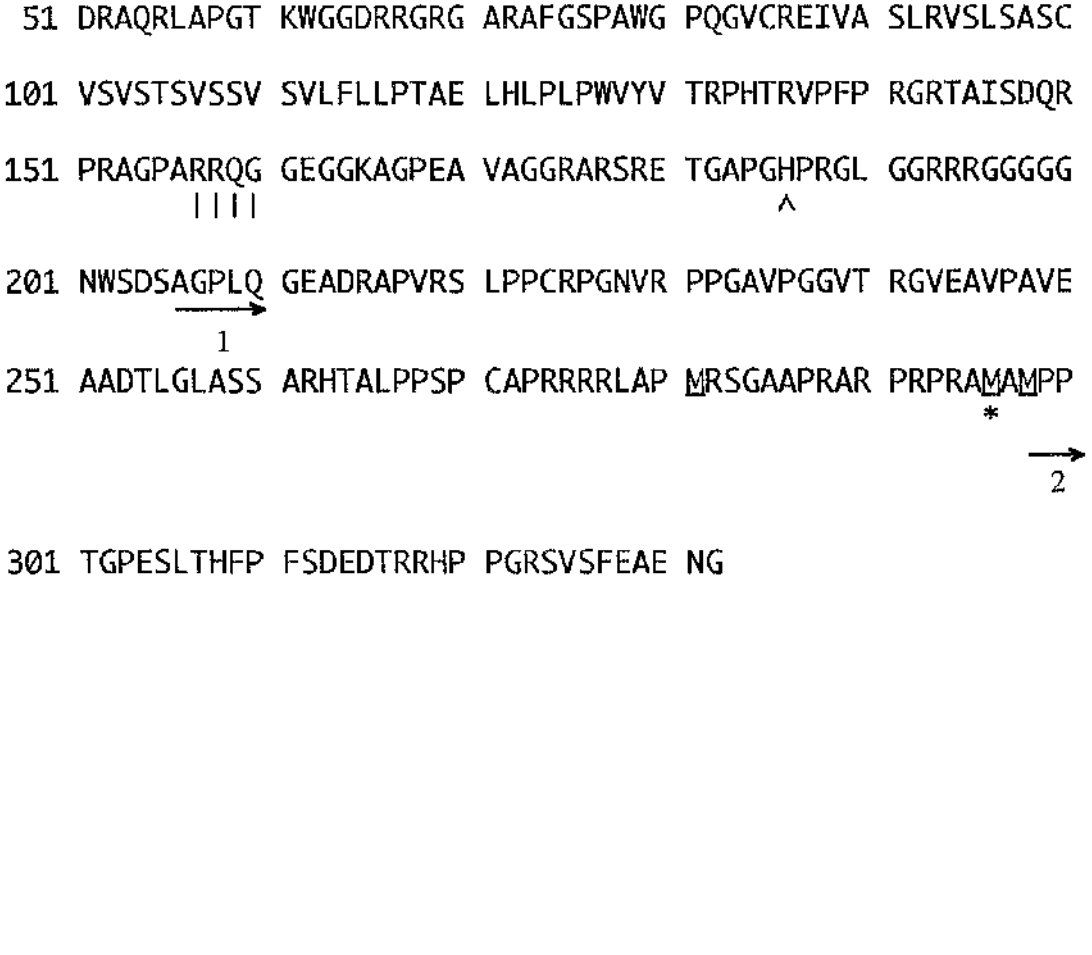

Figure 6.10.1.c Candidate Initiator Methionines for PDE4A10
Putative peptide sequence is shown from the first in-frame methionine of the open reading frame of the PDE4A10 genomic sequence. Potential initiator methionines are underlined. Observations from experiments and sequence analysis which are relevant are mapped to their positions in this peptide sequence.

KEY:
| | | |: Position of the DNA encoding the putative CRE
^: The 5' extent of PDE4A10/pSV SPORT construct (See next section).

1 : Furthest extent of human PDE4A10 detectable by RT-PCR (primer GR114, see section 6.10)

2 : Furthest extent of rat or mouse PDE4A10 detectable by RT-PCR (primer GR10, see section 6.10)

```
  1 MAMPPTGPES LTHFPFSDED TRRHPPGRSV SFEAENGPTP SPGRSPLDSQ
 51 ASPGLVLHAG AATSQRRESF LYRSDSDYDM SPKTMSRNSS VTSEAHAEDL
101 IVTPFAQVLA SLRSVRSNFS LLTNVPVPSN KRSPLGGPTP VCKATLSEET
151 CQQLARETLE ELDWCLEQLE TMQTYRSVSE MASHKFKRML NRELTHLSEM
201 SRSGNQVSEY ISTTFLDKQN EVEIPSPTMK EREKQQAPRP RPSQPPPPPV
251 PHLQPMSQIT GLKKLMHSNS LNNSNIPRFG VKTDQEELLA QELENLNKWG
301 LNIFCVSDYA GGRSLTCIMY MIFQERDLLK KFRIPVDTMV TYMLTLEDHY
351 HADVAYHNSL HAADVLQSTH VLLATPALDA VFTDLEILAA LFAAAIHDVD
401 HPGVSNQFLI NTNSELALMY NDESVLENHH LAVGFKLLQE DNCDIFQNLS
451 KRQRQSLRKM VIDMVLATDM SKHMTLLADL KTMVETKKVT SSGVLLLDNY
501 SDRIQVLRNM VHCADLSNPT KPLELYRQWT DRIMAEFFQQ GDRERERGME
551 ISPMCDKHTA SVEKSQVGFI DYIVHPLWET WADLVHPDAQ EILDTLEDNR
601 DWYYSAIRQS PSPPPEEESR GPGHPPLPDK FQFELTLEEE EEEEISMAQI
651 PCTAQEALTA QGLSGVEEAL DATIAWEASP AQESLEVMAQ EASLEAELEA
701 VYLTQQAQST GSAPVAPDEF SSREEFVVAV SHSSPSALAL QSPLLPAWRT
751 LSVSEHAPGL PGLPSTAAEV EAQREHQAAK RACSACAGTF GEDTSALPAP
801 GGGGSGGDPT
```

Figure 6.10.1.d The full peptide sequence of PDE4A10.

The sequence shown above is the full sequence of the most likely open reading frame of PDE4A10.

6.10.2. Analysis of the unique 5' exon of PDE4A10 and putative promoter sequence

The predicted amino acid sequence of PDE4A10 contains an N-terminal unique sequence of 30 amino acids. For comparison with other 'long' PDE4A forms, HPDE46 has 106 unique amino acids, RPDE66 has 65 amino acids and RPDE39 has 20 amino acids. When compared in a FASTA similarity search the sequence shows no significant homology with any sequences in the Genbank nucleotide and EST databases. A second search, using the most N-terminal sequence conserved in PDE4As was similarly unable to identify a PDE4A10-like sequence in the databases. This finding indicates that a novel splice variant has been identified. ~2.2kB of DNA has been isolated upstream of the putative initiator methionine of PDE4A10. There is no TATA box within this sequence but there are a number of GC rich stretches which are associated with promoter loci which lack a TATA box (240) (see figure 6.10.1). A number of putative Sp1 regulatory motifs (239), which promote transcription initiation from these GC boxes, are identified in the upstream sequence (figure 6.10.1). Most interesting however, is the near-perfect consensus cAMP response element sequence (238) upstream of the initiator methionine. This suggests that PDE4A10 expression could be dynamically regulated and may explain why, though it can be amplified at low levels in RNA from a range of cell-lines, PDE4A10 has not been identified previously by others.

6.11 CONSTRUCTION OF THE FULL CODING SEQUENCE OF PDE4A10 IN THE MAMMALIAN EXPRESSION VECTOR PSV SPORT

6.11.1. Construction of human PDE4A10 5'/pCR2.1

A human PDE4A10 5' end construct was made in pCR2.1 TA cloning vector. This construct represents the expected unique coding exon of PDE4A10. The construct was made from a Sau3A I fragment of the 5' exon of PDE4A10 from colony 67. This was ligated to unphosphorylated adaptors. These adaptors extend the PDE4A10 sequence beyond the exon boundary into sequence conserved with HPDE46. The adaptor-ligated Sau3A I fragment was then TA cloned into pCR2.1 to

produce PDE4A10 5'/pCR2.1. The adaptors incorporate a BstB I site. Partial cleavage of this site enabled production of a cohesive end compatible with PDE46 digested with Taq I.

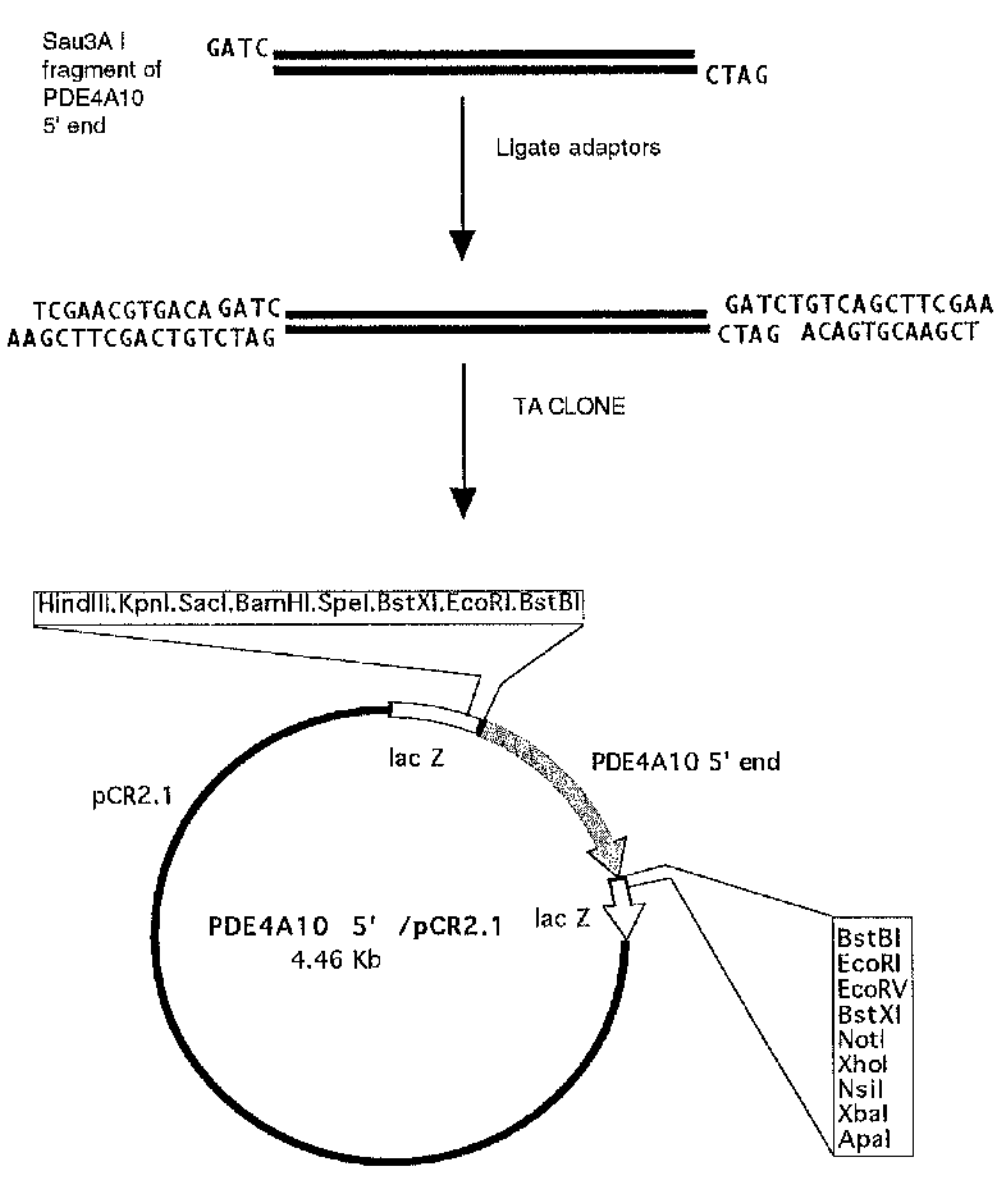

Figure 6.11.1 Construction and plasmid map of PDE4A10 5'/pCR2.1
A Sau3A I fragment of colony 67 was TA cloned by ligation of an adaptor with a T overhang. This produces an insert with sequence which stretches beyond the alternative splicing junction of PDE4A10 into conserved PDE4A sequence. This exon can be fused to PDE46 to produce full-length PDE4A10 (see figure 6.11.2a, b)

6.11.2. Construction of human PDE4A10/pSV SPORT

Construction of human PDE4A10/pSV SPORT incorporated a partial digestion. HPDE46/pSV SPORT was singly digested with Taq I. Singly cut plasmid was separated from uncut and multiply cut plasmid by gel electrophoresis. This product was then digested with Nar I and Kpn I, both of which digest HPDE46/pSV SPORT once (figure 6.11.2.a). The Kpn I digestion is to enable the human PDE4A10 exon to be ligated in. The Nar I digestion site is in the 5' end of HPDE46. This digestion was performed to reduce the probability of recircularisation of HPDE46/pSV SPORT. PDE4A10 5' /pCR2.1 was digested with Kpn I and partially digested with BstB I and then ligated to the HPDE46/pSV SPORT construct which had been digested as already described (figure 6.11.2.b). The construct was analysed by PCR and restriction digestion (figure 6.11.2.c.)

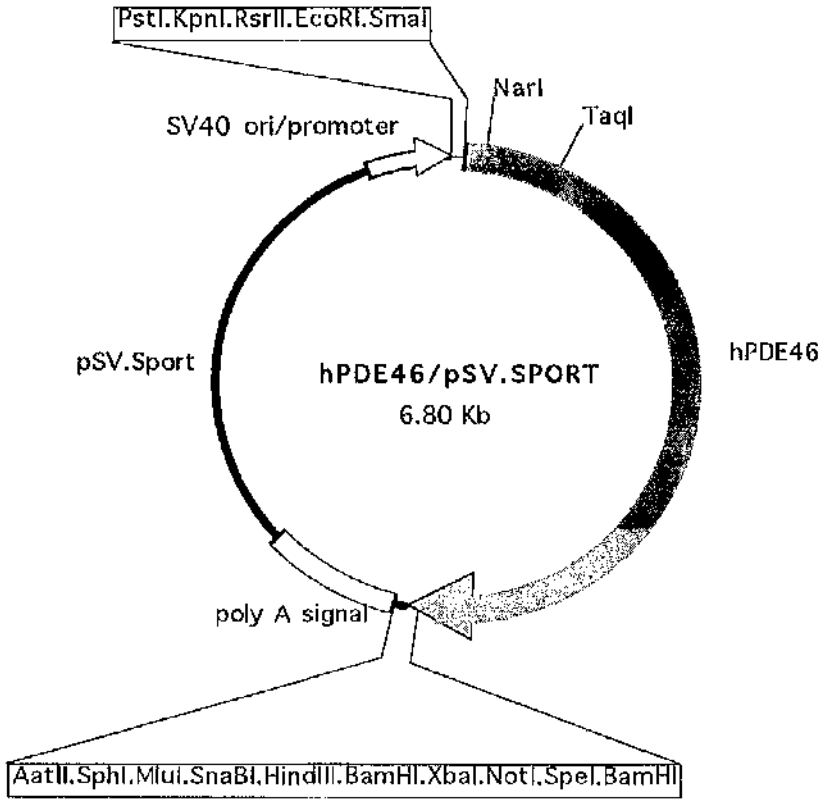

Figure 6.11.2.a. Plasmid map of hPDE46/pSV SPORT

hPDE46/pSV SPORT was digested singly with each of Taq I (partial digest, but the intended insertion site is displayed), Kpn I and Nar I (see section 6.11.2.). Components of the plasmid are as labelled.

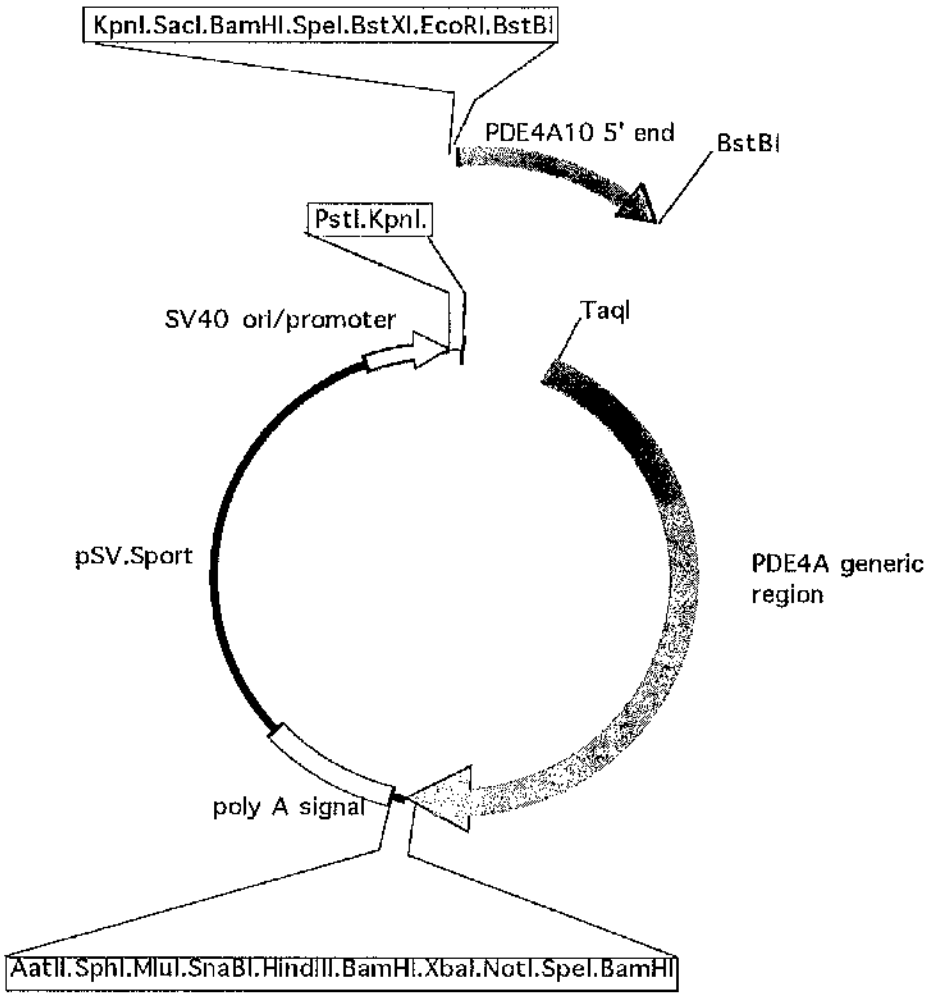

Figure 6.11.2.b. Construction of PDE4A10/ pSV SPORT

The schematic above shows the Kpn I /BstB I fragment of PDE4A10 5' end. This was ligated into a Kpn I/ Taq I PDE46/pSVSPORT digestion to produce PDE4A10/pSV SPORT

(i)

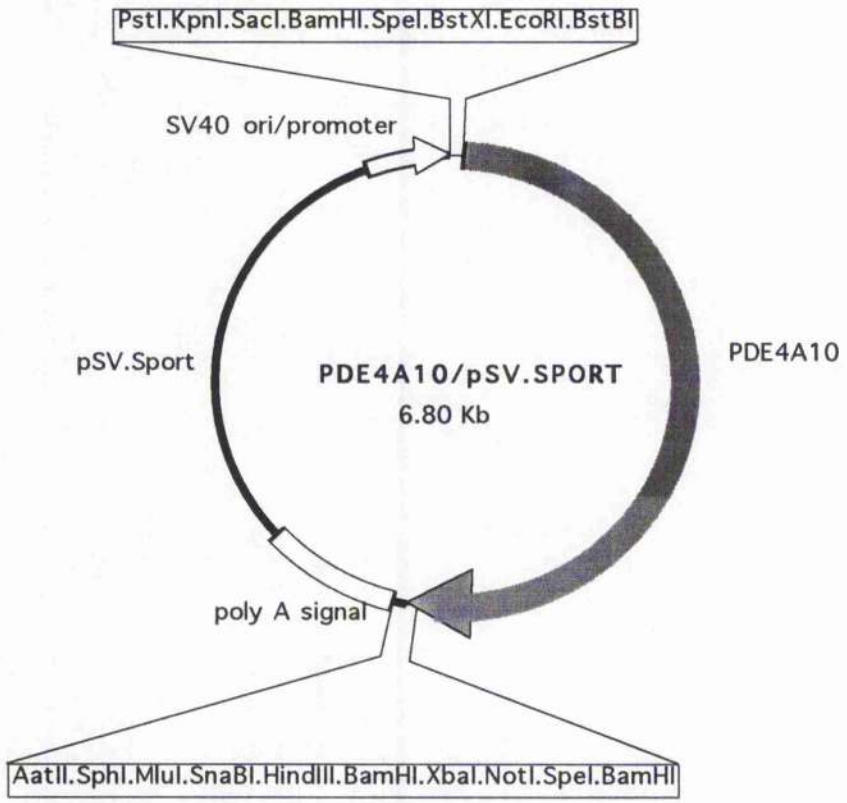

(ii)

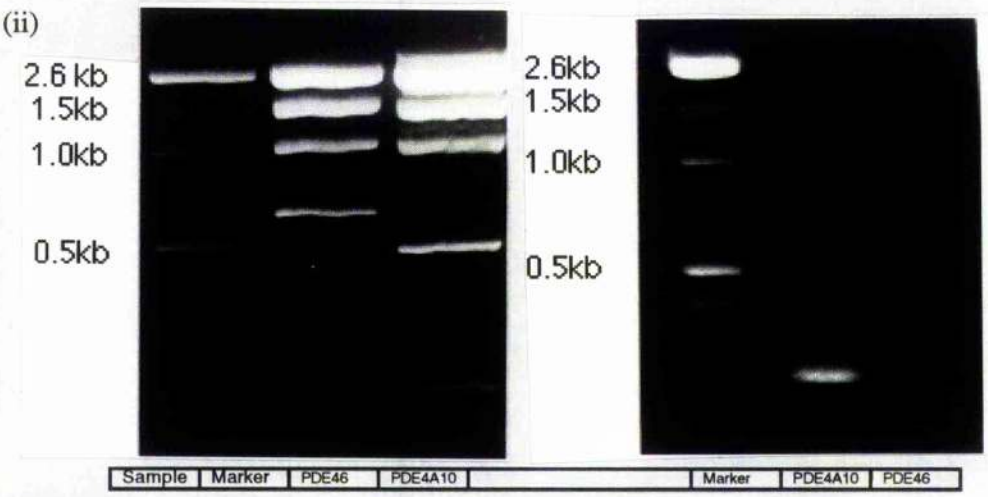

Figure 6.11.2.c Plasmid map of PDE4A10/pSV SPORT

(i) A schematic map of the PDE4A10/pSVSPORT construct. (ii) Evidence that the correct construct has been synthesised. As well as sequencing, the PDE4A10/pSV SPORT construct was subjected to restriction digestion with Sma I (left panel). This shows that the 5' end of PDE46, which is the 0.7kb band, is removed missing in PDE4A10. The smaller bands which then appear are because Sma I cuts several times in the PDE4A10 5' end. A PCR screen with PDE4A10 specific 5' primer GR114 and PDE4A specific primer GR84 (reaction D, see figure 6.10.1.b). produces a band of the correct size with the PDE4A10 construct but not PDE46 (right panel.)

6.12 EXPRESSION OF PDE4A10/pSV SPORT IN COS-7 CELLS

The new construct PDE4A10/pSV SPORT was transfected in COS-7 cells to allow over-expression of the PDE encoded by the plasmid. Cell lysates were then immunoblotted. Lysates of COS-7 cells transfected with PDE46/pcDNA3 were run alongside PDE4A10 lysates as a positive control for the PDE4A monoclonal antibody. These results clearly show a band migrating at the expected weight, which is markedly different to that of PDE46. PDE4A10/pSV SPORT apparently expresses as a doublet. This may be due to initiation occurring at the weak initiation ATG which is upstream of the correct ATG. As with other PDE4A forms HSPDE4A10 appears to run more slowly on an SDS-PAGE gel than one would expect from its calculated molecular weight of 90kD. Both of the PDE4A10 expression products are entirely cytosolic.

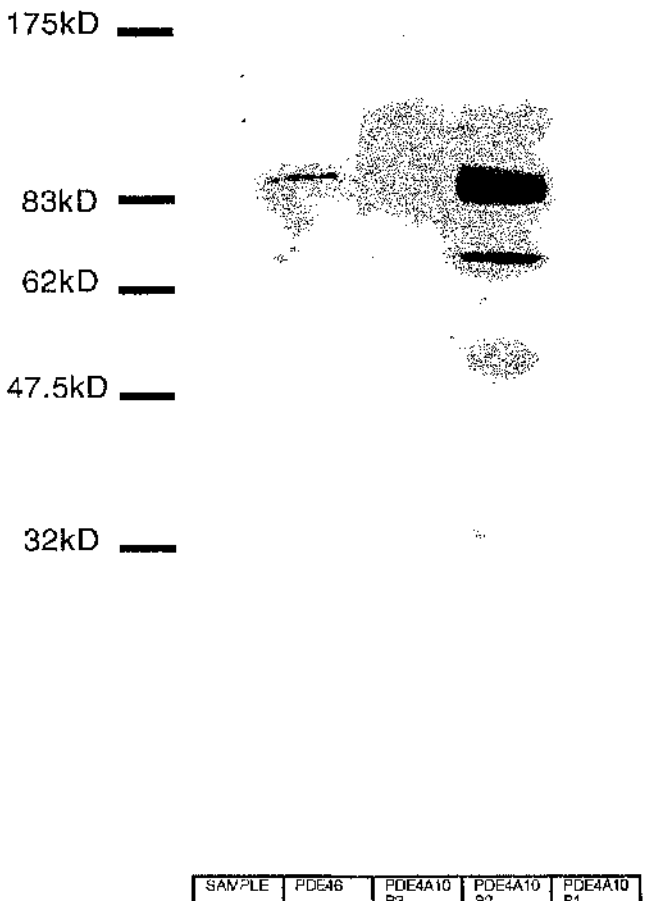

Figure 6.12 Over-expression of PDE4A10 in COS-7 cells

COS-7 cells were transfected with PDE4A10/pSV SPORT. Cells were fractionated and the lysates were then immunoblotted with the PDE4A specific PDE4A monoclonal antibody. Lanes are labelled S2, for the high speed soluble fraction, P2 for the high speed particulate fraction and P1 for the low speed particulate fraction. The molecular weight markers are shown. The apparent molecular weight of the PDE4A10 band is ~95kD. Labels under the lanes show which fraction of each sample (P2, P1, S2) was run. PDE46, which migrates more slowly, is shown as a positive control for the antibody and for comparison with PDE4A10.

CONCLUSION

6.13 FAILURE OF PCR-BASED METHODOLOGIES TO ISOLATE ANY EXTRA SEQUENCE OF RNPDE4A10

Four PCR based methodologies failed to isolate any further DNA sequence of PDE4A10, though the reasons for this remain obscure. The sequence, now identified by other means, shows that conditions were not propitious for PCR-based protocols. The sequence is GC rich, including one sequence of 25 consecutive G or C bases directly upstream of the known sequence. It is well established (228) that such regions provide a poor template for the PCR reaction. Knowledge of the sequence has allowed alteration of denaturing temperatures and DMSO concentrations in PCR reactions of the N-terminal of PDE4A10. This work has revealed that, for the human sequence at least, only at conditions more extreme than those in the RACE PCR is the correct PCR band obtained. Therefore this is in itself reason enough why none of the PCR-based protocols worked. A further more basic problem is that in none of these protocols could the size of the PCR fragment be predicted and this thus removed a major way of discriminating artefactual amplification products. The use of two alternative gene specific primers (see section 6.7.2.) in parallel PCRs did not identify genuine PDE4A amplification products. These primers would have been better indicators of genuine amplification products if they had been placed further apart making the size differential of genuine amplification products larger between the two PCR reactions. Furthermore, given the likelihood that RNA Ligase Mediated (RLM) RACE will, in any case, produce a range of sizes of genuine amplification products (153), the chances of detecting the shifting of all these bands against the kind of background noise I have seen suggests that this innovation will be of limited value. A positive control sequence, which could have been RACE amplified alongside PDE4A10 could have shown that all the enzymes used in the RACE were active but this too would be of questionable value where sequence specific effects are so important on the outcome of an experiment (153).

There were further drawbacks specific to each protocol: (1) The ligase free cloning strategy which is integral to the Terminal Deoxynucleotidyl Transferase (TdT)

RACE kit meant that each primer in the PCR was greater than 30 base pairs long. This is considerably longer than is recommended in most RACE protocols (153). This may have been part of the reason why no amplification products were obtained with this system; (2) The inverse PCR of circularised single stranded cDNA protocol clearly suffered from insufficient removal of cDNA primer because these were seen ligated in polymers in PCR clones. The other 'tag' oligonucleotides were chemically modified at their 3' ends such that they would not be substrates for downstream ligations and it may be that this drawback is the reason why similar protocols have not previously been reported.

6.14 DISCOVERY OF A NEW PDE4A SPLICE VARIANT IN HUMAN AND RAT

This project began with an incomplete novel rat PDE4A clone, rat PDE4A10. By screening of PDE4A cosmid DNA with probes designed to the 5' end of this novel PDE4A cDNA, sequence has been isolated for the full open reading frame of a novel human PDE4A splice variant, HSPDE4A10. A 2.5 kb fragment of sequence which contains putative PDE4A10 promoter elements has also been isolated. The existence of HSPDE4A10 and RNPDE4A10 has been confirmed by RT-PCR in RNA from native tissues and for HSPDE4A10 in cell lines. Sequence information was obtained from these RT-PCR fragments in order to validate the authenticity of the PDE4A10 sequence that I had identified in human genomic DNA. This sequence information did indeed show that the extra PDE4A10 sequence identified by me in human genomic DNA is expressed in PDE4A10 RNA.

The failed attempts to obtain any evidence of the RPDE66 specific exon in genomic cosmids could be because a notional HPDE66 is not sufficiently homologous with RPDE66 or because such an exon is found beyond the 210Kb contig of PDE4A sequence so far isolated or because a homologue of RPDE66 is not found in human. Failure to identify RPDE66 species in RNA may additionally be due to the expected narrow expression profiles of these two splice variants.

6.14.1 Identification of the initiator methionine of PDE4A10

The initiator methionine of human PDE4A10 has been identified on the basis of a number of criteria. Firstly, of the four in-frame methionines downstream of the first in-frame stop codon, only two (iii and iv) are contained within the context of a Kozak consensus. Site (iv) is not conserved in the rat sequence. Secondly, RT-PCR analyses show apparent lack of conservation of sequence further upstream between species, consistent with this upstream sequence being a UTR. Thirdly, the sequence upstream from site (iii) contains several sequence motifs which are commonly identified in promoters. These results are all consistent with the notion that site (iii) is the initiator methionine. These experiments represent a far more rigorous analysis of the initiation site than is normally carried out in the PDE field. The position of the human initiator methionine suggests that the original rat ORF is missing only one codon.

6.14.2. Primary structure and expression of human PDE4A10

As is the case with many other PDE4 forms there are a large number of prolines, serines and arginines in the N-terminal unique sequence of PDE4A10. Prolines and arginines often direct kinases to phosphorylate serines (215) and so it is clearly possible that kinases could phosphorylate PDE4A10. Possible phosphorylation sites are shown below the alignment of rat and human PDE4A10 sequence (figure 6.14.2). The predicted peptide sequence of the human and rat PDE4A10 forms (figure 6.14.2) is well conserved. This is expected to be due to some conserved functions. These still need to be identified but could include conserved regulatory phosphorylation sites. The level of conservation between human and rat PDE4A10 is similar to that of PDE46 and RPDE6 with ~20% substitution in both cases. This contrasts sharply with the 100% conservation of unique exon sequence between human RD1, rat RD1 and RD1 homologues from a number of other species. This distinction further underlines the strict evolutionary constraints which the N-terminus of RD1 seems to be under and which I argued in chapter 5 may be due to a conserved molecular recognition. As with RD1, it is anticipated that the human and rat PDE4A10 homologues will vary most at

their LR2 domain, where human PDE4A10 will have LR2HP whereas rat PDE4A10 will have an LR2P motif. Thus, rat and human PDE4A10 will be another pair of clones in which the function of LR2H can be studied.

The fullest extent of human PDE4A10 cDNA has been expressed in COS-7 cells. This construct expresses protein which is readily detectable by a PDE4A antibody. The doublet produced may be due to aberrant initiation similar to that apparently observed in RD1 PDE4A overexpression (114). Alternatively the doublet may be due to some as yet unidentified postranslational modification.

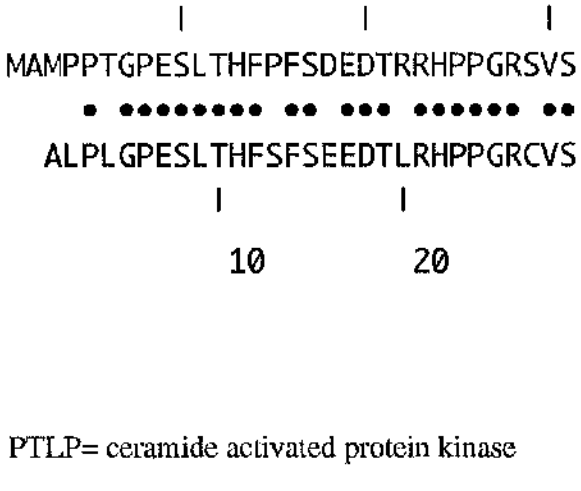

PTLP= ceramide activated protein kinase

XSXXE/DX (where X is preferred acidic) = casein kinase-2

ES= ßARK motif

Figure 6.14.a Peptide sequence conservation between the human and rat homologues of PDE4A10.

The unique splice variant specific sequence of human (TOP) and rat (BOTTOM) PDE4A10 are shown aligned together.

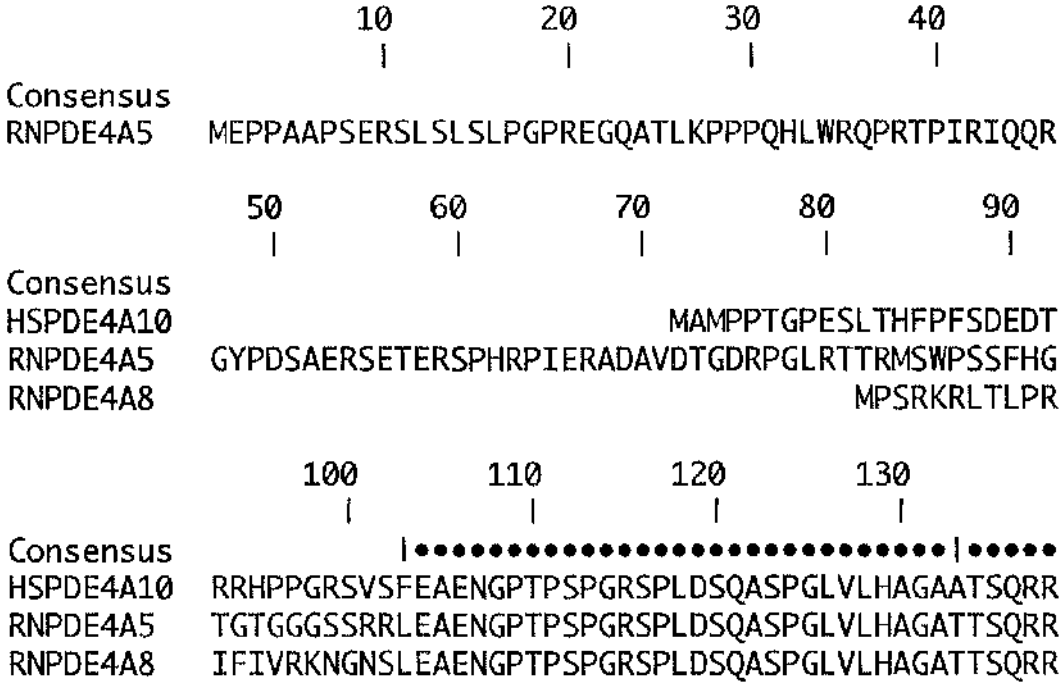

Figure 6.14.b. Alignment of PDE4A splice variants

HSPDE4A10 is compared with the other known 'long' form PDE4A splice variants. These are, with the Genbank accession number in brackets, RNPDE4A5 (68) (L27057), RNPDE4A8 (77) (L36437). Each splice variant sequence diverges from the others at the same splice junction upstream of the conserved rat/human (F/L)EAENG motif.

6.15 OVERLAPPING SHOTGUN TA CLONING: A STRAIGHTFORWARD, RELIABLE METHOD FOR CLONING, SEQUENCING OR RESTRICTION MAPPING PROJECTS.

A method has been described for producing overlapping clones for any shotgun cloning project. These clones could then be used to create a sequence contig or very long single enzyme restriction maps. Any enzyme which gives recessed 3' ends and which cuts away from the recognition sequence could be used in these projects, as presented in table 6.15. As can be seen they can be used to give a range of fragment sizes. A technical drawback is that if two restriction sites are very close together cutting of one may disrupt cutting of the other or both may cut to give a very small fragment which could be missed by downstream processing such as blue/white colour selection for recombinant clones. This is not a major difficulty however because, at worst, such sites will simply interrupt the contig; the size of the interruption may even be gauged by comparison of the length of the contigs with the length of the original DNA sequence

Restriction Enzyme	Recognition Sequence	Frequency of cutting (bp)	Probability of chance overlap match[1] (bp)	Global probability of match[2] (Kb)
Alw26 I Bbv I BsmA I BsmF I Bst71 I Fok I[3] SfaN I	GTCTC(N)1/5 GCAGC(N)8/12 GTCTC(N)1/5 GTCCC(N) 10/14 GCAGC(N)8/12 GGATG(N)9/13 GCATC(N)5/9	1/512	1/256	1/131Kb
Hga I	GACGC(N)5/10	1/512	1/1024	1/524Kb
Eam1104 I Ear I/Ksp632 I	CTCTTC(N)1/4	1/2048	1/64	1/131Kb
Bbs I/Bbv16 II Bpi I/BpuA I Bsa I/Eco31 I BsmB I/Esp3 I BspM I Gdi II[4]	GAAGAC(N)2/6 GGTCTC(N)1/5 CGTCTC(N)1/5 ACCTGC(N)4/8 CGGCCR(N)1/5	1/2048	1/256	1/524Kb
Sap I	GCTCTTC(N)1/4	1/8192	1/64	1/524Kb

[1] Probability of chance match between two unrelated overhangs.

[2] Global probability of a random match between two unrelated overhangs. (Example calculation: Each Alw26 I end has will cut on average every 512 bp of DNA. Each of these overhangs has a 1/256 chance of matching. Thus the global probability of there being a random matching overlap is;
the probability of Alw26 I cutting a piece of DNA x probability of an end matching
1/512 x 1/256 = 1/131Kb
Therefore the global chance of a random overlap is 1 in 131Kb

[3] Fok I possesses considerable 'star' activity (this is where the enzyme cuts at sites other than those it is supposed to digest). The effects that this might have on this cloning strategy are unknown.

[4] Gdi II is not commercially available

Table 6.15. Restriction enzymes suitable for overlapping shotgun TA cloning.

All commercially available enzymes suitable for the novel cloning technique described herein are shown above (source: MBI Fermentas catalogue). These are all restriction enzymes that cut beyond the recognition sequence leaving a recessed 3' end.

6.15.1 Overlapping TA shotgun cloning might be used for very large sequencing projects

Hga I is particularly attractive for overlapping TA shotgun cloning because it can be used to cut large amounts of DNA down to portions that can be sequenced. However, the probability of having ends matching by chance is extremely low, typically about 1 chance overlap per 0.5 Mb (see table 6.15). For comparison the typical bacterial genome is around 4Mb and the human genome is 3000Mb long. Furthermore, even if there are a few random overlaps some permutations could be discounted immediately, for example those that produce a circular contig for a DNA fragment that is clearly linear. Other permutations could be discounted by looking for the permutation with the least number of contigs (see figure 6.15.1). For the production of very large scale contigs with the possibility of an increased number of chance matches this might become a difficult task. However this provides no obvious bar to automation of a 'least number of contigs permutation' search. Missing sequences disrupting the contig are unlikely to perturb these searches because any such gap would be present in both correct and incorrect contig permutations. It is difficult to determine how long sequences would have to be for use in this method before contig alignment becomes impossible. What is clear, from table 6.13, is that the technique described herein will be eminently suitable for contig creation for the many existing vectors designed to hold large amounts of DNA. For example, The Institute for Genome Research (TIGR) is currently engaged in 'end-sequencing' all of its Bacterial Artificial Chromosomes (BAC). This endeavour will provide some information to allow positioning and ordering of the sequence of these constructs within the human genome. If, instead, they were to employ my technique in sequencing their chromosomes, they could rapidly produce large contigs and restriction maps, as I have described, with very little more additional effort. These contigs and digestion maps would allow simpler isolation of new genes and more complete ordering of BAC contigs.

The application of this technique on small scale (gene/PCR products) sequencing projects contig construction will be straightforward because overlaps will

generally either not occur or occur extremely rarely with around a 1/10 chance in a 50kB cosmid cut with Hga I. The only drawback to gene sequencing by overlapping TA shotgun cloning is that the digestion sites may not be well placed to obtain all the sequence. However, as shown in figure 6.13, there are a number of enzymes with different specificities to choose from. In any case, use of my new protocol does not preclude the use of other protocols to fill in any gaps.

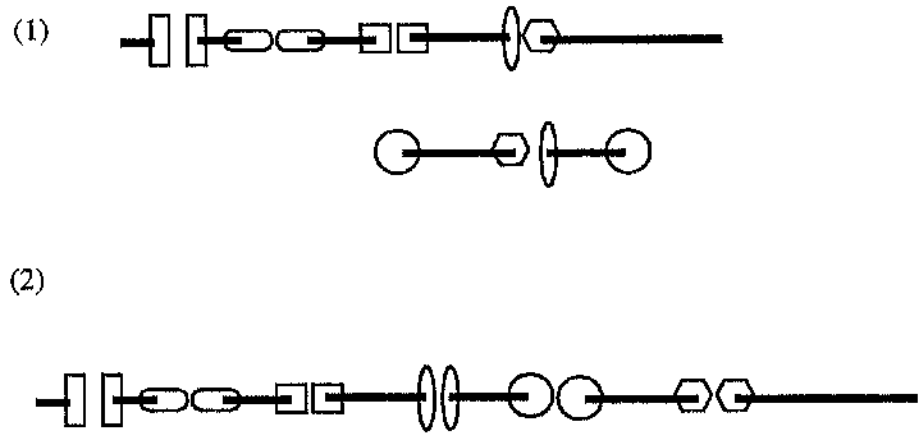

Figure 6.15.1. Schematic of the simplest 'Least number of contigs permutation search'

Small numbers of random overlap matches can be resolved by finding the permutation which gives the least number of cosmids. In the example above the upright oval overlap matches the hexagon overlap, giving two possible permutations for the contig (1,2). The correct contig is the longer one (2).

6.15.2 Overlapping TA shotgun cloning has practical advantages over existing methods of contig assembly.

Overlapping TA shotgun cloning offers considerable advantages over classical shotgun cloning in that much more information is obtained with very few extra experimental steps. The new method also has several practical advantages over the exonuclease/mung bean nuclease protocol which is currently the standard method for sequencing long pieces of DNA (241).

(1) Range. The exonuclease/mung bean nuclease protocol will only work if the restriction enzymes used are not present in the insert. For cosmids and other vectors which carry large inserts then most restriction enzymes will cut many times in the insert so that the exonuclease/mung bean protocol cannot be used (241).

(2) Reliability. The new technique I have described here uses the most robust DNA ligation reaction in TA cloning and only one other reaction, restriction digestion, which can be monitored by gel electrophoresis. Conversely, the full activity of exonuclease III and mung bean nuclease, as well as the proper specificity of the latter, depend on the efficient removal of small pieces of DNA and RNA and nicked DNA (241). S1 nuclease, which has been used in place of mung bean nuclease is even more promiscuous (241).

(3) Ease. The need for pure DNA means that for the best chance of success the exo/mung bean nuclease protocol incorporates phenol chloroform extractions/ spin column extractions (241) whereas the new protocol will work with more straightforward gel purification and ethanol precipitation. Also, the exo/mung bean protocol becomes less attractive the larger the DNA insert gets. This is not only because of the extra risk of restriction digestion sites in the insert (see 1) but also because the positioning of the sequence of interest gets less certain so more time points have to be taken for the exonuclease digestion and these time points are longer. There are no time courses in the new protocol. Another practical difficulty with the exo/mung bean nuclease protocol is that there is no easy control for the second restriction digestion and yet the efficiency of this digestion is vital for the whole experiment's efficiency.

6.15.3 Use of overlapping TA shotgun cloning in creating gel-free long restriction maps

Overlapping TA shotgun cloning could also be used to produce very long restriction maps. To date, these are typically constructed by logical deduction from double digests, or by consistency in the digestion patterns of overlapping clones. Technical difficulties of gel analysis of digests limit the lengths that such maps can be. As has already been discussed, the new method has more relaxed limitations and thus it should be possible to restriction map very large pieces of DNA. Drawbacks to the new approach are that this procedure requires sequencing data and can only use enzymes like those presented in table. Enzymes frequently used in restriction mapping, such as Eco RI or Not I cannot be used.

6.15 FUTURE PROSPECTS

There is now the prospect that this protocol may supersede others to allow identification of contiguous sequences (see figure) without recourse to time-consuming conventional restriction mapping or nuclease treatments. Continuing research into new restriction enzymes with longer overlaps and/or recognition sequences is the key to extending the already wide range of sequence lengths that can be used in this technique.

7. FINAL CONCLUSION

As was discussed in the Introduction, cAMP signals are produced as a result of many external stimuli and these cAMP signals are able to alter cell functioning in distinct ways. This thesis details work towards an understanding of compartmentalisation of cAMP signals at the molecular level. Models for control of compartmentalisation of cAMP by PDEs were elaborated in the introduction. These depend on the existence of a large array of functionally different PDEs. The first two results chapters in this thesis concerned themselves with characterising these functional differences.

In chapter 3 of this thesis I examined the mechanism by which the insulin sensitive PDE3B associates with particulate cell fractions. To do this I made three constructs of various sections of PDE3B. Using these constructs I was able to solubilise full-length PDE3B by treatment with either non-ionic detergent or triethanolamine. The immunoblots of these solubilisations are the first to show solubilisation of full-length PDE3B. I have been able to map a new membrane association domain beyond that described by Taira et al (54) but which is implicit in other data (52,56).

In chapter 4 I examined a PKC-mediated induction of PDE1 in chinese hamster ovary cells in collaboration with co-worker Dr Sandra Spence (163,207). By use of RT-PCR I was able to show that there was an induction in the level of PDE1 transcripts (163). I was further able to show that this induction was a selective induction of PDE1B (207). This is the first example of an induction of an identified PDE by PKC. My results are also the first identification of an induction of PDE1 and similar results, implicating the same PDE in PKC-mediated stimulation, have since been reported by others (35). As such, the data from this chapter represent a significant contribution to understanding of PDE1 regulation.

Chapters 5 and 6 of this thesis were devoted to furthering knowledge of the number and primary structure of PDEs, an endeavour which, in the long term, should also deepen knowledge of the role of different PDEs in compartmentalisation. The work described in chapter 5 showed that I was able to identify mammalian

homologues for the rat PDE RD1. Human RD1 (hRD1) is only the second PDE4A which has been identified in both human and rat. The putative membrane association sequences of RD1 are perfectly conserved across a number of mammalian species, supporting the notion that the sequences may have a conserved functional role. Serendipitously, this work exposed a rodent-lineage specific deletion of apparently ancient PDE4A sequence. This finding, which may be associated with functional alterations, may be a first step in the production of single state PDE inhibitors, since it suggests a possible target for such inhibitors. The deletion may also be of considerable interest to molecular taxonomists as a phylogenetic marker with the potential to solve previously intractable controversies over rodent phylogeny.

In chapter 6 of this thesis I identified, cloned and expressed a novel human PDE4A splice variant, PDE4A10. I have also made a survey of endogenous expression of this PDE in native brain and cell lines by RT-PCR. I have isolated almost the full open reading frame of the rat homologue of this splice variant. This PDE is therefore the third PDE4A which has been identified in both rat and human and the work presented in this chapter therefore represents a major contribution to understanding of the molecular biology of PDEs. The work in chapter 6 also makes a wider contribution, by describing a novel method for producing precise overlaps in clones of DNA. The impact that this technique will make remains to be established. If the technique supplants less reliable, more laborious existing techniques, the facile contig assembly and restriction mapping of very large pieces of DNA that it enables could speed large sequencing projects such as the Human Genome Project. The technique should also be applicable to smaller sequencing projects, where it can be used in conjunction with existing protocols to produce full sequences.

Taken together, the work presented in this thesis represents a significant contribution to understanding of phosphodiesterase isozymes.

APPENDIX: Tested sequences for reverse transcription polymerase chain reaction (RT-PCR) detection of PDEs

A first step towards understanding the basis of compartmentalisation is to identify which of the possible molecular participants are present in the system under investigation. RT-PCR is an attractive technique to employ for this because the necessary probes are easily made and the reactions themselves are robust and rapid. RNA isolated from tissues is reverse transcribed into cDNA and then a fragment of this cDNA is amplified by repeated rounds of specifically primed DNA polymerisation in the PCR reaction.

The primers presented here have been used successfully to detect PDEs from a number of rat tissue and cell line sources (Graham Rena, Li Zeng, Mischa Kostic unpublished) and also mouse (Alex Peden unpublished). The high conservation of PDE sequence between species means that when used at low stringency they are likely to be able to detect the relevant PDE in a range of species, as shown by identification of homologues for RD1 (RNPDE4A1) in a range of species (82).

Design of primers for each published rat PDE4 splice variant

I have designed and tested primers for RT-PCR detection of PDE4 splice variants reported in the rat.

(1) The longest reported sequences for each PDE4 splice variant were downloaded from GenBank. These were used in multiple pairwise alignments on the GeneJockey II program (by Biosoft) to delimit how much unique sequence was contained in each splice variant . Primer pairs were designed to these unique sequences for RNPDE4A8 and RNPDE4A5. Even though there was often enough unique sequence for amplifying a good-sized fragment from the unique sequence alone, I designed most of my primers some way in from the 5' end having found that some primers designed to the extreme 5' ends are poor amplifiers in PCR (data not shown). Therefore, for RNPDE4A1, RNPDE4B2, RNPDE4B1, RNPDE4D1 and RNPDE4D3 we used a splice variant specific primer coupled to a gene specific (but not splice variant specific) downstream primer. RNPDE4D2 has no unique sequence relative to RNPDE4D3 so primers were

designed which allow discrimination from RNPDE4D1 by the size of the fragment (see below). RNPDE4B1 and RNPDE4C1 are likely to represent truncated sequence present in a number of splice variants (85) and so any primers designed to these sequences are probably detecting more than one transcript. My primers to RNPDE4D3 are also likely to be able to cross-detect the as yet uncloned rat homologues of HSPDE4D4 and HSPDE4D5.

(3) Candidate primer pairs are screened against a library of PDE sequences to make sure that they do not anneal to sequences other than those to which they were designed. They are also checked for internal or intermolecular complementarity. Primer sequences of between 18 and 26 base pairs are chosen and the melting temperature of each pair is matched (~65°C)

Tested primers for splice variant specific RT-PCR in the rat.

Splice Variant	SENSE primer	Starts	ANTISENSE primer	Ends at	Size
PDE4A					
RD1 M26715	GR37 ttcttctgcgagaccctgctccaagc	71	GR36 caggccccatttgctcaagttctcc	442	372
RPDE6 (L27057)	GR1 aaggagcctgtctctctctctcccg	1425	GR2 ggtaccggtgccgtggaagga	1683	259
PDE4B					
DPD (J04563)	GR3 aaaccttcaccggagcaccgaacaagagg	39	GR4 gccacgttgaagatgttaaggccccatt	545	507
PDE4 (M25350)	GR17 ttggtagatcactgacacctcatcccg	20	GR4 gccacgttgaagatgttaaggccccatt	686	667
PDE4C					
RPDE36 (L27061)	GS32 ccatggcccagatcactgggctg	459	GR9 ggacttcctggtccgcattaggctaat	1708	1250
PDE4D					
PDE3.1 (M25349)	GR7 tccggtgaagcgcttaagaactgagtcc	237	GR6 cctggttgccagaccgactcatttca	463	227
PDE3.1 (M25349)	GR8 acgtcaagctggagcatctcggc	66	GR6 cctggttgccagaccgactcatttca	463	398
PDE3.2 (U09456)	GR8 acgtcaagctggagcatctcggc	1	GR6 cctggttgccagaccgactcatttca	321	321
PDE3.3 (U09457)	GR5 ctaatttgcaagatcgcgcaccccagc	323	GR6 cctggttgccagaccgactcatttca	577	255

References

1. Scott, J. D. (1991) *Pharmacology and Therapeutics* **50**(1), 123-145

2. Strosberg, A. D., and Pietri-Rouxel, F. (1996) *Trends In Pharmacological Sciences* **17**, 373-381

3. Birnbaumer, L., Abramowitz, J., and Brown, A. M. (1990) *Biochimica et Biophysica Acta - Reviews on Biomembranes* **1031**(2), 163-224

4. Neer, E. J. (1995) *Cell* **80**, 249-257

5. Houslay, M. D. (1991) *Cellular Signalling* **3**, 1-10

6. Taussig, R., and Gilman, A. G. (1995) *Journal of Biological Chemistry* **270**(1), 1-4

7. Houslay, M. D., and Milligan, G. (1997) *Trends in the Biochemical Sciences*, **22**, 217-224

8. Cooper, D. M. F., Mons, N., and Karpen, J. W. (1995) *Nature* **374**(6521), 421-424

9. Pilkis, S. J., Claus, T. H., Johnson , R. A., and Park, C. A. (1975) *Journal of Biological Chemistry* **250**, 6328-6336

10. Houslay, M. D. (1991) *European Journal of Biochemistry* **195**(1), 9-27

11. Beavo, J. A., Conti, M., and Heaslip, R. J. (1994) *Molecular Pharmacology* **46**(3), 399-405

12. Beavo, J. A. (1995) *Physiological Reviews* **75**(4), 725-748

13. Conti, M., Jin, S. L. C., Monaco, L., Repaske, D. R., and Swinnen, J. V. (1991) *Endocrine Reviews* **12**(3), 218-234

14. Conti, M., Nemoz, G., Sette, C., and Vicini, E. (1995) *Endocrine Reviews* **16**(3), 370-389

15. Manganiello, V. C., Murata, T., Taira, M., Belfrage, P., and Degerman, E. (1995) *Archives of Biochemistry and Biophysics* **322**(1), 1-13

16. Manganiello, V. C., Taira, M., Degerman, E., and Belfrage, P. (1995) *Cellular Signalling* **7**(5), 445-455

17. Thompson, W. J. (1991) *Pharmacology and Therapeutics* **51**(1), 13-33

18. Torphy, T. J., Dewolf, W., Green, D. W., and Livi, G. P. (1993) *Agents and Actions* **43**(S), 51-71

19. Houslay, M. D., Sullivan, M., and Bolger, G. B. *Advances in Pharmacology* **In press**

20. Scott, J. D. (1991) *Pharmacol. Ther.* **50**, 123-145

21. Rubin, C. S. (1994) *Biochimica et Biophysica Acta* **1224**(3), 467-479

22. Faux, M. C., and Scott, J. D. (1996) *Cell* **85**, 9-12

23. Klauck, T. M., and Scott, J. D. (1995) *Cellular Signalling* **7**(8), 747-757

24. Hempel, C. M., Vincent, P., Adams, S. R., Tsien, R. Y., and Selverston, A. I. (1996) *Nature* **384**(6605), 166-169

25. Jurevicius, J., and Fischmeister, R. (1996) *Proceedings of the National*

Academy of Sciences USA **93**(1), 295-299

26. Chini, C. C. S., Grande, J. P., Chini, E. N., and Dousa, T. P. (1997) *Journal of Biological Chemistry* **272**(15), 9854-9859

27. Yan, C., Bentley, J. K., Sonnenburg, W. K., and Beavo, J. A. (1994) *Journal of Neuroscience* **14**(3 I), 973-984

28. Polli, J. W., and Kincaid, R. L. (1992) *Proceedings of the National Academy of Sciences USA* **89,** 11079-11083

29. Loughney, K., Martins, T. J., Harris, E. A. S., Sadhu, K., Hicks, J. B., Sonnenburg, W. K., Beavo, J. A., and Ferguson, K. (1996) *Journal of Biological Chemistry* **271**(2), 796-806

30. Yan, C., Zhao, A. Z., Bentley, J. K., and Beavo, J. A. (1996) *Journal of Biological Chemistry* **271**(41), 25699-25706

31. Yan, C., Zhao, A. Z., Bentley, J. K., Loughney, K., Ferguson, K., and Beavo, J. A. (1995) *Proceedings of the National Academy of Sciences USA* **92**(21), 9677-9681

32. Sonnenburg, W. K., Seger, D., and Beavo, J. A. (1993) *Journal of Biological Chemistry* **268**(1), 645-652

33. Sonnenburg, W. K., Seger, D., Kwak, K. S., Huang, J., Charbonneau, H., and Beavo, J. A. (1995) *Journal of Biological Chemistry* **270**(52), 30989-31000

34. Bentley, J. K., Kadlecek, A., Sherbert, C. H., Seger, D., Sonnenburg, W. K., Charbonneau, H., Novack, J. P., and Beavo, J. A. (1992) *Journal of Biological Chemistry* **267**(26), 18676-18682

35. Jiang, X., Li, J., Paskind, M. and Epstein, P. M., (1996) *Proceedings of the National Academy of Sciences USA* **93,** 11237-11241

36. Repaske, D. R., Swinnen, J. V., Jin, S. L. C., Van Wyk, J. J., and Conti, M. (1992) *Journal of Biological Chemistry* **267**(26), 18683-18688

37. Hashimoto, Y., Sharma, R. K., and Soderling, T. R. (1989) *Journal of Biological Chemistry* **264,** 10884-10887

38. Sharma, R. K., and Wang, J. H. (1985) *Proceedings of the National Academy of Sciences USA* **82**, 2603-2607

39. Sonnenburg, W. K., Mullaney, P. J., and Beavo, J. A. (1991) *Journal of Biological Chemistry* **266**(26), 17655-17661

40. Pyne, N. J., Cooper, M. E., and Houslay, M. D. (1986) *Biochemical Journal* **234**(2), 325-334

41. Stroop, S. D., Charbonneau, H., and Beavo, J. A. (1989) *Journal of Biological Chemistry* **264**(23), 13718-13725

42. Stroop, S. D., and Beavo, J. A. (1991) *Journal of Biological Chemistry* **266**(35), 23802-23809

43. Turko, I. V., Haik, T. L., McAllisterLucas, L. M., Burns, F., Francis, S. H., and Corbin, J. D. (1996) *Journal of Biological Chemistry* **271**(36), 22240-22244

44. Degerman, E., Belfrage, P., and Manganiello, V. C. (1996) *Biochemical Society Transactions* **24**(4), 1010-1014

45. Beavo, J. A. (1995) *Journal of Clinical Investigation* **95**(2), 445

46. Maurice, D. H., and Haslam, R. J. (1990) *Molecular Pharmacology* **37**(5), 671-681

47. Rascon, A., Lindgren, S., Stavenow, L., Belfrage, P., Andersson, K. E., Manganiello, V. C., and Degerman, E. (1992) *Biochimica et Biophysica Acta - Molecular Cell Research* **1134**(2), 149-156

48. Schmidt, H. H. H. W., Lohmann, S. M., and Walter, U. (1993) *Biochimica et Biophysica Acta* **1178,** 153-175

49. Smith, C. J., Vasta, V., Degerman, E., Belfrage, P., and Manganiello, V. C. (1991) *Journal of Biological Chemistry* **266**(20), 13385-13390

50. Zhao, A. Z., Zhao, H., Teague, J., Fujimoto, W., and Beavo, J. A. (1997) *Proceedings of the National Academy of Sciences USA* **94,** 3223-3228

51. Meacci, E., Taira, M., Moos Jr, M., Smith, C. J., Movsesian, M. A., Degerman, E., Belfrage, P., and Manganiello, V. (1992) *Proceedings of the National Academy of Sciences USA* **89,** 3721-3725

52. Kasuya, J., Goko, H., and Fujita-Yamaguchi, Y. (1995) *Journal of Biological Chemistry* **270,** 14305-14312

53. Miki, T., Taira, M., Hockman, S., Shimada, F., Lieman, J., Napolitano, M., Ward, D., Taira, M., Makino, H., and Manganiello, V. C. (1996) *Genomics* **36,** 476-485

54. Taira, M., Hockman, S. C., Calvo, J. C., Taira, M., Belfrage, P., and Manganiello, V. C. (1993) *Journal of Biological Chemistry* **268**(25), 18573-18579

55. Tang, K. M., Jang, E. K., and Haslam, R. J. (1997) *Biochemical Journal* **323,** 217-224

56. Leroy, M.-J., Degerman, E., Taira, M., Murata, T., Wang, L. H., Movsesian, M. A., Meacci, E., and Manganiello, V. C. (1996) *Biochemistry* **35,** 10194-10202

57. Reinhardt, R. R., Chin, E., Zhou, J., Taira, M., Murata, T., Manganiello, V. C., and Bondy, C. A. (1995) *Journal of Clinical Investigation* **95**(4), 1528-1538

58. Degerman, E., Belfrage, P., and Manganiello, V. C. (1997) *Journal of Biological Chemistry* **272,** 6823-6826

59. Marcoz, P., Nemoz, G., Prigent, A. F., and Lagarde, M. (1993) *Biochimica et Biophysica Acta* **1176,** 129-136

60. Beebe, S. J., Redmon, J. B., Blackmore, P. F., and Corbin, J. D. (1985) *Journal of Biological Chemistry* **260**(29), 15781-15788

61. Eriksson, J. W., Lonnroth, P., Bosner, B. I., Shaver, A., Wesslau, C., and Smith, U. P. G. (1996) *Diabetologia* **39,** 235-242

62. Eriksson, H., Ridderstrale, M., Degerman, E., Ekholm, D., Smith, C. J.,

Manganiello, V. C., Belfrage, P., and Tornqvist, H. (1995) *Biochimica et Biophysica Acta - Molecular Cell Research* **1266**(1), 101-107

63. Makino, H., Manganiello, V. C., and Kono, T. (1994) *Annual Review of Physiology* **56,** 273-295

64. Smith, C. J., and Manganiello, V. C. (1989) *Molecular Pharmacology* **35**(3), 381-386

65. Davis, R. L., Takayasu, H., Eberwine, M., and Myres, J. (1989) *Proceedings of the National Academy of Sciences USA* **86,** 3604-3608

66. Colicelli, J., Birchmeir, C., Michaeli, T., O'Neill, K., Riggs, M., and Wigler, M. (1989) *Proceedings of the National Academy of Sciences USA* **86,** 3599-3603

67. Swinnen, J. V., Joseph, D. R., and Conti, M. (1989) *Proceedings of the National Academy of SciencesUSA* **86**(14), 5325-5329

68. Bolger, G., Michaeli, T., Martins, T., St John, T., Steiner, B., Rodgers, L., Riggs, M., Wigler, M., and Ferguson, K. (1993) *Molecular and Cellular Biology* **13**(10), 6558-6571

69. Milatovich, A., Bolger, G., Michaeli, T., and Francke, U. (1994) *Somatic Cell and Molecular Genetics* **20,** 75-86

70. Horton, Y. M., Sullivan, M., and Houslay, M. D. (1995) *Biochemical Journal* **312**(3), 991

71. Horton, Y. M., Sullivan, M., and Houslay, M. D. (1995) *Biochemical Journal* **308**(2), 683-691

72. Szpirer, C., Szpirer, J., Riviere, M., Swinnen, J., Vicini, E., and Conti, M. (1995) *Cytogenetics and Cell Genetics* **69**(1-2), 11-14

73. Jin, S. L. C., Swinnen, J. V., and Conti, M. (1992) *Journal of Biological Chemistry* **267**(26), 18929-18939

74. Sullivan, M., Egerton, M., Shakur, Y., Marquardson, A., and Houslay, M. D. (1994) *Cellular Signalling* **6**(7), 793-812

75. Livi, G. P., Kmetz, P., McHale, M. M., Cieslinski, L. B., Sathe, G. M., Taylor, D. P., Davis, R. L., Torphy, T. J., and Balcarek, J. M. (1990) *Molecular and Cellular Biology* **10**(6), 2678-2686

76. Bolger, G. B., Rodgers, L., and Riggs, M. (1994) *Gene* **149**(2), 237-244

77. Bolger, G. B., McPhee, I., and Houslay, M. D. (1996) *Journal of Biological Chemistry* **271**(2), 1065-1071

78. Owens, R. J., Lumb, S., Rees-Milton, K., Russell, A., Baldock, D., Lang, V., Crabbe, T., Ballesteros, M., and Perry, M. J. (1997) *Cellular Signalling* **9,** (in press)

79. Obernolte, R., Bhakta, S., Alvarez, R., Bach, C., Zuppan, P., Mulkins, M., Jarnagin, K., Shelton, E. R. (1993) *Gene* **129,** 239-247

80. Baecker, P. A., Obernolte, R., Bach, C., Yee, C., and Shelton, E. R. (1994) *Gene* **138,** 253-256

81. Bolger, G. (1994) *Cellular Signalling* **6,** 851-859

82. Sullivan, M., Rena, G., Gordon, L., Olsen, A. S., and Houslay, M. D. (1997) , (m/s submitted)

83. McLaughlin, M. M., Cieslinski, L. B., Burman, M., Torphy, T. J., and Livi, G. P. (1993) *Journal of Biological Chemistry* **268**(9), 6470-6476

84. Swinnen, J. V., Tsikalas, K. E., and Conti, M. (1991) *Journal of Biological Chemistry* **266**(27), 18370-18377

85. Engels, P., Sullivan, M., Muller, T., and Lubbert, H. (1995) *FEBS Letters* **358**(3), 305-310

86. Nemoz, G., Zhang, B., Sette, C., and Conti, M. (1996) *FEBS Letters* **384**(1), 97-102

87. Bolger, G. B., Erdogan, S., Jones, R. E., Loughney, K., Wilkinson, I., Farrell, C., and Houslay, M. D. (1997) **328,** 539-548

88. Sette, C., Vicini, E., and Conti, M. (1994) *Journal of Biological Chemistry* **269**(28), 18271-18274

89. Sette, C., Vicini, E., and Conti, M. (1994) *Journal of Biological Chemistry* **269**(32), 20806

90. Huston, E., Lumb, S., Russell, A., Catterall, C., Ross, A. H., Steele, M. R., Bolger, G. B., Perry, M., Owens, R., and Houslay, M. D. (1997) **328,** 549-558

91. Obernolte, R., Ratzliff, J., Baecker, P. A., Daniels, D. V., Zuppan, P., Jarnagin, K., and Shelton, E. R. (1997) *Biochimica et Biophysica Acta,* **1353,** 287-297

92. Qiu, Y., Chen, C. N., Malone, T., Richter, L., Beckendorf, S. K., and Davis, R. L. (1991) *Journal of Molecular Biology* **222**(3), 553-565

93. Qiu, Y., and Davis, R. L. (1993) *Genes and Development* **7**(7 B), 1447-1458

94. Monaco, L., Vicini, E., and Conti, M. (1994) *Journal of Biological Chemistry* **269**(1), 347-357

95. Vicini, E., and Conti, M. (1997) *Molecular Endocrinology* **11,** 839-850

96. Beavo, J. A., and Reifsnyder, D. H. (1990) *Trends in Pharmacological Sciences* **11**(4), 150-155

97. Charbonneau, H. (1990) in *Cyclic nucleotide phosphodiesterases.* (Beavo, J., and Houslay, M. D., eds) Vol. 2, pp. 267-298, John Wiley, Chichester

98. Houslay, M. D. (1996) *Biochemical Society Transactions* **24**(4), 980-986

99. Erdogan, S., and Houslay, M. D. (1997) *Biochemical Journal* **271,** 165-175

100. Huston, E., Pooley, L., Julien, J., Scotland, G., McPhee, I., Sullivan, M., Bolger, G., and Houslay, M. D. (1996) *Journal of Biological Chemistry* **271,** 31334-31344

101. Lobban, M., Shakur, Y., Beattie, J., and Houslay, M. D. (1994) *Biochemical Journal* **304**(2), 399-406

102. Shakur, Y., Wilson, M., Pooley, L., Lobban, M., Griffiths, S. L., Campbell, A. M., Beattie, J., Daly, C., and Houslay, M. D. (1995) *Biochemical Journal* **306**(3), 801-809

103. Dudai, Y., Jan, Y. N., Byers, D., Quinn, W. G., and Benzer, S. (1976) *Proceedings of the National Academy of Sciences USA* **73,** 1684-1688.

104. Davis, R. L. (1993) *Neuron* **11**(1), 1-14

105. Byers, D., Davis, R. L., and Kiger, J. A. (1981) *Nature* **289,** 79-83

106. Chen, C. N., Denome, S., and Davis, R. L. (1986) *Proceedings of the National Academy of SciencesUSA* **83**(24), 9313-9317

107. Davis, R. L. (1996) *Physiology Reviews* **76,** 299-317

108. Dauwalder, B., and Davis, R. L. (1995) *Journal of Neuroscience* **15**(5 I), 3490-3499

109. Petrovitch, T. Z., Merakovsky, J., and Kelly, L. E. (1993) *Genetics* **133,** 955-965

110. Shakur, Y., Pryde, J. G., and Houslay, M. D. (1993) *Biochemical Journal* **292**(3), 677-686

111. Scotland, G., and Houslay, M. D. (1995) *Biochemical Journal* **308**(2), 673-681

112. McPhee, I., Pooley, L., Lobban, M., Bolger, G., and Houslay, M. D. (1995) *Biochemical Journal* **310**(3), 965-974

113. Houslay, M. D., Scotland, G., Pooley, L., Spence, S., Wilkinson, I., McCallum, F., Julien, P., Rena, N. G., Michie, A. M., Erdogan, S., Zeng, L., Oconnell, J. C., Tobias, E. S., and MacPhee, I. (1995) *Biochemical Society Transactions* **23**(2), 393-398

114. Smith, K. J., Scotland, G., Beattie, J., Trayer, I. P., and Houslay, M. D. (1996) *Journal of Biological Chemistry* **271**(28), 16703-16711

115. Pooley, L., Shakur, Y., Rena, G., and Houslay, M. D. (1997) *Biochemical Journal* **321,** 177-185

116. O'Connell, J. G., McCallum, J. F., McPhee, I., Wakefield, J., Houslay, E. S., Wishart, W., Bolger, G., Frame, M., and Houslay, M. D. (1996) *Biochemical Journal* **318**(1), 255-261

117. Engels, P., Fichtel, K., and Lubbert, H. (1994) *FEBS Letters* **350**(2-3), 291-295

118. Engels, P., AbdelAl, S., Hulley, P., and Lubbert, H. (1995) *Journal of Neuroscience Research* **41,** 169-178

119. Sette, C., Iona, S., and Conti, M. (1994) *Journal of Biological Chemistry* **269**(12), 9245-9252

120. Heyworth, C. M., Wallace, A. V., and Houslay, M. D. (1983) *Biochemical Journal* **214**(1), 99-110

121. Ricard, J., Meunier, J. C., and Buc, J. (1974) *European Journal of*

Biochemistry **49,** 195-208

122. Souness, J. E., and Rao, S. (1997) *Cellular Signalling* **9,** 227-236

123. Kelly, J. J., Barnes, P. J., and Giembycz, M. A. (1996) *Biochemical Journal* **318**(2), 425-436

124. Schneider, H. H., Schmiechen, R., Brezinski, M., and Seidler, J. (1986) *European Journal of Pharmacology* **127**(1-2), 105-115

125. Souness, J. E., and Scott, L. C. (1993) *Biochemical Journal* **291**(2), 389-395

126. Wilson, M., Sullivan, M., Brown, N., and Houslay, M. D. (1994) *Biochemical Journal* **304**(2), 407-415

127. Jacobitz, S., McLaughlin, M. M., Livi, G. P., Burman, M., and Torphy, T. J. (1996) *Molecular Pharmacology* **50,** 891-899

128. Muller, T., Engels, P., and Fozard, J. R. (1996) *Trends in Pharmacological Sciences* **17**(8), 294-298

129. Owens, R. J., Catterall, C., Batty, D., Jappy, J., Russell, A., Smith, B., O'Connell, J., and Perry, M. (1997) *Biochemical Journal* **326,** 53-60

130. Torphy, T. J., Stadel, J. M., Burman, M., Cieslinski, L. B., McLaughlin, M. M., White, J. R., and Livi, G. P. (1992) *Journal of Biological Chemistry* **267**(3), 1798-1804

131. Souness, J. E., Hassall, G. A., and Parrott, D. P. (1992) *Biochemical Pharmacology* **44**(5), 857-866

132. Duplantier, A. J., Biggers, M. S., Chambers, R. J., Cheng, J. B., Cooper, K., Damon, D. B., Eggler, J. F., Kraus, K. G., Marfat, A., Masamune, H., Pillar, J. S., Shirley, J. T., Umland, J. P., and Watson, J. W. (1996) *Journal of Medical Chemistry* **39,** 120-125

133. Souness, J. E., Griffin, M., Maslen, C., Ebsworth, K., Scott, L. C., Pollock, K., Palfreyman, M. N., and Karlsson, J. A. (1996) *British Journal of Pharmacology* **118**(3), 649-658

134. Souness, J. E., Houghton, C., Sardar, N., and Withnall, M. T. (1997) *British Journal of Pharmacology* **121**(4), 743-750

135. Souness, J. E., Maslen, C., and Scott, L. C. (1992) *FEBS Letters* **302**(2), 181-184

136. Thompson, W. J., Tan, B. H., and Strada, S. J. (1991) *Journal of Biological Chemistry* **266**(26), 17011-17019

137. Sette, C., and Conti, M. (1996) *Journal of Biological Chemistry* **271**(28), 16526-16534

138. Lenhard, J. M., Kassel, D. B., Rocque, W. J., Hamacher, L., Holmes, W. D., Patel, I., Hoffman, C., and Luther, M. (1996) *Biochemical Journal* **316**(3), 751-758

139. Sette, C., Vicini, E., and Conti, M. (1994) *Molecular and Cellular*

Endocrinology
100 , 75-79
140. DiSanto, M. E., Glaser, K. B., and Heaslip, R. J. (1995) *Cellular Signalling* **7,** 827-835
141. Nemoz, G., Sette, C., and Conti, M. (1997) *Molecular Pharmacology* **51**(2), 242-249
142. Francis, S. H., and Corbin, J. D. (1988) *Methods in Enzymology* **159,** 722-729
143. Thomas, M. K., Francis, S. H., and Corbin, J. D. (1990) *Journal of Biological Chemistry* **265**(25), 14964-14970
144. Thomas, M. K., Francis, S. H., and Corbin, J. D. (1990) *Journal of Biological Chemistry* **265**(25), 14971-14978
145. Francis, S. H., Colbran, J. L., McAllisterLucas, L. M., and Corbin, J. D. (1994) *Journal of Biological Chemistry* **269**(36), 22477-22480
146. Wilkins, M. R., Settle, S. L., Stockmann, P. T., and Needleman, P. (1990) *Proceedings of the National Academy of Sciences USA* **87,** 6465-6469
147. Wilkins, M. R., Settle, S. L., and Needleman, P. (1990) *Journal of Clinical Investigation* **85,** 1274-1279
148. Boolell, M., Gepi-Attee, S., Gingell, J. C., and Allen, M. J. (1996) *British Journal of Urology* **78,** 257-261
149. Lagnado, L., and Baylor, D. (1992) *Neuron* **8,** 995-1002
150. Lavan, B. E., Lakey, T., and Houslay, M. D. (1989) *Biochemical Pharmacology* **38**(22), 4123-4136
151. Bloom, T. J., and Beavo, J. A. (1996) *Proceedings of the National Academy of Sciences USA* **93**(24), 14188-14192
152. Michaeli, T., Bloom, T. J., Martins, T., Loughney, K., Ferguson, K., Riggs, M., Rodgers, L., Beavo, J. A., and Wigler, M. (1993) *Journal of Biological Chemistry* **268**(17), 12925-12932
153. Schaefer, B. C. (1995) *Analytical Biochemistry* **227**(2), 255-273
154. Hengen, P. N. (1995) *Trends in Biochemical Sciences* **20**(9), 372-373
155. Chen, Z., Faaberg, K. S., and Plagemann, P. G. W. (1994) *Journal of General Virology* **75**(4), 925-930
156. Triglia, T., Peterson, M. G., and Kemp, D. J. (1988) *Nucleic Acids Research* **16**(16), 8186
157. Laemmli, U. K. (1970) *Nature (London)* **222,** 680-682
158. Thompson, W. J., and Appleman, M. M. (1971) *Biochemistry* **10,** 311-316
159. Rutten, W. J., Schoot, B. M., and Dupont, J. S. H. (1973) *Biochimica Biophysica Acta* **315,** 378-383
160. Marchmont, R. J., and Houslay, M. D. (1980) *Biochemical Journal* **187,** 381-392

161. Hidaka, H., Hayashi, H., Kohri, H., Kimura, Y., Hospkawa, T., Igawa, T., and Saitoh, Y. (1979) *Journal of Pharmacology & Experimental Therapeutics* **211**(1), 26-30

162. Wachtel, H. (1982) *Psychopharmacology* **77,** 309-314

163. Spence, S., Rena, G., Sweeney, G., and Houslay, M. D. (1995) *Biochemical Journal* **310**(3), 975-982

164. Hay, R., Macy, M., Chen, T. R., McClintock, P., and Reid, Y. (1988) *American Type Culture Collection (ATCC) Catalogue of Cell Lines & Hybridomas*, Rockville

165. Puck, T. T. (1958) *Journal of Experimental Medicine* **108,** 945

166. Ponten, J. (1968) *Acta Pathologica et Microbiologica Scandinavica* **74,** 465-486

167. Biedler, J. L., Helson, L., and Spengler, B. A. (1973) **33,** 2643-2652

168. Sundstrom, C., and Nilsson, K. (1976) *International Journal of Cancer* **17,** 565-577

169. Puck, T. T., Marcus, P. I., and Cieciura, S. J. *Journal of Experimental Medicine* **103,** 273

170. Kaplan, J., Tilton, J., and Peterson, W. D. J. (1976) *American Journal of Hematology* **1,** 219-225

171. Hoelting, T., Tezelman, S., Siperstein, A. E., Duh, Q.-Y., and Clark, O. H. (1993) *Biochemical and Biophysical Research Communications* **195,** 1230-1236

172. Manganiello, V. C., and Vaughan, M. (1973) *Journal of Biological Chemistry* **248,** 7164-7170

173. Jennings, M. L. (1989) *Annual Review of Biochemistry* **58,** 999-1027

174. Pillai, R., Staub, S. F., and Colicelli, J. (1994) *Journal of Biological Chemistry* **269**(48), 30676-30681

175. He, R., Komas, N., Ekholm, D., Murata, T., Taira, M., Hockman, S., Degerman, E., and Manganiello, V. C. *Cellular Signalling* , In Press

176. Degerman, E., Smith, C. J., Tornqvist, H., Vasta, V., Belfrage, P., and Manganiello, V. C. (1990) *Proceedings of the National Academy of Sciences USA* **87**(2), 533-537

177. Shibata, H., Robinson, F. W., Soderling., T. R., and Kono, T. (1991) *Journal of Biological Chemistry* **266,** 17948-17953

178. Shibata, H., and Kono, T. (1990) *Biochemical and Biophysical Research Communications* **167,** 614-620

179. Shibata, H., and Kono, T. (1990) *Biochemical and Biophysical Research Communications* **170,** 533-539

180. LopezAparicio, P., Belfrage, P., Manganiello, V. C., Kono, T., and Degerman, E. (1993) *Biochemical and Biophysical Research Communications* **193**(3), 1137-1144

181. Rascon, A., Degerman, E., Taira, M., Meacci, E., Smith, C. J., Manganiello, V. C., Belfrage, P., and Tornqvist, H. (1994) *Journal of Biological Chemistry* **269,** 11962-11966

182. Rahn, T., Ronnstrand, L., Leroy, M.-J., Wernstedt, C., Tornqvist, H., Manganiello, V. C., Belfrage, P., and Manganiello, V. C. (1995) *Journal of Biological Chemistry* **271,** 11575-11580

183. Rahn, T., Ridderstrale, M., Tornqvist, H., Manganiello, V., Fredrikson, G., Belfrage, P., and Degerman, E. (1994) *FEBS Letters* **350,** 314-318

184. Cheatham, B., Vlahos, C. J., Cheatham, L., Wang, L., Blenis, J., and Kahn, C. R. (1994) *Molecular and Cellular Biology* **14,** 4902-4911

185. Chung, J., Grammer, T. C., Lemon, K. P., Kazlauskas, A., and Blenis, J. (1994) *Nature* **370,** 71-75

186. Cross, D. A. E., Alessi, D. R., Cohen, P., Andjelkovich, M., and Hemmings, B. (1995) *Nature* **378,** 785-789

187. Franke, T., Yang, S., Chan, T. O., Datta, K., Kazlauskas, A., Morrison, D. K., Kaplan, D. R., and Tsichlis, P. N. (1995) *Cell* **81,** 727-736

188. Alessi, D. R., Andjelkovic, M., Caudwell, B., Cron, P., Morrice, N., Cohen, P., and Hemmings, B. A. (1996) *EMBO Journal* **15,** 6541-6551

189. Kyte, J., and Doolittle, R. F. (1982) *Journal of Molecular Biology* **157,** 105-132

190. Kozak, M. (1986) *Cell* **44,** 283-292

191. Makino, H., and Kono, T. (1980) *Journal of Biological Chemistry* **255,** 7850-7854

192. Franciolini, F., and Nonner, W. (1994) *Journal of General Physiology* **104,** 711-723

193. Heuser, J., and Kirchhausen, T. (1985) *Journal of Ultrastructure and Molecular Structure Research* **92,** 1-27

194. Macphee, C. H., Reifsnyder, D. H., Moore, T. A., Lerea, K. M., and Beavo, J. A. (1988) *Journal of Biological Chemistry* **263**(21), 10353-10358

195. Wijkander, J., Rahn Landstrom, T., Manganiello, V., Belfrage, P., and Degerman, E. (1998) *Endocrinology* **139,** 219-227

196. Quick, J., Ware, J. A., and Driedger, P. E. (1992) *Biochemical and Biophysical Research Communications* **187,** 657-663

197. Berridge, M. J. (1984) *Advances in Cyclic Nucleotide Protein Phosphorylation Research* **17,** 329-335

198. Berridge, M. J., and Irvine, R. F. (1989) *Nature* **341,** 197-205

199. Hug, H., and Sarre, T. F. (1993) *Biochemical Journal* **291,** 329-343

200. Dekker, L. V., and Parker, P. J. (1994) *Trends in the Biochemical Sciences* **19,** 73-77

201. Ohno, S., Mizuna, K., Adachi, Y., Hata, A., Akita, Y., Akimoto, K.,

Osada, S., Hirai, S., and Suzuki, K. (1994) *Journal of Boilogical Chemistry* **269,** 17495-17501

202. Morris, N. J., Bushfield, M., Lavan, B. E., and Houslay, M. D. (1994) *Biochemical Journal* **301**(3), 693-702

203. Kawabe, J., Iwami, G., Ebina, T., Ohno, S., Kataoa, T., Veda, Y., Homcy, C. J., and Ishikawa, Y. (1994) *Journal of Biological Chemistry* **269,** 16554-16558

204. Yoshimura, M., and Cooper, D. M. F. (1993) *Journal of Biological Chemistry* **268,** 4604-4607

205. Jacobowitz, O., Chen, J., Premont, R. T., and Iyengar, R. (1993) *Journal of Biological Chemistry.* **268,** 4604-4607

206. Irvine, F., Pyne, N. J., and Houslay, M. D. (1986) *FEBS Letters* **208**(2), 455-459

207. Spence, S., Rena, G., Sullivan, M., Erdogan, S., and Houslay, M. D. (1997) *Biochemical Journal* **321,** 157-163

208. Iredale, P. A., and Hill, S. J. (1993) *British Journal of Pharmacology* **110,** 1305-1310

209. Megson, A. C., Dickenson, J. M., Townsend-Nicholson, A., and Hill, S. J. (1995) *British Journal of Pharmacology* **115**(1415-1424)

210. Hoelting, T., Zielke, A., Siperstein, A. E., Clark, O. H., and Duh, Q. Y. (1994) *Clinical and Experimental Metastasis* **12**(4), 315-323

211. Hoelting, T., Zielke, A., Siperstein, A. E., Clark, O. H., and Duh, Q. Y. (1994) *Journal of Clinical Endocrinology and Metabolism* **79**(3), 806-813

212. Hoelting, T., Tezelman, S., Siperstein, A. E., Duh, Q. Y., and Clark, O. H. (1995) *Thyroid* **5**(1), 35-40

213. Hoelting, T., Siperstein, A. E., Duh, Q. Y., and Clark, O. H. (1995) *Journal of Clinical Endocrinology and Metabolism* **80**(1), 308-313

214. Hoelting, T., Siperstein, A. E., Clark, O. H., and Duh, Q. Y. (1995) *European Journal of Endocrinology* **132**(2), 229-235

215. Kemp, B. E. (ed) (1990) *Peptides and Protein Phosphorylation*, Uniscience CRC Press

216. Usdin, K., Chevret, P., Catzeflis, F. M., Verona, R., and Furano, A. V. (1995) *Molecular Biology and Evolution* **12,** 73-82

217. Furano, A. V., and Usdin, K. (1995) *Journal of Biological Chemistry* **270,** 25301-25304

218. Modi, W. S. (1996) *Molecular Biology and Evolution* **13,** 633-641

219. Graur, D., Duret, L., and Gouy, M. (1996) *Nature* **379,** 333-335

220. Li, W. H., Gouy, M., Sharp, P. M., OhUigin, C., and Yang, Y. W. (1990) *Proceedings of the National Academy of Sciences USA* **87,** 6703-6707

221. Nakatani, T., Suzuki, Y., Yoshida, K., and Sinohara, H. (1995) *Biochimica*

et Biophysica Acta **1263,** 245-248

222. d'Erchia, A. M., Gissi, C., Pesole, G., Saccone, C., and Arnason, U. (1996) *Nature* **381,** 597-600

223. Graur, D., Hide, W. A., Zharkikh, A., and Li, W. H. (1992) *Comparative Biochemistry and Physiology* **101,** 495-498

224. Noguchi, T., Fujiwara, S., Hayashi, S., and Sakaruba, H. (1994) *Comparative Biochemistry and Physiology* , 179-182

225. Ohara, O., Dorit, R., and Gilbert, W. (1989) *Proceedings of the National Academy of Sciences USA* **89,** 9823-9825

226. Loh, E. Y., Elliot, J. F., Cwirla, S., Lanier, L. L., and Davis, M. M. (1989) *Science* **243,** 217-220

227. Frohman, M. A., Dush, M. K., and Martin, G. R. (1988) *Proceedings of the National Academy of Sciences USA* **85**(23), 8998-9002

228. Chen, Z. (1996) *Trends in Genetics* **12,** 87-88

229. Dumas Milne Edwards, J. B., Delort, J., and Mallet, J. (1991) *Nucleic Acids Research* **19,** 5227-5232

230. Dumas Milne Edwards, J. B., Delort, J., and Mallet, J. (1993) in *Methods in Molecular Biology* (White, B. A., ed) Vol. 15, pp. 365-385, Humana Press, Totowa, NJ

231. Troutt, A. B., McHeyzerWilliams, M. G., Pulendran, B., and Nossal, G. J. V. (1992) *Proceedings of the National Academy of Sciences USA* **89**(20), 9823-9825

232. Troutt, A. B. (1994) in *PCR Technology: Current Innovations* (Griffin, H. G., and Griffin, A. M., eds), pp. 141-145, CRC Press, Boca Raton, FL

233. Apte, A., and Siebert, P. D. (1993) *BioTechniques* **15,** 890-893

234. Brennan, C. A., Manthey, A. E., and Gumport, R. I. (1983) *Methods in Enzymology* **100,** 38-52

235. Uhlenbeck, O. C. (1983) *Trends in the Biochemical Sciences* **8,** 94-96

236. Liu, X., and Gorovsky, M. A. (1993) *Nucleic Acids Research* **21**(21), 4954-4960

237. Clark, J. (1988) *Nucleic Acids Research* **16,** 9677-9686

238. Montminy, M. (1997) *Annual Review of Biochemistry* **66,** 807-822

239. Hagen, G., Muller, S., Beato, M., and Suske, G. (1992) *Nucleic Acids Research* **20,** 5519-5525

240. Bucher, P. (1990) *Journal of Molecular Biology* **212,** 563-578

241. Maniatis, T., Fritsch, E. F., and Sambrook, J. (1982) . Molecular cloning: a laboratory manual., Cold Spring Harbor Laboratory, Cold Spring Harbor, N.Y.